EID 30th ANNIVERSARY 1995–2025

CDC U.S. CENTERS FOR DISEASE CONTROL AND PREVENTION

EMERGING INFECTIOUS DISEASES®

Mycobacterial and Fungal Infections

March 2026

Joseph Severn, *Portrait of Keats Listening to a Nightingale on Hampstead Heath*, 1845. Oil on canvas. 114 cm × 97 cm (45 in × 38 in). Guildhall Art Gallery, London, UK. On display at Keats House, Hampstead, UK.

Pages 315–476

EMERGING INFECTIOUS DISEASES

A Peer-Reviewed Journal Tracking and Analyzing Disease Trends

Emerging Infectious Diseases is published monthly by the Centers for Disease Control and Prevention, 1600 Clifton Rd NE, Mailstop H16-2, Atlanta, GA 30329-4018, USA. Telephone 404-639-1960; email eideditor@cdc.gov

EMERGING INFECTIOUS DISEASES®

Mycobacterial and Fungal Infections **March 2026**

On the Cover

Joseph Severn, *Portrait of Keats, Listening to a Nightingale on Hampstead Heath*, 1845. Oil on canvas. 114 cm × 97 cm (45 in × 38 in). Guildhall Art Gallery, London, UK. On display at Keats House, Hampstead, UK.

About the Cover p. 473

Synopses

Research

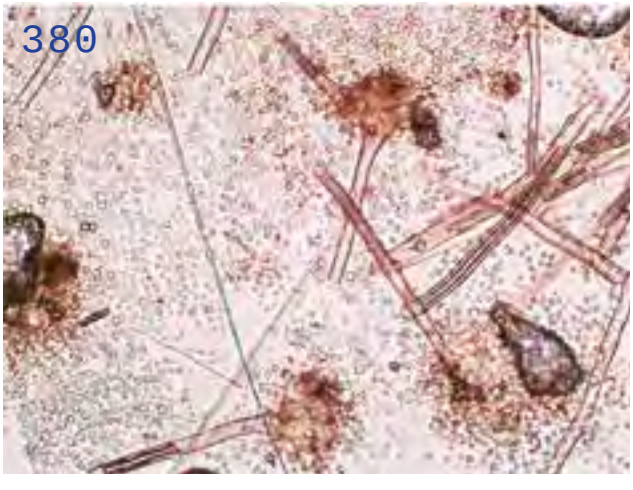

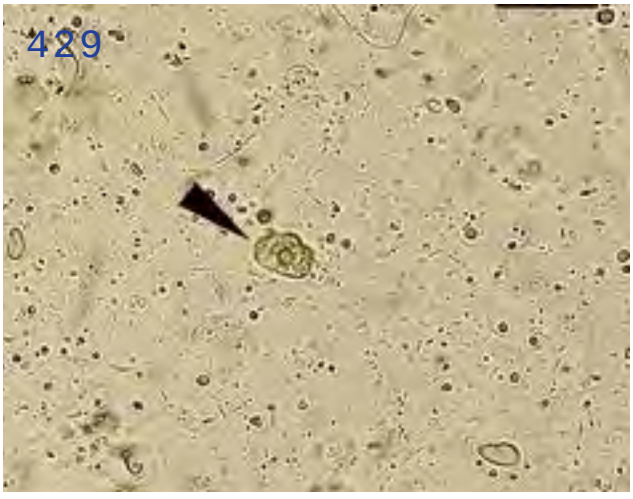

Policy Review

Dispatches

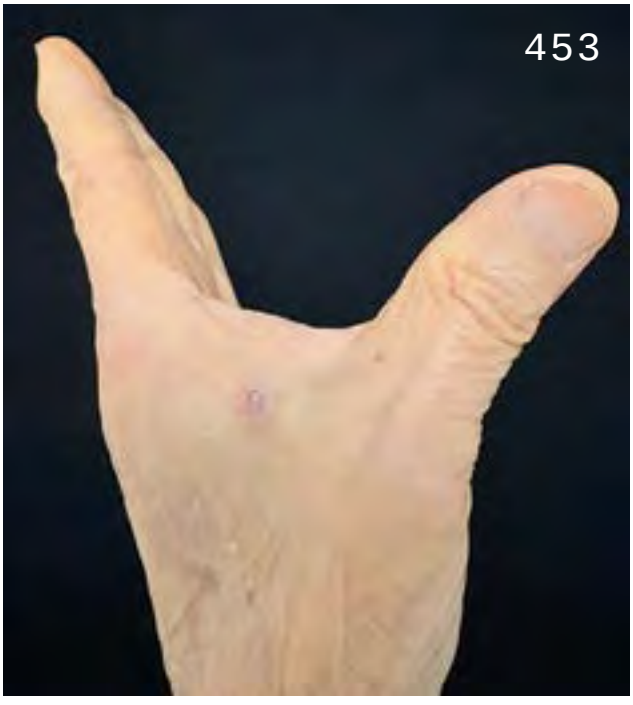

EMERGING INFECTIOUS DISEASES®
March 2026

Another Dimension

Research Letters

EMERGING INFECTIOUS DISEASES®
March 2026

Emerging Infection Networks Letter

About the Cover

Online Report

Correction

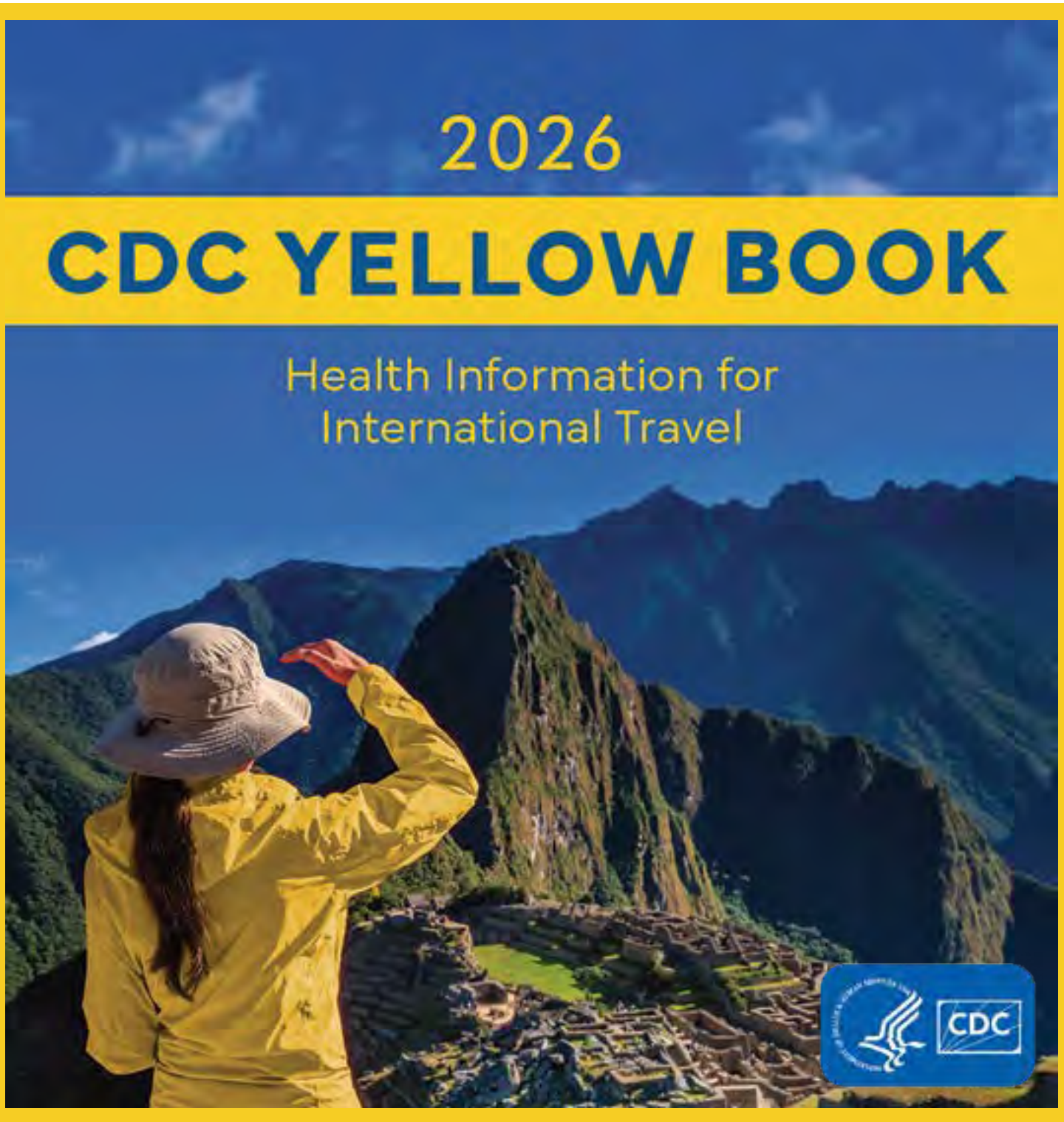

Launch of CDC Yellow Book 2026– A Trusted Travel Medicine Resource

CDC is pleased to announce the launch of the **CDC Yellow Book 2026**. The CDC Yellow Book is a resource containing the U.S. government's travel medicine recommendations and has been trusted by the travel medicine community for over 50 years. Healthcare professionals can use the print and digital versions to find the most up-to-date travel medicine information to better serve their patients' healthcare needs.

The CDC Yellow Book is available online now at www.cdc.gov/yellowbook and in print starting in June 2025 through Oxford University Press and other major online booksellers.

Stenotrophomonas maltophilia Bloodstream Infection Outbreak in Acute Care Hospital, California, USA, 2022–2023[1]

Sana M. Khan, Axel A. Vazquez Deida, Steven Langerman, Jennifer C. Hunter, Rebeca Elliott, Alison Laufer Halpin, Alyssa G. Kent, Paige Gable, Heather A. Moulton-Meissner, Frances C. Knight, Thomas Ewing, Kristen Clancy, Amit Chitnis, Eileen F. Dunne, Dustin Heaton, Barbara Allen, Hillary Metcalf, Munira Shemsu, Kathleen Nava, Suada Abdic, Kiran M. Perkins, Elsa Villarino, Jeffrey Silvers, Kavita K. Trivedi

Stenotrophomonas maltophilia is an opportunistic bacterial pathogen found in healthcare settings. During May 2022–September 2023, an acute care hospital in northern California, USA, identified 13 *S. maltophilia* bloodstream infections among intensive care unit patients. Whole-genome sequencing showed the isolates were highly related. We identified risk factors for infection by conducting a matched case–control study, targeted assessment of infection prevention and control practices, and laboratory testing of suspected environmental reservoirs. Among 13 case-patients and 39 control-patients, patients exposed to iodinated contrast (odds ratio [OR] 12.0; 95% CI 2.1–∞), injectable propofol (OR 12.2; 95% CI 1.5–101.4), or fentanyl (OR 9.2; 95% CI 1.8–∞) had increased odds of *S. maltophilia* bloodstream infection. Although we did not have culture confirmation of a source, we suspect *S. maltophilia* was transmitted by exposure to nonsterile water from a common source. We recommended infection prevention and control practices to reduce risk for contamination from nonsterile water.

Stenotrophomonas maltophilia is a gram-negative bacterium found in aqueous environments, including hospital water systems. *S. maltophilia* causes opportunistic healthcare-associated infections that can result in increased illness and death among hospitalized patients, especially critically ill or immunocompromised patients (*1*,*2*). *S. maltophilia* often leads to respiratory tract infection but can also cause bloodstream, intraabdominal, urinary, catheter, and implanted device–associated infections (*2*,*3*). The crude mortality rate for *S. maltophilia* bloodstream infections (BSIs) ranges from 14% to 69% (*2*,*4*–*6*). Risk factors for healthcare-associated *S. maltophilia* bacteremia include indwelling devices, prior antimicrobial drug therapy, and prolonged hospitalization (*1*,*7*). Past outbreaks of *S. maltophilia* infections in healthcare settings have been attributed to exposure to nonsterile water and contaminated medical devices, medications, or patient care products (*8*–*10*). *S. maltophilia* infections are particularly concerning because the bacterium is often resistant to multiple classes of antibiotics, and treatment options are limited (*2*,*11*).

In May 2022, an acute care hospital in California, USA, alerted its local public health department about 2 patients with *S. maltophilia* BSIs in an intensive care unit (ICU). The hospital identified a third case in July 2022 and reported it to the local health department, after which the hospital and local health department consulted the California Department of Health (CDPH). The hospital infection control team identified an additional 6 *S. maltophilia* BSIs during July–

Author affiliations: Centers for Disease Control and Prevention, Atlanta, Georgia, USA (S.M. Khan, A.A. Vazquez Deida, S. Langerman, J.C. Hunter, A. Laufer Halpin, A.G. Kent, P. Gable, H.A. Moulton-Meissner, F.C. Knight, T. Ewing, K. Clancy, K.M. Perkins); Alameda County Public Health Department, San Leandro, California, USA (S.M. Khan, A. Chitnis, E.F. Dunne, D. Heaton, M. Shemsu, K.K. Trivedi); California Department of Public Health, Richmond, California, USA (R. Elliott, B. Allen, H. Metcalf, E. Villarino); Sutter Health, Sacramento, California, USA (K. Nava, S. Abdic, J. Silvers)

DOI: https://doi.org/10.3201/eid3203.250835

[1]Preliminary results were presented at the Society for Healthcare Epidemiology of America Spring Conference; April 16–19, 2024; Houston, Texas, USA.

September 2022 at the same ICU. The local health department and CDPH consulted the Division of Healthcare Quality Promotion (DHQP), National Center for Emerging and Zoonotic Infectious Diseases, Centers for Disease Control and Prevention (CDC; Atlanta, Georgia), on August 22, 2022, for technical assistance, including whole-genome sequencing (WGS). WGS on 6 available patient isolates showed that all isolates were sequence type (ST) 239 and highly related. No source for the infections was identified at that time, but CDPH and the local health department provided infection control recommendations to the facility during on-site visits in 2022. After a 6-month lapse in cases, the facility reported 4 additional *S. maltophilia* BSIs during April–September 2023, and DHQP provided onsite assistance during August 28–September 12, 2023. We describe the initial and follow-up investigations in response to *S. maltophilia* BSIs.

Methods

Epidemiologic Investigation

We conducted a matched case–control study to determine risk factors for *S. maltophilia* BSI. We identified case-patients via *S. maltophilia*–positive blood cultures. After the initial case was identified in May 2022, we subsequently identified cases by using blood and respiratory cultures from hospital inpatients who had *S. maltophilia* isolated. We defined a case-patient as a febrile (temperature ≥38°C) ICU patient with *S. maltophilia* isolated from a blood culture during May 2022–September 2023.

For each case-patient, we assessed exposures during a reference period, which we defined as the number of days from hospital admission to index specimen collection. The index specimen was the first specimen from which *S. maltophilia* was isolated for a given case-patient. We selected 3 control-patients for each case-patient by matching the closest hospital admission in calendar time and an ICU stay greater than or equal to the matched case-patient's reference period.

We abstracted patient information and relevant healthcare exposures from electronic medical records. For case-patients, we abstracted exposures during the reference period; for control-patients, we abstracted information on the basis of their matched case-patient's reference period. For example, if a case-patient had 5 days between date of admission and date of index specimen collection, we abstracted exposures for 5 days after admission for the matched control-patients. Abstracted information included demographic characteristics, procedures conducted, admission location, medications administered, and any indwelling medical devices (e.g., central venous catheters or urinary catheters placed during admission). Clinical and laboratory data collected included admission diagnoses and microbiology results.

This activity was defined by CDC as a public health investigation and therefore institutional review board approval was required. This activity was reviewed by CDC and was consistent with applicable federal law and CDC policy (see e.g., 45 C.F.R. part 46.102(l)(2), 21 C.F.R. part 56; 42 U.S.C. §241(d); 5 U.S.C. §552a; 44 U.S.C. §3501 et seq.).

Statistical Analysis

We summarized patient characteristics by using descriptive statistics and used univariate conditional logistic regression to estimate the unadjusted odds ratio (OR) and 95% CIs for each possible risk factor, such as exposure to any imaging and invasive procedures, injectable medications received, and presence of indwelling devices. We used exact conditional logistic regression for characteristics in which all case-patients or all control-patients had the exposure of interest. We performed statistical analysis by using SAS version 9.4 (SAS Institute Inc., https://www.sas.com).

Onsite Infection Control Assessment

During the 2022 and 2023 site visits, we observed infection prevention and control (IPC) practices in patient care areas where most case-patients received care, including the emergency department (ED), ICU, ICU step-down unit, and interventional radiology (IR) and computed tomography (CT) suites. We also observed environmental cleaning and disinfection practices. In addition to direct observation of IPC practices, we conducted informal interviews with staff in each department. In 2023, we additionally observed bedside blood draws, trauma patient intake, IR and CT procedures, and maintenance of the contrast injection system in the CT suite.

The facility conducted a review of case-patient hospital stays to assess whether drug diversion occurred. Staff reviewed relevant activity documented in the electronic health records and the automated medication dispensing systems from the time of admission through index culture collection for the affected patients.

Environmental Sampling, WGS, and Bioinformatic Analysis

We conducted 2 rounds of environmental sampling. During August–October 2022, we collected water

and swab samples from sink drains and faucets from the ED, operating rooms, radiology suites, and certain case-patient rooms in the ICU. In September 2023, we collected environmental and product samples informed by direct observation and epidemiologic hypotheses for exposure on the basis of review of preliminary statistical analysis of potential risk factors. We also collected samples from the ED critical care bay, the CT suite, and the ICU, including swabs of sink drains, sponge-wipes used on the contrast autoinjector, and first-catch water samples from 2 sinks in the ED and both CT suite rooms. We obtained samples from the contrast autoinjector in each CT room by using a swab and sponge-wipe. We also obtained materials used during the autoinjector's maintenance for sampling, such as towels used to clean the machine.

We evaluated water samples for *S. maltophilia* by concentration with membrane filtration standard methods (*12*). We filtered 10 mL, 100 mL, and 200 mL of water through a 0.45-micron pore filter (Pall Corporation, https://www.pall.com) and placed filtered samples onto MacConkey agar (MAC; BD Biosciences, https://www.bdbiosciences.com) or directly into 30-mL of tryptic soy broth (TSB; Hardy Diagnostics, http://www.hardydiagnostics.com). We separated sponge-wipes from their handles before processing by using neutralizing buffer (Neogen, https://www.neogen.com), then homogenized at 200 rpm in a Stomacher Circulator 400C (Seward, https://www.seward.co.uk) in phosphate-buffered saline containing 0.02% Tween 80. We then removed the sponge portion and concentrated the homogenate by centrifugation at 2,700 × *g* for 20 minutes. We discarded most of the supernatant and resuspended the pellet in the residual supernatant, which was ≈5 mL. We then plated 100 μL of the concentrated eluent onto MAC and trypticase soy agar with 5% sheep blood (BAP; BD Biosciences) and placed the remaining eluent in 10 mL of TSB. We placed amies transport media swabs directly into 10 mL of TSB. We incubated all broths and culture agar plates for 18–24 hours at 35°C. After incubation, we plated turbid broth enrichments onto MAC and BAP agar and incubated for 18–24 hours at 35°C. We screened all plate cultures for suspected *S. maltophilia*. We used MALDI Biotyper (Bruker Daltonics, https://www.bruker.com) matrix-associated laser desorption/ionization time-of-flight and CDC's MicrobeNet (https://microbenet.cdc.gov) databases to identify suspected *S. maltophilia* and considered scores ≥2.0 confident for species-level identification.

Of 13 case-patients, 10 (77%) had ≥1 clinical blood isolate with *S. maltophilia* growth available for WGS. We also collected 8 clinical respiratory isolates with *S. maltophilia* growth from non–case-patients for WGS. We used Maxwell 16 Cell with Low Elution volume DNA Purification Kit, (both Promega, https://www.promega.com) to extracted DNA from pure isolates and subsequently sheared DNA by using the ME200 Focused-Ultrasonicator (Covaris, https://www.covaris.com). We prepared indexed libraries on the Zephyr G3 NGS workstation (PerkinElmer https://www.perkinelmer.com) by using Ovation Ultralow System V2 Kit (Tecan Life Sciences, https://lifesciences.tecan.com) and analyzed on the Fragment Analyzer System with Standard Sensitivity NGS Fragment Analysis Kit (both Agilent, https://www.agilent.com). We performed WGS on the MiSeq sequencer by using the MiSeq Reagent Kit v2 (Illumina, https://www.illumina.com), which generated 2 × 250 paired-end reads.

We processed raw sequencing reads through DHQP's in-house QuAISAR-H pipeline (https://github.com/DHQP/QuAISAR_singularity). Specifically, we processed sequences by using BBDuk version 38.90 (https://jgi.doe.gov/data-and-tools/bbtools) for adaptor and PhiX removal, and fastp version 0.20.1 to quality trim sequences (*13*). We performed de novo assembly of samples by using SPAdes version 3.15.0 (*14*). After assembly, we removed small scaffolds (<500 bp). We used the PubMLST database and mlst version 2.19 (*15*) to assign STs. We generated maximum-likelihood phylogenetic trees from high-quality single-nucleotide variant (hqSNV) alignments by using SNVPhyl–Nextflow version 1.0.0 to assess isolate relatedness (*16*). We also ran identified clusters separately to calculate cluster hqSNV distances and core-genome estimates. For all SNVPhyl analyses, the reference was the centroid of the isolate set determined by using mash version 2.0 b (*17*). We deposited sequences in the National Center for Biotechnology Information's Sequence Read Archive (BioProject PRJNA288601, BioSample nos. SAMN45204371–413).

Results

Epidemiologic Investigation

We identified 13 case-patients who were hospitalized during May 2022–September 2023 (Figure 1); we selected 39 control-patients for matching. After the initial case was identified in May 2022, blood and respiratory isolates for all hospital inpatients were assessed for *S. maltophilia* growth; no *S. maltophilia* BSIs were identified in patients outside the ICU. Case-patients had a lower median age, 45 (IQR 36.0–68.0) years, than control-patients, who had a median age of

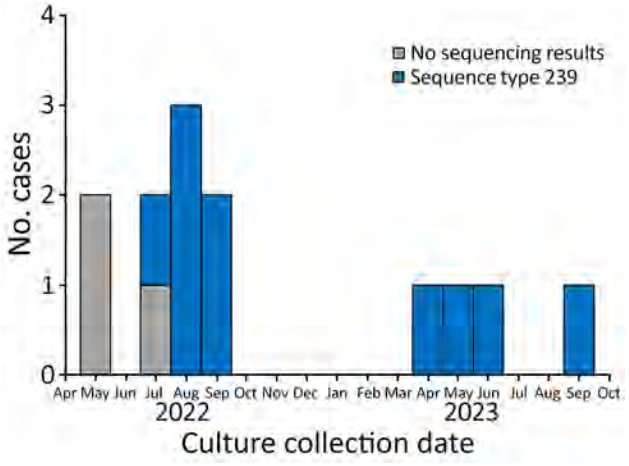

Figure 1. Number of cases per month in *Stenotrophomonas maltophilia* bloodstream infection outbreak in acute care hospital, California, USA, 2022–2023. Graph includes isolates with whole-genome sequencing results showing sequence type 239.

64.0 (IQR 60.0–75.0) years (Table 1). The median reference period was 5 (IQR 3–10) days.

Most (92.3%, 48/52) patients were admitted to the ICU from the ED. A larger percentage (76.9%, 10/13) of case-patients than control-patients (66.7%, 26/39) were admitted through the critical care bay in the ED (Table 2). All 13 case-patients received iodinated contrast, either through an IR procedure or CT scan, compared with only 64.1% (25/39) control-patients. In addition, all 13 case-patients were exposed to injectable fentanyl and 12 (92.3%) were exposed to injectable propofol, but for control-patients, only 64.1% (25/39) were exposed to injectable fentanyl and 61.5% (24/39) to propofol. Case-patients and control-patients had similar rates of antimicrobial drug exposure (84.6% [11/13] vs. 82.1% [32/39]).

Statistical Analysis

A conditional logistic regression analysis revealed that case status was significantly associated with exposure to iodinated contrast either through CT imaging or an IR procedure (OR 12.0 [95% CI 2.1–∞]) (Table 2). Case status was also significantly associated with exposure to injectable fentanyl (OR 9.2 [95% CI 1.8–∞]) or propofol (OR 12.2 [95% CI 1.5–101.4]). Other risk factors associated with being a case-patient included having a bedside procedure (OR 10.2 [95% CI 1.1–93.0]) or having an arterial line (OR 4.1 [95% CI 1.1–16.2]). However, neither of those risk factors had >70% exposure among case-patients.

Onsite Infection Control Assessment

We identified opportunities for improved IPC practices in certain hospital areas, including the CT suite and ICU, during our 2022 site visits. We conducted additional onsite IPC assessments in July, August, and September 2023, in response to identifying

Table 1. Characteristics of case-patients and control patients in a *Stenotrophomonas maltophilia* bloodstream infection outbreak in acute care hospital, California, USA, 2022–2023*

Characteristics	No. (%) case-patients, n = 13	No. (%) control-patients, n = 39
Median age, y (IQR)	45 (36.0–68.0)	64.0 (60.0–75.0)
Sex		
M	9 (69.2)	27 (69.2)
F	4 (30.8)	12 (30.8)
Race		
White	5 (46.2)	14 (35.9)
Black/African American	2 (15.4)	9 (23.1)
Asian	1 (7.7)	8 (20.5)
American Indian/Alaska Native	1 (7.7)	0
Native Hawaiian or other Pacific Islander	0	2 (5.1)
Other	4 (23.1)	6 (15.4)
Ethnicity		
Hispanic	3 (23.0)	8 (22.2)
Non-Hispanic	10 (77.0)	28 (77.8)
No. underlying conditions†		
0	6 (46.2)	9 (23.1)
1	6 (46.2)	13 (33.3)
2	1 (7.7)	10 (25.6)
3	0	4 (10.3)
4	0	3 (7.7)
Admitted to ICU from ED	12 (92.3)	36 (92.3)
Critical care bay of ED	10 (76.9)	26 (66.7)
On immunosuppressant treatments	1 (7.7)	3 (7.7)
Median no. (IQR) days between admission and positive culture collection	5 (3–10)	NA

*ED, emergency department; ICU, intensive care unit; NA, not applicable.
†Underlying conditions were assessed by using electronic health records and included coronary artery disease, congestive heart failure, diabetes, peripheral vascular disease, gastrointestinal disease, liver disease, chronic kidney disease, obesity, cancer, and hypertension.

additional case-patients. Interviews with staff revealed that nonsterile tap water was used extensively to clean the contrast autoinjector, particularly to clean spilled iodinated contrast on and within the autoinjector. Service records for the CT autoinjectors indicated device exposure to tap water in the past, including an incident where standing water was discovered within one of the devices. We reviewed the manufacturer's instructions for use (IFU), which state, "Do not use strong cleaning agents and solvents. Warm water and a mild disinfectant are all that are required to clean the [...] module" (*18*). The facility followed the manufacturer's guidelines and, therefore, followed proper infection prevention protocols. The facility recommended that, in the CT suite, the staff use sterile water and not tap water for cleaning the contrast injection system to prevent possible contamination of the autoinjector with water-associated organisms, such as *S. maltophilia*, even though the use of warm tap water is allowed for cleaning per the manufacturer's IFU.

In reviewing case-patient hospital stays to assess for drug diversion, the facility's drug diversion committee did not find any evidence of drug diversion. The committee reviewed case-patient electronic health records and the automated medication dispensing systems from the time of admission through the culture collection for the affected patients and found no staff commonalities that would suggest drug diversion.

Environmental Sampling, WGS, and Bioinformatic Analysis

Environmental samples from the CT autoinjectors and ICU patient room sink yielded no growth for any gram-negative organisms. *S. maltophilia* was isolated from multiple sink drains and from a first-catch water sample collected from the sink in one of the CT rooms, but those isolates were not genetically linked to the outbreak strain (Figure 2). We sequenced 42 *S. maltophilia* isolates, including 13 (31%) blood, 8 (19%) respiratory, and 21 (50%) environmental samples (Figure 2). The 11 clinical blood isolates available for sequencing from 10 case-patients were highly related.

We sequenced 2 additional blood isolates from 2 non–case-patients who had *S. maltophilia* bacteremia at hospital admission. Those 2 isolates were not genetically linked to each other or to the outbreak strain. Of 8 clinical respiratory isolates collected from non–case-patients during the same period, most (n = 7) did not match the *S. maltophilia* outbreak strain.

Our analyses showed 4 distinct *S. maltophilia* clusters among the 42 isolates. Cluster 1 comprised 12 clinical isolates (11 from blood); all were ST239 and differed by 0–4 pairwise hqSNVs across 98.55% of the reference core genome. Clusters 2–4 included only environmental isolates (no clinical isolates) and included highly related isolates (cluster 2 hqSNV range 1–21, cluster 3 hqSNV difference 12, and cluster 4 hqSNV difference 2) from different sampling locations. The other isolates represented unique sequence types, except for 2 ST5, 2 ST23, and 2 ST224 isolates; isolates in those pairs were unrelated by phylogenetic analyses despite being the same sequence type.

Discussion

This outbreak was unusual in the number of patients with BSIs with the same ST239 *S. maltophilia* identified during an 18-month period, including a 6-month interval without any cases. Prior to the outbreak period, only 1 *S. maltophilia* BSI was identified at this acute care hospital since 2020. Although we did not identify a single common source, *S. maltophilia* was likely transmitted through exposure to tap water through medications, medical devices, or patient care items. *S. maltophilia* is a biofilm-forming pathogen and might exist in a biofilm within the hospital's water drain system despite the facility's robust water management program. Nonsterile water might have contaminated patient care items, injectable contrast, or other medications that were used or prepared in a sink's splash zone area. However, patients were hospitalized in multiple different rooms on different wings of the ICU and water sampling did not identify the *S. maltophilia* outbreak strain. ICU rooms had freestanding sinks without counter tops, making exposure of patient care items to tap water less likely in the ICU. Both rooms in the CT suite had sinks where injectable contrast or other medications could have been prepared for administration, and both sinks had attached countertops and no splash guards in place.

S. maltophilia BSIs most often affect immunocompromised patients and have been associated with ICU admission, indwelling devices, and prior antibiotic use (*3*,*19*,*20*). *S. maltophilia* often leads to infection of the respiratory tract but can also cause BSIs through hematogenous dissemination from the respiratory tract (*21*). This outbreak was unusual in that the case-patients exhibited signs of *S. maltophilia* BSI without a prior or concomitant *S. maltophilia* respiratory infection. In addition, antibiotic exposures were of short duration and were similar between case- and control-patients. Of note, the ST239 *S. maltophilia* strain implicated in this outbreak seemed to have unusually low virulence because no case-patients developed sepsis or died from their bacteremia. In addition, most (7/8) clinical respiratory isolates collected from non–case-patients

during the same period did not match the outbreak strain of *S. maltophilia*. One clinical respiratory isolate in September 2023 did match the *S. maltophilia* outbreak strain. That patient was not considered a case-patient because the patient did not have a BSI and thus did not meet the case definition for this outbreak investigation. However, a review of that patient's medical chart revealed that the patient underwent a CT with contrast, was admitted to the ICU, and was exposed to both fentanyl and propofol between the time of admission and *S. maltophilia* culture collection date. That finding might be explained by opportunities for improvement of IPC practices that might have exposed the patient's respiratory tract to the same unidentified nonsterile water source.

Although we isolated *S. maltophilia* from multiple water and sink drain samples, none of those isolates were related to the outbreak strain by WGS. In addition, sampling of the 2 CT autoinjectors did not reveal *S. maltophilia* growth. However, our observations of cleaning and maintenance practices revealed opportunities for potential contamination of the autoinjectors with nonsterile water. Previous studies have demonstrated that rinsing medical equipment with

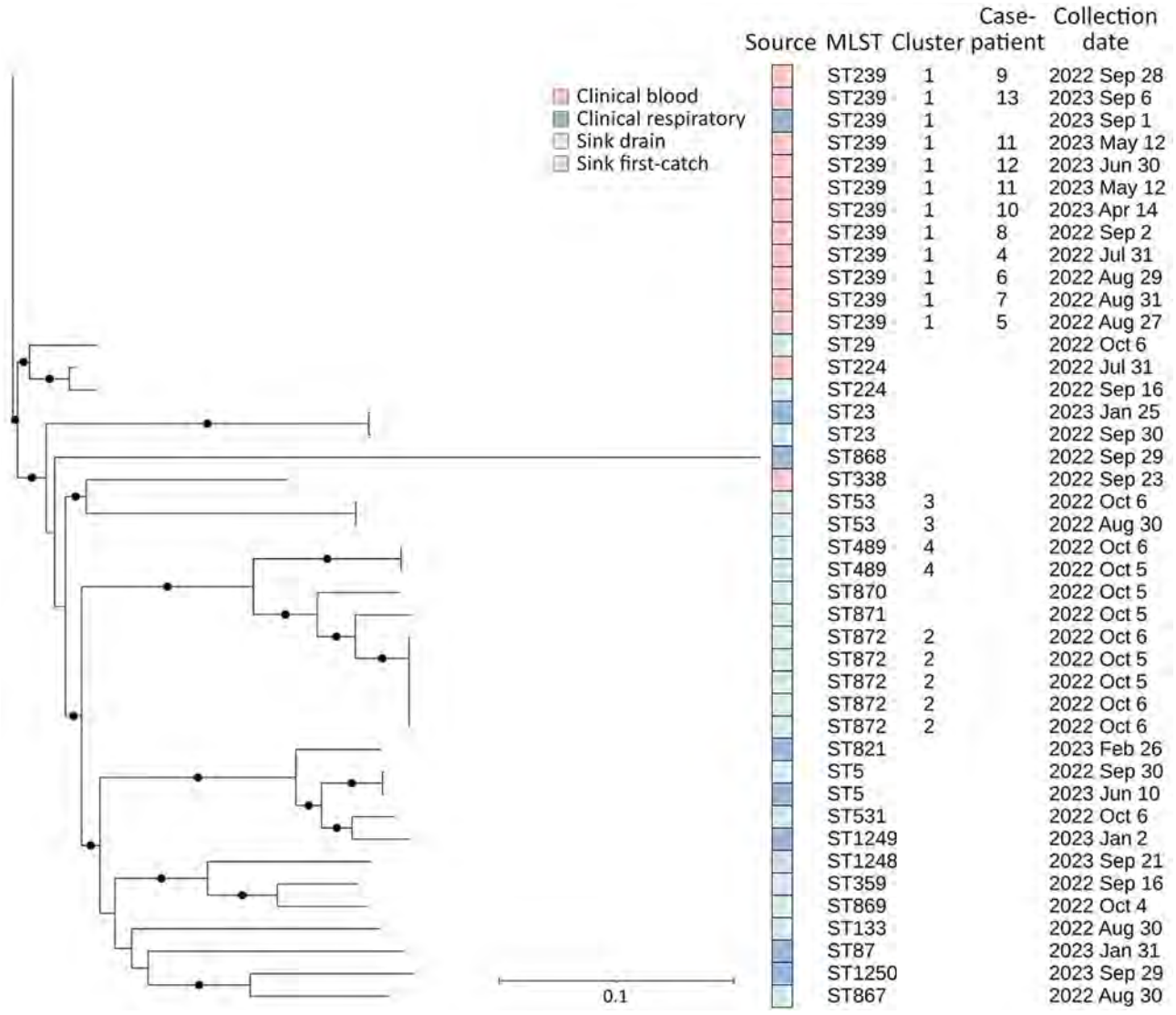

Figure 2. Phylogeny of *Stenotrophomonas maltophilia* detected in bloodstream infection outbreak in acute care hospital, California, United States, 2022–2023. Case-patient numbering starts at 4 because isolates for the first 3 cases were unavailable for sequencing. Full circles on the phylogenetic tree indicate evolutionary branching in the tree with a high value (n = 1) or strong support for the hypothesis that the branching is true. Cluster 1 (n = 12) differed by 0–4 pairwise high-quality single-nucleotide variants (hqSNVs), across 98.54% of the reference isolate core-genome. Cluster 2 (n = 5) differed by 1–21 hqSNVs, across 97.56% of the core-genome. Cluster 3 (n = 2) differed by 12 hqSNVs, across 98.68% of the core-genome. Cluster 4 (n = 2) differed by 3 hqSNVs, across 99.01% of the core-genome. Scale bar indicates nucleotide substitutions per site.

Table 2. Conditional logistic regression models on risk factors of interest for a *Stenotrophomonas maltophilia* bloodstream infection outbreak in acute care hospital, California, USA, 2022–2023*

Risk factors	No. (%) case-patients, n = 13	No. (%) control-patients, n = 39	OR (95% CI)
Imaging procedures			
Any CT†‡	13 (100)	37 (94.9)	0.81 (0.10–∞)
CT with contrast	11 (91.7)	23 (63.9)	8.5 (0.9–78.2)
Ultrasound	8 (61.5)	23 (59.0)	1.1 (0.3–4.5)
MRI	1 (7.7)	9 (23.1)	0.3 (0.03–2.3)
Injectable medications			
Exposure to any contrast†§	13 (100)	25 (64.1)	12.0 (2.1–∞)
Fentanyl†*	13 (100)	24 (61.5)	9.2 (1.8–∞)
Propofol	12 (92.3)	19 (48.7)	12.2 (1.5–101.4)
Famotidine	9 (69.2)	29 (74.4)	0.8 (0.2–3.0)
Locations			
CT room 2	9 (69.2)	15 (38.5)	3.6 (0.9–14.7)
CT room 1	8 (61.5)	23 (59.0)	1.1 (0.3–3.6)
Critical care bay	10 (76.9)	26 (66.7)	1.6 (0.4–6.9)
Procedures			
Any procedure¶	10 (76.9)	22 (56.4)	2.6 (0.6–10.5)
Surgery	7 (53.9)	12 (30.8)	2.6 (0.7–9.7)
Any transfusions	7 (53.9)	15 (38.5)	1.9 (0.5–7.1)
Operating room procedure	6 (46.2)	12 (30.8)	1.9 (0.5–6.8)
Interventional radiology procedure	4 (30.8)	12 (30.8)	1.0 (0.2–4.2)
Bedside procedure	4 (30.8)	2 (5.1)	10.2 (1.1–93.0)
Indwelling devices			
Any tube#	12 (92.3)	30 (76.9)	3.3 (0.4–28.3)
Peripheral line	12 (92.3)	36 (92.3)	1.0 (0.06–16.0)
Mechanical ventilator	10 (76.9)	28 (71.8)	1.3 (0.3–6.2)
Arterial line	9 (69.2)	13 (33.3)	4.1 (1.1–16.2)
Central venous catheter	8 (61.5)	22 (56.4)	1.2 (0.4–4.3)
Other indwelling device**	7 (53.9)	36 (92.3)	0.12 (0.03–0.6)
Other factors			
Presence of wound	6 (46.2)	20 (51.3)	0.8 (0.2–2.9)
Antibiotic drug exposure	11 (84.6)	32 (82.1)	1.2 (0.2–7.0)

*CT, computed tomography; MRI, magnetic resonance imaging; OR, odds ratio.
†Exact odds ratio; median unbiased estimate and 1-sided p value.
‡Brain, chest, abdomen, pelvis, maxillofacial, spine, head and neck, and other CT imaging.
§Contrast administered during CT or other interventional radiologic procedure,
¶Procedures were surgery, transfusions, procedures in an operating room, interventional radiology, or bedside procedures.
#Nasogastric, orogastric, percutaneous endoscopic gastronomy, and other tubes.
**Suprapubic catheter, Foley catheter, dialysis line, surgical drain, or other devices.

nonsterile water during cleaning can result in contamination of equipment and lead to subsequent BSIs among patients (*22*). In the setting of this outbreak, we recommended that the facility continue to identify opportunities to minimize the use of nonsterile water during maintenance and routine cleaning of the equipment to prevent additional *S. maltophilia* BSIs and other gram-negative bacterial infections. Since the outbreak, the facility has revised internal preventive maintenance guidelines for CT autoinjectors to include use of sterile water in place of the manufacturer's IFU that states warm tap water may be used. In addition, staff working in the CT suite have implemented a daily deep cleaning of the injector heads using hospital-approved disinfectant wipes and a contrast cleaner for cleaning drips or spills. A 2-person approach was also implemented to eliminate use of the countertop next to the sink during the preparation and administration of contrast.

Several outbreaks, including ones involving bacterial infections, have been reported in healthcare settings as a result of drug diversion; some outbreaks involved tampering with injectable fentanyl (*23*). Drug diversion occurs when a prescription drug is removed from its intended path from the manufacturer to the patient. A 2015 review of the published literature and internal CDC records related to infections from drug diversion found 6 outbreaks over a 10-year period, 4 of which involved tampering with syringes or vials containing fentanyl (*23*). Tampering with syringes can include replacement of medication with saline or nonsterile water, enabling introduction of environmental pathogens to the bloodstream. Dilution of analgesic medication using nonsterile water has also been linked to an outbreak of *Sphingomonas paucimobilis*, another water-associated pathogen that rarely causes bloodstream infections (*24*). We found that exposure to fentanyl increased the odds of being a case-patient by 9.2 times and exposure to propofol increased the odds by 12.2 times. However, the facility's drug diversion committee did not find evidence of drug diversion related to this outbreak. The review did not reveal any patterns

or commonalities among the case-patients, such as a common anesthesia provider or nursing staff. The facility also contacted the contracted pharmacies and confirmed no medication recalls had been issued to ensure no intrinsic contamination of intravenous medications occurred during this time.

Although other risk factors were statistically associated with being a case-patient in this case–control study, we focused our investigation and discussion on iodinated contrast and injectable fentanyl, because almost all case-patients were exposed those risk factors. The possibility that the infection point source was a risk factor that was not common among case-patients is less likely.

The first limitation of this investigation is that, because of technical difficulties during environmental sampling, only 1 of 2 autoinjectors from the CT suite could be sampled initially. The local public health department returned to the facility on September 29, 2023, to sample the second autoinjector and the drain in the second CT room. *S. maltophilia* was not isolated from those samples, which might have been attributable to a 5-day delay between sample collection and culturing caused by shipping disruption between sample collection and receipt by the CDC laboratory. Potential temperature deviations during delayed shipping might have contributed to loss of organism viability. Second, biofilms are dynamic in nature, and the environmental samples collected might have been insufficient to capture a portion of the biofilm that contained the pathogen of interest (*25*). The negative environmental samples do not definitively rule out the presence of the *S. maltophilia* outbreak strain in the sampled environments. Despite those challenges, the matched case–control study and IPC observations provided the facility with focus areas for re-educating staff and auditing IPC practices surrounding using nonsterile water for cleaning and preparing injectable medication in the CT suite.

In summary, this epidemiologic investigation of 13 *S. maltophilia* BSIs did not find a point source for this outbreak but revealed intravenous contrast as a possible risk factor of concern. Although sampling of the 2 CT autoinjectors was negative for *S. maltophilia*, the facility implemented measures to decrease the risk for contamination from nonsterile water beyond what was recommended in the manufacturer's IFU. Intensive investigations during outbreaks frequently do not identify a common source. However, addressing identified opportunities in infection control often results in a halt of transmission, and as of August 2025, no additional cases had been identified. Healthcare settings should discourage using nonsterile water for medical devices that could contact patient medications or care products to reduce the risk of contamination with waterborne pathogens such as *S. maltophilia*.

About the Author

Dr. Khan is an Epidemic Intelligence Service officer at the Centers for Disease Control and Prevention and is assigned to the Alameda County Public Health Department, California, USA. Her research interests include antimicrobial stewardship and health equity.

References

1. Brooke JS. *Stenotrophomonas maltophilia*: an emerging global opportunistic pathogen. Clin Microbiol Rev. 2012;25:2–41. https://doi.org/10.1128/CMR.00019-11
2. Gibb J, Wong DW. Antimicrobial treatment strategies for *Stenotrophomonas maltophilia*: a focus on novel therapies. Antibiotics (Basel). 2021;10:1226. https://doi.org/10.3390/antibiotics10101226
3. del Toro MD, Rodríguez-Bano J, Herrero M, Rivero A, García-Ordoñez MA, Corzo J, et al.; Grupo Andaluz para el Estudio de las Enfermedades Infecciosas. Clinical epidemiology of *Stenotrophomonas maltophilia* colonization and infection: a multicenter study. Medicine (Baltimore). 2002;81:228–39. https://doi.org/10.1097/00005792-200205000-00006
4. Friedman ND, Korman TM, Fairley CK, Franklin JC, Spelman DW. Bacteraemia due to *Stenotrophomonas maltophilia*: an analysis of 45 episodes. J Infect. 2002;45:47–53. https://doi.org/10.1053/jinf.2002.0978
5. Jang TN, Wang FD, Wang LS, Liu CY, Liu IM. *Xanthomonas maltophilia* bacteremia: an analysis of 32 cases. J Formos Med Assoc. 1992;91:1170–6.
6. Micozzi A, Venditti M, Monaco M, Friedrich A, Taglietti F, Santilli S, et al. Bacteremia due to *Stenotrophomonas maltophilia* in patients with hematologic malignancies. Clin Infect Dis. 2000;31:705–11. https://doi.org/10.1086/314043
7. Lai CH, Chi CY, Chen HP, Chen TL, Lai CJ, Fung CP, et al. Clinical characteristics and prognostic factors of patients with *Stenotrophomonas maltophilia* bacteremia. J Microbiol Immunol Infect. 2004;37:350–8.
8. Alfieri N, Ramotar K, Armstrong P, Spornitz ME, Ross G, Winnick J, et al. Two consecutive outbreaks of *Stenotrophomonas maltophilia* (*Xanthomonas maltophilia*) in an intensive-care unit defined by restriction fragment-length polymorphism typing. Infect Control Hosp Epidemiol. 1999;20:553–6. https://doi.org/10.1086/501668
9. Guyot A, Turton JF, Garner D. Outbreak of *Stenotrophomonas maltophilia* on an intensive care unit. J Hosp Infect. 2013;85:303–7. https://doi.org/10.1016/j.jhin.2013.09.007
10. Sakhnini E, Weissmann A, Oren I. Fulminant *Stenotrophomonas maltophilia* soft tissue infection in immunocompromised patients: an outbreak transmitted via tap water. Am J Med Sci. 2002;323:269–72. https://doi.org/10.1097/00000441-200205000-00008
11. Keaton A, Fike L, Spicer K, Kallen A, Perkins K. Healthcare-associated *Stenotrophomonas maltophilia* infections in the United States, 2018–2022. Antimicrob Steward Healthc Epidemiol. 2023;3:s89. https://doi.org/10.1017/ash.2023.352
12. Standard Methods for the Examination of Water and Wastewater. 9215 Heterotrophic plate count [cited 2025 May

7]. https://www.standardmethods.org/doi/abs/10.2105/SMWW.2882.188
13. Chen S, Zhou Y, Chen Y, Gu J. fastp: an ultra-fast all-in-one FASTQ preprocessor. Bioinformatics. 2018;34:i884–90. https://doi.org/10.1093/bioinformatics/bty560
14. Bankevich A, Nurk S, Antipov D, Gurevich AA, Dvorkin M, Kulikov AS, et al. SPAdes: a new genome assembly algorithm and its applications to single-cell sequencing. J Comput Biol. 2012;19:455–77. https://doi.org/10.1089/cmb.2012.0021
15. Jolley KA, Bray JE, Maiden MCJ. Open-access bacterial population genomics: BIGSdb software, the PubMLST.org website and their applications. Wellcome Open Res. 2018;3:124. https://doi.org/10.12688/wellcomeopenres.14826.1
16. Petkau A, Mabon P, Sieffert C, Knox NC, Cabral J, Iskander M, et al. SNVPhyl: a single nucleotide variant phylogenomics pipeline for microbial genomic epidemiology. Microb Genom. 2017;3:e000116. https://doi.org/10.1099/mgen.0.000116
17. Ondov BD, Treangen TJ, Melsted P, Mallonee AB, Bergman NH, Koren S, et al. Mash: fast genome and metagenome distance estimation using MinHash. Genome Biol. 2016;17:132. https://doi.org/10.1186/s13059-016-0997-x
18. MEDRAD Stellant imaging system interface (ISI) 800 module operation & installation manual. Bayer Medical Care Inc; 2019 [cited 2025 May 7]. https://www.manualslib.com/manual/1808572/Bayer-Healthcare-Medrad-800-Module.html
19. Sumida K, Chong Y, Miyake N, Akahoshi T, Yasuda M, Shimono N, et al. Risk factors associated with *Stenotrophomonas maltophilia* bacteremia: a matched case-control study. PLoS One. 2015;10:e0133731. https://doi.org/10.1371/journal.pone.0133731
20. Denton M, Kerr KG. Microbiological and clinical aspects of infection associated with *Stenotrophomonas maltophilia*. Clin Microbiol Rev. 1998;11:57–80. https://doi.org/10.1128/CMR.11.1.57
21. Garazi M, Singer C, Tai J, Ginocchio CC. Bloodstream infections caused by *Stenotrophomonas maltophilia*: a seven-year review. J Hosp Infect. 2012;81:114–8. https://doi.org/10.1016/j.jhin.2012.02.008
22. Boyce JM, Dumigan DG, Havill NL, Hollis RJ, Pfaller MA, Moore BA. A multi-center outbreak of *Candida tropicalis* bloodstream infections associated with contaminated hemodialysis machine prime buckets. Am J Infect Control. 2021;49:1008–13. https://doi.org/10.1016/j.ajic.2021.02.014
23. Schaefer MK, Perz JF. Outbreaks of infections associated with drug diversion by US health care personnel. Mayo Clin Proc. 2014;89:878–87. https://doi.org/10.1016/j.mayocp.2014.04.007
24. Wasiura J, Segal BH, Mullin KM. Cluster of *Sphingomonas paucimobilis* bacteremias linked to diversion of intravenous hydromorphone. N Engl J Med. 2019;381:584–5. https://doi.org/10.1056/NEJMc1902973
25. Bamford NC, MacPhee CE, Stanley-Wall NR. Microbial primer: an introduction to biofilms—what they are, why they form and their impact on built and natural environments. Microbiology (Reading). 2023;169:8. https://doi.org/10.1099/mic.0.001338

Address for correspondence: Kavita K. Trivedi, Alameda County Public Health Department, 1100 San Leandro Blvd, San Leandro, CA 94577, USA; email: kavita.trivedi@acgov.org

Lymphocytic Choriomeningitis Virus Seroprevalence among Urban Pregnant Women and Newborns, Philadelphia, Pennsylvania, USA, 2021

Dustin D. Flannery,[1] Caitlin M. Cossaboom,[1] Timothy D. Flietstra, Alvaro Zevallos Barboza, Heather H. Burris, Karen M. Puopolo, Aridth Gibbons, Deborah L. Cannon, Inna Krapiunaya, Leanna Sayyad, Katrin S. Sadigh, Kami Smith, Joel M. Montgomery, Trevor Shoemaker, John D. Klena, Scott M. Gordon

Lymphocytic choriomeningitis virus (LCMV) is a globally distributed rodentborne pathogen that can cause severe congenital infections. We conducted a retrospective cross-sectional seroepidemiologic study using remnant serum samples from pregnant women and newborns at 2 hospitals in Philadelphia, Pennsylvania, USA. We tested samples for LCMV IgG and IgM in 3 phases: a high-risk group determined by neighborhood deprivation index scores, a random sample of all birthing women, and a group with prenatally diagnosed neurologic malformations. We found LCMV IgG seroprevalence was 2.4% among 700 high-risk and 2.7% among 300 randomly selected pregnant women. Seroprevalence varied by hospital site, maternal race or ethnicity, and neighborhood deprivation level. All seropositive maternal samples were IgM-negative. Thirty-seven pregnant women carrying fetuses with neurologic malformations were seronegative. Our findings highlight the risk for LCMV exposure in urban settings and emphasize the need for pregnant women to avoid contact with rodents to prevent this rare but serious congenital infection.

Lymphocytic choriomeningitis virus (LCMV) is a rodentborne pathogen that can cause severe congenital infections (*1*). LCMV is commonly carried by the house mouse (*Mus musculus*) (*2*). The virus is a member of the Arenaviridae family and is distributed globally in urban and rural settings; however, the burden of infection is not well defined. Infections have been reported throughout North and South America, Europe, Asia, and Australia (*3*).

In adult humans, LCMV infection typically is associated with asymptomatic or mild illness, but severe disease can occur in immunocompromised patients (*4*). The virus has disproportionate health effects on fetuses and newborns when infection occurs during pregnancy and can lead to chorioretinitis, intracranial calcifications, a variety of neurologic malformations, intellectual disability, neurodevelopmental problems, and fetal death (*1*,*5*–*7*).

Although LCMV is a devastating congenital human pathogen, sparse epidemiologic data describe domestic LCMV seroprevalence in the United States (*8*). Previous serosurveys of adult urban dwellers in the United States in the 1980s and early 1990s found an LCMV seroprevalence of 2%–5%, suggesting that LCMV exposure might be common (*9*,*10*). Data collected during 1984–1989 showed an average of 9% of house mice trapped across Baltimore, Maryland, USA, had detectable LCMV antibodies (*2*). Infected animals were identified at 6 of 8 sites, and LCMV seroprevalence among mice varied from 3.9% to 13.4%. The sampled site with the highest seroprevalence was an inner-city residential area where positive mice were clustered within city blocks

Author affiliations: Children's Hospital of Philadelphia, Philadelphia, Pennsylvania, USA (D.D. Flannery, A. Zevallos Barboza, H.H, Burris, K.M. Puopolo, S.M. Gordon); University of Pennsylvania Perelman School of Medicine, Philadelphia (D.D. Flannery, H.H. Burris, K.M. Puopolo, S.M. Gordon); Centers for Disease Control and Prevention, Atlanta, Georgia, USA (C.M. Cossaboom, T.D. Flietsra, A. Gibbons, D.L. Cannon, I. Krapiunaya, L. Sayyad, K.S. Sadigh, K. Smith, J.M. Montgomery, T. Shoemaker, J.D. Klena)

DOI: https://doi.org/10.3203/eid3203.250910

[1]These first authors contributed equally to this article.

and households, and that clustering correlated with estimates of mouse density (*2*).

Scant data on LCMV seropositivity among urban pregnant women or general cohorts of infants with neurologic malformations are available for the United States (*8*). Although rapid genetic sequencing has identified more causes of congenital neurologic malformations, most (50%–60%) remain idiopathic (*11*,*12*). One prior Chicago, Illinois, USA–based serosurvey of a limited number of children with congenital chorioretinitis showed that LCMV exposure in that group was common, supporting the notion that congenital LCMV might be underdiagnosed (*13*). Therefore, to understand current perinatal LCMV seroprevalence and its implications, we aimed to estimate LCMV seroprevalence among a targeted high-risk sample of pregnant women, and a random sample of women who gave birth in urban Philadelphia, Pennsylvania, USA. We also aimed to assess LCMV antibody transfer to newborns of LCMV seropositive birth mothers and determine LCMV seroprevalence among newborns with neurologic malformations and their birth mothers.

Materials and Methods

Study Design and Serum Sample Collection

We conducted a retrospective cross-sectional seroepidemiologic study of available remnant serum samples from pregnant women and newborns at 2 birth hospitals, Pennsylvania Hospital and Hospital of the University of Pennsylvania, and a freestanding children's hospital special delivery unit, all located in Philadelphia. As part of routine clinical care at the 2 birth hospitals, at admission for delivery, pregnant women have blood drawn for rapid plasma reagin testing to screen for syphilis, per public health guidelines (*14*). We obtained residual serum from that testing from the clinical laboratory at the time it was scheduled for disposal. We linked residual serum samples to demographic and clinical data abstracted from medical records and then deidentified data for analysis. All data abstraction occurred before serologic testing, and the analyst responsible for clinical data was blinded to serologic testing results. We also obtained serum samples from pregnant women referred to the Children's Hospital of Philadelphia (CHOP) Special Delivery Unit for childbirth because of known fetal neurologic malformations. CHOP Birth Defects Biorepository routinely collects newborn serum samples. We deidentified all specimens used in this study, and specimens could not be linked to specific patients. The study was reviewed and deemed non–human subjects research as a public health surveillance project by the institutional review boards at the University of Pennsylvania and CHOP, with a waiver of informed consent. This activity was also reviewed by the Centers for Disease Control and Prevention (CDC) and was conducted consistent with applicable federal law and CDC policy (e.g., 45 C.F.R. part 46.102(a)).

We conducted the study in 3 phases. For phases 1 and 2 (Figure), we included serum samples from pregnant women who were admitted for childbirth during January 1–December 31, 2021, and who had an available remnant serum sample in the biobank registry. At 1 of the 2 birth hospitals, we included available remnant cord blood serum samples from newborns of seropositive women to assess placental antibody transfer.

For phase 1, we defined a high-risk group, assuming a likely association between residence in neighborhoods of lower socioeconomic status and higher mouse exposure (*15*). For that group, we selected serum samples from pregnant women residing in census tracts with the highest quartile of neighborhood deprivation according to the Community Deprivation Index (https://github.com/geomarker-io/dep_index) on the basis of the geocoded address reported at the time of admission for childbirth (*16*,*17*). Community Deprivation Index scores range from 0 to 1 and are divided into 4 quartiles from least deprived (Q1) to most deprived (Q4) as follows: Q1 is <0.324, Q2 is 0.324–0.449, Q3 is 0.45–0.579, and Q4 is ≥0.58 (*17*,*18*). The index was developed using a principal component analysis of the 2018 American Community Survey census tract fraction of the population with incomes below the federal poverty level, at least a high school education, lacking health insurance, receiving public assistance for income or food, median household income, and the fraction of vacant homes (*18*).

For phase 2, to obtain a seroprevalence estimate for the study population at large, we selected serum samples from a random sample of pregnant women who gave birth during the study period. For phases 1 and 2, we excluded serum samples from pregnant women who had a missing deprivation index; resided outside of the Philadelphia city limits; had an imprecise geocode, defined as a geocode match score ≤0.8 the range; or with <300 μL of available serum (Figure). We excluded samples from the 700 pregnant women in phase 1 from selection in phase 2 to avoid double selection considering that a large pool of samples remained and resampling was not necessary. We abstracted clinical data from the electronic medical record for all pregnant women with included serum samples.

For phase 3, we sought to estimate LCMV seroprevalence among a cohort of pregnant women with

known fetal neurologic and ocular malformations and their newborns. We obtained maternal plasma and cord blood samples from the CHOP Birth Defects Biorepository for births during June 1, 2019–June 1, 2023. We used Human Phenotype Ontology (HPO) terms to define neurologic and ocular findings (*19*); those terms were developed to standardize the descriptions of phenotypes observed across human disease.

LCMV Serologic and Molecular Testing

During September 2023–June 2024, we shipped samples from all 3 study phases to CDC (Atlanta, Georgia, USA) for laboratory testing. As previously described (*20*), the laboratory used a CDC-developed ELISA to determine the presence of LCMV IgG. The laboratory subsequently tested IgG-positive samples by using a CDC-developed IgM ELISA (*20*). For IgM-positive samples, the laboratory subsequently extracted RNA from the original clinical specimen and tested for LCMV nucleic acid using a real-time reverse transcription PCR targeting the large segment of LCMV (*21*).

Statistical Analysis

For phase 1, from preliminary deprivation index data and historical childbirth volumes, we estimated that we would need 700 maternal serum samples to detect seroprevalence ≥0.5%: 500 samples for screening and 200 samples for validation to confirm the seroprevalence estimate. For phase 2, on the basis of preliminary findings from phase 1, we selected 300 random maternal samples stratified by deprivation index quartiles (75 samples per quartile) to obtain a seroprevalence estimate for the study population. For phase 3, we used a convenience sample, as described above. We reported the percentage of seropositive cases for each phase and computed 95% CIs by using the binomial distribution.

We used a 2-sample *z*-test for proportions and Fisher exact test to compare serostatus by available demographic data and clinical characteristics for phases 1 and

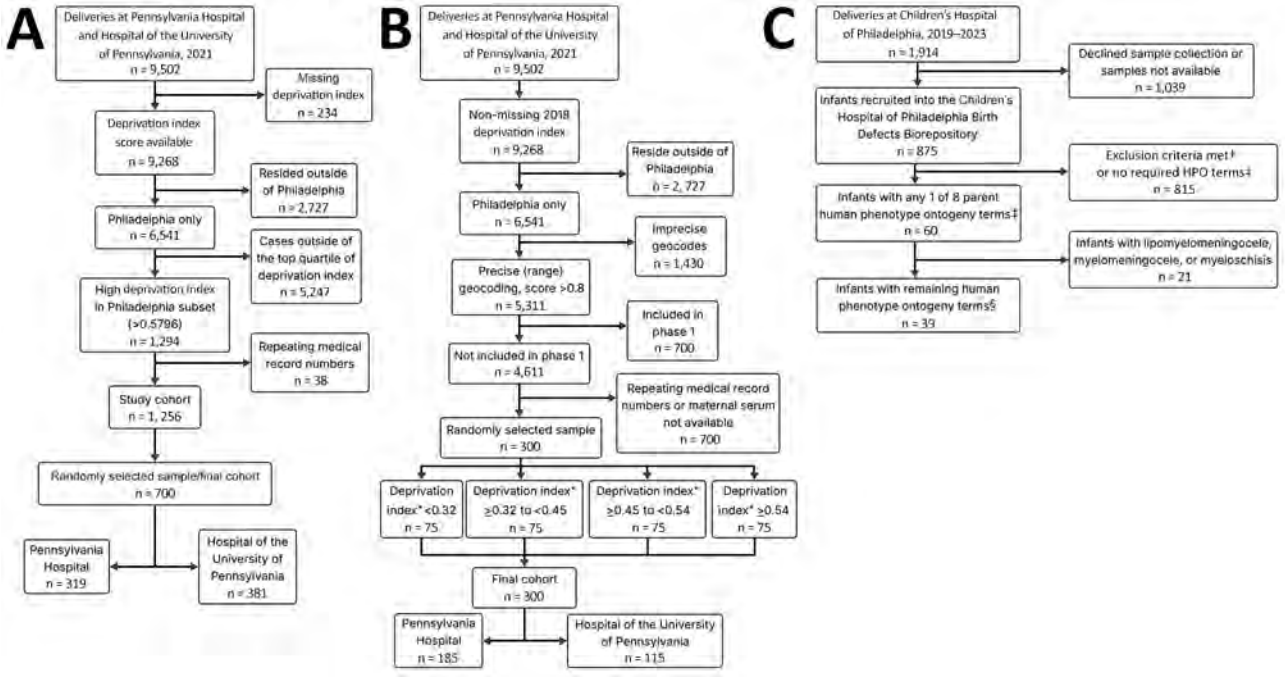

Figure. Flowchart of 3 phases of a study of lymphocytic choriomeningitis virus seroprevalence among urban pregnant women and newborns, Philadelphia, Pennsylvania, USA, 2021. A) Phase 1; B) phase 2; C) phase 3. Phases 1 and 2 used deliveries at Pennsylvania Hospital and the Hospital of the University of Pennsylvania in 2021 as the starting population. Repeated medical record numbers indicate parturient patients with multiple deliveries or >1 delivery during the study period, which would result in replicate maternal serum samples if retained. Phase 3's starting population was the Children's Hospital of Philadelphia Special Delivery Unit newborns delivered from the inception of the Birth Defects Biorepository during June 1, 2019–June 1, 2023. *Deprivation index ranges were determined using the Community Deprivation Index (https://github.com/geomarker-io/dep_index) on the basis of the geocoded address and quartile values were calculated on the full eligible cohort before phase-specific exclusions (n = 4,611). †Exclusion criteria included no cytomegalovirus testing on file, no placenta tissue available, and plasma not available for both maternal/infant matched samples even within the first few weeks after delivery. ‡The 8 overall HPO terms (https://hpo.jax.org) used encompassed 615 conditions. Those 8 HPO terms were abnormal choroid morphology, abnormal retinal morphology, cerebral calcification, intracranial cystic lesion, abnormality of neuronal migration, abnormal cerebral morphology, open neural tube defect, and abnormal cerebral ventricle morphology. §After excluding lipomyelomeningocele, myelomeningocele, and myeloschisis, 612 children's HPO conditions remained. HPO, Human Phenotype Ontology.

2 combined. Because phase 3 results were not comparable to phases 1 and 2, we did not include phase 3 in that analysis. To address potential collinearity, we used an analysis of variance (ANOVA) model with hospital, ethnicity, race, maternal age, and deprivation index quartile variables as the independent variables and serostatus as the response variable. Because we selected all samples from phase 1 from Q4, we used the deprivation index quartile in the ANOVA model to ensure that the overrepresentation did not bias the results. We then fit a multivariable logistic regression model with maternal LCMV serostatus as the binary outcome. We used stepwise variable selection to derive a final parsimonious model and calculated adjusted odds ratios (ORs) with 95% CIs. We used MATLAB (MathWorks, https://www.mathworks.com) to perform all statistical analyses and considered $p<0.05$ statistically significant.

Results

In 2021, the 2 hospitals reported that 9,286 women gave birth to 9,502 newborns. For phases 1 and 2 combined, the median maternal age at delivery was 29 (IQR 24–34) years, and 109 (9.8%) patients gave birth before 37 weeks' gestation. Of the 700 selected maternal serum samples from the high-risk group screened in phase 1, a total of 17 (2.4%, 95% CI 1.4%–3.9%) were positive for LCMV IgG, among which none were IgM-positive. We had 11 paired cord blood samples available from the 17 IgG-positive maternal serum samples, all of which tested positive for IgG directed to LCMV but were IgM-negative.

In phase 2, a total of 8 (2.7%, 95% CI 1.2%–5.2%) of the 300 random maternal serum samples were IgG-positive for LCMV. None of those serum samples were IgM-positive. Six paired cord blood samples were available from the 8 IgG-positive maternal serum samples; all were IgG-positive for LCMV but were IgM-negative (Table 1).

We compared serostatus by clinical and demographic characteristics for phases 1 and 2 combined (Table 2). The overall ANOVA model was statistically significant. The independent variables showed high collinearity in the initial model with an average variance inflation factor (VIF) of 1.57. The final ANOVA model (F statistic = 24.375; p = 0.0004) that used stepwise regression removed much of the collinearity from the initial model, resulting in an average VIF of 1.14. The statistically significant factors were the birth hospital (Pennsylvania Hospital ranked higher than Hospital of the University of Pennsylvania; p = 0.01), maternal race (all other races were higher than White race; p = 0.0003), and maternal ethnicity (Hispanic ethnicity ranked higher than non-Hispanic; p = 0.02).

Table 1. Phase-specific lymphocytic choriomeningitis virus seroprevalence among urban pregnant women, Philadelphia, Pennsylvania, USA*

Analysis phase	No. (%) seropositive
Pregnant women, n = 1,000	25 (2.5)
Phase 1, n = 700	17 (2.4)
Phase 2, n = 300	8 (2.7)
Pregnant women with antenatally diagnosed fetal brain anomaly; phase 3, n = 37	0

*Maternal lymphocytic choriomeningitis virus (LCMV) seroprevalence detected by LCMV IgG during pregnancy. For phases 1 and 2, neighborhood deprivation at the census tract level calculated by using the Community Deprivation Index (*17*,*18*). Scores are divided into 4 quartiles from least deprived (Q1) to most deprived (Q4). Scores are as follows: Q1 is <0.324; Q2 is 0.324–0.449; Q3 is 0.45–0.579; and Q4 is >0.58. Phase 1 included persons residing in the highest quartile of neighborhood deprivation; phase 2, included residents of all 4 quartiles of neighborhood deprivation. Phase 3 included persons with fetal brain anomalies diagnosed antenatally.

We additionally calculated ORs from those significant variables, as well as maternal age and deprivation index (Table 3).

In phase 3, we assessed LCMV seroprevalence among a cohort of pregnant women carrying fetuses with prenatally diagnosed congenital malformations (Figure). We used HPO terms to identify neurologic or ocular malformations discovered prenatally or during an infant's hospital stay. We tested for LCMV IgG in plasma from 37 pregnant women and cord blood samples from their 39 affected children (including 2 sets of twins) from June 1, 2019–June 1, 2023. Malformations included microcephaly (n = 17), ventriculomegaly (n = 10), corpus callosum abnormalities (n = 5), encephalocele (n = 2), retinal hemorrhage (n = 2), Dandy-Walker malformation (n = 1), absent septum pellucidum (n = 1), and posterior fossa cyst (n = 1). None of the samples from the 37 pregnant women or their 39 children were seropositive for LCMV IgG (Table 1; Figure); therefore, we did not test for IgM levels.

Discussion

In this study of LCMV seroprevalence among a large and contemporary cohort of pregnant women in Philadelphia, we found that ≈2%–3% had evidence of exposure to the virus on the basis of detectable LCMV IgG. None of the seropositive samples had confirmed LCMV IgM, and cord blood samples from seropositive cases all had detectable LCMV IgG but no detectable LCMV IgM. Those findings suggest that ≈2–3 of 100 pregnant women in Philadelphia had past exposure to LCMV, although none had acute infection at the time of blood sample collection. The results also are consistent with passive antibody transfer from exposed pregnant women to their newborns because all cord blood samples from seropositive patients were also IgG positive. Our data provide insights into exposure of a large

random sample of pregnant women and a targeted sample of high-risk pregnant women to a high-consequence and underrecognized congenital pathogen.

The seroprevalence estimates from this study align with data from other LCMV seroprevalence reports in the United States and worldwide (*8*). The largest prior LCMV serosurvey was conducted 35 years ago in urban Baltimore (*9*). That study included 1,149 persons who sought care at a sexually transmitted infections clinic. Among that patient cohort, 94% were African American (*9*), but pregnancy status was not reported. In that study, 54/1,149 (4.7%) patients were IgG seropositive (*9*), a modestly higher percentage than in our study. Those differences might be explained by differences in rodent exposure risk between the Baltimore and Philadelphia study populations or differences in LCMV carrier rates among mice in Baltimore versus Philadelphia during the study periods. Philadelphia is the sixth-largest US city and has >1.5 million inhabitants and ≈19,000 births annually (*22*). If our estimate of LCMV seroprevalence among pregnant women is generalizable to the overall population of Philadelphia, we can extrapolate that nearly 30,000–45,000 persons have been exposed to LCMV, including 400–600 pregnant women. Those data support that exposure to rodents shedding LCMV is common. Therefore, we support developing guidance for pregnant women to avoid rodent excreta to the extent possible, given risks of severe congenital disease, which can range from neurologic and ocular malformations to hydrops and fetal or neonatal death (*6*,*7*). Similar guidance is already in place to minimize risk of contracting other congenital pathogens, including *Listeria*, cytomegalovirus, *Toxoplasma*, *Treponema*, rubella, varicella, Zika, and others (*23*).

Although we hypothesized that residents in census tracts with higher neighborhood deprivation would have higher rates of LCMV seroprevalence

Table 2. Demographic and clinical characteristics of maternal patients in a study of lymphocytic choriomeningitis virus seroprevalence among urban pregnant women and newborns, Philadelphia, Pennsylvania, USA, 2021*

Characteristic	No. seropositive (%) [95% CI]	p value
Maternal age range, y		
14–23, n = 246	4 (1.6) [0.44–4.11]	0.2488
24–34, n = 570	19 (3.3) [2.02–5.16]	Referent
35–49, n = 184	2 (1.1) [0.13–3.87]	0.1268
Prepregnancy BMI†		
Underweight, BMI <18.5, n = 26	0 [0–10.88]	NA
Normal, BMI 18.5 to <25.0, n = 332	4 (1.2) [0.33–3.06]	0.3344
Overweight, BMI 25.0 to <30.0, n = 240	6 (2.5) [0.92–5.36]	Referent
Obese, BMI ≥30.0, n = 381	14 (3.7) [2.02–6.09]	0.4905
Group B *Streptococcus* status		
Positive, n = 295	4 (1.4) [0.37–3.43]	0.1695
Negative, n = 593	17 (2.9) [1.68–4.55]	Referent
Unknown, n = 112	4 (3.6) [0.98–8.89]	0.7600
Live-born infant		
Y, n = 995	25 (2.5) [1.63–3.69]	Referent
N, n = 5	0 [0–45.07]	NA
Gestational age at delivery		
<37 weeks, n = 108	3 (2.8) [0.58–7.90]	0.7836
≥37 weeks, n = 892	22 (2.5) [1.55–3.71]	Referent
Birth hospital		
Pennsylvania Hospital, n = 504	17 (3.4) [1.98–5.35]	Referent
Hospital of the University of Pennsylvania, n = 496	8 (1.6) [0.70–3.15]	0.1036
Race‡		
Black, n = 655	22 (3.3) [2.12–5.04]	Referent
White, n = 243	1 (0.4) [0.01–2.27]	0.0086
Other, n = 86	1 (1.2) [0.03–6.31]	0.7154
Ethnicity§		
Hispanic, n = 153	7 (2.9) [1.17–5.84]	Referent
Non-Hispanic, n = 837	16 (1.9) [1.10–3.09]	0.0712
Neighborhood deprivation¶		
Q1, least deprived, n = 75	0 [0–3.92]	0.2406
Q2, n = 75	2 (2.7) [0.32–9.30]	1.0
Q3, n = 75	2 (2.7) [0.32–9.30]	1.0
Q4, most deprived, n = 75	21 (2.7) [1.68–4.11]	Referent

*BMI, body mass index; NA, not applicable.
†Excludes 21 unknown, of which 1 was positive (not represented in table).
‡Excludes 16 unknown, of which 1 was positive (not represented in table).
§Excludes 10 unknown, of which 2 were positive (not represented in table).
¶Neighborhood deprivation at the census tract level calculated by using the Community Deprivation Index (*17*,*18*). Scores are divided into 4 quartiles from least deprived (Q1) to most deprived (Q4). Scores are as follows: Q1 is <0.324; Q2 is 0.324–0.449; Q3 is 0.45–0.579; and Q4 is >0.58.

compared with the random sample, that was not the case. We did not find a statistically significant difference between deprivation index quartiles, but the quartile with the least deprivation had zero seropositive samples identified among the 75 tested samples (Table 2). We acknowledge that census tract–level data might not accurately reflect a person's risk for exposure to LCMV-infected rodents. Of note, the difference in seropositivity between the 2 hospitals might be explained by potential demographic and socioeconomic differences in the populations served. Larger cohorts, including patients and samples from multiple urban and rural areas, are needed to fully determine the relationship between specific housing and neighborhood characteristics and risk for LCMV exposure.

None of the cases of congenital neurologic malformations in phase 3 of this study appear to have been related to congenital LCMV infection, most likely because of the small sample size of infants with a variety of congenital neurologic malformations. None of those infants exhibited chorioretinitis, which is the common clinical feature among all reported live-born cases of congenital LCMV (*6*). Although the sensitivity of chorioretinitis in congenital LCMV remains to be determined in larger studies, we recommend that all infants with congenital neurologic malformations receive a thorough retinal exam and that those with evidence of chorioretinitis then be evaluated for LCMV antibodies. Larger cohorts of samples from affected newborns are needed to more accurately estimate the effects of LCMV infection during pregnancy on the fetus. In addition, prospective sampling of women before and during pregnancy will be required to associate seroconversion more definitively with adverse fetal outcomes. Efforts to increase awareness of LCMV infection during pregnancy and to educate clinicians about LCMV are warranted because of the potential for this virus to cause fetal neurologic disease.

Strengths of this study include the relatively large sample size of phases 1 and 2, identification of 3 populations of interest, and use of a detailed serologic testing strategy devised in collaboration with experts from CDC. The first limitation of this study is that using remnant samples could introduce selection bias; however, of the 9,502 deliveries from Pennsylvania Hospital and Hospital of the University of Pennsylvania in 2021, maternal samples were available for ≈8,739 (92%). Second, including samples from pregnant women residing in single urban area in a single year might mean results are not generalizable to other populations or later timeframes; however, LCMV seroprevalence would not be expected to change substantially within the same geographic area over short time intervals. Third, we used deprivation index data from 2018, and that temporal mismatch could lead to misclassification error. Fourth, we did not test all maternal samples for IgM in the absence of IgG, meaning that very early maternal infection might not have been detected. Finally, the CHOP Birth Defects Biorepository contained limited maternal and cord blood samples, leading us to test only for IgG in cord blood samples from infants born with congenital neurologic malformations and their respective maternal samples. In a prior case series, IgG titers were unequivocally positive at birth in infants with diagnosed congenital LCMV, and IgM might be absent in neonates. Although we did not definitively rule out early infection in this cohort, we do not suspect congenital LCMV in the absence of pathognomonic chorioretinitis and IgG seropositivity. Future prospective studies should be undertaken to clarify LCMV transmission dynamics and fetal risks among additional urban and rural populations to best inform clinical and preventive guidance.

In conclusion, our findings confirm the ongoing exposure of urban dwellers to LCMV and demonstrate the potential for maternal-to-fetal transfer of LCMV IgG. Our data update decades-old US prevalence estimates and highlight a continued risk of

Table 3. Factors associated with maternal seroprevalence in a study of lymphocytic choriomeningitis virus seroprevalence among urban pregnant women and newborns, Philadelphia, Pennsylvania, USA, 2021*

Characteristic	Odds ratio (95% CI)
Maternal age range, y	
14–23	0.4793 (0.1614–1.4239)
24–34	Referent
35–49	0.3187 (0.0735–1.3814)
Birth hospital†	
Pennsylvania Hospital	2.1294 (0.9104–4.9802)
Hospital of the University of Pennsylvania	Referent
Race†	
Black	8.4107 (1.1275–62.7395)
White	Referent
Other	2.8471 (0.1761–46.0206)
Ethnicity†	
Hispanic	2.4602 (0.9948–6.0842)
Non-Hispanic	Referent
Neighborhood deprivation‡	
Q1, least deprived	NA§
Q2	0.9837 (0.2261–4.279)
Q3	0.9837 (0.2261–4.279)
Q4, most deprived	Referent

*NA, not applicable.
†Statistically significant variable in final analysis of variance model.
‡Neighborhood deprivation at the census tract level calculated by using the Community Deprivation Index (*17*,*18*). Scores are divided into 4 quartiles from least deprived (Q1) to most deprived (Q4). Scores are as follows: Q1 is <0.324; Q2 is 0.324–0.449; Q3 is 0.45–0.579; and Q4 is >0.58.
§NA indicates that no positive results were recorded within Q1, resulting in this odds ratio being undefined.

rodentborne virus exposure during pregnancy. Given LCMV's potential to cause severe congenital disease, targeted public health messaging could help prevent exposure during pregnancy, especially in high-risk communities. We believe that LCMV risk should be included in standard education about congenital infections and that pregnant women and clinicians should be made aware of risks associated with LCMV infection during pregnancy.

Acknowledgments

We thank our colleagues from the Philadelphia Department of Health, the Pennsylvania Department of Health, and the Viral Special Pathogens Branch, Division of High-Consequence Pathogens and Pathology, National Center for Emerging and Zoonotic Infectious Diseases, CDC, for their support of this study. We thank Madhavi Sriram at CDC for assistance establishing the interinstitutional Research Collaboration Agreement for this study. We thank Janine McNelia (data analyst) and Donna Stephan (abstractionist) for assistance pulling and reviewing data from the Children's Hospital of Philadelphia Birth Defects Biorepository.

Dr. Flannery reports receiving K08 funding from the Agency for Healthcare Research and Quality. Dr. Gordon reports receiving K08 funding from the National Institute of Allergy and Infectious Diseases.

About the Author

Dr. Flannery is an attending neonatologist and an assistant professor of pediatrics at the Children's Hospital of Philadelphia and the University of Pennsylvania Perelman School of Medicine, Philadelphia, Pennsylvania, USA. His primary research interests include perinatal infection epidemiology, with an emphasis on neonatal early-onset sepsis and antimicrobial stewardship. Dr. Cossaboom is a veterinary epidemiologist in the Division of High-Consequence Pathogens and Pathology, National Center for Emerging and Zoonotic Infectious Diseases, CDC, Atlanta, Georgia, USA. Her primary research interests include epidemiology and outbreak response for zoonotic diseases of public health importance.

References

1. Bonthius DJ. Lymphocytic choriomeningitis virus: an underrecognized cause of neurologic disease in the fetus, child, and adult. Semin Pediatr Neurol. 2012;19:89–95. https://doi.org/10.1016/j.spen.2012.02.002
2. Childs JE, Glass GE, Korch GW, Ksiazek TG, Leduc JW. Lymphocytic choriomeningitis virus infection and house mouse (*Mus musculus*) distribution in urban Baltimore. Am J Trop Med Hyg. 1992;47:27–34. https://doi.org/10.4269/ajtmh.1992.47.27
3. Childs JE, Klein SL, Glass GE. A case study of two rodent-borne viruses: not always the same old suspects. Front Ecol Evol. 2019;7:35–55. https://doi.org/10.3389/fevo.2019.00035
4. Fischer SA, Graham MB, Kuehnert MJ, Kotton CN, Srinivasan A, Marty FM, et al.; LCMV in Transplant Recipients Investigation Team. Transmission of lymphocytic choriomeningitis virus by organ transplantation. N Engl J Med. 2006;354:2235–49. https://doi.org/10.1056/NEJMoa053240
5. Bonthius DJ. Lymphocytic choriomeningitis virus: a prenatal and postnatal threat. Adv Pediatr. 2009;56:75–86. https://doi.org/10.1016/j.yapd.2009.08.007
6. Bonthius DJ, Wright R, Tseng B, Barton L, Marco E, Karacay B, et al. Congenital lymphocytic choriomeningitis virus infection: spectrum of disease. Ann Neurol. 2007;62:347–55. https://doi.org/10.1002/ana.21161
7. Meritet JF, Krivine A, Lewin F, Poissonnier MH, Poizat R, Loget P, et al. A case of congenital lymphocytic choriomeningitis virus (LCMV) infection revealed by hydrops fetalis. Prenat Diagn. 2009;29:626–7. https://doi.org/10.1002/pd.2240
8. Olivieri NR, Othman L, Flannery DD, Gordon SM. Transmission, seroprevalence, and maternal-fetal impact of lymphocytic choriomeningitis virus. Pediatr Res. 2024;95:456–63. https://doi.org/10.1038/s41390-023-02859-w
9. Childs JE, Glass GE, Ksiazek TG, Rossi CA, Barrera Oro JG, Leduc JW. Human-rodent contact and infection with lymphocytic choriomeningitis and Seoul viruses in an inner-city population. Am J Trop Med Hyg. 1991;44:117–21. https://doi.org/10.4269/ajtmh.1991.44.117
10. Stephensen CB, Blount SR, Lanford RE, Holmes KV, Montali RJ, Fleenor ME, et al. Prevalence of serum antibodies against lymphocytic choriomeningitis virus in selected populations from two U.S. cities. J Med Virol. 1992;38:27–31. https://doi.org/10.1002/jmv.1890380107
11. Kooshavar D, Amor DJ, Boggs K, Baker N, Barnett C, de Silva MG, et al. Diagnostic utility of exome sequencing followed by research reanalysis in human brain malformations. Brain Commun. 2024;6:fcae056. https://doi.org/10.1093/braincomms/fcae056
12. Srivastava S, Cohen JS, Vernon H, Barañano K, McClellan R, Jamal L, et al. Clinical whole exome sequencing in child neurology practice. Ann Neurol. 2014;76:473–83. https://doi.org/10.1002/ana.24251
13. Mets MB, Barton LL, Khan AS, Ksiazek TG. Lymphocytic choriomeningitis virus: an underdiagnosed cause of congenital chorioretinitis. Am J Ophthalmol. 2000;130:209–15. https://doi.org/10.1016/S0002-9394(00)00570-5
14. American College of Obstetricians & Gynecologists. Screening for syphilis in pregnancy [cited 2024 Sep 27]. https://www.acog.org/clinical/clinical-guidance/practice-advisory/articles/2024/04/screening-for-syphilis-in-pregnancy
15. Chew GL, Perzanowski MS, Miller RL, Correa JC, Hoepner LA, Jusino CM, et al. Distribution and determinants of mouse allergen exposure in low-income New York City apartments. Environ Health Perspect. 2003;111:1348–51. https://doi.org/10.1289/ehp.6124
16. Brokamp C, Beck AF, Goyal NK, Ryan P, Greenberg JM, Hall ES. Material community deprivation and hospital utilization during the first year of life: an urban population-based cohort study. Ann Epidemiol. 2019;30:37–43. https://doi.org/10.1016/j.annepidem.2018.11.008
17. Brokamp C, Wolfe C, Lingren T, Harley J, Ryan P. Decentralized and reproducible geocoding and

characterization of community and environmental exposures for multisite studies. J Am Med Inform Assoc. 2018;25:309–14. https://doi.org/10.1093/jamia/ocx128
18. Brokamp C, Rasnick Manning E. A nationwide community deprivation index [cited 2025 Jan 31]. https://github.com/geomarker-io/dep_index
19. Gargano MA, Matentzoglu N, Coleman B, Addo-Lartey EB, Anagnostopoulos AV, Anderton J, et al. The Human Phenotype Ontology in 2024: phenotypes around the world. Nucleic Acids Res. 2024;52(D1):D1333–46. https://doi.org/10.1093/nar/gkad1005
20. Park JY, Peters CJ, Rollin PE, Ksiazek TG, Katholi CR, Waites KB, et al. Age distribution of lymphocytic choriomeningitis virus serum antibody in Birmingham, Alabama: evidence of a decreased risk of infection. Am J Trop Med Hyg. 1997;57:37–41. https://doi.org/10.4269/ajtmh.1997.57.37
21. Dyal J, Gandhi S, Cossaboom CM, Leach A, Patel K, Golden M, et al. Lymphocytic choriomeningitis virus in person living with HIV, Connecticut, USA, 2021. Emerg Infect Dis. 2023;29:1886–9. https://doi.org/10.3201/eid2909.230087
22. Philadelphia Department of Public Health. PhilaStats [cited 2025 Jann 10]. https://philadelphiapublichealth.shinyapps.io/philastats
23. American College of Obstetricians & Gynecologists. Reducing risks of birth defects [cited 2025 Mar 31]. https://www.acog.org/womens-health/faqs/reducing-risks-of-birth-defects

Address for correspondence: Dustin D. Flannery, Children's Hospital of Philadelphia Newborn Care, 800 Spruce St, Philadelphia, PA 19107, USA; email: flanneryd@chop.edu

Projected Effects of Changing Global Tuberculosis Epidemiology on *Mycobacterium tuberculosis* Immunoreactivity Prevalence, 2024–2050

Michelle Machado, Aria Ed Jordan, Alvaro Schwalb, Rein M.G.J. Houben, Peter J. Dodd, Katie Dale, Kevin Schwartzman, Jonathon R. Campbell

We assessed how evolving global tuberculosis (TB) trends might influence *Mycobacterium tuberculosis* immunoreactivity and TB risk among persons immigrating to low-incidence countries. We projected annual risk for infection (ARI) in 168 countries for 2024–2050, focusing on China, India, the Philippines, and Vietnam. We applied projections to the age profile of immigrants to 4 low-incidence countries to estimate changes in *M. tuberculosis* immunoreactivity prevalence and TB risk under status quo and accelerated ARI decline scenarios. In the status quo 2024 estimate, *M. tuberculosis* immunoreactivity prevalence ranged from 14.7% in China to 40.1% in the Philippines, declining to 5.8% in China and 23.0% in the Philippines by 2050; TB risk also declined. Accelerated ARI reductions yielded greater relative decreases in disease risk than immunoreactivity prevalence. Declining global TB incidence could reduce *M. tuberculosis* immunoreactivity and disease risk among immigrant populations, which could inform cost–benefit analyses for future TB screening strategies in low-incidence settings.

Tuberculosis (TB) remains a major global public health challenge. In 2024, an estimated 10.7 million persons had TB develop, and ≈1.23 million persons died (*1*). TB, caused by *Mycobacterium tuberculosis*, begins as an asymptomatic infection but can progress to infectious disease at any time (*2*). Among persons with evidence of *M. tuberculosis* infection, risk of developing TB is highest in the first 2 years after infection (*3*). Persons with evidence of *M. tuberculosis* infection go through a short high-risk period, followed by a prolonged low-risk period (*1*–*3*).

M. tuberculosis infection is diagnosed by absence of clinical findings indicating TB disease, plus immunoreactivity to *M. tuberculosis* antigens measured by skin tests or interferon-γ release assays (*4*,*5*). Immunoreactivity can exhibit reversion (*6*) but is assumed to be lifelong for many infected persons. Immunoreactivity tests cannot distinguish persons at high risk for TB progression (i.e., recently infected [≤2 years]) from those at low risk (i.e., remotely infected [>2 years]). The number of recently infected versus remotely infected persons will vary by local epidemiology, driven by the force of *M. tuberculosis* transmission.

In many low-incidence countries, TB disproportionately affects immigrant populations, largely because of progression of *M. tuberculosis* infection acquired in higher transmission settings before immigration. For that reason, several countries have

Author affiliations: McGill University, Montreal, Quebec, Canada (M. Machado, K. Schwartzman, J.R. Campbell); University of Minnesota Foundation, Minneapolis, Minnesota, USA (A.E. Jordan); Instituto de Medicina Tropical Alexander von Humboldt, Universidad Peruana Cayetano Heredia, Lima, Peru (A. Schwalb); TB Modelling Group, TB Centre, London School of Hygiene and Tropical Medicine, London, UK (A. Schwalb, R.M.G.J. Houben); Sheffield Centre for Health and Related Research, School of Medicine and Population Health, University of Sheffield, Sheffield, UK (P.J. Dodd); Victorian Tuberculosis Program, Royal Melbourne Hospital, at the Peter Doherty Institute for Infection and Immunity, Melbourne, Victoria, Australia (K. Dale); The University of Melbourne, at the Peter Doherty Institute for Infection and Immunity, Melbourne (K. Dale); McGill International TB Centre, Montreal (K. Schwartzman, J.R. Campbell); Centre for Outcomes Research and Evaluation, Research Institute of the McGill University Health Centre, Montreal (K. Schwartzman, J.R. Campbell)

DOI: https://doi.org/10.3201/eid3203.251340

implemented or considered large-scale *M. tuberculosis* infection screening and treatment programs among new immigrants (*7*,*8*). Critical to the cost-effectiveness of those programs are *M. tuberculosis* immunoreactivity prevalence and the likelihood of subsequent TB disease (*9*). TB risk is directly correlated with the percentage of recently infected persons; thus, understanding how changing TB epidemiology affects immunoreactivity prevalence and percentages of persons recently or remotely infected can have implications for cost-effectiveness and efficiency of TB programs.

In this study, we aimed to gain insights into how changing TB epidemiology would affect the *M. tuberculosis* immunoreactivity prevalence and risk for developing TB disease among new immigrants to low-incidence countries. Using the age distribution of new immigrants to 4 immigrant-receiving low-incidence countries, we estimated temporal changes in the overall *M. tuberculosis* immunoreactivity prevalence and risk for progression to TB disease in the year of arrival among immigrants from 168 countries. We focused on immigrants from 4 moderate- to high-incidence countries, India, China, the Philippines, and Vietnam, and modeled how further changes in *M. tuberculosis* transmission could affect those outcomes for 2024–2050.

Methods

Countries Evaluated

For this analysis, we considered persons immigrating from 168 countries (Appendix Table 1, https://wwwnc.cdc.gov/EID/article/32/3/25-1340-App1.pdf). Of those, we selected 4 moderate- to high-incidence countries (annual TB incidence ≥50/100,000 population) to examine more closely: China, India, the Philippines, and Vietnam. We selected those countries because all 4 are common countries of origin for immigrants moving to 4 common immigrant-receiving countries. In 2023, those 4 countries combined accounted for 54% of new immigrants to Canada, 19% to the United States, 12% to the United Kingdom, and 47% to Australia (*10*–*13*).

Annual Risk for *M. tuberculosis* Infection Measured by Immunoreactivity

The diagnosis of *M. tuberculosis* infection is based on immunoreactivity to skin tests or interferon-γ release assays and cannot be empirically confirmed; thus, we focused on immunoreactivity. We estimated the annual risk for infection (ARI), which is the probability that in a given year someone will become *M. tuberculosis* immunoreactive, by leveraging methods and estimates generated for a previously published analysis (*14*). Estimates included 200 different ARI projections from 1889–2021. When available, we used historical tuberculin skin test surveys as the basis for ARI; in all other instances, we estimated ARI by using a modified Styblo rule, which relates the prevalence of smear-positive TB disease to the ARI. In both methods, ARI is related to measured immunoreactivity prevalence, and immunoreactivity is assumed to be lifelong. To estimate ARI beyond 2021, we estimated the average annual change in ARI during 2000–2021 and projected the same annual change from 2022 to 2050 for each country and ARI projection.

Estimation of *M. tuberculosis* Immunoreactivity Prevalence

To estimate *M. tuberculosis* immunoreactivity prevalence, we adapted methods from a previously published study modeling immunoreactivity prevalence among foreign-born residents of Canada (*14*). In brief, we calculated the cumulative probability of *M. tuberculosis* immunoreactivity by integrating the ARI over time stratified by country of origin, year of birth, and year of migration. We applied annual ARI values sequentially up to each time point, assuming independent infection risk from year to year.

For each country, we used the 200 ARI trajectories estimated for 2024 to 2050 to generate 200 corresponding estimates of immunoreactivity prevalence for each year of migration and year of birth. We then applied those estimates to the age distribution of new immigrants from 4 immigrant-receiving low-incidence countries, to attain estimates of overall immunoreactivity prevalence for each year. Similarly, we used those same ARI trajectories to estimate the prevalence of recently acquired *M. tuberculosis* immunoreactivity (i.e., persons who became immunoreactive ≤2 years), using the ARI over a 2-year period. We selected a 2-year period for recent immunoreactivity because that timeframe corresponds to the highest risk period for progression to TB (*3*,*5*,*15*).

Projections of *M. tuberculosis* Immunoreactivity Prevalence and TB Risk

To estimate the age distribution of immigrants, we analyzed immigration data from Canada, the United States, the United Kingdom, and Australia, which detail the demographic characteristics of new immigrants each year (Appendix). We categorized those values into 6 age ranges: 0–14, 15–29, 30–44, 45–59, 60–74, and ≥75 years (*16*). We assumed the age distribution was the same for each country of origin and that specific ages were equally distributed within each range.

To project the age distribution into the future, we calculated the mean percentage and SD of new immigrants belonging to each age group in the most recent year from which data were available (2023–2024) across countries by using equal weighting and assumed that distribution remained stable from 2024 to 2050. We fit each age category to a β distribution (Appendix Table 2), and generated 200 sets of age distribution estimates, scaling values to ensure each set summed to 100%. Therefore, we estimated that, of all new immigrants, 16.4% (95% uncertainty interval [UI] 10.3%–24.9%) would be 0–14 years of age, 25.2% (95% UI 14.4%–36.8%) would be 15–29 years of age, 34.5% (95% UI 24.4%–47.0%) would be 30–44 years of age, 15.3% (95% UI 8.5%–24.8%) would be 45–59 years of age, 6.3% (95% UI 2.7%–11.4%) would be 60–74 years of age, and 1% (95% UI 0.3%–2.5%) would be ≥75 years of age at the time of immigration.

For each year during 2024–2050, we used each of the 200 ARI trajectories to estimate the overall *M. tuberculosis* immunoreactivity prevalence among persons immigrating from each country, as well as the acquired immunoreactivity prevalence in the previous 2 years under a status quo scenario (i.e., no change in projected ARI trajectories). Using the projections of overall and recent *M. tuberculosis* immunoreactivity, we estimated the average annual TB incidence in the year of arrival among new immigrants overall from each country, as well as the TB incidence in the year of arrival restricted to those with underlying *M. tuberculosis* immunoreactivity.

To estimate risk for TB progression, we assumed that the annual risk for TB progression for persons who recently acquired immunoreactivity was similar to that estimated in a large systematic review of TB risk among contacts (*17*). For persons with remotely (>2 years before immigration) acquired immunoreactivity, we based estimates on observed TB incidence data in Canada (Appendix). We used those data sources to fit risks to lognormal distributions (Appendix) and generated 200 estimates, which resulted in estimates of TB risk in the year of arrival at 1.7% (95% UI 1.3%–2.2%) among persons with recent *M. tuberculosis* immunoreactivity and at 0.07% (95% UI 0.06%–0.09%) among persons with remote *M. tuberculosis* immunoreactivity.

To assess how reducing *M. tuberculosis* transmission would affect each of those outcomes, we modeled 3 different scenarios in which we reduced the ARI trajectories in our status quo projections beginning in 2025 to an absolute 1% additional reduction, 3% additional reduction, and 5% additional reduction in ARI. For example, if the status quo scenario had an estimated annual relative ARI decrease of 3% for a given country, we modeled scenarios in which the relative ARI decrease was 4%, 6%, or 8% annually. We calculated absolute and relative reductions by comparing each reduction scenario to the status quo. We stratified data by country and by age groups to identify trends and differences in estimates among strata.

We conducted a sensitivity analysis in which we loosened our assumption that *M. tuberculosis* immunoreactivity was lifelong, allowing for reversion (*6*,*18*). Because our ARI estimates are based on measured immunoreactivity, if reversion occurred, we would estimate the same level of overall measured immunoreactivity prevalence, but ARI would necessarily need to be higher to achieve that prevalence. Using those higher ARIs, recently acquired immunoreactivity prevalence would increase. Therefore, to maintain observed levels of immunoreactivity in our sensitivity analysis, we estimated the attendant increase in the ARI assuming an annual reversion rate of 10%, per previously described data (*18*,*19*). Thus, considering reversion was equivalent to a 2.9-fold increase in ARI, and we used that assumption to reestimate the prevalence of recently acquired immunoreactivity and the average annual risk for TB progression for the years 2024–2050.

We reported estimates as medians and 95% UIs (2.5th and 97.5th percentiles) across the 200 ARI trajectories. We compared outputs of *M. tuberculosis* immunoreactivity prevalence and TB disease risk to previous estimates for face validity (Appendix). We conducted all analyses in R version 4.3.1 (The R Project for Statistical Computing, https://www.r-project.org). We performed preliminary data organization and cleaning using Excel 2024 (Microsoft, https://www.microsoft.com). We created graphic representations using the ggplot2 package version 3.5.1 (https://github.com/cran/ggplot2) and GraphPad (GraphPad Software Inc., https://www.graphpad.com). This study used publicly available deidentified, aggregate data, and did not include personal identifiers in any data analyzed; thus, approval from a research ethics board was not required.

Results

Estimated Changes in ARI

We estimated the Philippines would have the highest 2024 ARI at 0.98% (95% UI 0.46%–2.2%), followed by India at 0.48% (95% UI 0.24%–0.95%), Vietnam at 0.41% (95% UI 0.13%–1.20%), and China at 0.19% (95% UI 0.08%–0.47%) (Table 1; Appendix Figure 1). Across all 4 countries, the estimated ARI generally

Table 1. Projected annual risk for infection in a study of global tuberculosis epidemiology on *Mycobacterium tuberculosis* and immunoreactivity prevalence, 2024–2050*

	Status quo ARI, % (95% UI)		2050 ARI, % (95% UI), under additional ARI reduction scenarios		
Country	2024	2050	Additional 1% reduction	Additional 3% reduction	Additional 5% reduction
China	0.19 (0.08–0.47)	0.07 (0.01–0.47)	0.05 (0.01–0.35)	0.03 (0.01–0.19)	0.02 (0–0.11)
India	0.48 (0.24–0.95)	0.17 (0.04–0.98)	0.13 (0.03–0.74)	0.07 (0.01–0.41)	0.04 (0.01–0.22)
Philippines	0.98 (0.46–2.2)	0.44 (0.08–2.7)	0.32 (0.06–2.0)	0.18 (0.03–1.1)	0.09 (0.02–0.62)
Vietnam	0.41 (0.13–1.2)	0.16 (0.01–1.7)	0.12 (0.01–1.3)	0.06 (0.01–0.70)	0.03 (0–0.38)

*Analysis of percentage ARI under the status quo scenario and 3 scenarios of additional ARI reduction of 1%, 3%, and 5%. ARI, annual risk for infection; UI, uncertainty interval.

declined during 2000–2021, although in all countries except India, a small number of trajectories projected increases. Specifically, we estimated the ARI would fall at a relative rate of 3.8% per year (95% UI 7.3% decline to 0.2% increase) in China, 4.1% per year (95% UI 7.1% decline to 0.2% decline) in India, 3.1% per year (95% UI 7.1% decline to 0.7% increase) in the Philippines, and 3.8% per year (95% UI 8.8% decline to 1.6% increase) in Vietnam. Following those projections, compared with 2024, the 2050 ARI was 61.8% lower (95% UI 84.7% lower to 5.0% higher) in China, 64.7% lower (95% UI 84.0% lower to 5.5% higher) in India, 53.8% lower (95% UI 83.9% lower to 19.5% higher) in the Philippines, and 61.6% lower (95% UI 89.7% lower to 46.8% higher) in Vietnam. We also calculated ARI trends for all 168 countries (Appendix Table 3).

Projected Changes in Immunoreactivity Prevalence

In general, declining ARI trends translated into reductions in the point estimates of immunoreactivity prevalence among immigrant populations from China, India, the Philippines, and Vietnam. In 2024, we estimated prevalence among new immigrants from each country to be 14.7% (95% UI 10.7%–22.7%) for China, 25.4% (95% UI 20.4%–30.8%) for India, 40.1% (95% UI 32.6%–49.8%) for the Philippines, and 27.7% (95% UI 19.5%–41.2%) for Vietnam (Figure 1). By 2050, we projected prevalence would decrease to 5.8% (95% UI 3.4%–13.5%) for China, 13.2% (95% UI 7.7%–26.2%) for India, 23.0% (95% UI 14.3%–48.5%) for the Philippines, and 11.7% (95% UI 6.9%–30.5%) for Vietnam (Appendix Tables 4, 5).

The prevalence of recent immunoreactivity remained relatively stable over time in the status quo scenario. By 2050, we projected the prevalence of recently acquired immunoreactivity would be 0.14% (95% UI 0.03%–0.78%) for China, 0.30% (95% UI 0.07%–1.40%) for India, 0.67% (95% UI 0.14%–2.6%) for the Philippines, and 0.28% (95% UI 0.03%–2.1%) for Vietnam (Appendix Table 6). In our reversion sensitivity analysis, corresponding estimates in 2050 were 0.4% (95% UI 0.08%–2.3%) for China, 0.86% (95% UI 0.21%–4.1%) for India, 1.9% (95% UI 0.41%–7.4%) for the Philippines, and 0.80% (95% UI 0.08%–6.0%) for Vietnam (Appendix Table 6).

Increasing the rate of ARI decline had modest effects on the absolute decline in immunoreactivity prevalence, regardless of the increase in the rate

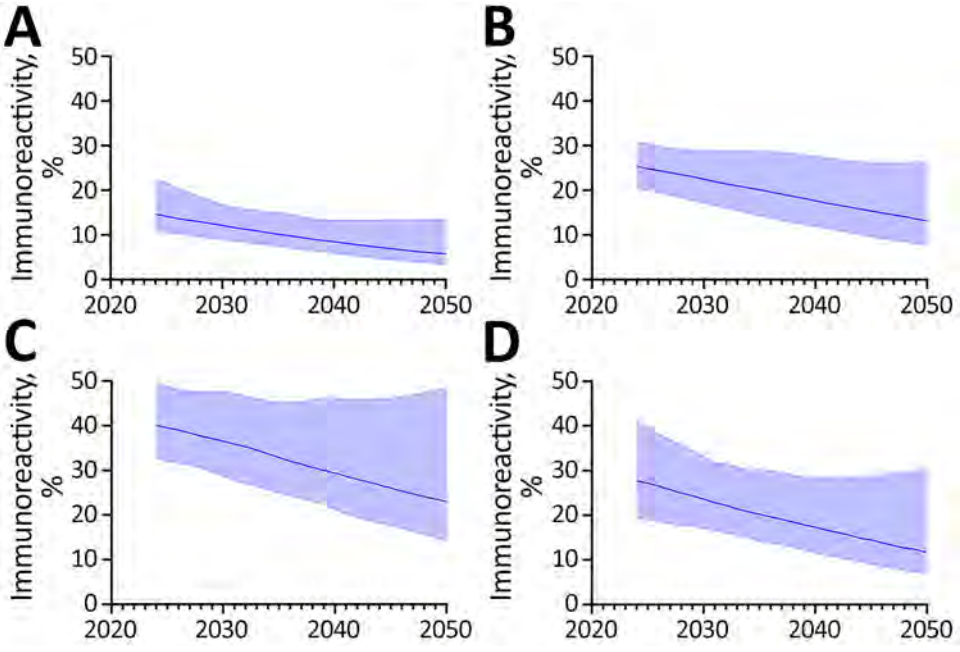

Figure 1. Projected immunoreactivity in study of effects of global tuberculosis epidemiology on *Mycobacterium tuberculosis* immunoreactivity prevalence, 2024–2050. Graphs show projected prevalence of *M. tuberculosis* immunoreactivity prevalence among immigrants from China (A), India (B), the Philippines (C), and Vietnam (D) under the status quo scenario, i.e., assuming continuation of projected annual risk for infection trends without additional reduction. Solid lines represent median estimates, and shaded areas indicate 95% uncertainty intervals.

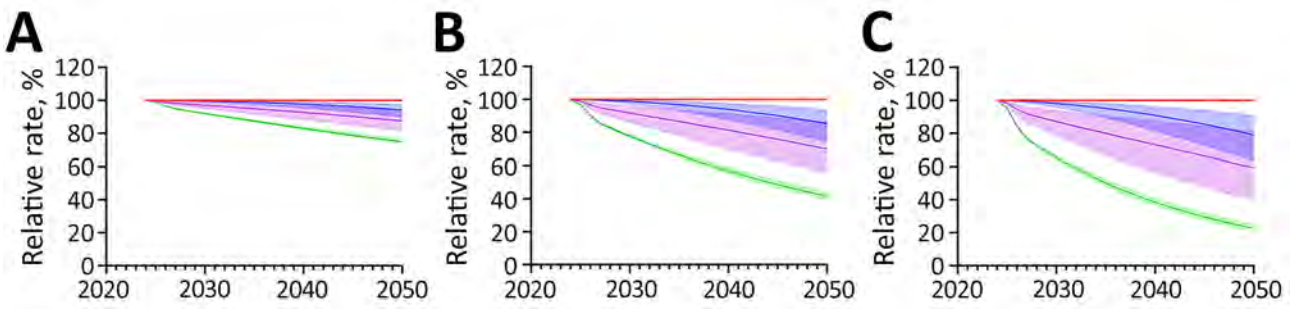

Figure 2. Projected effects on tuberculosis (TB) incidence and *Mycobacterium tuberculosis* immunoreactivity in study of effects of global tuberculosis epidemiology on *M. tuberculosis* immunoreactivity prevalence, 2024–2050. Graphs show effects over time among immigrants from China under 3 scenarios for reduction in annual risk for infection: A) 1% additional reduction; B) 3% additional reduction; C) 5% additional reduction. Solid lines represent median estimates; shaded areas indicate 95% uncertainty intervals. Red line indicates status quo scenario (i.e., no change in percent immunoreactivity or TB incidence); blue indicates overall *M. tuberculosis* immunoreactivity; green indicates recent (≤2 years) *M. tuberculosis* immunoreactivity; and purple indicates TB disease risk in the year of immigration to low-incidence country.

of decline (Appendix Tables 7, 8). We noted much greater effects on the prevalence of recent *M. tuberculosis* immunoreactivity under ARI decline scenarios (Figures 2–5). Under the additional 1% ARI decline scenario, we projected the overall immunoreactivity prevalence across China, India, the Philippines, and Vietnam would decrease by ≈6% by 2050 relative to the status quo scenario. However, recent immunoreactivity prevalence fell more sharply, declining by ≈25%. Under the additional 5% ARI decline scenario, those reductions were more pronounced; overall immunoreactivity prevalence decreased by up to 21%–23%, and recent immunoreactivity prevalence fell by 75%–77% relative to the status quo.

Age-stratified projections revealed that declines in immunoreactivity prevalence varied by age group and had a strong inverse relationship between age and reduction magnitude. Younger cohorts, having experienced fewer cumulative years of exposure, received the largest benefits from reduced ARI. For instance, by 2050 under the additional 3% ARI decline scenario, we projected the immunoreactivity in children 0–14 years of age would fall below 1% among children from China, India, and Vietnam, although it remained slightly above 1% for children from the Philippines. In contrast, older adults retained higher immunoreactivity levels due to prior exposures accumulated over their lifetimes (Appendix Table 9). The most substantial declines occurred in settings with initially high transmission, notably the Philippines and India, where the effects of accelerated ARI reductions were substantial. As expected, the percentage of recently acquired immunoreactivity was highest in the youngest age groups and increased in sensitivity analyses that incorporated reversion (Appendix Tables 10, 11).

Projected Changes in the Average TB Risk

Under the status quo scenario, we estimated overall annual TB incidence per 100,000 new immigrants arriving in 2024 would be 16.4 (95% UI 11.0–24.9) among those from China, 29.7 (95% UI 20.1–47.4) among

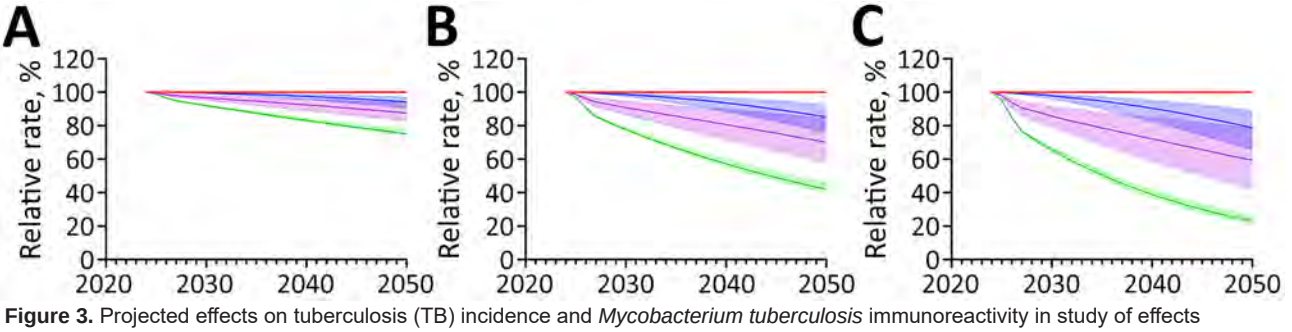

Figure 3. Projected effects on tuberculosis (TB) incidence and *Mycobacterium tuberculosis* immunoreactivity in study of effects of global tuberculosis epidemiology on *M. tuberculosis* immunoreactivity prevalence, 2024–2050. Graphs show effects over time among immigrants from India under 3 scenarios for reduction in annual risk for infection: A) 1% additional reduction; B) 3% additional reduction; C) 5% additional reduction. Solid lines represent median estimates; shaded areas indicate 95% uncertainty intervals. Red line indicates status quo scenario (i.e., no change in percent immunoreactivity or TB incidence); blue indicates overall *M. tuberculosis* immunoreactivity; green indicates recent (≤2 years) *M. tuberculosis* immunoreactivity; and purple indicates TB disease risk in the year of immigration to low-incidence country.

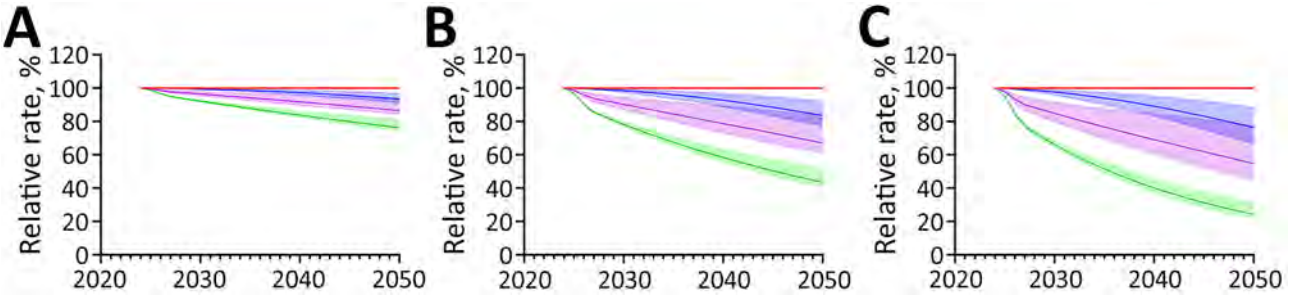

Figure 4. Projected effects on tuberculosis (TB) incidence and *Mycobacterium tuberculosis* immunoreactivity in study of effects of global tuberculosis epidemiology on *M. tuberculosis* immunoreactivity prevalence, 2024–2050. Graphs show effects over time among immigrants from the Philippines under 3 scenarios for reduction in annual risk for infection: A) 1% additional reduction; B) 3% additional reduction; C) 5% additional reduction. Solid lines represent median estimates; shaded areas indicate 95% uncertainty intervals. Red line indicates status quo scenario (i.e., no change in percent immunoreactivity or TB incidence); blue indicates overall *M. tuberculosis* immunoreactivity; green indicates recent (≤2 years) *M. tuberculosis* immunoreactivity; and purple indicates TB disease risk in the year of immigration to low-incidence country.

those from India, 47.9 (95% UI 34.5–72.0) among those from the Philippines, and 30.2 (95% UI 21.2–47.3) among those from Vietnam. We projected that by 2050 those risks among new immigrants would fall to 6.4 (95% UI 3.0–22.7) among those from China, 14.5 (95% UI 6.8–41.9) among those from India, 27.1 (95% UI 12.2–76.0) among those from the Philippines, and 12.9 (95% UI 5.9–53.9) among those from Vietnam (Table 2; Appendix Table 12). As a result of the higher estimated prevalence of recently acquired immunoreactivity, we estimated TB incidence in the arrival year would be nearly double in sensitivity analyses incorporating immunoreactivity reversion (Table 2; Appendix Tables 13, 14).

Accelerating declines in ARI led to further reductions in TB risk, largely driven by reductions in the prevalence of recently acquired *M. tuberculosis* immunoreactivity (Appendix Figure 2). Under the additional 3% ARI decline scenario, we estimated the annual risk per 100,000 new immigrants arriving in 2050 would be 4.4 (95% UI 2.3–12.7) among those from China, 10.1 (95% UI 5.4–24.2) among those from India, 18.5 (95% UI 9.0–48.7) among those from the Philippines, and 9.1 (95% UI 5.0–32.8) among those from Vietnam (Table 2). As with immunoreactivity prevalence, we noted greater declines in TB risk in younger age categories (Appendix Tables 12, 13). When we estimated TB risk in arrival year only among those with *M. tuberculosis* immunoreactivity, TB risk fell by ≈7% in the additional 1% ARI decline scenario, 18% in the 3% scenario, and 25% in the 5% scenario relative to the status quo (Appendix Table 15).

Discussion

In this study, we found that among 4 countries with moderate to high TB incidence, China, India, the Philippines, and Vietnam, recent trends suggest ARI is falling 2%–3% per year. Accordingly, we projected *M. tuberculosis* immunoreactivity prevalence, a proxy for *M. tuberculosis* infection, and average TB risk would decrease among immigrants from those countries by 2050, and the Philippines would have

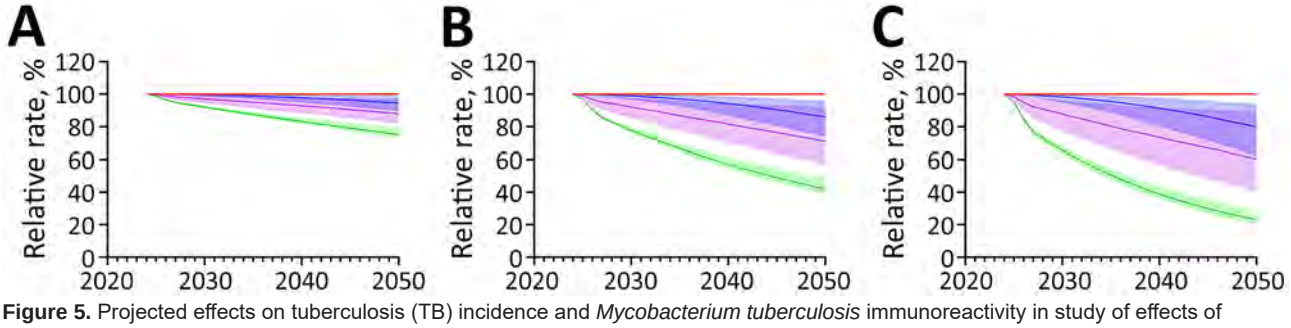

Figure 5. Projected effects on tuberculosis (TB) incidence and *Mycobacterium tuberculosis* immunoreactivity in study of effects of global tuberculosis epidemiology on *M. tuberculosis* immunoreactivity prevalence, 2024–2050. Graphs show effects over time among immigrants from Vietnam under 3 scenarios for additional reduction in annual risk for infection: A) 1% additional reduction; B) 3% additional reduction; C) 5% additional reduction. Solid lines represent median estimates; shaded areas indicate 95% uncertainty intervals. Red line indicates status quo scenario (i.e., no change in percent immunoreactivity or TB incidence); blue indicates overall *M. tuberculosis* immunoreactivity; green indicates recent (≤2 years) *M. tuberculosis* immunoreactivity; and purple indicates TB disease risk in the year of immigration to low-incidence country.

Table 2. Projected annual tuberculosis disease incidence among new immigrants in a study of effects of global tuberculosis epidemiology on *Mycobacterium tuberculosis* immunoreactivity prevalence, 2024–2050*

Country	Status quo incidence (95% UI)		2050 incidence (95% UI) under additional ARI reduction scenarios		
	2024	2050	Additional 1% reduction	Additional 3% reduction	Additional 5% reduction
Primary analysis					
China	16.4 (11.0–24.9)	6.4 (3.0–22.7)	5.5 (2.7–18.6)	4.4 (2.3–12.7)	3.8 (2.1–9.1)
India	29.7 (20.1–47.4)	14.5 (6.8–41.9)	12.7 (6.3–34.7)	10.1 (5.4–24.2)	8.5 (4.9–18.3)
Philippines	47.9 (34.5–72.0)	27.1 (12.2–76.0)	23.5 (11.0–65.6)	18.5 (9.0–48.7)	15.2 (8.1–36.7)
Vietnam	30.2 (21.2–47.3)	12.9 (5.9–53.9)	11.1 (5.5–45.5)	9.1 (5.0–32.8)	7.9 (4.6–24.4)
Sensitivity analysis†					
China	26.0 (16.9–50.2)	10.6 (3.7–48.7)	8.8 (3.4–38.5)	6.2 (2.9–24.1)	4.7 (2.4–15.6)
India	51.1 (30.9–96.4)	23.5 (9.2–86.9)	19.5 (8.1–70.1)	14.2 (6.6–45.8)	10.8 (5.5–30.5)
Philippines	83.7 (51.5–139.5)	48.5 (15.6–149.4)	39.4 (14.0–122.4)	27.5 (11.8–86.5)	20.2 (9.4–61.2)
Vietnam	46.9 (29.4–92.1)	20.8 (7.2–113.0)	17.4 (6.6–92.3)	12.6 (5.6–61.2)	9.6 (5.0–38.6)

*Annual incidence per 100,000 persons under the status quo scenario and 3 scenarios of additional ARI reduction of 1%, 3%, and 5%. ARI, annual risk for infection; UI, uncertainty interval.
†Assuming increased risk for recently acquired *M. tuberculosis* immunoreactivity.

the greatest absolute declines. Accelerating ARI declines, even by modest amounts, had larger relative effects on TB risks compared with *M. tuberculosis* immunoreactivity prevalence, primarily driven by declines in recently acquired immunoreactivity.

The cost-effectiveness of immigration *M. tuberculosis* infection screening and treatment programs is an ongoing area of debate. Some analyses have found such programs to be highly cost-prohibitive (*20*–*22*), but others have found them to be cost-effective compared with traditionally accepted willingness-to-pay thresholds (*23*,*24*). However, the major drivers of the cost effectiveness of any *M. tuberculosis* infection screening program are the underlying prevalence of *M. tuberculosis* immunoreactivity and risk of developing TB. Our analysis projects the cost effectiveness of those programs to generally worsen over time as the immunoreactivity prevalence and risk of developing TB decline. For instance, our estimates showed that, among new immigrants from the Philippines, immunoreactivity prevalence would drop from 40.1% in 2024 to 23.0% in 2050 and TB risk in the year of arrival would fall from 47.9/100,000 immigrants in 2024 to 27.1/100,000 immigrants in 2050. However, those effects are unlikely to be homogenous within and between countries. That finding highlights the need for constant evaluation of TB screening programs where they are implemented (*25*) to ensure efficient use of healthcare funds.

A 2024 modeling study highlighted the potential economic and health benefits of improvements in global TB prevention and care in low-incidence settings (*26*). In line with those findings, we found substantial reductions in the population-level TB risk in scenarios with accelerated ARI declines. We also found that in those scenarios, TB risk declined more rapidly than overall *M. tuberculosis* immunoreactivity prevalence. That finding suggests that, in addition to the overall decline in population-level TB risk, the individual-level risk–benefit calculus of providing TB preventive treatment could change. Therefore, if declines in global TB incidence accelerate in the future, programs would need to anticipate and adapt to those changes, such as by using more targeted approaches to TB screening and treatment.

We found consideration of *M. tuberculosis* immunoreactivity reversion increased estimates of TB disease risks in the year of arrival for new immigrants, driven by higher ARIs and therefore increased prevalence of recently acquired *M. tuberculosis* immunoreactivity. That aspect has been identified by others (*27*). However, cohort data have shown TB risk persists, albeit reduced, among persons who had immunoreactivity reversion, and that reversion might not be stable (i.e., persons reconvert to immunopositive) (*6*). The extent of stable immunoreactivity reversion thus has implications on the value of prompt immunoreactivity testing and treatment after immigration (*28*), when risk for recent exposure would be highest.

Key strengths of this study are the consideration of multiple policy-relevant outcomes, use of previously reported data and methodology to perform the analyses, and consistency of our estimates with existing empiric literature. In addition, we included a breadth of countries and focused on countries comprising a large number of new immigrants to low-incidence countries. We also used uncertainty in several key underlying parameters and explored the effects of underlying assumptions around immunoreactivity reversion.

The first limitation of our study is that our analysis equated *M. tuberculosis* immunoreactivity to infection. Because current technologies to identify *M. tuberculosis* infection rely on immunoreactivity and data underlying TB progression rates reflect observations based on immunoreactivity, that was a reasonable approach. However, our main analysis assumed *M. tuberculosis* immunoreactivity would be lifelong, which

might underestimate prevalence of recently acquired immunoreactivity. Therefore, we evaluated the effect of that assumption in a sensitivity analysis. When we incorporated immunoreactivity reversion, which implies a higher estimated prevalence of recently acquired immunoreactivity, the estimated TB risks increased. Second, we made several simplifying assumptions to focus the analysis on the potential effect of changing infection risks. We projected ARI trends beyond 2021 on the basis of trends from 2000–2021 and used a similar age distribution for immigrants from all countries. Those assumptions might not hold true for all countries if immigration patterns change or if global TB funding is interrupted (*1*,*29*). Third, we did not consider protection from reinfection in our model (*30*), which might lead to slight overestimation of the percentage of persons with recent infection. Fourth, we assumed no heterogeneity in risk for *M. tuberculosis* immunoreactivity or TB progression by demographic, clinical, or other factors among immigrants from each country. We did not explicitly model specific high-risk groups (e.g., persons with HIV) within immigrant cohorts and did not consider immigrants to differ systematically from nonimmigrants within any given country when considering infection or TB progression.

In summary, we found changing global TB epidemiology could lead to reduced *M. tuberculosis* immunoreactivity and TB risk among immigrants to low-incidence countries. Such changes might worsen the cost-effectiveness of *M. tuberculosis* infection screening and treatment programs, requiring further targeting of these programs over time, as well as alter the individual-level balance of risks and benefits of TB preventive treatment.

All code and data underlying the analysis are available at https://github.com/michelle-machado/TB-immigrants-risk-projection/tree/main.

This work was funded by the Canadian Institutes of Health Research (grant nos. PJT-190227 and PJT-173348).

J.R.C. receives salary support from the McGill University Health Centre Foundation and the McGill University Department of Medicine and holds a Chercheur-boursier award from the Fonds de recherche du Québec—Santé (no. 330287 https://doi.org/10.69777/330287).

Author contributions: J.R.C. and K.S. initially conceptualized the study; M.M., A.E.J., and J.R.C. conducted analysis; M.M. and J.R.C. wrote the first draft; and all authors contributed to study development and interpretation and revised the final draft. All authors meet ICMJE criteria for authorship and have seen and approved the final submitted version.

About the Author

Ms. Machado works in health economics and outcomes research McGill University, Montreal, Quebec, Canada. Her research interests focus on generating evidence to support health equity and access to care, particularly among vulnerable populations.

References

1. World Health Organization. Global tuberculosis report 2025. Geneva: The Organization; 2025.
2. Trajman A, Campbell JR, Kunor T, Ruslami R, Amanullah F, Behr MA, et al. Tuberculosis. Lancet. 2025;405:850–66. https://doi.org/10.1016/S0140-6736(24)02479-6
3. Getahun H, Matteelli A, Abubakar I, Aziz MA, Baddeley A, Barreira D, et al. Management of latent *Mycobacterium tuberculosis* infection: WHO guidelines for low tuberculosis burden countries. Eur Respir J. 2015;46:1563–76. https://doi.org/10.1183/13993003.01245-2015
4. Gupta RK, Calderwood CJ, Yavlinsky A, Krutikov M, Quartagno M, Aichelburg MC, et al. Discovery and validation of a personalized risk predictor for incident tuberculosis in low transmission settings. Nat Med. 2020;26:1941–9. https://doi.org/10.1038/s41591-020-1076-0
5. Houben RMGJ, Dodd PJ. The global burden of latent tuberculosis infection: a re-estimation using mathematical modelling. PLoS Med. 2016;13:e1002152. https://doi.org/10.1371/journal.pmed.1002152
6. Dale KD, Schwalb A, Coussens AK, Gibney KB, Abboud AJ, Watts K, et al. Overlooked, dismissed, and downplayed: reversion of *Mycobacterium tuberculosis* immunoreactivity. Eur Respir Rev. 2024;33:240007. https://doi.org/10.1183/16000617.0007-2024
7. Kunst H, Burman M, Arnesen TM, Fiebig L, Hergens MP, Kalkouni O, et al. Tuberculosis and latent tuberculous infection screening of migrants in Europe: comparative analysis of policies, surveillance systems and results. Int J Tuberc Lung Dis. 2017;21:840–51. https://doi.org/10.5588/ijtld.17.0036
8. Pareek M, Baussano I, Abubakar I, Dye C, Lalvani A. Evaluation of immigrant tuberculosis screening in industrialized countries. Emerg Infect Dis. 2012;18:1422–9. https://doi.org/10.3201/eid1809.120128
9. Mahon J, Beale S, Holmes H, Arber M, Nikolayevskyy V, Alagna R, et al. A systematic review of cost-utility analyses of screening methods in latent tuberculosis infection in high-risk populations. BMC Pulm Med. 2022;22:375. https://doi.org/10.1186/s12890-022-02149-x
10. Government of Canada. Permanent residents—monthly IRCC updates—Canada—permanent residents by country of citizenship [cited 2025 Apr 25]. https://open.canada.ca/data/en/dataset/f7e5498e-0ad8-4417-85c9-9b8aff9b9eda/resource/d1c1f4f3-2d7f-4e02-9a79-7af98209c2f3
11. Ward A. U.S. lawful permanent residents. Washington: US Department of Homeland Security; 2023.
12. GOV.UK. How many people are granted settlement or citizenship? [cited 2025 Apr 25]. https://www.gov.uk/government/statistics/immigration-system-statistics-year-ending-december-2023/how-many-people-are-granted-settlement-or-citizenship
13. Australian Government, Department of Home Affairs [cited 2025 Apr 25]. https://www.homeaffairs.gov.au
14. Jordan AE, Nsengiyumva NP, Houben RMGJ, Dodd PJ, Dale KD, Trauer JM, et al. The prevalence of tuberculosis

infection among foreign-born Canadians: a modelling study. CMAJ. 2023;195:E1651–9. https://doi.org/10.1503/cmaj.230228
15. Pinto PFPS, Teixeira CSS, Ichihara MY, Rasella D, Nery JS, Sena SOL, et al. Incidence and risk factors of tuberculosis among 420 854 household contacts of patients with tuberculosis in the 100 Million Brazilian Cohort (2004–18): a cohort study. Lancet Infect Dis. 2024;24:46–56. https://doi.org/10.1016/S1473-3099(23)00371-7
16. Government of Canada. Permanent residents—monthly IRCC updates [cited 2025 May 6]. https://open.canada.ca/data/en/dataset/f7e5498e-0ad8-4417-85c9-9b8aff9b9eda
17. Campbell JR, Winters N, Menzies D. Absolute risk of tuberculosis among untreated populations with a positive tuberculin skin test or interferon-gamma release assay result: systematic review and meta-analysis. BMJ. 2020;368:m549. https://doi.org/10.1136/bmj.m549
18. Schwalb A, Emery JC, Dale KD, Horton KC, Ugarte-Gil CA, Houben RMGJ. Impact of reversion of *Mycobacterium tuberculosis* immunoreactivity tests on the estimated annual risk of tuberculosis infection. Am J Epidemiol. 2023;192:1937–43. https://doi.org/10.1093/aje/kwad028
19. Schwalb A, Dodd PJ, Rickman HM, Ugarte-Gil CA, Horton KC, Houben RMGJ. Estimating the global burden of viable *Mycobacterium tuberculosis* infection: a mathematical modelling study. PLoS Med. 2026;23:e1004920. https://doi.org/10.1371/journal.pmed.1004920
20. Campbell JR, Johnston JC, Sadatsafavi M, Cook VJ, Elwood RK, Marra F. Cost-effectiveness of post-landing latent tuberculosis infection control strategies in new migrants to Canada. PLoS One. 2017;12:e0186778. https://doi.org/10.1371/journal.pone.0186778
21. Dale KD, Abayawardana MJ, McBryde ES, Trauer JM, Carvalho N. Modeling the cost-effectiveness of latent tuberculosis screening and treatment strategies in recent migrants to a low-incidence setting. Am J Epidemiol. 2022;191:255–70. https://doi.org/10.1093/aje/kwab150
22. Shedrawy J, Deogan C, Öhd JN, Hergens MP, Bruchfeld J, Jonsson J, et al. Cost-effectiveness of the latent tuberculosis screening program for migrants in Stockholm region. Eur J Health Econ. 2021;22:445–54. https://doi.org/10.1007/s10198-021-01265-5
23. Linas BP, Wong AY, Freedberg KA, Horsburgh CR Jr. Priorities for screening and treatment of latent tuberculosis infection in the United States. Am J Respir Crit Care Med. 2011;184:590–601. https://doi.org/10.1164/rccm.201101-0181OC
24. Tasillo A, Salomon JA, Trikalinos TA, Horsburgh CR Jr, Marks SM, Linas BP. Cost-effectiveness of testing and treatment for latent tuberculosis infection in residents born outside the United States with and without medical comorbidities in a simulation model. JAMA Intern Med. 2017;177:1755–64. https://doi.org/10.1001/jamainternmed.2017.3941
25. Centers for Disease Control and Prevention. Immigrant and refugee health—tuberculosis [cited 2025 May 9]. https://www.cdc.gov/immigrant-refugee-health/hcp/civil-surgeons/tuberculosis.html
26. Menzies NA, Swartwood NA, Cohen T, Marks SM, Maloney SA, Chappelle C, et al. The long-term effects of domestic and international tuberculosis service improvements on tuberculosis trends within the USA: a mathematical modelling study. Lancet Public Health. 2024;9:e573–82. https://doi.org/10.1016/S2468-2667(24)00150-6
27. Dowdy DW, Behr MA. Are we underestimating the annual risk of infection with *Mycobacterium tuberculosis* in high-burden settings? Lancet Infect Dis. 2022;22:e271–8. https://doi.org/10.1016/S1473-3099(22)00153-0
28. Greenaway C, Diefenbach-Elstob T, Schwartzman K, Cook VJ, Giovinazzo G, Njoo H, et al. Tuberculosis surveillance and tuberculosis infection testing and treatment in migrants. In: Canadian tuberculosis standards, 8th edition. Menzies D, editor. Montreal: Canadian Thoracic Society; 2022. p. 194–204.
29. Clark RA, McQuaid CF, Richards AS, Bakker R, Sumner T, Prŷs-Jones TO, et al. The potential impact of reductions in international donor funding on tuberculosis in low-income and middle-income countries: a modelling study. Lancet Glob Health. 2025;13:e1517–24. https://doi.org/10.1016/S2214-109X(25)00232-3
30. Andrews JR, Noubary F, Walensky RP, Cerda R, Losina E, Horsburgh CR. Risk of progression to active tuberculosis following reinfection with *Mycobacterium tuberculosis*. Clin Infect Dis. 2012;54:784–91. https://doi.org/10.1093/cid/cir951

Address for correspondence: Jonathon R. Campbell, McGill University, Office 3D.55, 5252 Blvd de Maisonneuve O, Montreal, QC H4A 3S5, Canada; email: jonathon.campbell@mcgill.ca

Genetically Similar High-Risk Strains of Carbapenemase-Producing Enterobacterales in Humans and Companion Animals, United States

Lingzi Xiaoli, Allison E. James, Anna L. Stahl, Maho Okumura, Stephen D. Cole, Jaclyn M. Dietrich, Molly M. Leeper, Jordan K. Putney, Maroya Spalding Walters, Richard A. Stanton

To elucidate the zoonotic potential of carbapenemase-producing carbapenem-resistant Enterobacterales (CP-CRE) in US companion animals (i.e., dogs and cats), we queried the National Center for Biotechnology Pathogen Detection database to identify One Health clusters containing CP-CRE isolates from companion animals and humans. The 11 One Health clusters we found included most (69% [169/246]) publicly available CP-CRE sequences from US companion animals and were from 8 internationally disseminated, high-risk sequence types from 3 bacterial species (*Escherichia coli*, *Klebsiella pneumoniae*, and *Enterobacter cloacae*). All clustered isolates had New Delhi metallo-β-lactamase–family carbapenemases, and most (92%) carried the $bla_{\text{NDM-5}}$ allele. The One Health clusters included several closely related subclusters with geographically linked isolates from both humans and companion animals. Those results suggest that CP-CRE is an emerging One Health issue and that direct or indirect transmission of CP-CRE is occurring between humans and companion animals in the United States.

Carbapenem-resistant Enterobacterales (CRE) are among the highest priority antimicrobial-resistant pathogen threats to public health in the United States and globally (*1*,*2*). Defined by resistance to the "last resort" carbapenem antibiotics, CRE infections are difficult to treat and associated with high mortality (*3*). CRE is a major cause of human healthcare-associated infections and have recently emerged as a clinical, and potentially zoonotic, pathogen in companion animals (i.e., dogs and cats) (*4*).

Enterobacterales are a taxonomic order of gram-negative bacteria that include commensal and pathogenic gastrointestinal tract organisms, such as *Escherichia coli*, *Klebsiella pneumoniae*, and *Enterobacter* spp. Carbapenem resistance in Enterobacterales species can be conferred by several different mechanisms; among those, acquisition of genes that encode carbapenemases (enzymes that inactivate carbapenems and other β-lactam antibiotics) represents the most serious public health threat (*5*). Because carbapenemase genes are often located on mobile genetic elements, they can spread rapidly through both horizontal transfer and clonal expansion (*6*,*7*). The 5 most common and widely disseminated carbapenemase families are *K. pneumoniae* carbapenemase (KPC), imipenemase metallo-β-lactamase, New Delhi metallo-β-lactamase (NDM), Verona integron-encoded metallo-β-lactamase, and oxacillinase (OXA) 48–like (*8*,*9*).

CRE isolates with carbapenemases from each of the 5 major families have been recovered from companion animals across the globe (*10*). In the United States, the earliest reported carbapenemase-producing CRE (CP-CRE) detections from companion animals were NDM-producing *E. coli* isolates collected during 2008–2009 (*11*). CP-CRE from several bacterial species and carbapenemase families have since been

Author affiliations: Centers for Disease Control and Prevention, Atlanta, Georgia, USA (L. Xiaoli, A.E. James, A.L. Stahl, M.M. Leeper, J.K. Putney, M.S. Walters, R.A. Stanton); University of Pennsylvania School of Veterinary Medicine, Philadelphia, Pennsylvania, USA (M. Okumura, S.D. Cole, J.M. Dietrich); Applied Science Research and Technology, Inc., Smyrna, Georgia, USA (J.K. Putney); US Public Health Service, Rockville, Maryland, USA (M.S. Walters)

DOI: https://doi.org/10.3201/eid3203.251458

isolated from dogs and cats in multiple states (*12*–*18*). Although the prevalence of CP-CRE colonization (i.e., asymptomatic carriage in the gastrointestinal tract) in US companion animals was recently estimated to be only 0.2% (*16*), NDM-producing *E. coli* has caused several large outbreaks among dogs and cats in veterinary hospitals and animal rescue facilities beginning in 2018 (*14*,*17*,*18*).

Transmission of CP-CRE between humans and animals has been documented only a few times, 1 time in a household in Finland (*19*) and 2 times in veterinary hospitals in Europe and the United States (*20*,*21*). However, CP-CRE outbreaks in companion animals have included strains associated with outbreaks in human healthcare facilities, highlighting the potential for transmission between human and animal hosts (*13*,*14*,*16*,*22*). Thanks to the widespread adoption of whole-genome sequencing (WGS) for research, surveillance, and outbreak response, thousands of CP-CRE sequences from human and nonhuman sources are now publicly available. We leveraged those data to analyze the relatedness of strains circulating between humans and animals to elucidate the zoonotic potential of CP-CRE in companion animals in the United States. This activity was reviewed by the Centers for Disease Control and Prevention (CDC), deemed research not involving human subjects, and was conducted consistent with applicable federal law and CDC policy (see e.g., 45 C.F.R. part 46; 21 C.F.R. part 56; 42 U.S.C. §241(d), 5 U.S.C. §552a, 44 U.S.C. §3501 et seq.).

Materials and Methods

Companion Animal Isolate and One Health Cluster Identification

We queried the National Center for Biotechnology Information (NCBI) Pathogen Detection database (https://www.ncbi.nlm.nih.gov/pathogens) on October 24, 2023, to identify Enterobacterales isolates from US dogs and cats containing any of the 5 major carbapenemase gene families (*23*) (Figure 1). We designated Pathogen Detection clusters (predefined by NCBI as isolates within ≤25 allele differences from species-specific, whole-genome multilocus sequence typing schemes) containing CP-CRE collected from companion animal and human sources from the United States as One Health clusters for further analysis. We continued to add isolates to the One Health clusters through February 23, 2024.

Metadata and Epidemiologic Data Collection

We downloaded metadata for isolates belonging to One Health clusters from the Pathogen Detection database (including host species, location, isolation source, etc.). Additional anonymized isolate and patient characteristic data were obtained for analyses, including patient state of residence, isolation source, and specimen type (i.e., colonization or clinical test). When specimen type information was missing, rectal swab samples were categorized as colonization tests, and samples from all other body sites were considered clinical specimens. Those additional data were obtained from the CDC Antimicrobial Resistance Laboratory Network (AR Lab Network), the University of Pennsylvania Veterinary Diagnostic Laboratory, and the Microbiology Laboratory at Texas A&M University Veterinary Medical Teaching Hospital. Linked data were not available or not requested from 7 human-origin sequences and 4 animal-origin sequences; for those sequences only, we used the metadata available in Pathogen Detection. To ensure confidentiality, state of residence for both human and animal patients were classified only by their AR Lab Network region of residence (*24*).

Bioinformatics Analysis

For each One Health cluster, we downloaded available isolate sequence assemblies from NCBI or generated with SKESA version 3.0.0 (*25*) with reads downloaded from the NCBI Sequence Read Archive (https://www.ncbi.nlm.nih.gov/sra) for samples without available assemblies. We identified the multilocus sequence types (STs) for all isolates using mlst version 2.23.0 (https://github.com/tseemann/mlst) with PubMLST typing schemes (*26*). We determined genetic similarity among CP-CRE sequences of human-origin and animal-origin isolates within the same ST by core-genome multilocus sequence typing (cgMLST) to provide a standardized basis of comparison across multiple STs and cluster sizes. We applied publicly available cgMLST schemes for *E. coli* (2,513 loci) from EnteroBase (*27*) and *K. pneumoniae* (2,537 loci) from Institut Pasteur (*28*) as previously described (*29*). For *Enterobacter cloacae*, we constructed an ad hoc cgMLST scheme with 4,229 loci from the 41 CP-CRE isolates within the identified One Health clusters using Roary (https://github.com/rastanton/cgMLST_Scripts; *30*). We constructed phylogenetic dendrograms from cgMLST allele differences using the unweighted pair group method with arithmetic mean. We annotated the cgMLST trees with AR Lab Network regions of collection and host species (dog, cat, and human) using iToL version 4.0 (https://github.com/tseemann/mlst). We calculated the cgMLST allele differences within each cluster for different host pairs (e.g., human–human, human–

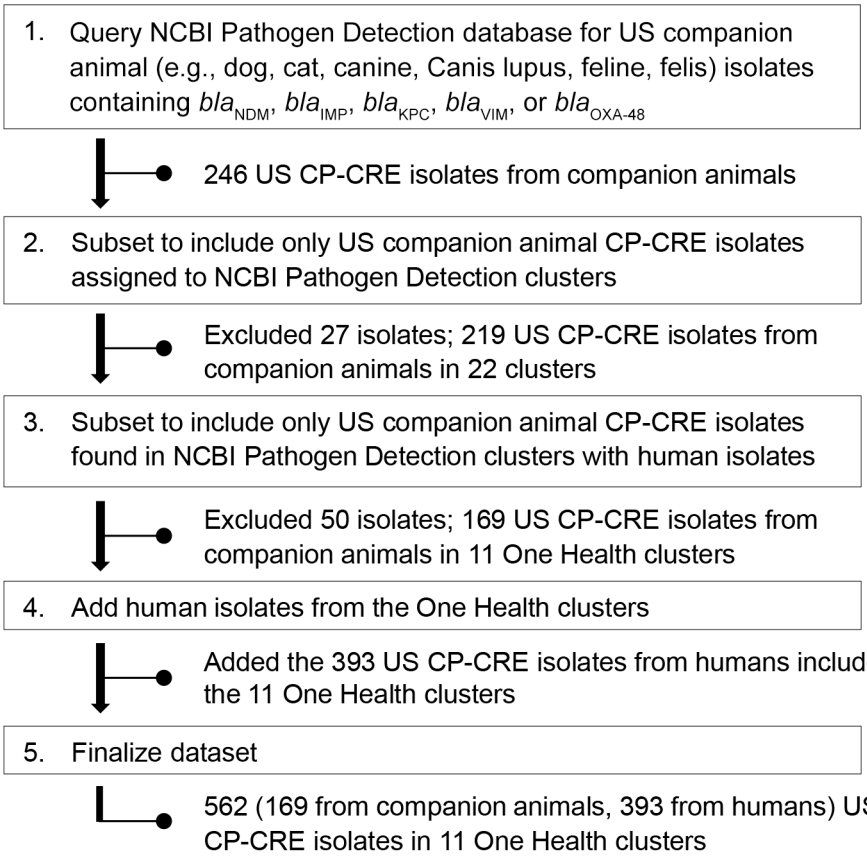

Figure 1. Workflow for identification and inclusion of genetically related US companion animal and human CP-CRE isolates using the NCBI Pathogen Detection database used in study of genetically similar high-risk strains of carbapenemase-producing Enterobacterales in humans and companion animals, United States. CP-CRE, carbapenemase-producing carbapenem-resistant Enterobacterales; IMP, imipenemase metallo-β-lactamase; KPC, K. pneumoniae carbapenemase; NCBI, National Center for Biotechnology Information; NDM, New Delhi metallo-β-lactamase; OXA, oxacillinase; VIM, Verona integron-encoded metallo-β-lactamase.

animal, animal–animal) and summarized them using statistics tools from NumPy (*31*).

Data Validation

We verified isolate host information with epidemiologic data. We excluded isolate sequences if they were from sources other than humans or companion animals, they were duplicate sequences from the same isolate, if an isolate was ≤3 cgMLST allele differences from another isolate collected from the same patient on the same day, or if the sequence was not from paired-end reads.

Results

Dataset Generation

As of February 23, 2024, a total of 246 CP-CRE isolate sequences from US companion animals were available in the NCBI Pathogen Detection database (Figure 1), 26 isolates from cats (11%) and 220 isolates from dogs (89%). Most isolates harbored bla_{NDM} (236 [96%]). Among the isolates with bla_{NDM}, 56% (n = 131) were *E. coli*, 31% were *E. cloacae* (n = 72), and 14% were *K. pneumoniae* (n = 33). Nine isolates harbored bla_{KPC}; 7 were *E. cloacae*, 1 was *E. coli*, and 1 was *Klebsiella oxytoca*. A single OXA-48–like–producing *K. oxytoca* isolate from companion animals was also identified.

Among the 246 US isolates from companion animals, 169 (69%) belonged to 11 One Health clusters (Table 1; Appendix 1 Table 1, https://wwwnc.cdc.gov/EID/article/32/3/25-1458-App1.xlsx), which included 393 human-origin isolates. All clustered isolates were collected during January 2016–February 2024, a period that marked a rapid increase in the use of WGS; 10 times more US CP-CRE sequences were uploaded to NCBI in 2023 than were uploaded in 2016 (Appendix 2 Figure 1, https://wwwnc.cdc.gov/EID/article/32/3/25-1458-App2.pdf).

Isolate and Patient Characteristics

Among the 562 isolates in One Health CP-CRE clusters, *E. coli* was the most common species (88%, n = 493), followed by *E. cloacae* (7%, n = 41) and *K. pneumoniae* (5%, n = 28) (Table 2). All isolates harbored NDM-family carbapenemases; 92% (n = 519) had bla_{NDM-5} and 8% (n = 43) had bla_{NDM-7}. Seven isolates from humans, all from the largest *E. coli* One Health cluster (ST167 cluster 3) (Table 2), also carried carbapenemases from different families (4 with OXA-48–like and 3 with KPC genes) (Appendix 1 Table 2) in addition to bla_{NDM-5}.

Table 1. Companion animal and human CP-CRE isolates included in One Health clusters in study of genetically similar high-risk strains of carbapenemase-producing Enterobacterales in humans and companion animals, United States*

Characteristic	Companion animal	Human
No. isolates†	169	393
Specimen type	n = 168	n = 388
Colonization test	126 (75)	21 (5)
Clinical test	42 (25)	367 (95)
Source (for clinical tests)	n = 42	n = 365
Respiratory Tract	14 (33)	8 (2)
Urine	11 (26)	261 (72)
Wound	12 (29)	17 (5)
Blood	0	48 (13)
Other	5 (12)	31 (8)
No. unique patients	n = 158‡	n = 386§
Dogs	145 (92)	NA
Cats	13 (8)	NA
Patient region of residence¶	n = 154	n = 379
Central	9 (6)	32 (8)
Mid-Atlantic	78 (51)	60 (16)
Midwest	22 (14)#	41 (11)
Mountain	1 (1)	89 (23)
Northeast	41 (27)	57 (15)
Southeast	3 (2)	36 (9)
West	0	64 (17)

*Values are no. (%) except as indicated. CP-CRE, carbapenemase-producing carbapenemase-resistant Enterobacterales; NA, not applicable.
†Isolates or patients with missing data were excluded from corresponding denominators.
‡Eleven unique isolates were collected from 1 cat and 6 dogs.
§Seven unique isolates were collected from 5 humans.
¶Centers for Disease Control and Prevention Antimicrobial Resistance Laboratory Network regions (*24*).
#Includes 18 animals known to have been imported from other countries.

Among isolates with available data, 75% (126/168) of companion animal-origin isolate sequences were collected for colonization screening, compared with 5% (21/388) of the human isolates (Table 1). Seventy-two percent of human clinical isolates were collected from urine (261/365), whereas those from companion animals were divided roughly equally among the respiratory tract (tracheal wash or bronchoalveolar lavage samples, 33%, 14/42), wounds (29%, 12/42), and urine (26%, 11/42).

The One Health cluster isolates were from 386 unique human patients and 158 companion animal patients. Compared with the broad geographic distribution of human-origin isolates, companion animal isolates were concentrated in 2 neighboring regions; 77% (119/154) were from the Mid-Atlantic or Northeast.

Cluster Characteristics and Genetic Analyses

Of the 11 One Health clusters, 8 were from *E. coli*. The 11 clusters were composed of 8 unique STs; 2 *E. coli* STs were associated with multiple clusters (ST162 [2 clusters] and ST167 [3 clusters]) (Table 2). The size of the clusters varied from 2 isolates (*E. coli* ST162 cluster 1) to 285 isolates (*E. coli* ST167 cluster 3) (Table 2). Seven clusters contained isolates collected from dogs, cats, and humans, whereas 4 contained isolates collected from humans and dogs only. The fraction of human isolates within clusters varied from 6% (*K. pneumoniae* ST11 [1/18]) to 96% (*E. coli* ST167 cluster 3 [275/285]). Of the CP-CRE isolates from companion animals that were not part of One Health clusters, 59% (49/77) were from the same STs as the One Health clusters (*E. coli* ST162 and ST167, *K. pneumoniae* ST307, and *E. cloacae* ST171) (Appendix 1 Table 1).

To investigate whether the isolates from humans and companion animals within One Health clusters were genetically distinct from one another, we compared cgMLST allele differences between human–human, human–animal, and animal–animal isolate pairs (Figure 2). The interquartile ranges overlapped across all 3 pairwise categories. The median allele difference for human–animal pairs was lower than that for human–human pairs across all 3 CP-CRE species. Plots of the relative frequencies of within-cluster pairwise allele differences by CP-CRE species also showed overlapping human–human and human–animal pair distributions (Appendix 2 Figure 2).

Eight of the One Health clusters (representing each of the 3 species and all STs) contained human–animal isolate pairs that were 0–1 cgMLST allele differences apart (Appendix 1 Table 2). Seven of those clusters included human–animal pairs that were related within 0–1 cgMLST allele differences and collected from the same region (examples in Figure 3).

Discussion

Our analysis of CP-CRE sequences in the NCBI Pathogen Detection database found >240 isolates collected from US companion animals; nearly 70% clustered with isolates from humans. Those One Health clusters included isolates from 3 different bacterial species and 8 unique STs, and all harbored NDM-family carbapenemase genes. All cluster isolates were collected during a period that coincided with the rapid emergence of the NDM family of carbapenemase genes in US human patients (*32*,*33*). The One Health clusters included very closely genetically related isolate pairs from human and companion animals and many geographically linked genetic subclusters. Those findings support that emerging CP-CRE populations carried by companion animals are not genetically distinct from those isolated from humans and that strains are likely being shared among hosts.

Each of the STs identified in this analysis have been recognized as globally disseminated, high-risk strains (i.e., known to disseminate antimicrobial resistance genes) and have previously been isolated from

companion animals (*13*,*16*,*34*–*38*). *E. coli* with bla_{NDM-5} was the most frequent species and carbapenemase allele combination in One Health clusters. Of the 5 *E. coli* STs (ST167, ST410, ST361, and ST617) identified, 4 are also among the most common NDM-5–producing human strains worldwide and were recently linked to community associated NDM-producing CRE cases in the United States (*39*–*41*). The most frequently identified of those, NDM-5–producing *E. coli* ST167, has caused outbreaks among companion animals at a veterinary hospital and an animal rescue facility in the United States and has been implicated in transmission between humans and companion animals in Europe (*19*,*20*).

Although our results provide evidence that exchange of CP-CRE between humans and companion animals is occurring in the United States, no established thresholds of relatedness (i.e., cgMLST allele differences) can be interpreted as absolute evidence of direct or indirect transmission (e.g., by exposure to a shared contaminated environment) or directionality (i.e., whether transmission occurred from humans to animals or vice versa) in the absence of clear epidemiologic links. The data do suggest that the emergence of CP-CRE among humans and companion animals in the United States is primarily driven by clonal expansion of strains that might be better suited for community spread, instead of horizontal transfer of carbapenemase genes into otherwise unrelated strains.

Most (75%) animal CP-CRE isolates in this study were found through colonization screening; those tests are used to identify persons or animals that might be asymptomatically shedding the organisms, usually to contain outbreaks or prevent introducing CP-CRE into healthcare facilities or veterinary hospitals (*42*). That finding confirms other reports that companion animals can silently carry zoonotic CP-CRE, which might accelerate spread of such organisms in community settings (*43*,*44*). Our findings of shared strains between companion animals and humans, as well as reports of outbreaks in veterinary facilities, highlight the potential risks of transmission to other companion animals, pet owners, and veterinary staff. Although the frequency of transmission is unknown, a study in Switzerland found 2 separate instances of veterinary hospital employees colonized with the same strain that had been identified in animals in their respective veterinary hospitals (*20*). That finding reinforces the importance of adhering to routine infection prevention and control measures to prevent spread within veterinary hospitals, among animal patients, and between animal patients and veterinary staff (*14*,*18*,*20*,*37*,*45*,*46*).

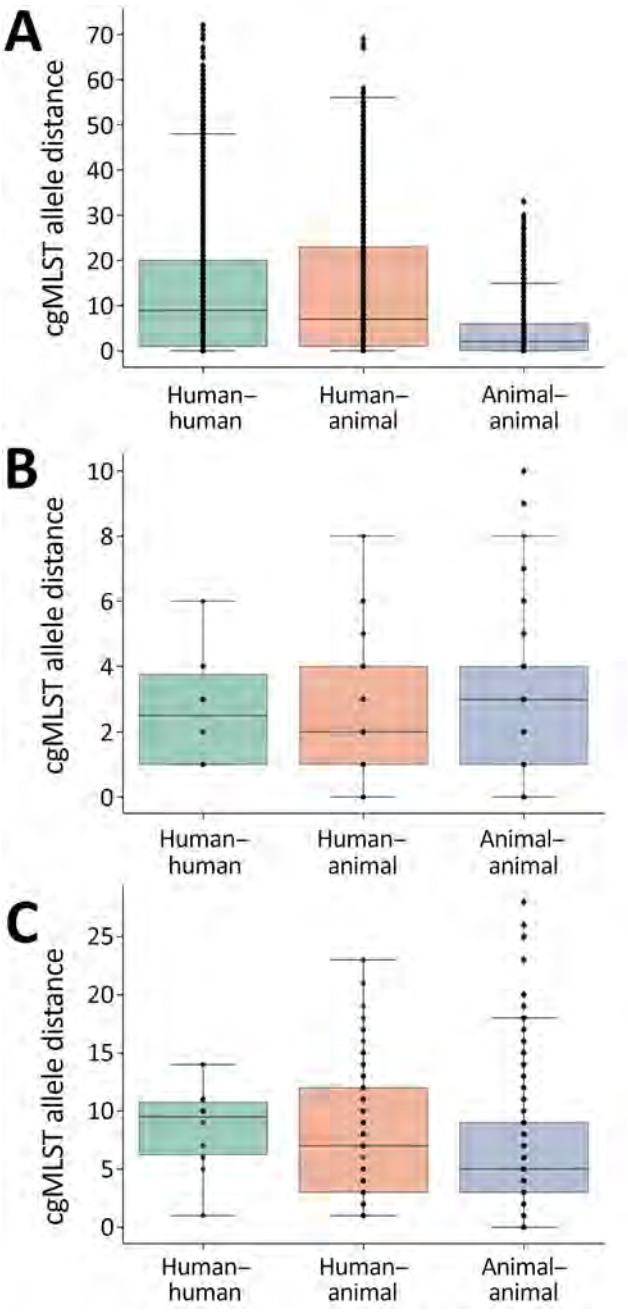

Figure 2. Frequency boxplots of pairwise within-cluster cgMLST allele distances among carbapenemase-producing carbapenem-resistant Enterobacterales isolates collected from humans and companion animals in study of genetically similar high-risk strains of carbapenemase-producing Enterobacterales in humans and companion animals, United States. Pairwise cgMLST allele distances were calculated between pairs within individual clusters and depicted by bacterial species with *Escherichia coli* (A), *Klebsiella pneumoniae* (B), and *Enterobacter cloacae* (C). Box top and bottom boundaries depict 25th and 75th quartiles, horizontal lines within boxes depict median values, dots represent individual data points, and whiskers represent datapoints within 1.5 times the interquartile range. cgMLST, core-genome multilocus sequence typing.

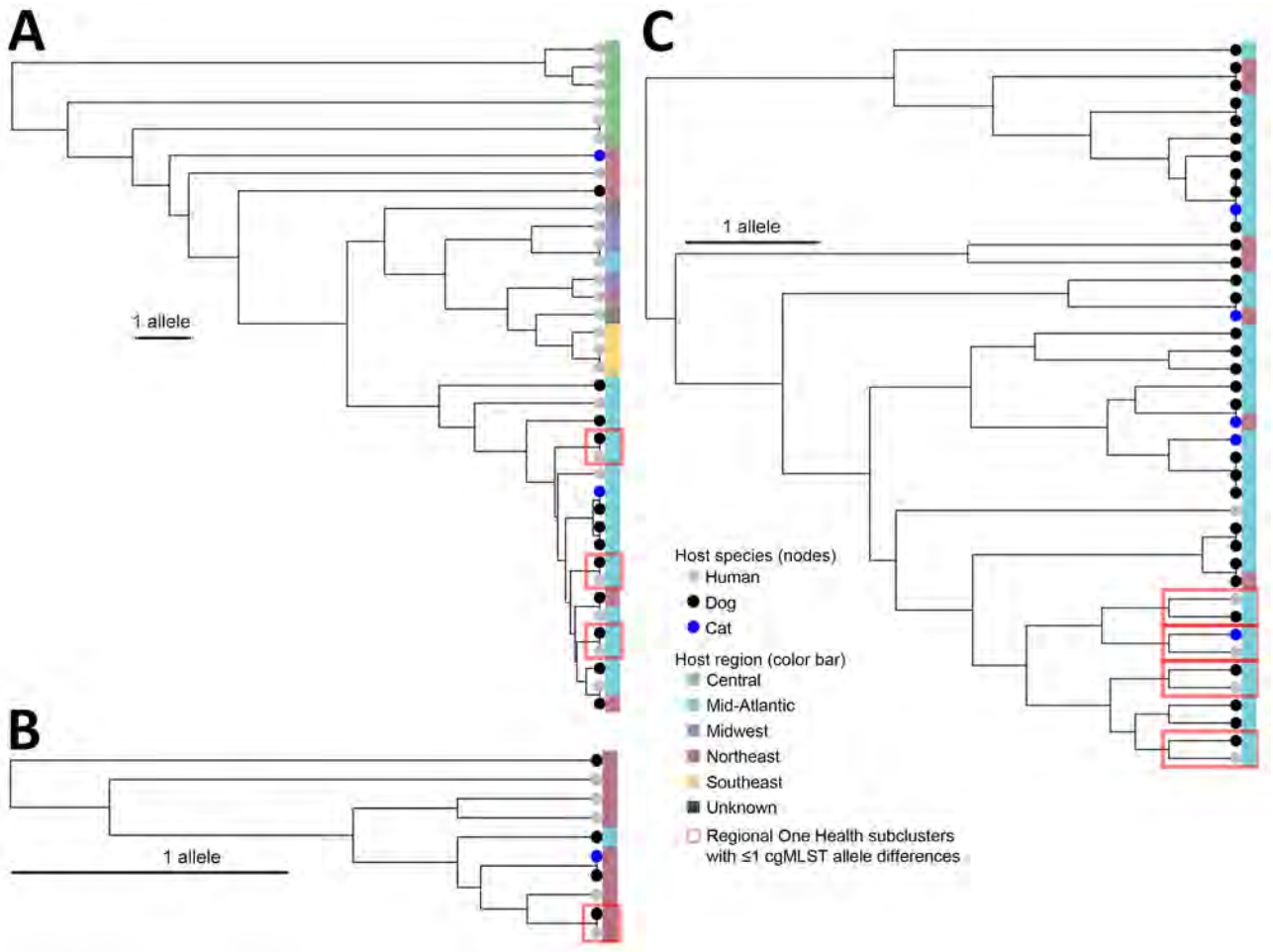

Figure 3. Phylogenetic core-genome multilocus sequence typing trees of *Escherichia coli* sequence type (ST) 617, *Klebsiella pneumoniae* ST307, and *Enterobacter cloacae* ST171 One Health clusters in study of genetically similar high-risk strains of carbapenemase-producing Enterobacterales in humans and companion animals, United States. The tree nodes are colored by host species, and the bands on the right are colored by the region of patient residence. cgMLST, core-genome multilocus sequence typing.

The first limitation of our study is that we used a convenience sample of publicly available WGS data, which are not representative of the true burden or characteristics of CP-CRE in companion animals or humans and might be skewed by the overrepresentation of closely related sequences associated with outbreaks (e.g., the *E. coli* sequences included dozens of sequences from 2 known companion animal outbreaks). In addition, most companion animal samples were from only 2 regions, the Mid-Atlantic and Northeast, the same regions in which CP-CRE outbreaks in US veterinary hospitals have been reported (*14*,*18*). Therefore, the results might underestimate the diversity and distribution of CP-CRE in companion animals across the United States.

Our results demonstrate that CP-CRE in companion animals and humans are genetically very similar and include many diverse, high-risk sequence types commonly associated with infections and outbreaks in human healthcare settings. That finding suggests that both companion animals and humans serve as reservoirs for high-risk CP-CRE strains; community reservoirs of historically healthcare-associated pathogens have the potential to increase CP-CRE infections in otherwise healthy humans and pets. Coordinated efforts between human and animal health sectors are warranted to mitigate further spread of such highly antimicrobial-resistant bacteria.

Acknowledgments

We thank Sara Lawhon for her assistance in providing epidemiological information for a companion animal patient.

S.D.C. has received honoraria for speaking engagements and consultations for Idexx Laboratories and bioMérieux. He has also received travel support for his role as advisor

and working group chairholder for the Clinical and Laboratory Standards Institute and for being a guest speaker for the Council of State and Territorial Epidemiologists.

About the Author

Dr. Xiaoli completed this work during her Molecular Epidemiology Fellowship at the Centers for Disease Control and Prevention. Her research interests include pathogen genomics, microbiology, and pathogenesis, with a focus on integrating multidisciplinary data to advance outbreak responses and disease surveillance.

References

1. Centers for Disease Control and Prevention. Antibiotic resistance threats in the United States 2019 [cited 2025 Mar 10]. https://www.cdc.gov/antimicrobial-resistance/media/pdfs/2019-ar-threats-report-508.pdf
2. World Health Organization. WHO bacterial priority pathogens list, 2024 [cited 2025 Mar 10]. https://iris.who.int/server/api/core/bitstreams/1a41ef7e-dd24-4ce6-a9a6-1573562e7f37/content
3. Zhou R, Fang X, Zhang J, Zheng X, Shangguan S, Chen S, et al. Impact of carbapenem resistance on mortality in patients infected with *Enterobacteriaceae*: a systematic review and meta-analysis. BMJ Open. 2021;11:e054971. https://doi.org/10.1136/bmjopen-2021-054971
4. Silva JMD, Menezes J, Marques C, Pomba CF. Companion animals—an overlooked and misdiagnosed reservoir of carbapenem resistance. Antibiotics (Basel). 2022;11:533. https://doi.org/10.3390/antibiotics11040533
5. Gupta N, Limbago BM, Patel JB, Kallen AJ. Carbapenem-resistant *Enterobacteriaceae*: epidemiology and prevention. Clin Infect Dis. 2011;53:60–7. https://doi.org/10.1093/cid/cir202
6. Naas T, Cuzon G, Villegas MV, Lartigue MF, Quinn JP, Nordmann P. Genetic structures at the origin of acquisition of the β-lactamase bla_{KPC} gene. Antimicrob Agents Chemother. 2008;52:1257–63. https://doi.org/10.1128/AAC.01451-07
7. Mathers AJ, Cox HL, Kitchel B, Bonatti H, Brassinga AK, Carroll J, et al. Molecular dissection of an outbreak of carbapenem-resistant Enterobacteriaceae reveals intergenus KPC carbapenemase transmission through a promiscuous plasmid. MBio. 2011;2:e00204–11. https://doi.org/10.1128/mBio.00204-11
8. Nordmann P, Poirel L. Epidemiology and diagnostics of carbapenem resistance in gram-negative bacteria. Clin Infect Dis. 2019;69(Suppl 7):S521–8. https://doi.org/10.1093/cid/ciz824
9. Wise MG, Karlowsky JA, Mohamed N, Hermsen ED, Kamat S, Townsend A, et al. Global trends in carbapenem- and difficult-to-treat-resistance among World Health Organization priority bacterial pathogens: ATLAS surveillance program 2018–2022. J Glob Antimicrob Resist. 2024;37:168–75. https://doi.org/10.1016/j.jgar.2024.03.020
10. Sellera FP, Da Silva LCBA, Lincopan N. Rapid spread of critical priority carbapenemase-producing pathogens in companion animals: a One Health challenge for a post-pandemic world. J Antimicrob Chemother. 2021;76:2225–9. https://doi.org/10.1093/jac/dkab169
11. Shaheen BW, Nayak R, Boothe DM. Emergence of a New Delhi metallo-β-lactamase (NDM-1)-encoding gene in clinical *Escherichia coli* isolates recovered from companion animals in the United States. Antimicrob Agents Chemother. 2013;57:2902–3. https://doi.org/10.1128/AAC.02028-12
12. Liu X, Thungrat K, Boothe DM. Occurrence of OXA-48 carbapenemase and other β-lactamase genes in ESBL-producing multidrug resistant *Escherichia coli* from dogs and cats in the United States, 2009–2013. Front Microbiol. 2016;7:1057. https://doi.org/10.3389/fmicb.2016.01057
13. Daniels JB, Chen L, Grooters SV, Mollenkopf DF, Mathys DA, Pancholi P, et al. *Enterobacter cloacae* complex sequence type 171 isolates expressing KPC-4 carbapenemase recovered from canine patients in Ohio. Antimicrob Agents Chemother. 2018;62:e01161-18. https://doi.org/10.1128/AAC.01161-18
14. Cole SD, Peak L, Tyson GH, Reimschuessel R, Ceric O, Rankin SC. New Delhi metallo-β-lactamase-5-producing *Escherichia coli* in companion animals, United States. Emerg Infect Dis. 2020;26:381–3. https://doi.org/10.3201/eid2602.191221
15. Lavigne SH, Cole SD, Daidone C, Rankin SC. Risk factors for the acquisition of a bla_{NDM-5} carbapenem-resistant *Escherichia coli* in a veterinary hospital. J Am Anim Hosp Assoc. 2021;57:101–5. https://doi.org/10.5326/JAAHA-MS-7105
16. Dietrich J, LeCuyer TE, Hendrix GK, Burbick CR, Jacob ME, Byrne BA, et al. Prevalence and molecular epidemiology of carbapenemase-producing Enterobacterales isolated from dog and cat faeces submitted to veterinary laboratories in the USA. Zoonoses Public Health. 2024;71:538–48. https://doi.org/10.1111/zph.13144
17. McNamara K, Habrun C, Wilson W, Kollmann L, Stapleton G, Stanton R, et al. New Delhi metallo-β-lactamase–producing *Escherichia coli* among dogs at an animal rescue facility—Wisconsin, 2022. Antimicrob Steward Health Epidemiol. 2023;3:s90. https://doi.org/10.1017/ash.2023.354
18. DeStefano I, Fellman CL, Bergeron AC, Golato LM, Doron S, Cumming M, et al. Effective mitigation of an outbreak of New Delhi metallo-β-lactamase-producing *Escherichia coli* infections in a small animal veterinary teaching hospital. J Am Vet Med Assoc. 2025;263:1–10. https://doi.org/10.2460/javma.24.09.0572
19. Grönthal T, Österblad M, Eklund M, Jalava J, Nykäsenoja S, Pekkanen K, et al. Sharing more than friendship—transmission of NDM-5 ST167 and CTX-M-9 ST69 *Escherichia coli* between dogs and humans in a family, Finland, 2015. Euro Surveill. 2018;23:1700497. https://doi.org/10.2807/1560-7917.ES.2018.23.27.1700497
20. Endimiani A, Brilhante M, Bernasconi OJ, Perreten V, Schmidt JS, Dazio V, et al. Employees of Swiss veterinary clinics colonized with epidemic clones of carbapenemase-producing *Escherichia coli*. J Antimicrob Chemother. 2020;75:766–8. https://doi.org/10.1093/jac/dkz470
21. DeStefano IM, Fellman CL, Vagnone PMS, Cumming MA, Dale JL, Ruhland A, et al. Human cases of carbapenemase-producing *Escherichia coli* linked to spread between animals and the environment in a veterinary facility—Massachusetts, USA, 2023. Clin Infect Dis. 2025;ciaf541. https://doi.org/10.1093/cid/ciaf541
22. Campos-Madueno EI, Moser AI, Jost G, Maffioli C, Bodmer T, Perreten V, et al. Carbapenemase-producing *Klebsiella pneumoniae* strains in Switzerland: human and non-human settings may share high-risk clones. J Glob Antimicrob Resist. 2022;28:206–15. https://doi.org/10.1016/j.jgar.2022.01.016

23. National Center for Biotechnology Information. Pathogen detection help document [cited 2025 May 2]. https://www.ncbi.nlm.nih.gov/pathogens/pathogens_help
24. Centers for Disease Control and Prevention. Antimicrobial Resistance Laboratory Network [cited 2025 May 2]. https://www.cdc.gov/antimicrobial-resistance-laboratory-networks/php/about/domestic.html
25. Souvorov A, Agarwala R, Lipman DJ. SKESA: strategic k-mer extension for scrupulous assemblies. Genome Biol. 2018;19:153. https://doi.org/10.1186/s13059-018-1540-z
26. Jolley KA, Bray JE, Maiden MCJ. Open-access bacterial population genomics: BIGSdb software, the PubMLST.org website and their applications. Wellcome Open Res. 2018; 3:124. https://doi.org/10.12688/wellcomeopenres.14826.1
27. Dyer NP, Päuker B, Baxter L, Gupta A, Bunk B, Overmann J, et al. EnteroBase in 2025: exploring the genomic epidemiology of bacterial pathogens. Nucleic Acids Res. 2025;53(D1):D757–62. https://doi.org/10.1093/nar/gkae902
28. Bialek-Davenet S, Criscuolo A, Ailloud F, Passet V, Jones L, Delannoy-Vieillard A-S, et al. Genomic definition of hypervirulent and multidrug-resistant *Klebsiella pneumoniae* clonal groups. Emerg Infect Dis. 2014;20:1812–20. https://doi.org/10.3201/eid2011.140206
29. Stanton RA, McAllister G, Daniels JB, Breaker E, Vlachos N, Gable P, et al. Development and application of a core genome multilocus sequence typing scheme for the health care-associated pathogen *Pseudomonas aeruginosa.* J Clin Microbiol. 2020;58:e00214-20. https://doi.org/10.1128/JCM.00214-20
30. Page AJ, Cummins CA, Hunt M, Wong VK, Reuter S, Holden MT, et al. Roary: rapid large-scale prokaryote pan genome analysis. Bioinformatics. 2015;31:3691–3. https://doi.org/10.1093/bioinformatics/btv421
31. Harris CR, Millman KJ, van der Walt SJ, Gommers R, Virtanen P, Cournapeau D, et al. Array programming with NumPy. Nature. 2020;585:357–62. https://doi.org/10.1038/s41586-020-2649-2
32. Sader HS, Mendes RE, Carvalhaes CG, Kimbrough JH, Castanheira M. Changing epidemiology of carbapenemases among carbapenem-resistant Enterobacterales from United States hospitals and the activity of aztreonam-avibactam against contemporary Enterobacterales (2019–2021). Open Forum Infect Dis. 2023;10:ofad046. https://doi.org/10.1093/ofid/ofad046
33. Devinney K, Burton N, Alroy KA, Crawley A, Da Costa-Carter CA, Kratz MM, et al. Notes from the field: increase in New Delhi metallo-β-lactamase-producing carbapenem-resistant Enterobacterales—New York City, 2019–2024. MMWR Morb Mortal Wkly Rep. 2025;74:401–3. https://doi.org/10.15585/mmwr.mm7423a2
34. Caddey B, Fisher S, Barkema HW, Nobrega DB. Companions in antimicrobial resistance: examining transmission of common antimicrobial-resistant organisms between people and their dogs, cats, and horses. Clin Microbiol Rev. 2025;38:e0014622. https://doi.org/10.1128/cmr.00146-22
35. de Mendieta JM, Argüello A, Menocal MA, Rapoport M, Albornoz E, Más J, et al. Emergence of NDM-producing Enterobacterales infections in companion animals from Argentina. BMC Vet Res. 2024;20:174. https://doi.org/10.1186/s12917-024-04020-z
36. Brookshire C, Robinson D, Seo K. Carbapenemase-producing ST307 *Klebsiella pneumoniae* in dogs. Am J Med Sci. 2023;365:S313–4. https://doi.org/10.1016/S0002-9629(23)00584-0
37. Brilhante M, Gobeli Brawand S, Endimiani A, Rohrbach H, Kittl S, Willi B, et al. Two high-risk clones of carbapenemase-producing *Klebsiella pneumoniae* that cause infections in pets and are present in the environment of a veterinary referral hospital. J Antimicrob Chemother. 2021;76:1140–9. https://doi.org/10.1093/jac/dkab028
38. Garcia-Fierro R, Drapeau A, Dazas M, Saras E, Rodrigues C, Brisse S, et al. Comparative phylogenomics of ESBL-, AmpC- and carbapenemase-producing *Klebsiella pneumoniae* originating from companion animals and humans. J Antimicrob Chemother. 2022;77:1263–71. https://doi.org/10.1093/jac/dkac041
39. Linkevicius M, Bonnin RA, Alm E, Svartström O, Apfalter P, Hartl R, et al. Rapid cross-border emergence of NDM-5-producing *Escherichia coli* in the European Union/European Economic Area, 2012 to June 2022. Euro Surveill. 2023;28:2300209. https://doi.org/10.2807/1560-7917.ES.2023.28.19.2300209
40. Jones S, Stanton R, D'Angeli M, Brezak A, Sinkevitch J, Sredl M, et al. Community-associated New Delhi metallo-beta-lactamase-producing carbapenem-resistant Enterobacterales: multiple states, from September 2021 through September 2022. Infect Control Hosp Epidemiol. 2025;46:1–4. https://doi.org/10.1017/ice.2025.28
41. Xia C, Yan R, Liu C, Zhai J, Zheng J, Chen W, et al. Epidemiological and genomic characteristics of global *bla*NDM-carrying *Escherichia coli*. Ann Clin Microbiol Antimicrob. 2024;23:58. https://doi.org/10.1186/s12941-024-00719-x
42. Centers for Disease Control and Prevention. MDRO prevention strategies [cited 2025 Aug 12]. https://www.cdc.gov/healthcare-associated-infections/php/preventing-mdros/mdro-prevention-strategies.html
43. Dazio V, Nigg A, Schmidt JS, Brilhante M, Campos-Madueno EI, Mauri N, et al. Duration of carriage of multidrug-resistant bacteria in dogs and cats in veterinary care and co-carriage with their owners. One Health. 2021;13:100322. https://doi.org/10.1016/j.onehlt.2021.100322
44. Nigg A, Brilhante M, Dazio V, Clément M, Collaud A, Gobeli Brawand S, et al. Shedding of OXA-181 carbapenemase-producing *Escherichia coli* from companion animals after hospitalisation in Switzerland: an outbreak in 2018. Euro Surveill. 2019;24:1900071. https://doi.org/10.2807/1560-7917.ES.2019.24.39.1900071
45. Schmidt JS, Kuster SP, Nigg A, Dazio V, Brilhante M, Rohrbach H, et al. Poor infection prevention and control standards are associated with environmental contamination with carbapenemase-producing Enterobacterales and other multidrug-resistant bacteria in Swiss companion animal clinics. Antimicrob Resist Infect Control. 2020;9:93. https://doi.org/10.1186/s13756-020-00742-5
46. Haenni M, Boulouis HJ, Lagrée AC, Drapeau A, Va F, Billet M, et al. Enterobacterales high-risk clones and plasmids spreading $bla_{ESBL/AmpC}$ and bla_{OXA-48} genes within and between hospitalized dogs and their environment. J Antimicrob Chemother. 2022; 77:2754–62. https://doi.org/10.1093/jac/dkac268

Address for correspondence: Allison E. James, Centers for Disease Control and Prevention, 1600 Clifton Rd NE, Mailstop H20-3, Atlanta, GA 30329-4018, USA; email: hwj7@cdc.gov

Strongyloides Genetic Diversity among Humans, Dogs, and Nonhuman Primates, Central African Republic, 2016–2022

Eva Nosková, Vladislav Ilík, Frédéric Stéphane Singa Niatou, Laurent Dumas, Terence Fuh, Jean-Francais Dicky, Terézia Kurucová, Vojtech Baláž, Klára Judita Petrželková, Barbora Pafčo

Strongyloides stercoralis nematode infection occurs in ≈600 million persons worldwide and is listed by the World Health Organization as a neglected tropical disease. Understanding zoonotic potential is critical, especially in areas where humans, domestic animals, and wildlife interact. We explored cross-species sharing of *Strongyloides* roundworms by analyzing fecal samples from humans, dogs, and nonhuman primates in the Dzanga-Sangha Protected Areas, Central African Republic. We detected positive samples by quantitative PCR and assessed genetic diversity through amplification of the 18S rRNA HVR-IV region and *cox1*, followed by high-throughput sequencing. *Strongyloides* prevalence was high in humans, dogs, and gorillas. *S. stercoralis* haplotype A roundworm dominated in humans but appeared in dogs and apes, whereas *S. fuelleborni* nematode was present in all hosts. Shared species and haplotypes indicated zoonotic transmission. Our findings highlight the need for molecular surveillance and emphasize the role of dogs and nonhuman primates as reservoirs, complicating efforts to control infections in human populations.

Strongyloidiasis, caused by *Strongyloides* nematodes, is a zoonotic disease with public health and veterinary implications worldwide (*1*). The World Health Organization classifies strongyloidiasis among neglected tropical diseases requiring urgent control in endemic regions (*2*). Current estimates suggest that >600 million persons are infected globally, predominantly in tropical and subtropical areas (*3*). *Strongyloides stercoralis* and *S. fuelleborni* nematodes are the main species infecting humans; transmission typically occurs through transcutaneous exposure. More severe infections are primarily attributed to *S. stercoralis* nematodes, which are capable of autoinfection and can lead to severe systemic disease, particularly in immunocompromised persons; infection can result in death in extreme cases. Uncomplicated infections often manifest in gastrointestinal, pulmonary, or dermatological symptoms (*4*).

Molecular analyses of *S. stercoralis* nematodes have revealed 2 primary lineages: the potentially zoonotic lineage A, which involves dogs as potential reservoirs for human infection, and lineage B, which is largely restricted to canine hosts (*5*,*6*). Conversely, *S. fuelleborni* nematodes, although less common, are confined to nonhuman primates (NHPs) in Africa and Asia, occasionally spilling over to humans (*1*). Despite numerous documented cases, the true global prevalence of strongyloidiasis remains uncertain because of limited surveillance and underdiagnosis, compounded by the asymptomatic nature of many infections and the lack of standardized diagnostic tools (*7*,*8*).

The Central African Republic (CAR), one of the world's most resource-constrained countries (*9*), ranks 191st out of 193 on the 2022 United Nations Human Development Index (*10*). Its tropical ecosystems, which are rich in biodiversity and wildlife (*11*), create favorable conditions for zoonotic disease circulation (*12*). Frequent interactions

Author affiliations: Masaryk University, Brno, Czech Republic (E. Nosková, V. Ilík, B. Pafčo); Masaryk University, Central European Institute of Technology, Brno (T. Kurucová); Czech Academy of Sciences, Institute of Vertebrate Biology, Brno (E. Nosková, V. Ilík, K.J. Petrželková, B. Pafčo); Czech Academy of Sciences, Biology Center, Institute of Parasitology, Ceske Budejovice, Czech Republic (K.J. Petrželková); WWF Central African Republic Programme Office, Dzanga Sangha Protected Areas, Bangui, Central African Republic (F.S. Singa Niatou, T. Fuh); Toulouse National School of Veterinarians, Toulouse, France (L. Dumas); University of Veterinary Sciences, Brno (V. Baláž)

DOI: https://doi.org/10.3201/eid3203.250526

among humans, NHPs, domestic animals, and wildlife encourage the spread of infectious diseases (*13*), including *Strongyloides* nematodes (*14*). Dogs often act as ecologic bridges as a result of their hunting and scavenging behaviors (*15*). Soil-transmitted helminth infections remain among the most prevalent public health challenges in CAR (*16*); *Strongyloides* nematodes pose a particular concern for both human and NHP populations (*14*,*17*).

This study investigates the role of potential animal reservoirs in human *Strongyloides* infections within the Dzanga-Sangha Protected Areas (DSPA), CAR, where humans, NHPs, and domestic dogs interact closely at the human–wildlife interface. By using molecular genotyping, we analyzed the diversity and sharing of *Strongyloides* haplotypes among humans, NHPs, and dogs to inform control strategies in complex multihost systems.

Materials and Methods

Study Design and Participants

The study was conducted in the DSPA in CAR (Figure 1) during 2016–2022, a location known for habituation of western lowland gorillas (*Gorilla gorilla gorilla*) to human presence and home of traditional BaAka hunter-gatherer communities living in close contact with wildlife. DSPA consists of several zones at varying levels of protection, including the strictly protected Dzanga-Ndoki National Park and the Dzanga-Sangha Special Reserve, a multiuse area where human activities are regulated to varying extents (Figure 1). The research complied with the legal requirements of the CAR and with all research, ethical, and sample transport approvals (Appendix 1, https://wwwnc.cdc.gov/EID/article/32/3/25-0526-App1.pdf).

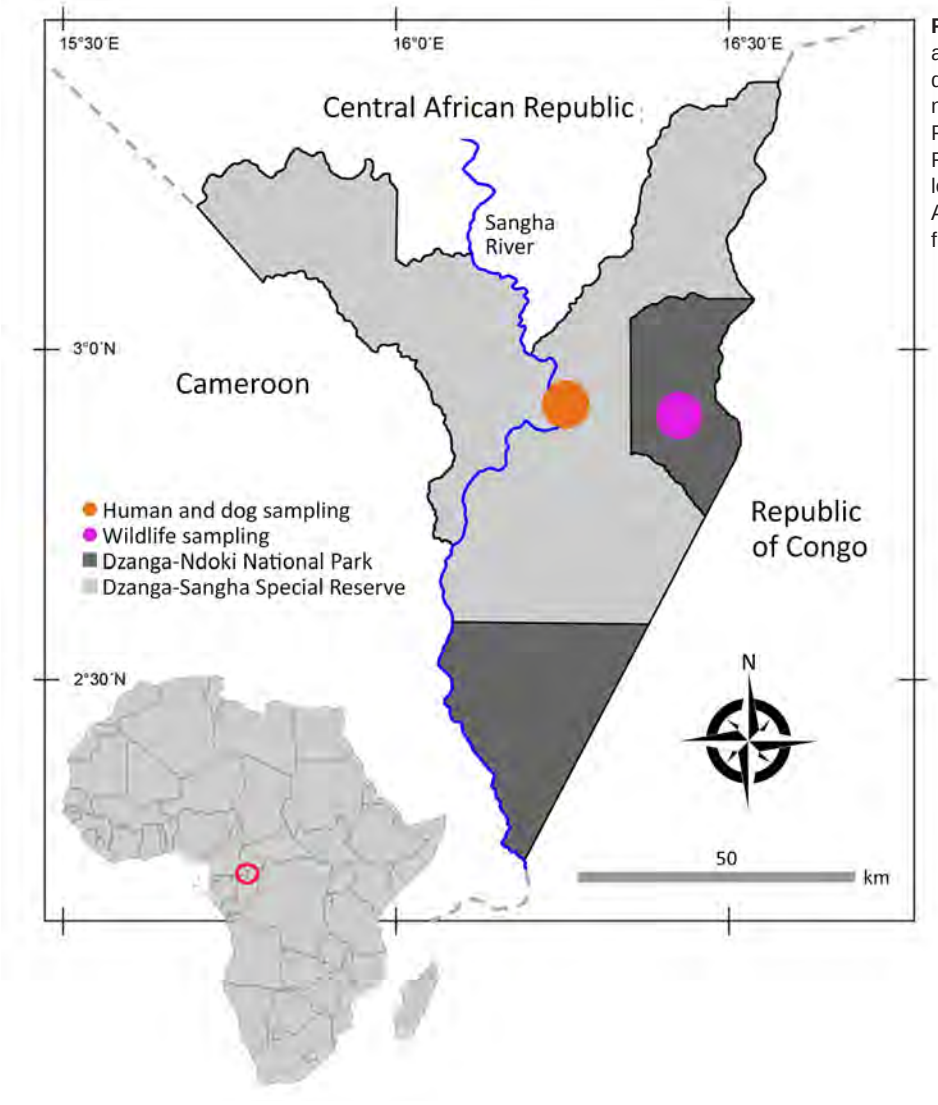

Figure 1. Location of study site in analysis of *Strongyloides* genetic diversity among humans, dogs, and nonhuman primates, Dzanga-Sangha Protected Areas, Central African Republic, 2016–2022. Inset shows location of Central African Republic in Africa. Figure adapted and adjusted from Hasegawa et al. (*18*).

Samples were collected from humans and domestic dogs from 2 villages located within the Special Reserve, whereas wildlife samples were collected in the National Park. Fresh stool samples were obtained from BaAka trackers who worked directly with NHPs in the National Park and also entered the Special Reserve (n = 18), as well as from humans residing in the villages (n = 32), who access the Special Reserve for daily activities such as gathering or hunting. Samples were also collected from dogs (n = 47), which were further categorized as hunting dogs entering the Special Reserve (n = 35) and guarding dogs (n = 12). Wildlife samples consisted of samples from western lowland gorillas (n = 101) at different levels of habituation, unhabituated central chimpanzees (*Pan troglodytes troglodytes*, n = 7), and a habituated group of agile mangabeys (*Cercocebus agilis*, n = 50). Samples were collected as part of health surveillance efforts (Appendix 2 Table 1, https://wwwnc.cdc.gov/EID/article/32/3/25-0526-App2.xlsx). Approximately 1 g of feces was collected and immediately fixed in 96% ethanol and stored at –20°C before DNA isolation.

Procedures

We dried fecal samples overnight at 37°C to evaporate the ethanol. We isolated total DNA using the PowerSoil DNA isolation kit (QIAGEN, https://www.qiagen.com). The extracted DNA was first screened by quantitative PCR (qPCR) targeting the small subunit (18S) rRNA gene specific to the genus *Strongyloides* (*19*) using the LightCycler 480 Real-Time PCR system (Roche, https://www.roche.com). We only included samples positive for *Strongyloides* in high-throughput library preparation. We used DNA extractions from *Strongyloides* PCR-negative feces and water as negative controls, whereas *S. stercoralis* first-stage larva was the positive control. All samples were prepared in technical PCR replicates (*20*). We prepared the high-throughput sequencing library using a 3-step PCR approach (Appendix 2 Table 2). We designed primers for the first PCR step, nested for the hypervariable region IV (HVR-IV) of the 18S rRNA gene and seminested for a portion of the mitochondrial cytochrome c oxidase subunit 1 gene (*cox1*), to increase sensitivity and ensure sufficient yield of amplicons for downstream sequencing (Appendix 1). In the second PCR step, we amplified the HVR-IV-18S rRNA and *cox1* (*21*). In the final PCR step, we applied Nextera primers with unique barcodes for each technical PCR replicate. We performed paired-end sequencing (2 × 300 bp) on the MGI DNBSEQ-G400 platform (MGI Tech, https://mgi-tech.eu).

We first demultiplexed raw fastq sequences and trimmed primer sequences using skewer version 0.2.2 (*22*). We then filtered, dereplicated, and denoised trimmed sequences and merged paired reads in R version 4.2.2 using the dada2 package (*23*). After processing, the final amplicon lengths were 255 bp for the 18S rRNA region and 217 bp for the *cox1*. During merging, we marked amplicon sequencing variants (ASVs) inconsistently present in both PCR technical replicates as potential artifacts and removed them from downstream analyses. We searched for corresponding sequences against the National Center for Biotechnology Information Nucleotide database (downloaded in February 2024) and excluded environmental, uncultured, <85% identity, and <90% coverage hits. We downloaded taxonomy using taxonomizer and used the created reference database to assign a taxonomic classification in our dataset through dada2's Assign Taxonomy method (*24*).

Statistical Analysis

We analyzed all data using the statistical software RStudio (https://www.rstudio.com). We assessed statistical differences in *Strongyloides* occurrence between trackers and villagers and between hunting and guard dogs using the χ^2 test. We generated a bar plot to depict the proportion of *Strongyloides* haplotypes of HVR-IV-18S rRNA in each sample for better resolution. For *cox1* haplotypes, we constructed a median-joining network and visualized using Population Analysis with Reticulate Trees (PopART, https://popart.maths.otago.ac.nz). In addition, we performed a phylogenetic analysis using the MrBayes plugin in Geneious 9.1.5 (https://www.geneious.com) to complement the network approach and assess the phylogenetic placement of the detected haplotypes. To examine differences in α diversity, assessed as ASVs richness (number of ASVs per sample), we applied a generalized linear model (GLM) with a quasipoisson error distribution. We conducted posthoc pairwise comparisons using the Tukey test to identify specific differences among the studied host groups. We evaluated community composition diversity by analyzing the relative representation of HVR-IV-18S rRNA and *cox1* ASVs using Bray-Curtis ecologic distances. We visualized the clustering patterns with principal coordinate analysis (PCoA). To test for interspecific differences in *Strongyloides* nematode community composition among hosts, we performed a permutational analysis of variance (PERMANOVA), followed by similarity analysis (ANOSIM).

Results

Strongyloides qPCR Detection

The number of *Strongyloides*-positive samples by qPCR was high across all studied host species; rates were 76% (38/50) in humans, 60% (28/47) in dogs, 59% (58/101) in gorillas, 43% (3/7) in chimpanzees, and 38% (19/50) in mangabeys. Among humans, BaAka gorilla trackers exhibited a slightly higher, although nonsignificant ($\chi^2 = 0.83$; $p = 0.36$), prevalence of infection (83.3% [15/18]) than that observed in villagers (71.9% [23/32]). Similarly, hunting dogs, which actively venture into the forest, showed a significantly ($\chi^2 = 12.32$; $p = 0.0004$) higher prevalence (74.3% [26/35]) than did guard dogs, which remain in villages (16.7% [2/12]). All qPCR-positive samples were further successfully sequenced with both targets (HVR-IV-18S rRNA and *cox1*), except for 3 mangabey samples that were near the detection threshold (cycle threshold ≈33–34), which likely explains their sequencing failure.

Strongyloides HVR-IV-18S rRNA Diversity

Genotyping identified a total of 11,472,181 high-quality HVR-IV-18S rRNA reads, with a median sequencing depth of 74,200 (range 1,221–302,518) per sample. Taxonomic analysis identified a total of 24 ASVs (Table). Six clustered into already known *Strongyloides* haplotypes: haplotype A of *S. stercoralis* and haplotypes K, L, M, P, and T of *S. fuelleborni*. Five *S. fuelleborni* ASVs did not match with any previously described haplotypes. Those ASVs were detected in only 9 samples (9/140 [6.4%]). Three haplotypes were host-specific (detected exclusively in human, dog, or gorilla), whereas 2 haplotypes were shared (1 between gorilla and mangabey and the other between human and dog). Six ASVs were classified as uncharacterized *Strongyloides* species and were found in 14 samples (14/140 [10%]). Three ASVs were detected in a single host, each occurring exclusively in mangabeys, whereas the remaining 3 were shared (2 between humans and dogs, and 1 within mangabeys). Last, 7 unassigned ASVs, detected in 19% of the samples, were tentatively classified as being most closely related to the order Rhabditida.

Overall, *S. fuelleborni* nematodes dominated across all studied hosts; haplotype L was the most prevalent variant (93.8% of total prevalence). Potentially zoonotic haplotype A of *S. stercoralis* nematodes was detected in 29% of samples from humans, dogs, and gorillas (Table). Relative abundances bar plot of *Strongyloides* HVR-IV-18S rRNA ASVs shows interspecific differences in *Strongyloides* community composition depending on host species (Figure 2). Humans were predominantly infected with *S. fuelleborni* haplotype L and *S. stercoralis* haplotype A (Table; Figure 2, panel A). *S. stercoralis* haplotype A was detected less frequently in BaAka gorilla trackers (67%) than in their village-dwelling relatives (78%), although that difference was not statistically significant ($\chi^2 = 0.63$; $p = 0.43$); haplotype A was absent in guard dogs but present in 30% of hunting dogs. NHPs were mainly infected with *S. fuelleborni* haplotype L. Unclassified *S. fuelleborni* and other unassigned *Strongyloides* variants were predominantly found in mangabeys (Table).

Zoonotic Potential of *Strongyloides* Roundworm on the Basis of HVR-IV-18S rRNA

The highest number of *Strongyloides* HVR-IV-18S rRNA ASVs (8) was shared between humans and dogs, accounting for 33.3% of all observed ASVs. Those included haplotype A of *S. stercoralis*, haplotypes K, L, M, and P of *S. fuelleborni*, 1 unclassified *S. fuelleborni* (ASV_19), and 2 unidentified *Strongyloides* spp. (ASV_14 and ASV_21). Four ASVs (16.6% of all observed ASVs), haplotype A of *S. stercoralis,* and haplotypes K, L, and P of *S. fuelleborni* were shared between humans and NHPs. Haplotype A of *S. stercoralis* and haplotypes K, L, and P of *S. fuelleborni* were shared across humans, dogs, and gorillas (Figure 2, panel A).

Differences in *Strongyloides* HVR-IV-18S rRNA Communities

The number of ASVs per sample did not differ significantly among host species, as determined by a GLM ($p>0.1$) and subsequent Tukey test (Figure

Table. Prevalence of individual *Strongyloides* hypervariable region IV 18S rRNA haplotypes assessed from quantitative PCR–positive samples across host species in study of *Strongyloides* genetic diversity, Central African Republic, 2016–2022

	No. (%)				
Haplotype	Humans, n = 38	Dogs, n = 28	Gorillas, n = 58	Chimpanzees, n = 3	Mangabeys, n = 16
S. stercoralis A	28 (73.7)	7 (25)	7 (12.1)	0	0
S. fuelleborni K	9 (23.7)	6 (21.4)	4 (6.9)	0	0
S. fuelleborni L	38 (100)	26 (92.8)	54 (93.1)	3 (100)	13 (81.3)
S. fuelleborni M	7 (18.4)	9 (32.1)	0	0	0
S. fuelleborni P	1 (2.6)	1 (3.6)	38 (65.5)	3 (100)	10 (62.5)
S. fuelleborni T	1 (2.6)	0	0	0	0
S. fuelleborni unclassified	2 (5.3)	3 (10.7)	2 (3.4)	0	2 (12.5)
Strongyloides unclassified	3 (7.9)	4 (14.3)	3 (5.2)	0	4 (25)

2, panel B). However, the PCoA diagram based on Bray-Curtis ecologic distances revealed distinct differences in *Strongyloides* community composition among humans, dogs, and NHPs (Figure 2, panel D). Those differences were further statistically confirmed by PERMANOVA ($F_{(4,137)} = 11.372$; $p = 0.001$) and ANOSIM

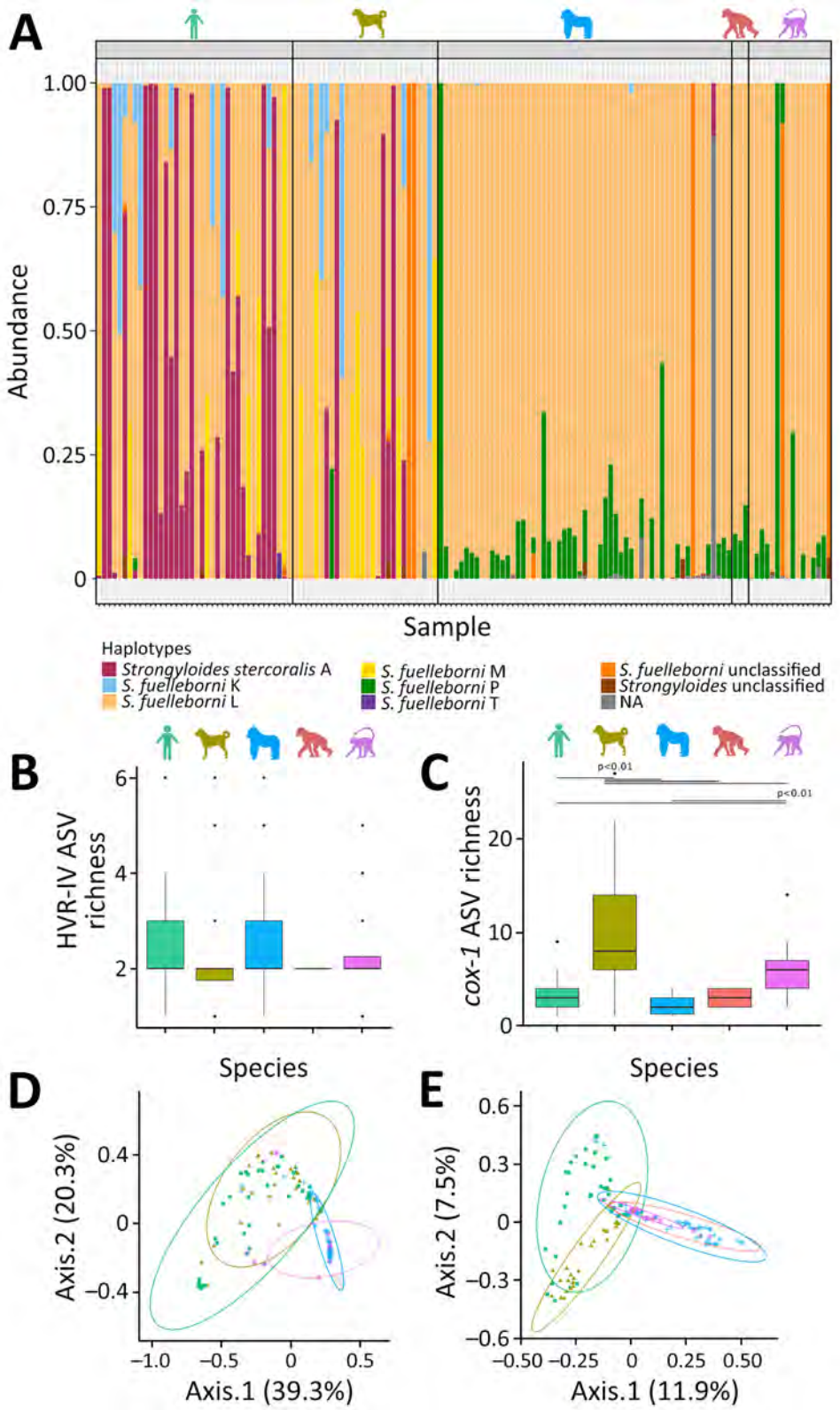

Figure 2. Relative community composition of *Strongyloides* HVR-IV-18S rRNA haplotypes across examined hosts in study of *Strongyloides* genetic diversity among humans, dogs, and nonhuman primates, Dzanga-Sangha Protected Areas, Central African Republic, 2016–2022. A) Relative abundance of haplotypes shown as color panels; each column represents a single sample. B) Boxplot showing the α diversity of *Strongyloides* HVR-IV 18S rRNA haplotypes, represented by the number of ASVs per sample (dots) grouped by host species. C) Boxplot showing the α diversity of *Strongyloides cox1* haplotypes represented by the number of ASVs per sample (dots) grouped by host species. D) Beta diversity of *Strongyloides* HVR-IV 18S rRNA haplotype communities, based on Bray-Curtis ecologic distances (relative abundance of reads), visualized using principal coordinate analysis ordination diagrams. E) Principal coordinate analysis showing the β diversity of *Strongyloides cox1* haplotypes. Color silhouettes (A-C) and data points (D, E) indicate host species: light green, human; olive green, dog; blue, gorilla; red, chimpanzee; violet, mangabey. ASV, amplicon sequencing variant; HVR-IV, hypervariable region IV.

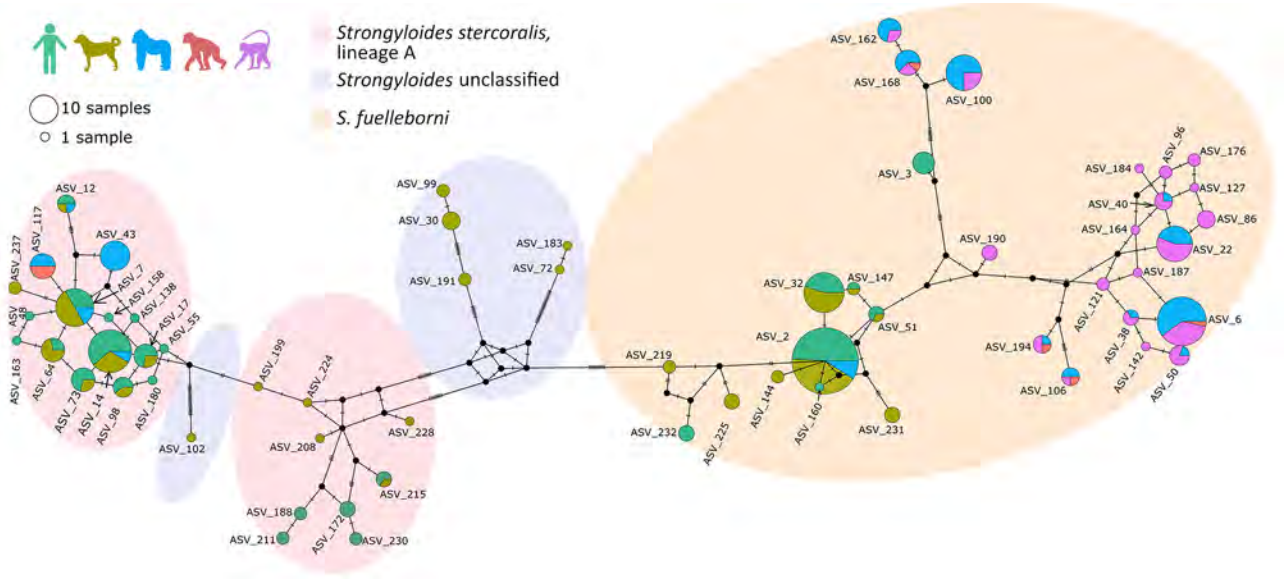

Figure 3. Median-joining *Strongyloides* haplotype network for the mitochondrial *cox1* gene studied in various host species in study of *Strongyloides* genetic diversity among humans, dogs, and nonhuman primates, Dzanga-Sangha Protected Areas, Central African Republic, 2016–2022. Each circle represents 1 haplotype; circle size indicates the number of hosts harboring the respective haplotype. The colors inside the circles indicate the host species: light green, human; olive green, dog; blue, gorilla; red, chimpanzee; violet, mangabey. The hatch marks beside the branches indicate the number of mutation steps between the haplotypes. Missing haplotypes are indicated by small black circles. Shaded ovals indicate species/lineage type. ASV, amplicon sequencing variant.

(R = 0.3435; p = 0.001) tests. The overlap in *Strongyloides* communities was greater between humans and dogs, whereas communities within NHPs were more similar but distinct from those of humans and dogs (Figure 2, panel D).

Strongyloides cox1 Diversity and Zoonotic Potential

We identified a total of 3,381,999 reads based on *cox1*; the median sequencing depth was 2,314 (range 75–56,108) per sample. Taxonomic assignment revealed 62 *Strongyloides* ASVs and 72 unassigned variants, which we tentatively classified as closest to the order Rhabditida. The 62 *Strongyloides* ASVs were used to construct a median-joining phylogenetic network (Figure 3) and Bayesian phylogeny (Figure 4).

The nucleotide diversity was high (N = 0.076), and 52 of the ASVs were parsimony informative. The haplotype network consisted of 25 *S. stercoralis*, 31 *S. fuelleborni*, and 6 unclassified *Strongyloides* ASVs. The network revealed divergence in ASVs on the basis of host specificity. *S. stercoralis* ASVs were primarily shared between humans and dogs, with occasional overlap with gorillas. Haplotype ASV_7 was most common in dogs, whereas ASV_14 was most frequent in humans. Chimpanzees shared only 1 haplotype (ASV_117) with gorillas, and intriguingly, haplotype ASV_43 was found exclusively in gorillas (Figure 3). In the phylogenetic tree, all ASVs of *S. stercoralis* cluster within potentially zoonotic lineage A (Figure 4). *S. fuelleborni* ASVs all clustered to *S. fuelleborni* Africa clade (Figure 4) and displayed host-specific divergence (Figure 3). Humans shared *S. fuelleborni* haplotypes mostly with dogs and occasionally with gorillas, whereas other haplotypes were restricted to NHPs. The ASV_2 haplotype was most common in both humans and dogs, whereas ASV_6 was predominant in gorillas and mangabeys. Haplotypes of unclassified *Strongyloides* species were detected only in dogs (Figure 4). The first cluster, consisting of ASV_30, ASV_99, and ASV_191, formed a well-supported branch closely related to *S. venezuelensis*. The second cluster, represented by ASV_183 and ASV_72, grouped between *S. planiceps* and *S. ratti* but with low nodal support. The final lineage, ASV_102, formed a separate, also weakly supported branch positioned between *S. ratti*, *S. procyonis*, and unclassified *Strongyloides* spp. found in Bornean slow lorises. Overall, the median-joining phylogenetic network and Bayesian phylogeny were highly complementary, revealing host-associated divergence in *S. stercoralis* and *S. fuelleborni* and highlighting distinct clustering of unclassified *Strongyloides* taxa.

Differences in *Strongyloides cox1* Communities

cox1 ASV richness differed significantly among the studied hosts (GLM $F_{(4,134)}$ = 253.93; p<0.0001). Tukey

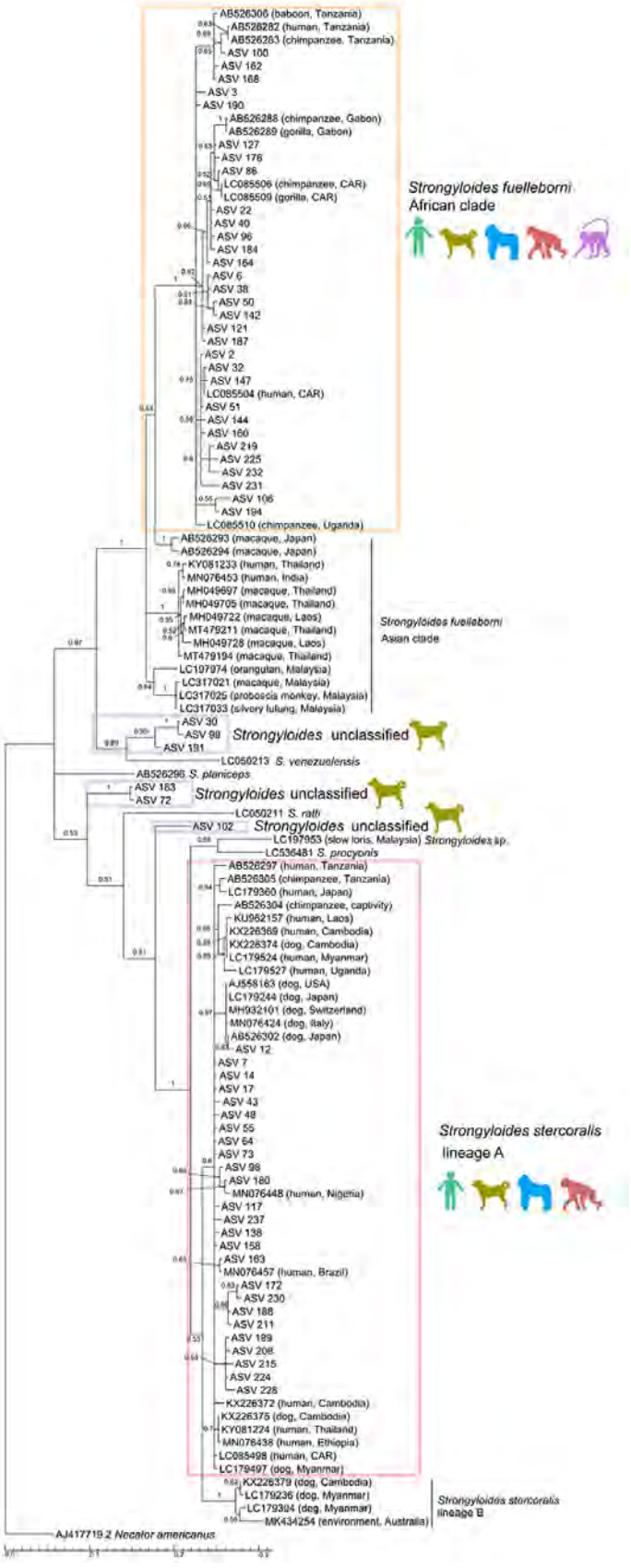

Figure 4. Bayesian phylogenetic tree based on *Strongyloides* spp. *cox1* (700 bp) sequences derived from study of *Strongyloides* genetic diversity among humans, dogs, and nonhuman primates, Dzanga-Sangha Protected Areas, Central African Republic, 2016–2022. Tree also includes sequences downloaded from GenBank; accession numbers are provided. The alignment was performed in Geneious (https://www.geneious.com) using the general time-reversible model of nucleotide substitution with gamma distribution. Branch lengths indicate expected substitutions per site. *Necator americanus* (accession no. AJ417719.2) was included as an outgroup. Node support was estimated from 10^6 iterations. Color silhouettes indicate host species: light green, human; olive green, dog; blue, gorilla; red, chimpanzee; violet, mangabey. Colored boxes indicate species/lineage type. ASV, amplicon sequencing variant; CAR, Central African Republic.

posthoc testing revealed that dogs differed significantly from all other hosts ($p<0.01$ for all pairwise comparisons), whereas mangabeys also differed significantly from humans and gorillas ($p<0.01$) (Figure 2, panel C). We observed no significant differences between the remaining host pairs. The PCoA diagram based on Bray-Curtis ecologic distances further confirmed clear differences between humans, dogs, and NHPs (Figure 2, panel E), supporting the findings of the haplotype network analysis. Those differences in the composition of *Strongyloides* infections between host species were further statistically confirmed by PERMANOVA ($F_{(4,135)} = 11.192$; $p = 0.001$) and ANOSIM ($R = 0.3438$; $p = 0.001$) tests.

Discussion

We investigated *Strongyloides* nematode diversity and haplotype sharing among humans, dogs, and NHPs cohabiting in the DSPA, CAR, to assess zoonotic potential and multihost transmission (*25*). A previous study from the DSPA investigated *Strongyloides* nematodes in humans, gorillas, and chimpanzees, reporting *S. stercoralis* exclusively in humans and identifying different haplotypes of *S. fuelleborni* in gorillas and chimpanzees than those found in humans (*14*). However, that study was limited by a small sample size of larvae and did not include dogs, which are potential hosts. Our study highlights the critical importance of employing modern diagnostic approaches and examining a broader range of hosts from the same locality to better understand *Strongyloides* sharing in the ecosystem.

Our genotyping approach revealed a remarkable degree of genetic diversity within *Strongyloides* species, reflecting the complexity of their populations, and further identified the sharing of specific haplotypes across different host species. Of note, *S. fuelleborni*, likely originating from NHPs, dominated across all hosts; haplotype L was the most prevalent variant. Zoonotic *S. stercoralis* haplotype A was observed primarily in humans, dogs, and gorillas. This variation in prevalence underscores the host-specific transmission dynamics and the role of local ecologic factors in determining *Strongyloides* distribution. Those findings emphasize the need for a One Health approach (*26*) because of the zoonotic potential of *S. stercoralis* nematodes and the species' strong connection to the environment.

Despite the identification of dominant haplotypes, the proportion of *Strongyloides* sequences remains unclassified, highlighting the limitations of short-marker–based phylogenetic inference. Unclassified *S. fuelleborni* haplotypes were detected in all host species except chimpanzees, for which only a limited dataset was available. Those sequences likely reflect previously undetected diversity, because additional haplotypes have been reported with expanded sampling. Given the limited data currently available from sites in Africa (*27*), further haplotypes are expected to emerge as sampling across hosts and regions improves.

Several unclassified ASVs clustered with *S. venezuelensis* with high nodal support, whereas other unclassified ASVs formed clusters with very low support, rendering their classification unreliable. The placement of such lineages, based solely on short *cox1* fragments, is highly challenging, because those sequences might lack sufficient phylogenetically informative sites to resolve relationships among closely related or cryptic taxa. Similar issues have been reported previously (e.g., short *cox1* fragments were insufficient for precise taxonomic resolution of cryptic *Strongyloides* in dogs [*28*]). Therefore, integrating comprehensive genetic data, such as longer mitochondrial sequences or genomic information from individual larvae, with morphological analyses of larvae and adult or paratenic females is crucial for resolving the taxonomy and evolutionary relationships of unclassified *Strongyloides* spp.

We recognize the inherent limitations of single-locus genotyping, because reliance on a single marker provides a restricted representation of genetic diversity and might not reflect genome-wide variation. That limitation means substantially larger host sample sizes are required to achieve the same statistical power and robustness that whole-genome data can provide, because only by averaging across many individuals can stochastical effects at a single locus be mitigated. We also acknowledge that our reliance on fecal DNA, although advantageous as a noninvasive sampling method, can introduce issues related to DNA degradation, contamination, and allelic dropout, further constraining data quality. Thus, our conclusions should be interpreted with caution and viewed as complementary to, rather than a substitute for, genome-wide analyses.

Strongyloides communities were more similar between humans and dogs than between either of those hosts and NHPs. The highest proportion of shared haplotypes was observed between humans and dogs, accounting for 33.3% of all detected ASVs. This pattern supports the involvement of dogs in the circulation of *S. stercoralis* nematodes alongside humans in the DSPA (*5*,*6*). Consistent with this pattern, *S. stercoralis* haplotype A predominated in humans, suggesting that human-associated circulation represents

a key component of *Strongyloides* nematodes occurrence in this setting and that dogs potentially act as secondary hosts.

Unexpectedly, sharing between humans and dogs was also observed for *S. fuelleborni* haplotypes K and M, a species previously considered to circulate primarily in NHPs (*14*). The presence of haplotype M in both humans and dogs, with higher prevalence in dogs, is notable given its limited geographic reporting to date in humans, restricted to Senegal (*21*) and CAR (*14*). The high prevalence in dogs suggests a potential contribution to the environmental dissemination of *S. fuelleborni* nematodes within DSPA, although spurious infections associated with coprophagy cannot be excluded (*29*). Experimental infections of dogs with *S. fuelleborni* nematodes have been demonstrated (*30*), but natural infections remain unconfirmed, and fecal metabarcoding alone cannot resolve the definitive host status of dogs.

ASVs shared between humans and NHPs included *S. stercoralis* haplotype A and *S. fuelleborni* haplotypes K, L, and P, accounting for 16.6% of all observed ASVs; all of those were also detected in dogs. *Strongyloides fuelleborni* haplotype L, which is well established across all studied hosts, was previously reported only in gorillas (*14*) and in African vervets on St. Kitts (*31*). Although its origin remains speculative, its presence across host species suggests extensive host sharing within the DSPA. In contrast, haplotype P was predominantly detected in NHPs, which likely represent a key source of exposure for humans and dogs. Together, these patterns indicate shared circulation of *Strongyloides* nematodes among humans, dogs, and NHPs in the DSPA.

Given the soil-transmitted nature of *Strongyloides* nematodes and the close coexistence of hosts in DSPA, environmental exposure represents a major challenge for disease control (*4*). Although chemotherapy is effective in the short term to treat strongyloidiasis (*32*), high reinfection rates, autoinfection, free-living stages in soil, multiple host species, and emerging concerns about drug resistance complicate long-term elimination, particularly in tropical settings (*33*,*34*), highlighting the need for a comprehensive strategy. A crucial aspect of controlling strongyloidiasis is recognizing the role of wildlife in transmission. Because treating wildlife such as free-ranging NHPs is not feasible, effective control requires a One Health approach that considers humans, domestic animals, and the environment (*26*). Practical measures, including proper latrine use and use of footwear to reduce soil contact, should complement treatment of infected persons (*35*). Ivermectin remains the treatment of choice (*33*), but its use must be carefully considered in regions with high *Loa loa* microfilaremia prevalence (*36*), as in CAR. Overall, the potential for rapid reinfection from multiple hosts underscores the need for integrated control strategies.

In conclusion, the close coexistence of multiple host species sharing *Strongyloides* infections in the DSPA likely contributes to the persistence of the parasite in this environment. Expanding investigations beyond humans to include domestic animals and wildlife is therefore essential, and our findings highlight the relevance of a One Health approach that integrates those host groups (*37*). The observed overlap of *S. stercoralis* and *S. fuelleborni* haplotypes among humans, dogs, and NHPs reflects the complexity of host associations within this ecosystem. By adopting a multihost diagnostic approach, we provide direct insights into *Strongyloides* nematode sharing among hosts in the DSPA, informing more realistic and sustainable control strategies.

Acknowledgments

We would like to express our gratitude to the government of the Central African Republic and the World Wildlife Fund for granting permission to conduct our research; the Ministre de l'Enseignement Supérieur, de la Recherche Scientifique et de l'Innovation Technologique, for providing research permits; and the Primate Habituation Programme for providing logistical support in the field. Finally, yet importantly, we would like to thank all the trackers and assistants in Dzanga-Sangha Protected Areas.

Raw HVR-IV-18S rRNA and *cox1* sequencing data are archived in the European Nucleotide Archive and are available project accession no. PRJEB101217. Accession numbers for each samples are available in Appendix 2 Table 3.

This project was supported by Czech Science Foundation 22-16475S and partially supported by Masaryk University internal grant no. MUNI/A/1602/2023. We acknowledge the CF Genomics supported by the NCMG research infrastructure (LM2023067 funded by MEYS CR) for their support with obtaining scientific data presented in this paper. Computational resources were provided by the e-INFRA CZ project (ID: 90254), supported by the Ministry of Education, Youth and Sports of the Czech Republic.

About the Author

Dr. Nosková is a parasitologist specializing in zoonotic nematodes and parasite transmission between humans, domestic animals, and wildlife. Her research focuses on

the molecular epidemiology, host specificity, and phylogeny of *Strongyloides* spp., with additional experience in veterinary parasitology, paleoparasitology, and wildlife conservation.

References

1. Bradbury RS, Pafčo B, Nosková E, Hasegawa H. *Strongyloides* genotyping: a review of methods and application in public health and population genetics. Int J Parasitol. 2021;51:1153–66. https://doi.org/10.1016/j.ijpara.2021.10.001
2. Asundi A, Beliavsky A, Liu XJ, Akaberi A, Schwarzer G, Bisoffi Z, et al. Prevalence of strongyloidiasis and schistosomiasis among migrants: a systematic review and meta-analysis. Lancet Glob Health. 2019;7:e236–48. https://doi.org/10.1016/S2214-109X(18)30490-X
3. Buonfrate D, Bisanzio D, Giorli G, Odermatt P, Fürst T, Greenaway C, et al. The global prevalence of *Strongyloides stercoralis* infection. Pathogens. 2020;9:468. https://doi.org/10.3390/pathogens9060468
4. Nutman TB. Human infection with *Strongyloides stercoralis* and other related *Strongyloides* species. Parasitology. 2017;144:263–73. https://doi.org/10.1017/S0031182016000834
5. Jaleta TG, Zhou S, Bemm FM, Schär F, Khieu V, Muth S, et al. Different but overlapping populations of *Strongyloides stercoralis* in dogs and humans-dogs as a possible source for zoonotic strongyloidiasis. PLoS Negl Trop Dis. 2017;11:e0005752. https://doi.org/10.1371/journal.pntd.0005752
6. Nagayasu E, Aung MPPTHH, Hortiwakul T, Hino A, Tanaka T, Higashiarakawa M, et al. A possible origin population of pathogenic intestinal nematodes, *Strongyloides stercoralis*, unveiled by molecular phylogeny. Sci Rep. 2017;7:4844. https://doi.org/10.1038/s41598-017-05049-x
7. Gordon CA, Utzinger J, Muhi S, Becker SL, Keiser J, Khieu V, et al. Strongyloidiasis. Nat Rev Dis Primers. 2024;10:6. https://doi.org/10.1038/s41572-023-00490-x
8. Buonfrate D, Requena-Mendez A, Angheben A, Cinquini M, Cruciani M, Fittipaldo A, et al. Accuracy of molecular biology techniques for the diagnosis of *Strongyloides stercoralis* infection-A systematic review and meta-analysis. PLoS Negl Trop Dis. 2018;12:e0006229. https://doi.org/10.1371/journal.pntd.0006229
9. Kuehne A, Roberts L. Learning from health information challenges in the Central African Republic: where documenting health and humanitarian needs requires fresh approaches. Confl Health. 2021;15:68. https://doi.org/10.1186/s13031-021-00405-1
10. United Nations Development Programme. Human development insights [cited 2025 Feb 6]. https://hdr.undp.org/data-center/country-insights#/ranks
11. Blom A, Yamindou J, Prins HHT. Status of the protected areas of the Central African Republic. Biol Conserv. 2004;118:479–87. https://doi.org/10.1016/j.biocon.2003.09.023
12. David PM, Nakouné E, Giles-Vernick T. Hotspot or blind spot? Historical perspectives on surveillance and response to epidemics in the Central African Republic. Int J Public Health. 2020;65:241–8. https://doi.org/10.1007/s00038-020-01338-x
13. Pedersen AB, Davies TJ. Cross-species pathogen transmission and disease emergence in primates. EcoHealth. 2009;6:496–508. https://doi.org/10.1007/s10393-010-0284-3
14. Hasegawa H, Kalousova B, McLennan MR, Modry D, Profousova-Psenkova I, Shutt-Phillips KA, et al. *Strongyloides* infections of humans and great apes in Dzanga-Sangha Protected Areas, Central African Republic and in degraded forest fragments in Bulindi, Uganda. Parasitol Int. 2016;65(5 Pt A):367–70. https://doi.org/10.1016/j.parint.2016.05.004
15. Wolfe ND, Dunavan CP, Diamond J. Origins of major human infectious diseases. Nature. 2007;447:279–83. https://doi.org/10.1038/nature05775
16. World Health Organization. Soil-transmitted helminthiases [cited 2025 Feb 6]. https://www.who.int/data/gho/data/themes/topics/soil-transmitted-helminthiases.
17. Pampiglione S, Ricciardi M. Parasitological survey on Pygmies in Central Africa. I. Babinga group (Central African Republic). Riv Parassitol. 1974;35:161–88.
18. Hasegawa H, Modrý D, Kitagawa M, Shutt KA, Todd A, Kalousová B, et al. Humans and great apes cohabiting the forest ecosystem in Central African Republic harbour the same hookworms. PLoS Negl Trop Dis. 2014;8:e2715. https://doi.org/10.1371/journal.pntd.0002715
19. Verweij JJ, Canales M, Polman K, Ziem J, Brienen EA, Polderman AM, et al. Molecular diagnosis of *Strongyloides stercoralis* in faecal samples using real-time PCR. Trans R Soc Trop Med Hyg. 2009;103:342–6. https://doi.org/10.1016/j.trstmh.2008.12.001
20. Pafčo B, Čížková D, Kreisinger J, Hasegawa H, Vallo P, Shutt K, et al. Metabarcoding analysis of strongylid nematode diversity in two sympatric primate species. Sci Rep. 2018;8:5933. https://doi.org/10.1038/s41598-018-24126-3
21. Barratt JLN, Lane M, Talundzic E, Richins T, Robertson G, Formenti F, et al. A global genotyping survey of *Strongyloides stercoralis* and *Strongyloides fuelleborni* using deep amplicon sequencing. PLoS Negl Trop Dis. 2019;13:e0007609. https://doi.org/10.1371/journal.pntd.0007609
22. Jiang H, Lei R, Ding SW, Zhu S. Skewer: a fast and accurate adapter trimmer for next-generation sequencing paired-end reads. BMC Bioinformatics. 2014;15:182. https://doi.org/10.1186/1471-2105-15-182
23. Callahan BJ, McMurdie PJ, Rosen MJ, Han AW, Johnson AJA, Holmes SP. DADA2: High-resolution sample inference from Illumina amplicon data. Nat Methods. 2016;13:581–3. https://doi.org/10.1038/nmeth.3869
24. Wang Q, Garrity GM, Tiedje JM, Cole JR. Naive Bayesian classifier for rapid assignment of rRNA sequences into the new bacterial taxonomy. Appl Environ Microbiol. 2007;73:5261–7. https://doi.org/10.1128/AEM.00062-07
25. Bradbury RS, Streit A. Is strongyloidiasis a zoonosis from dogs? Philos Trans R Soc Lond B Biol Sci. 2024;379:20220445. https://doi.org/10.1098/rstb.2022.0445
26. Lapat JJ, Opee J, Apio MC, Akello S, Ojul CL, Onekalit R, et al. A One Health approach toward the control and elimination of soil-transmitted helminthic infections in endemic areas. IJID One Health. 2024;2:100021. https://doi.org/10.1016/j.ijidoh.2024.100021
27. Nosková E, Sambucci KM, Petrželková KJ, Červená B, Modrý D, Pafčo B. *Strongyloides* in non-human primates: significance for public health control. Philos Trans R Soc Lond B Biol Sci. 2024;379:20230006. https://doi.org/10.1098/rstb.2023.0006
28. Beknazarova M, Barratt JLN, Bradbury RS, Lane M, Whiley H, Ross K. Detection of classic and cryptic *Strongyloides* genotypes by deep amplicon sequencing: A preliminary survey of dog and human specimens collected from remote Australian communities. PLoS Negl Trop Dis. 2019;13:e0007241. https://doi.org/10.1371/journal.pntd.0007241
29. Nijsse R, Mughini-Gras L, Wagenaar JA, Ploeger HW. Coprophagy in dogs interferes in the diagnosis of parasitic

infections by faecal examination. Vet Parasitol. 2014;204:304–9. https://doi.org/10.1016/j.vetpar.2014.05.019
30. Sandground JH. Biological studies on the life-cycle in the genus *Strongyloides grassi*, 1879. Am J Epidemiol. 1926;6:337–88. https://doi.org/10.1093/oxfordjournals.aje.a120018
31. Richins T, Sapp SGH, Ketzis JK, Willingham AL, Mukaratirwa S, Qvarnstrom Y, et al. Genetic characterization of *Strongyloides fuelleborni* infecting free-roaming African vervets (*Chlorocebus aethiops sabaeus*) on the Caribbean island of St. Kitts. Int J Parasitol Parasites Wildl. 2023;20:153–61. https://doi.org/10.1016/j.ijppaw.2023.02.003
32. Alum A, Rubino JR, Ijaz MK. The global war against intestinal parasites—should we use a holistic approach? Int J Infect Dis. 2010;14:e732–8. https://doi.org/10.1016/j.ijid.2009.11.036
33. Horton J. Global anthelmintic chemotherapy programs: learning from history. Trends Parasitol. 2003;19:405–9. https://doi.org/10.1016/S1471-4922(03)00171-5
34. White MAF, Whiley H, Ross KE. A review of *Strongyloides* spp. environmental sources worldwide. Pathogens. 2019;8:8.
35. Khieu V, Hattendorf J, Schär F, Marti H, Char MC, Muth S, et al. *Strongyloides stercoralis* infection and re-infection in a cohort of children in Cambodia. Parasitol Int. 2014;63:708–12. https://doi.org/10.1016/j.parint.2014.06.001
36. Kamgno J, Boussinesq M, Labrousse F, Nkegoum B, Thylefors BI, Mackenzie CD. Encephalopathy after ivermectin treatment in a patient infected with *Loa loa* and *Plasmodium* spp. Am J Trop Med Hyg. 2008;78:546–51. https://doi.org/10.4269/ajtmh.2008.78.546
37. Zinsstag J, Kaiser-Grolimund A, Heitz-Tokpa K, Sreedharan R, Lubroth J, Caya F, et al. Advancing One human-animal-environment Health for global health security: what does the evidence say? Lancet. 2023;401:591–604. https://doi.org/10.1016/S0140-6736(22)01595-1

Address for correspondence: Barbora Pafčo, Czech Academy of Sciences, Institute of Vertebrate Biology, Květná 8, Brno 603 00, Czech Republic; email: pafco@ivb.cz

Blastomyces Urine Antigen Testing for Active Case Identification During a Blastomycosis Outbreak

Allyson W. O'Connor,[1] Ian Hennessee,[1] Perri C. Callaway, Marcia L. Stanton, Xiaoming Liang, Ju-Hyeong Park, Ryan LeBouf, Rachel L. Bailey, Rebecca Reik, Mary Grace Stobierski, Michael Snyder, Robert Yin, Mitsuru Toda, Jean Cox-Ganser, Stella E. Hines

In support of improving patient care, this activity has been planned and implemented by Medscape, LLC and Emerging Infectious Diseases. Medscape, LLC is jointly accredited with commendation by the Accreditation Council for Continuing Medical Education (ACCME), the Accreditation Council for Pharmacy Education (ACPE), and the American Nurses Credentialing Center (ANCC), to provide continuing education for the healthcare team.

Medscape, LLC designates this Journal-based CME activity for a maximum of 1.00 ***AMA PRA Category 1 Credit(s)™***. Physicians should claim only the credit commensurate with the extent of their participation in the activity.

Successful completion of this CME activity, which includes participation in the evaluation component, enables the participant to earn up to 1.0 MOC points in the American Board of Internal Medicine's (ABIM) Maintenance of Certification (MOC) program. Participants will earn MOC points equivalent to the amount of CME credits claimed for the activity. It is the CME activity provider's responsibility to submit participant completion information to ACCME for the purpose of granting ABIM MOC credit.

All other clinicians completing this activity will be issued a certificate of participation. To participate in this journal CME activity: (1) review the learning objectives and author disclosures; (2) study the education content; (3) take the post-test with a 75% minimum passing score and complete the evaluation at https://www.medscape.org/qna/processor/76906?isAspenArticle=true&src=prt_jcme_eid_mscpedu; and (4) view/print certificate. For CME questions, see page 476.

NOTE: It is the policy of Medscape Education to avoid the mention of brand names or specific manufacturers in accredited educational activities. However, trade and manufacturer names in this activity are provided in an effort to provide clarity. The use of brand or manufacturer names should not be viewed as an endorsement by Medscape of any specific product or manufacturer.

Release date: March 19, 2026; Expiration date: March 19, 2027

Learning Objectives

Upon completion of this activity, participants will be able to:

- Describe the presentation of blastomycosis
- Assess different testing modalities for blastomycosis
- Analyze the performance of urine antigen testing for *Blastomyces* in the current study
- Evaluate variables that affect the positivity rate of urine antigen testing for *Blastomyces*

CME Editor

Bryce Simons, MPH, Technical Writer/Editor, Emerging Infectious Diseases. *Disclosure: Bryce Simons, MPH, has no relevant financial relationships.*

CME Author

Charles P. Vega, MD, Health Sciences Clinical Professor of Family Medicine, University of California, Irvine School of Medicine, Irvine, California. *Disclosure: Charles P. Vega, MD, has the following relevant financial relationships: served as consultant or advisor for Boehringer Ingelheim; Exact Sciences.*

Authors

Allyson W. O'Connor, PhD; Ian Hennessee, PhD; Perri C. Callaway, PhD; Marcia L. Stanton, BS; Xiaoming Liang, MS; Ju-Hyeong Park, ScD; Ryan LeBouf, PhD; Rachel L. Bailey, DO; Rebecca Reik, MPH; Mary Grace Stobierski, DVM; Michael Snyder, RS, MPA; Robert Yin, MD; Mitsuru Toda, PhD, MS; Jean Cox-Ganser, PhD; Stella E. Hines, MD, MSPH.

Blastomyces urine antigen testing is a sensitive blastomycosis diagnostic method, but its utility for active case identification during outbreaks is unknown. We evaluated urine antigen testing for identifying blastomycosis cases during a 2023 outbreak at a Michigan, USA, paper mill and assessed demographic and clinical factors associated with test positivity. Approximately 2 months after the outbreak was recognized, we collected work and health information for 603 employees; 95% (n = 578) underwent urine antigen testing and 9% (n = 52) tested positive, including 25 previously undetected cases. Blastomycosis-like symptoms were associated with test positivity (p<0.001), but 10% of employees with positive results were asymptomatic. Recent hospitalization for blastomycosis was associated with test positivity (p = 0.02) and higher antigen levels. Further research into urine antigen testing is needed to clarify its suitability for detecting mild and asymptomatic infections during outbreak investigations. Urine antigen testing had high acceptability among employees and effectively identified additional cases.

Blastomycosis is an environmentally acquired fungal disease caused by *Blastomyces* spp. Pulmonary and systemic manifestations such as cough, chest pain, and fever are the most common (*1*). Blastomycosis is often misdiagnosed, which can lead to inappropriate antibiotic drug use and increased use of healthcare services (*2*). Early detection and treatment can improve patient outcomes, particularly in immunocompromised patients with an elevated risk for severe disease (*3*).

Blastomycosis can be severe; a substantial proportion of cases reported through public health surveillance require hospitalization (*4*,*5*). However, an estimated 50% of infections are asymptomatic (*6*). Detecting asymptomatic infections is necessary for assessing exposure sources during outbreaks (*6*,*7*). Infections may be presymptomatic, and thus hard to detect, given the disease's long incubation period of 2 weeks to 3 months (*6*,*8*), and reactivation of latent infections can occur after subsequent immunosuppression (*9*).

In 2023, a large outbreak of blastomycosis caused by *Blastomyces gilchristii* occurred among employees at a paper mill in northern Michigan, USA (*10*). A total of 162 cases were identified over the course of the outbreak, with a case prevalence of almost 20% among the mill employees (*11*). As part of a multiagency response, the National Institute for Occupational Safety and Health (NIOSH) led a workplace evaluation and medical survey in late April 2023 that offered *Blastomyces* urine antigen testing to all mill employees and contractors (*11*,*12*). The aim was to identify previously undiagnosed cases among employees and to assess *Blastomyces* exposure to determine potential locations and activities within the mill where exposure might have occurred.

Exposure assessments during blastomycosis outbreaks traditionally evaluate immune responses against the fungus by serologic or skin testing (*6*,*7*,*13*–*15*). However, skin tests are no longer widely available, and most serologic tests have low sensitivity (*16*). Although a newly approved enzyme immunoassay antibody test offers improved sensitivity for serologic testing (*17*), it is unclear how long antibodies remain in blood, making it challenging to distinguish recent infections from historical exposures in endemic areas (*18*). Blood collection poses financial and logistical constraints for large-scale exposure assessments, requiring trained phlebotomists, attention to biosafety concerns, and intensive laboratory processing. Further, participant consent for blood collection during outbreak investigations can be lower than for other specimen types (*19*).

Blastomyces urine antigen testing has high sensitivity in symptomatic populations (*16*). Urine samples are easier to collect and process than blood, and urine has generally higher consent rates for sampling. Antigen levels can remain detectable in urine for months after infection (*20*), but antigen levels decline quicker than serum antibodies (*21*). Therefore, positive urine antigen tests might more accurately reflect recent infections, especially when used in endemic areas with potentially elevated background antibody levels among the population. The test also has high specificity, except for substantial cross-reactivity with *Histoplasma* and other fungal pathogens (*22*). The test can have cross-reactivity with other fungal pathogens because it targets galactomannan, a fungal cell wall component common to multiple fungal pathogens. However, cross-reactivity is of less importance in outbreak settings where patients share common exposures to a known fungal pathogen. In this outbreak, 15 cases were confirmed by

Author affiliations: Centers for Disease Control and Prevention, Morgantown, West Virginia, USA (A.W. O'Connor, P.C. Callaway, M.L. Stanton, X. Liang, J.-H. Park, R. LeBouf, R.L. Bailey, J. Cox-Ganser, S.E. Hines); Centers for Disease Control and Prevention, Atlanta, Georgia, USA (I. Hennessee, P.C. Callaway, M. Toda); Michigan Department of Health and Human Services, Lansing, Michigan, USA (R. Reik, M.G. Stobierski); Public Health Delta & Menominee Counties, Escanaba, Michigan, USA (M. Snyder, R. Yin)

DOI: https://doi.org/10.3201/eid3203.250973

[1]These first authors contributed equally to this article.

culture, and whole-genome sequencing of *Blastomyces* isolates from 8 patients revealed strong phylogenetic relatedness (*10*).

We used *Blastomyces* urine antigen testing for the medical survey because of its high sensitivity, higher likelihood of worker participation, and convenience. However, little is known about the test's effectiveness in identifying new cases during an outbreak. Using the medical survey results, we evaluated the performance of urine antigen testing in actively identifying potential blastomycosis cases without a recent diagnosis or with few or no symptoms and identified demographic and clinical factors associated with *Blastomyces* antigen test positivity.

Methods

Data and Population

All mill employees and contractors were invited to participate in NIOSH's medical survey during April 22–28, 2023, approximately 2 months after the first outbreak cases were recognized. The survey included an interviewer-administered work and health questionnaire and *Blastomyces* urine antigen testing (*12*). We sought written informed consent before participation in the medical survey and antigen testing. Of nearly 1,000 mill employees, 608 completed the survey. Among those who completed the survey, 95% (n = 578) underwent urine testing. We excluded 5 records because of missing or incomplete questionnaire data; 94% (n = 573) employees were included in urine antigen testing analyses. Previous reports describe the outbreak response and clinical characteristics of cases in detail (*10*,*11*). We supplemented survey data with case information collected by the Michigan Department of Health and Human Services (MDHHS) and the local health department through routine surveillance and case interviews. MDHHS relied on a modified version of the national surveillance standard case definition for blastomycosis to classify outbreak-associated blastomycosis cases on the basis of clinical and laboratory criteria (*10*).

Urine Antigen Testing

We refrigerated urine samples collected during the NIOSH survey and then sent the samples to a commercial laboratory for analysis using the MiraVista quantitative *Blastomyces* antigen enzyme immunoassay test (*22*). At the time of the survey, the test's quantifiable range for *Blastomyces* antigen was 0.2–14.7 ng/mL, within which antigen levels were reliably quantified. Positive results included any test with detectable antigen levels, including detectable levels that were below the lower limit of quantification (LLOQ) of 0.2 ng/mL and those within or above the quantifiable range. Tests with results below the LLOQ are not considered cases by standard surveillance case definition laboratory criteria, but we counted them as positive results in the modified outbreak case definition. We considered tests with no antigen detected negative. We mailed results to employees and their authorized healthcare providers; positive results were also communicated to employees by phone. Employees with positive results, including those with few or no symptoms, were encouraged to discuss their results with their healthcare providers.

Questionnaire Data

The interviewer-administered NIOSH questionnaire gathered work and health information from mill employees. We collected information on demographic characteristics, including age and sex, and clinical characteristics, including self-reported symptoms and medical findings, hospitalization and antifungal medication use, and history of potentially immunocompromising health conditions. The questionnaire sought information about symptoms including cough, fever or chills or night sweats, shortness of breath, poor appetite or weight loss, muscle aches or pain, joint or bone pain, and fatigue. We considered employees who did not report any of those symptoms asymptomatic. Medical findings included abnormal lung findings on chest imaging, skin lesions, brain inflammation, abscess, granuloma, other lesions, and bone or joint abnormalities. We collected information on reported symptoms and medical findings that were clinically compatible (*23*) with blastomycosis since October 1, 2022, the earliest date of possible exposure on the basis of available case information. We excluded reported symptoms and medical findings that occurred within 2 weeks of a self-reported COVID-19, influenza, or respiratory syncytial virus illness. We also collected self-reported information on potential immunocompromising conditions, including diabetes, autoimmune diseases, taking immunosuppressive medication, and history of an organ or stem cell transplant.

We classified employees as having a recent diagnosis of blastomycosis during the outbreak if they were listed as having a confirmed or probable case of blastomycosis on the MDHHS case list as of April 21, 2023, or if they self-reported a healthcare provider diagnosis since October 1, 2022, on the NIOSH questionnaire. We asked employees with recent blastomycosis diagnoses if they were hospitalized

for their recent illness and if they had initiated antifungal drug treatment.

Data Analysis

We summarized worker characteristics, including recent blastomycosis diagnoses during the outbreak, by urine antigen test positivity. We then assessed associations between clinical characteristics and test positivity among all participants who underwent testing and among employees with a recent blastomycosis diagnosis during the outbreak. We also examined clinical characteristics by antigen levels (below the LLOQ vs. within or above the quantifiable range) among employees with positive tests. We evaluated bivariate associations between worker or clinical characteristics and test positivity by using Wilcoxon rank sum tests for continuous variables (to compare the medians) and Pearson's χ^2 or Fisher exact tests for categorical variables, with 2-sided p values of 0.05 indicating statistical significance. We did not assess statistical associations for antigen levels because of the small numbers in this analysis.

We conducted statistical analyses by using SAS software version 9.4 (SAS Institute, Inc.). This activity was reviewed by the Centers for Disease Control and Prevention, was deemed not research, and was consistent with applicable federal law and Centers for Disease Control and Prevention policy.

Results

Among 573 employees who underwent *Blastomyces* urine antigen testing during the medical survey period, the median age was 47 years (interquartile range [IQR] 38–53 years); 82% were male and 18% female, and 12% had a recent diagnosis of blastomycosis during the outbreak (Table 1). Of the 573 employees, 52 (9%) received positive *Blastomyces* antigen test results; there were no significant differences in test positivity by age (p = 0.42) or sex (p = 0.61). A recent diagnosis of blastomycosis during the outbreak was associated with test positivity (p<0.001); of 71 participants with a recent diagnosis, 27 (38%) tested positive. In addition, 25 (48%) of 52 employees who tested positive were previously undiagnosed.

Among the 573 survey participants, 67% reported symptoms, and the number of symptoms differed significantly by test positivity (p<0.001). Among 52 employees with positive tests, 90% reported ≥1 symptom, compared with 65% of 521 employees who tested negative; 10% of test-positive employees were asymptomatic (Table 2). Four of the 5 asymptomatic cases were from previously undiagnosed employees (data not shown). Reporting any medical findings was also more common among test-positive employees (46%) than test-negative employees (13%; p<0.001). All individual blastomycosis-associated symptoms (e.g., cough, fever, shortness of breath) and medical findings (e.g., abnormal lung imaging) were also more common among test-positive employees (p<0.05) (Appendix Table 1, http://wwwnc.cdc.gov/EID/article/32/3/25-0973-App1.pdf). Immunocompromising conditions were not associated with test positivity for employees in the survey (p = 0.58).

Among 71 employees with a recent diagnosis of blastomycosis, 93% reported ≥1 symptom, and 77% reported ≥1 medical finding (Table 2). Unlike in the full survey population, the number of symptoms (p = 0.75) or medical findings (p = 0.96) did not differ significantly by test positivity among those employees. There was no statistical difference in the median time from symptom onset to the survey urine antigen testing between test-positive employees (47 days, IQR 31–70 days) and test-negative employees (52 days, IQR 40–69 days; p = 0.32). Sixty-five (93%) employees initiated antifungal treatment a median of 31 (IQR 18–41) days before survey testing. Neither treatment initiation (p = 0.64) nor time from initiation to testing during the survey (p = 0.36) were

Table 1. Characteristics of employees by UAT result from a medical survey conducted in a study of *Blastomyces* urine antigen testing for active case identification during a blastomcoysis outbreak, United States*

Characteristic	Total, n = 573	Positive UAT, n = 52	Negative UAT, n = 521	p value†
Median age, years (IQR)	47 (38–53)	46 (38–53)	47 (38–54)	0.42
Sex				
M	470 (82)	44 (85)	426 (82)	0.61
F	103 (18)	8 (15)	95 (18)	
Recent blastomycosis diagnosis‡				
Yes	71 (12)	27 (52)	44 (8)	<0.001
No	502 (88)	25 (48)	477 (92)	

*Values are no. (%) except as indicated. Numbers might not reach column total because of missing responses. UAT, urine antigen test; IQR, interquartile range.
†Wilcoxon rank sum tests for continuous variables and Pearson χ^2 tests or Fisher exact tests for categorical variables were used to test differences by urine antigen test result.
‡Recent diagnosis of blastomycosis included employees the Michigan Department of Health and Human Services identified as having confirmed or probable blastomycosis during the paper mill outbreak as of April 21, 2023, or self-reported healthcare provider-diagnosed blastomycosis on the medical survey questionnaire.

Table 2. Clinical factors by UAT result among employees from a medical survey conducted in a study of *Blastomyces* urine antigen testing for active case identification during a blastomycosis outbreak, United States*

	All employees				Employees with recent blastomycosis diagnosis‡			
Clinical factor	Total, n = 573	Positive UAT, n = 52	Negative UAT, n = 521	p value†	Total, n = 71	Positive UAT, n = 27	Negative UAT, n = 44	p value†
No. symptoms potentially related to blastomycosis								
0	184 (32)	5 (10)	179 (34)	<0.001	4 (6)	1 (4)	3 (7)	0.75
1	156 (27)	5 (10)	151 (29)		5 (7)	1 (4)	4 (9)	
≥2	231 (40)	42 (81)	189 (36)		62 (87)	25 (93)	37 (84)	
No. medical findings potentially related to blastomycosis								
0	479 (84)	28 (54)	451 (87)	<0.001	16 (23)	6 (22)	10 (23)	0.96
≥1	92 (16)	24 (46)	68 (13)		55 (77)	21 (78)	34 (77)	
Days from symptom onset to test, median (IQR)§	NA	NA	NA	NA	48 (39–69)	47 (31–70)	52 (40–69)	0.32
Potentially immunocompromised¶								
Yes	64 (11)	7 (13)	57 (11)	0.58	13 (18)	6 (22)	7 (16)	0.54
No	509 (89)	45 (87)	464 (89)		58 (82)	21 (78)	37 (84)	
Pneumonia diagnosis								
Yes	26 (5)	8 (15)	18 (3)	0.001	17 (24)	7 (26)	10 (23)	0.76
No	543 (95)	44 (85)	499 (97)		54 (76)	20 (74)	34 (77)	
Hospitalized for blastomycosis§								
Yes	NA	NA	NA		11 (16)	8 (31)	3 (7)	0.02
No	NA	NA	NA		58 (84)	18 (69)	40 (93)	
Antifungal drugs initiated§								
Yes	NA	NA	NA		65 (93)	25 (96)	40 (91)	0.64
No	NA	NA	NA		5 (7)	1 (4)	4 (9)	
Days from antifungal drug initiation to antigen test, median (IQR)§	NA	NA	NA		31 (18–41)	29 (13–41)	33 (22–40)	0.36

*Values are no. (%) except as indicated. Numbers might not reach column total because of missing responses. UAT, urine antigen test; IQR, interquartile range; NA, not applicable.
†Wilcoxon rank sum tests for continuous variables and Pearson χ^2 tests or Fisher exact tests for categorical variables were used to test differences by urine antigen test result.
‡Recent diagnosis of blastomycosis included employees the Michigan Department of Health and Human Services identified as having confirmed or probable blastomycosis during the paper mill outbreak as of April 21, 2023, or self-reported healthcare provider-diagnosed blastomycosis on the NIOSH medical survey questionnaire.
§Data were only collected for employees with a recent diagnosis of blastomycosis (n = 71) during the outbreak and thus not available for all employees.
¶Potentially immunocompromised was defined as reporting diabetes, an autoimmune disease, taking immunosuppressive medication, or an organ transplant.

associated with test positivity. Recent hospitalization for blastomycosis was associated with test positivity (p = 0.02); among 27 recently diagnosed employees with positive tests, 31% reported hospitalization, compared with 7% of 44 recently diagnosed employees who tested negative.

Among the 52 employees with positive tests, 17 (33%) employees had *Blastomyces* antigen results below the LLOQ (<0.2 ng/mL) and 35 (67%) employees had results within or above the quantifiable range (0.2–14.7 ng/mL) (Table 3). Three (18%) of 17 employees with results below the LLOQ reported no symptoms, and another 3 (18%) only reported 1 symptom. Among 35 employees with results within or above the quantifiable range, 2 (6%) were asymptomatic and another 2 (6%) only reported 1 symptom. For test-positive employees reporting symptoms, median time from symptom onset to testing was similar for employees with positive tests below the LLOQ (49 days, IQR 37–70 days) and within or above the quantifiable range (45 days, IQR 23–70 days). Of the 17 employees with results below the LLOQ, 8 employees reported having initiated antifungal drug treatment, whereas the remaining 9 were not asked about treatment because they had no prior blastomycosis diagnosis. The 8 test-positive employees with recent blastomycosis diagnoses who reported recent hospitalization all had test results within or above the quantifiable range, representing 28% of employees with results within or above the quantifiable range. None of the 17 employees with results below the LLOQ reported recent hospitalization.

Discussion

Our investigation used *Blastomyces* urine antigen testing to actively identify unknown or asymptomatic cases during a blastomycosis outbreak. The test successfully identified additional cases; nearly half the positive results came from employees without recent blastomycosis diagnoses during the outbreak. The 25 new cases identified through urine antigen testing, including cases in 4 employees who were asymptomatic, accounted for 15% of 162 cases ultimately identified during the outbreak. Urine antigen testing increased case identification beyond routine surveillance and contributed to a comprehensive outbreak investigation (*11*,*12*). Test acceptability was high,

with 95% of employees who completed the survey questionnaire also consenting to testing.

Although urine antigen testing identified undiagnosed symptomatic cases, it appeared less effective for identifying asymptomatic infections. *Blastomyces* urine antigen tests were not originally developed to detect *Blastomyces* infection in asymptomatic persons, and our findings suggest their utility in this context might be limited. Only 10% of employees with positive urine antigen tests during this evaluation were asymptomatic, whereas several prior investigations that used testing for specific immune responses estimated that ≈50% of *Blastomyces* infections are asymptomatic (*6*,*24*–*26*).

The lower-than-expected proportion of asymptomatic employees with positive tests suggests that urine antigen testing might be less sensitive than immunological testing for identifying asymptomatic or mild infections. Previous studies reported lower sensitivity and lower antigen levels among patients with mild disease compared with patients with more severe disease (*10*,*27*–*29*). Those data align with our findings that fewer employees reporting no symptoms or a single symptom had positive tests and antigen levels within or above the quantifiable range compared with those who had ≥2 symptoms. In addition, employees who were hospitalized for blastomycosis during the outbreak, an indicator of more severe disease, more frequently had test results within or above the quantifiable range compared with those who were not hospitalized.

Several factors related to the timing of testing could also explain the lower-than-expected rate of asymptomatic infections identified through urine antigen tests. *Blastomyces* exposures likely occurred over several months during this outbreak, peaking in January or February 2023 (*11*). For some employees, antigen levels might have declined by the time urine antigen testing was offered in late April; ≈80% of confirmed and probable cases reported to MDHHS had initial positive urine antigen tests (*10*), whereas only 38% of employees with recent diagnoses tested positive during this survey. However, we did not have information on what type of testing employees who self-reported recent blastomycosis diagnoses received, which limited our ability to directly assess declining antigen levels among this group. Antigen levels might have declined particularly quickly in employees with mild or asymptomatic infections, as antigen levels are positively associated with disease severity, and declining antigen levels correlate with clinical improvement (*20*,*30*). In contrast, all hospitalized employees with recent blastomycosis

Table 3. Clinical factors by UAT levels for employees with positive tests from the medical survey conducted in a study of urine *Blastomyces* antigen testing for active case identification during an outbreak, United States*

	Positive UAT result, n = 52	
Clinical factor	Below LLOQ, n = 17	Within or above quantifiable range, n = 35
No. symptoms potentially related to blastomycosis		
0	3 (18)	2 (6)
1	3 (18)	2 (6)
≥2	11 (65)	31 (89)
No. medical findings potentially related to blastomycosis		
0	10 (59)	18 (51)
≥1	7 (41)	17 (49)
Days from symptom onset to test, median (IQR)†	49 (37–70)	45 (23–70)
Potentially immunocompromised‡		
Yes	2 (12)	5 (14)
No	15 (88)	30 (86)
Had a recent blastomycosis diagnosis		
Yes	8 (47)	19 (54)
No	9 (53)	16 (46)
Pneumonia diagnosis		
Yes	2 (12)	6 (17)
No	15 (88)	29 (83)
Hospitalized for blastomycosis†		
Yes	0	8 (28)
No	17 (100)	21 (72)
Antifungal drug initiated†		
Yes	8 (100)	17 (94)
No	0	1 (6)
Days from antifungal drug initiation to antigen test, median (IQR)†	25 (15–38)	31 (13–43)

*Values are no. (%) except as indicated. Numbers might not reach column total because of missing responses. LLOQ was 0.2 ng/mL, quantifiable range was 0.2–14.7 ng/mL. UAT, urine antigen test; LLOQ, lower limit of quantification.
†Data were only collected for employees with a recent diagnosis of blastomycosis during the outbreak (n = 71) and thus not available for all employees.
‡Potentially immunocompromised was defined as reporting diabetes, an autoimmune disease, taking immunosuppressive medication, or an organ transplant.

diagnoses who tested positive in the survey had results within or above the quantifiable range at the time of the survey. It is also unknown whether sustained exposure over several months affects progression or detectability of antigenuria compared with shorter-term exposure.

Antigen levels might have also declined more rapidly in employees taking antifungal drugs; 93% of employees with recent diagnoses during the outbreak had received antifungal drugs. A previous study reported initial spikes in antigen levels ≈11 days after antifungal drug treatment and declining antigen levels in the following months, although the median time to first negative result was 200 days (*20*). We did not find an association between antigen test positivity during the survey and antifungal drug treatment or days from antifungal drug treatment initiation to testing, but we were likely limited in the power to detect any associations, because only 5 employees with recent diagnoses had not received antifungal drugs. Although no employees reported having a prior blastomycosis diagnosis before the outbreak, prior exposure or undiagnosed infections could have conferred immunity and influenced antigen levels in this population.

An alternative explanation to the low observed rate of asymptomatic infections could be that we overestimated the number of symptomatic employees. We collected symptom information over a 7-month period on the questionnaire. Although we excluded symptoms related to self-reported respiratory infections, such as COVID-19 or influenza, we might have attributed reported symptoms to blastomycosis when they were because of another illness. Another limitation was that this outbreak occurred in a relatively healthy cohort of employees, which might limit the generalizability of our findings to other populations. Although we did not detect an association between test positivity and potential immunocompromise, our cohort included few employees with immunocompromising conditions; however, we did not have complete information for conditions such as HIV or malignancy, which are associated with increased blastomycosis risk (*3*). Last, heightened awareness of the outbreak among employees at the mill and the local healthcare community likely led to early identification of more cases, including less severe ones, than standard public health surveillance (*10*). Early care seeking and treatment could have reduced the overall severity of cases in this outbreak and potentially influenced urine antigen test positivity rates.

In conclusion, our findings suggest urine antigen testing might be less effective for detecting asymptomatic infections during investigations where exposure assessment is the primary goal. In such situations, serologic testing might be a better choice, but longitudinal studies comparing methods for detecting asymptomatic and mild infections over several months after exposure are needed to help clarify this consideration. Despite being potentially less effective for asymptomatic testing, our findings do indicate that *Blastomyces* urine antigen testing is a viable option for actively identifying cases during future blastomycosis outbreaks, in part because of its logistical ease and high acceptability compared with methods that rely on blood collection. Urine antigen testing might be particularly advantageous when used during outbreaks within a large exposed population (*11*).

Acknowledgments

We thank the mill management, unions, and employees for their participation in the medical survey. We also extend our gratitude to Public Health Delta and Menominee and the Michigan Department of Health and Human Services for providing data, as well as to Public Health Delta and Menominee for their assistance with urine antigen testing. We thank Caroline Groth for reviewing this manuscript. We also thank the members of the Michigan blastomycosis outbreak investigation team for their work with this outbreak, including Sara Palmer, Jevon McFadden, R. Reid Harvey, Anne Foreman, Suzanne Tomasi, Ethan Fechter-Leggett, David N. Weissman, Dallas Shi, Marie A. de Perio, and Ana P. Litvintseva.

About the Author

Dr. O'Connor is an epidemiologist with the Department of Veterans Affairs whose research focuses on occupational respiratory conditions. Dr. Hennessee is an epidemiologist with the Carter Center's river blindness, lymphatic filariasis, schistosomiasis, and malaria program whose research focuses on epidemiology, prevention, and control of environmentally mediated infectious diseases.

References

1. Linder KA, Kauffman CA, Miceli MH. Blastomycosis: a review of mycological and clinical aspects. J Fungi (Basel). 2023;9:117. https://doi.org/10.3390/jof9010117
2. Alpern JD, Bahr NC, Vazquez-Benitez G, Boulware DR, Sellman JS, Sarosi GA. Diagnostic delay and antibiotic overuse in acute pulmonary blastomycosis. Open Forum Infect Dis. 2016;3:ofw078. https://doi.org/10.1093/ofid/ofw078
3. McBride JA, Sterkel AK, Matkovic E, Broman AT, Gibbons-Burgener SN, Gauthier GM. Clinical manifestations and outcomes in immunocompetent and immunocompromised patients with blastomycosis. Clin Infect Dis. 2021;72:1594–602. https://doi.org/10.1093/cid/ciaa276

4. Benedict K, Hennessee I, Gold JAW, Smith DJ, Williams S, Toda M. Blastomycosis-associated hospitalizations, United States, 2010–2020. J Fungi (Basel). 2023;9:867. https://doi.org/10.3390/jof9090867
5. Williams SL, Smith DJ, Benedict K, Ahlers JR, Austin C, Birn R, et al. Surveillance for coccidioidomycosis, histoplasmosis, and blastomycosis during the COVID-19 pandemic—United States, 2019–2021. MMWR Morb Mortal Wkly Rep. 2024;73:239–44. https://doi.org/10.15585/mmwr.mm7311a2
6. Klein BS, Vergeront JM, Weeks RJ, Kumar UN, Mathai G, Varkey B, et al. Isolation of *Blastomyces dermatitidis* in soil associated with a large outbreak of blastomycosis in Wisconsin. N Engl J Med. 1986;314:529–34. https://doi.org/10.1056/NEJM198602273140901
7. Caceres DH, Chiller T, Lindsley MD. Immunodiagnostic assays for the investigation of fungal outbreaks. Mycopathologia. 2020;185:867–80. https://doi.org/10.1007/s11046-020-00452-x
8. Chapman SW, Dismukes WE, Proia LA, Bradsher RW, Pappas PG, Threlkeld MG, et al.; Infectious Diseases Society of America. Clinical practice guidelines for the management of blastomycosis: 2008 update by the Infectious Diseases Society of America. Clin Infect Dis. 2008;46:1801–12. https://doi.org/10.1086/588300
9. Pappas PG, Pottage JC, Powderly WG, Fraser VJ, Stratton CW, McKenzie S, et al. Blastomycosis in patients with the acquired immunodeficiency syndrome. Ann Intern Med. 1992;116:847–53. https://doi.org/10.7326/0003-4819-116-10-847
10. Hennessee I, Palmer S, Reik R, Miles-Jay A, Nawaz MY, Blankenship HM, et al.; Michigan Blastomycosis Outbreak Investigation Team. Epidemiological and clinical features of a large blastomycosis outbreak at a paper mill in Michigan. Clin Infect Dis. 2025;80:356–63. https://doi.org/10.1093/cid/ciae513
11. Harvey RR, O'Connor AW, Stanton ML, Park J-H, Shi D, Callaway PC, et al. Outbreak of blastomycosis among paper mill workers—Michigan, November 2022–May 2023. MMWR Morb Mortal Wkly Rep. 2025;73:1157–62. https://doi.org/10.15585/mmwr735152a2
12. O'Connor AW, Park J-H, Stanton ML, Liang X, Shi D, Callaway PC, et al.; Michigan Blastomycosis Outbreak Investigation Team. Assessment of environmental risk factors for blastomycosis during a large outbreak at a Michigan paper mill. PLoS One. 2025;20:e0332398. https://doi.org/10.1371/journal.pone.0332398
13. Klein BS, Vergeront JM, DiSalvo AF, Kaufman L, Davis JP. Two outbreaks of blastomycosis along rivers in Wisconsin. Isolation of *Blastomyces dermatitidis* from riverbank soil and evidence of its transmission along waterways. Am Rev Respir Dis. 1987;136:1333–8. https://doi.org/10.1164/ajrccm/136.6.1333
14. Klein BS, Vergeront JM, Kaufman L, Bradsher RW, Kumar UN, Mathai G, et al. Serological tests for blastomycosis: assessments during a large point-source outbreak in Wisconsin. J Infect Dis. 1987;155:262–8. https://doi.org/10.1093/infdis/155.2.262
15. Baumgardner DJ, Burdick JS. An outbreak of human and canine blastomycosis. Rev Infect Dis. 1991;13:898–905. https://doi.org/10.1093/clinids/13.5.898
16. Linder KA, Kauffman CA. Current and new perspectives in the diagnosis of blastomycosis and histoplasmosis. J Fungi (Basel). 2020;7:12. https://doi.org/10.3390/jof7010012
17. Richer SM, Smedema ML, Durkin MM, Brandhorst TT, Hage CA, Connolly PA, et al. Development of a highly sensitive and specific blastomycosis antibody enzyme immunoassay using *Blastomyces dermatitidis* surface protein BAD-1. Clin Vaccine Immunol. 2014;21:143–6. https://doi.org/10.1128/CVI.00597-13
18. Segaloff HE, Wu K, Williams SL, Shaw S, Miko S, Parnell LA, et al. Human and canine blastomycosis cases associated with riverside neighborhood, Wisconsin, USA, December 2021–March 2022. Emerg Infect Dis. 2024;30:2633–8. https://doi.org/10.3201/eid3012.240390
19. Hall EW, Luisi N, Zlotorzynska M, Wilde G, Sullivan P, Sanchez T, et al. Willingness to use home collection methods to provide specimens for SARS-CoV-2/COVID-19 research: survey study. J Med Internet Res. 2020;22:e19471. https://doi.org/10.2196/19471
20. Frost HM, Novicki TJ. *Blastomyces* antigen detection for diagnosis and management of blastomycosis. J Clin Microbiol. 2015;53:3660–2. https://doi.org/10.1128/JCM.02352-15
21. Spector D, Legendre AM, Wheat J, Bemis D, Rohrbach B, Taboada J, et al. Antigen and antibody testing for the diagnosis of blastomycosis in dogs. J Vet Intern Med. 2008;22:839–43. https://doi.org/10.1111/j.1939-1676.2008.0107.x
22. Connolly P, Hage CA, Bariola JR, Bensadoun E, Rodgers M, Bradsher RW Jr, et al. *Blastomyces dermatitidis* antigen detection by quantitative enzyme immunoassay. Clin Vaccine Immunol. 2012;19:53–6. https://doi.org/10.1128/CVI.05248-11
23. Council of State and Territorial Epidemiologists. Standardized surveillance case definition for blastomycosis. 2019 [cited 2020 Mar 12]. https://cdn.ymaws.com/www.cste.org/resource/ resmgr/2019ps/final/19-ID-02_Blastomycosis_final.pdf
24. Chapman SW, Lin AC, Hendricks KA, Nolan RL, Currier MM, Morris KR, et al. Endemic blastomycosis in Mississippi: epidemiological and clinical studies. Semin Respir Infect. 1997;12:219–28.
25. Vaaler AK, Bradsher RW, Davies SF. Evidence of subclinical blastomycosis in forestry workers in northern Minnesota and northern Wisconsin. Am J Med. 1990;89:470–6. https://doi.org/10.1016/0002-9343(90)90378-Q
26. Smith JA, Kauffman CA. Blastomycosis. Proc Am Thorac Soc. 2010;7:173–80. https://doi.org/10.1513/pats.200906-040AL
27. O'Dowd TR, Mc Hugh JW, Theel ES, Wengenack NL, O'Horo JC, Enzler MJ, et al. Diagnostic methods and risk factors for severe disease and mortality in blastomycosis: a retrospective cohort study. J Fungi (Basel). 2021;7:888. https://doi.org/10.3390/jof7110888
28. Wheat LJ, Knox KS, Hage CA. Approach to the diagnosis of histoplasmosis, blastomycosis and coccidioidomycosis. Curr Treat Options Infect Dis. 2014;6:337–51. https://doi.org/10.1007/s40506-014-0020-6
29. Bariola JR, Hage CA, Durkin M, Bensadoun E, Gubbins PO, Wheat LJ, et al. Detection of *Blastomyces dermatitidis* antigen in patients with newly diagnosed blastomycosis. Diagn Microbiol Infect Dis. 2011;69:187–91. https://doi.org/10.1016/j.diagmicrobio.2010.09.015
30. Mongkolrattanothai K, Peev M, Wheat LJ, Marcinak J. Urine antigen detection of blastomycosis in pediatric patients. Pediatr Infect Dis J. 2006;25:1076–8. https://doi.org/10.1097/01.inf.0000241144.89426.2a

Address for correspondence: Mitsuru Toda, Centers for Disease Control and Prevention, 1600 Clifton Road NE, Mailstop H24-11, Atlanta, GA 30329-4018, USA; email: nrk7@cdc.gov

Seroincidence Rate of Typhoidal *Salmonella* in Children, Kenya, 2017–2018

Aslam Khan, Polina Kamenskaya, Izabela Rezende, Francis M. Mutuku, Bryson Ndenga, Zainab Jembe, Priscilla Maina, Philip Chebii, Charles Ronga, Victoria Okuta, Denise O. Garrett, Donal Bisanzio, Kristen Aiemjoy, Jason R. Andrews, A. Desiree LaBeaud,[1] Richelle Charles[1]

Enteric fever, caused by *Salmonella enterica* serovars Typhi and Paratyphi, results in high rates of illness and death globally. The lack of reliable diagnostic assays limits surveillance, leading to major gaps in understanding the population-level burden in low- and middle-income countries. We applied a novel serologic tool measuring IgG responses to hemolysin E to assess typhoidal *Salmonella* infection rates in children from 4 communities: 2 in western Kenya (Kisumu and Chulaimbo) and 2 in coastal Kenya (Ukunda and Msambweni). We found a substantially higher enteric fever seroincidence rate in coastal Kenya (37/100 person-years) than in western Kenya (3.6/100 person-years). We found a higher seroincidence rate in households with nonpiped water and lower incomes and in neighborhoods with higher population density. Our findings contribute to Kenya's limited enteric fever surveillance data, especially in the coastal regions. Such information underscores the need for public health interventions, such as typhoid conjugate vaccine introduction, in Kenya.

Enteric fever is a major health problem globally that has the potential to cause a spectrum of symptoms, including severe febrile illness and intestinal perforation (*1*). *Salmonella enterica* serovars Typhi and Paratyphi A, B, and C are responsible for enteric fever; *Salmonella* Typhi is the most prevalent, followed by *Salmonella* Paratyphi A. Whereas *Salmonella* Typhi is found throughout the world, *Salmonella* Paratyphi A is most prevalent in South and Southeast Asia and is not commonly found in Africa. Most illness occurs in low and middle-income countries (LMICs) that lack access to safe drinking water and improved sanitation; children and adolescents bear the highest burden of disease (*2*–*4*). Accurate diagnosis is challenging and often requires culture-based methods (*5*). The current reference standard is blood culture, which might be unavailable in many clinical settings where typhoid is endemic; it has an estimated sensitivity range of 51%–65% that varies by age, duration of symptoms, use of antimicrobial drugs before testing, and volume of blood collected (*5*,*6*). Alternative molecular testing using peripheral blood has low diagnostic sensitivity (*7*). Point-of-care serologic-based diagnostic tests, such as the Widal test, are also limited by low sensitivity and specificity (*5*). In addition to variable sensitivity and specificity, available testing for enteric fever might be cost prohibitive, resulting in underreporting of the true incidence of disease. Furthermore, because of public health allocations of resources focused on other infectious diseases, accurate surveillance remains an epidemiologic challenge. It is important to capture the effect of those infections to better prioritize preventive measures, including vaccine implementation (*3*,*4*).

Author affiliations: Stanford University School of Medicine, Stanford, California, USA (A. Khan, I. Rezende, J.R. Andrews, D. LaBeaud); Massachusetts General Hospital, Boston, Massachusetts, USA (P. Kamenskaya, R. Charles); Technical University of Mombasa, Mombasa, Kenya (F.M. Mutuku); Kenya Medical Research Institute, Kisumu, Kenya (B. Ndenga, C. Ronga, V. Okuta); Msambweni County Referral Hospital, Msambweni, Kenya (Z. Jembe, P. Maina, P. Chebii); Albert B. Sabin Vaccine Institute, Washington, DC, USA (D.O. Garrett); RTI International, Research Triangle Park, North Carolina, USA (D. Bisanzio); University of California, Davis, California, USA (K. Aiemjoy); Mahidol University, Bangkok, Thailand (K. Aiemjoy); Harvard Medical School, Boston (R. Charles); Harvard T.H. Chan School of Public Health, Boston (R. Charles)

DOI: https://doi.org/10.3201/eid3203.250469

[1]These senior authors contributed equally to this article.

Although geostatistical models estimate a high prevalence of enteric fever in sub-Saharan Africa, relatively few studies have provided direct disease burden estimates in the region (*2*,*8*). The available data suggest a very high burden of typhoid in Kenya; however, most studies focused primarily on the densely populated capital city of Nairobi and its surrounding areas, with limited data available from the western or coastal regions (*2*,*9*). Although the Kenya Ministry of Health offers typhoid vaccination for high-risk groups, it has not implemented a routine immunization series for all persons (*9*). To further understand the burden of typhoid in western and coastal region of Kenya, we implemented a serosurveillance tool to estimate the population-level enteric fever seroincidence rate and identify risk factors for infection among children.

Methods

Study Cohort

We used archived serum samples and accompanying survey data that evaluated the burden of chikungunya virus and dengue virus infections among children 2–18 years of age across 4 sites in Kenya (*10*). Although the parent study included a longitudinal cohort, this analysis is cross-sectional serosurvey using data and serum samples collected from a periodic sampling timepoint (April 2017–January 2018) and comprises a random subset of 1,408 children. Two geographically distinct areas in Kenya are represented in this analysis: coastal Kenya (Msambweni and Ukunda) and western Kenya (Chulaimbo and Kisumu). Those 2 areas have different baseline infrastructure (higher wealth in the west) and weather patterns (higher temperature and humidity and longer rainy seasons on the coast) (Appendix Table 1, https://wwwnc.cdc.gov/EID/article/32/3/25-0469-App1.pdf). We selected a rural town in each area, Msawbweni on the coast and Chulaimbo in the west, that had less infrastructure and fewer resources than its adjacent densely populated urban center (Appendix Table 2) (*10*). We recruited households by random enrollment within confined structured zones in each study community across a similar time period. We administered demographic surveys designed to collect information about the household, built infrastructure, and behavioral patterns related to mosquitoborne infections but also captured information relevant to food and waterborne illnesses, such as population density and access to piped water and latrines (*10*). The ethics review boards with the Kenya Medical Research Institute (approval no. SSC95 2611), Stanford University (approval no. 31488), and Mass General Brigham (approval no. 2019P000152) approved the study protocol.

Sample Collection and Testing

We collected blood samples during the same household visit at which we administered surveys. We centrifuged blood samples and stored serum aliquots at −70°C until testing. We used 1 serum sample from each participant to measure hemolysin E HlyE IgG levels at Massachusetts General Hospital (Boston, MA, USA) by kinetic ELISA, as previously described (*6*).

Statistical Analysis

We estimated seroconversion rates from cross-sectional serosurveys using models of HlyE IgG decay derived from blood culture–confirmed enteric fever cases (*6*). Those models account for peak antibody responses, decay rates, and variability in immune responses while incorporating multiple biomarkers, measurement noise, and cross-reactivity (*11*–*13*). We implemented our approach using the open-source R package serocalculator (https://cran.r-project.org/web/packages/serocalculator). We paired demographic information with the serologic results and analyzed for associations with age, population density, water source, latrine availability, and wealth. We calculated the population density using zonal statistics in QGIS version 3.28.9 (https://qgis.org), and obtained population counts from WorldPop (https://www.worldpop.org). We divided the population into quartiles representing increasing population density across the cohort. We calculated a wealth index by multiple correspondence analysis, using variables related to tangible assets (e.g., radio, motor vehicle, television, bicycle, telephone), house ownership and characteristics (e.g., number of rooms used for sleeping, persons per room, window screens, and building materials), and access to utilities and infrastructure (e.g., source of water, sanitation facility, and location) (*14*,*15*). We divided the scores into quartiles representing increasing socioeconomic status (SES) as a measure of wealth throughout the group (*14*). We performed all analysis in R version 4.4.3 (The R Project for Statistical Computing, https://www.r-project.org).

Results

Study Population

Of the 1,408 participants included in the study, 323 were from Kisumu (west), 323 from Chulaimbo (west), 299 from Ukunda (coast), and 473 from Msambweni (coast) (Table 1). The median age of participants

Table. Characteristics of study sites and participants in study of typhoidal *Salmonella* in children, Kenya, 2017–2018*

Characteristic	Study site				
	Kisumu, n = 323	Chulaimbo, n = 323	Ukunda, n = 299	Msambweni, n = 473	Overall, n = 1,408
Sex					
F	173 (54)	146 (45)	166 (56)	225 (48)	719 (51)
M	150 (46)	177 (55)	133 (44)	248 (52)	689 (49)
Age, y					
2–5	32 (10)	27 (8)	20 (7)	47 (10)	126 (9)
6–10	140 (44)	146 (46)	138 (46)	227 (48)	651 (46)
11–18	147 (46)	145 (46)	141 (47)	199 (42)	632 (45)
Median (IQR)	10.2 (7.8–12.6)	10.7 (7.8–13.5)	10.5 (7.93–13.1)	10.9 (7.9–13.6)	10.6 (7.8–13.1)
Piped water, n = 1,382	300/303 (>99)	80/300 (26)	275/299 (92)	71/480 (14)	656 (47)
Latrine access, n = 1,371	301/301 (100)	294/300 (98)	296/297 (>99)	193/473 (41)	1,084 (79)
Location	West	West	Coast	Coast	

*Values are no. (%) except as indicated. IQR, interquartile range.

was 10.6 (interquartile range [IQR] 7.8–13.1) years; the median age for each specific community was 10.2–10.9 years of age (Table). Wealth distribution and population density were higher in Kisumu and Ukunda than in Chulaimbo and Msambweni (Appendix Tables 1, 2).

Serology Findings

We found higher HlyE IgG levels in the coastal population than the western population (Figures 1, 2). Median HlyE IgG level in the coastal population was 7.73 (IQR 4.10–10.97) ELISA units. Median HlyE IgG level in the western population was 0.86 (IQR 0.38–2.73) ELISA units.

The overall seroincidence rate for the Kenya cohort was 9.1 (95% CI 8.4–9.8) per 100 person-years. In the coastal region, the seroincidence rate was 37 (95% CI 33.8–40.5) per 100 person-years, and in the western region, it was 3.6 per 100 person-years (95% CI 3.0–4.4). We found no significant difference when comparing seroincidence rates by age (<10 years or

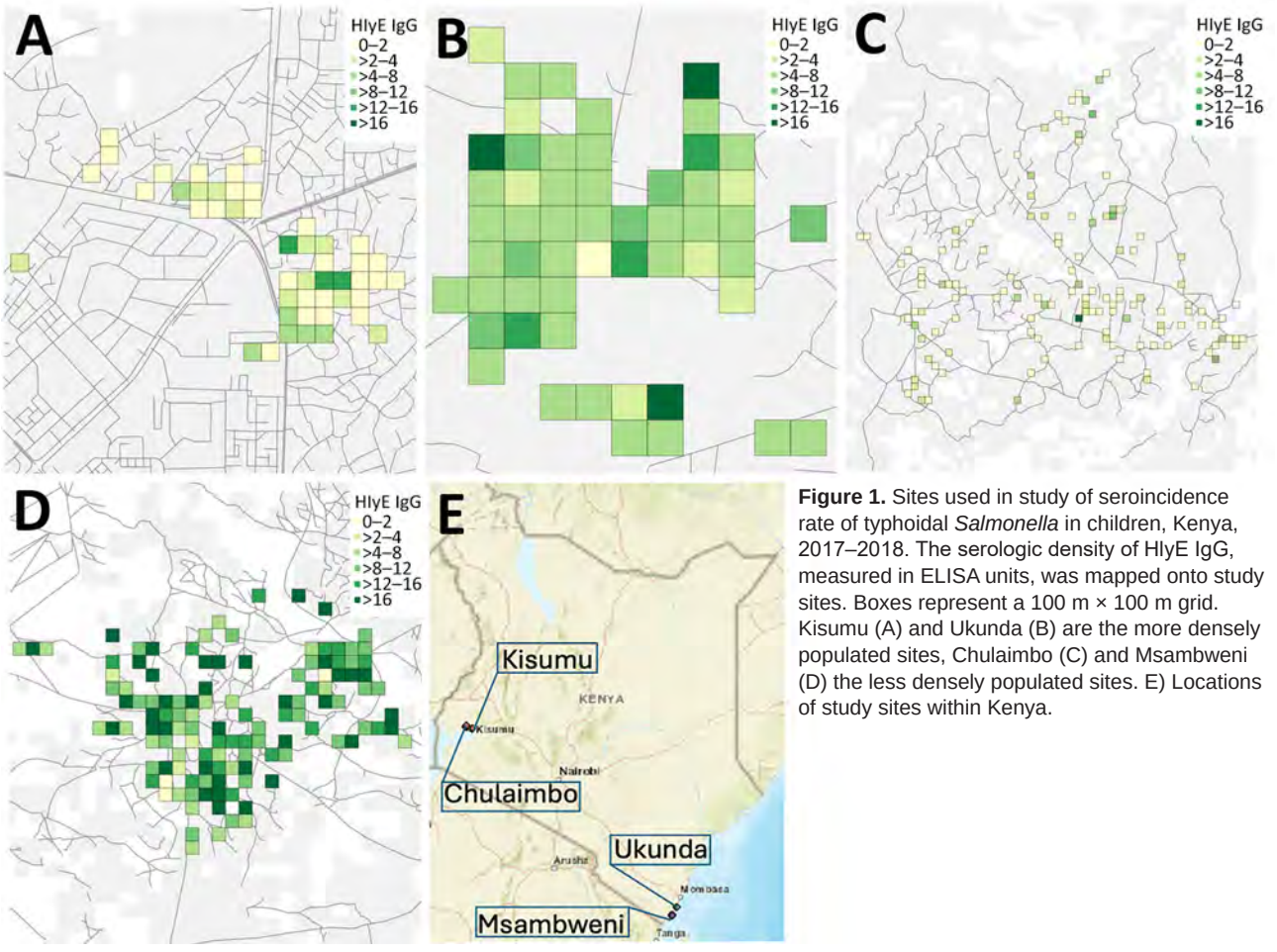

Figure 1. Sites used in study of seroincidence rate of typhoidal *Salmonella* in children, Kenya, 2017–2018. The serologic density of HlyE IgG, measured in ELISA units, was mapped onto study sites. Boxes represent a 100 m × 100 m grid. Kisumu (A) and Ukunda (B) are the more densely populated sites, Chulaimbo (C) and Msambweni (D) the less densely populated sites. E) Locations of study sites within Kenya.

≥10 years of age); however, there was a trend of higher seroincidence rates in the ≥10 years group (Figure 3). Piped water, higher wealth, latrine use, and urban location were associated with lower enteric fever seroincidence rates in the coastal region (Figure 4). No risk factors were significantly associated with seroincidence rates in the western region of Kenya.

Discussion

In this study, we leveraged archived serum samples from a large arbovirus cohort study in Kenya to obtain population-level enteric fever seroincidence rates based on HlyE IgG responses. We found an estimated 10-fold higher seroincidence rate of typhoidal *Salmonella* in the coastal region than the western region. The enteric fever seroincidence rate we estimated in coastal Kenya is similar to the rate estimated in Bangladesh, where ongoing blood culture surveillance for enteric fever has confirmed a high prevalence of *Salmonella* Typhi and Paratyphi A (*16*). The seroincidence rate we estimated in the western region of Kenya is closer to that of Kathmandu, Nepal (5.8/100 person-years), where the typhoid conjugate vaccine campaign was launched in 2022 (*6*,*16*).

The enteric fever seroincidence rates we estimated (9.1/100 person-years or 9,100/100,000 person-years overall) exceed those from previous culture-based studies in the region, for which an incidence rate of >100/100,000 persons/year is considered high for typhoid fever. Previous clinical surveillance studies have estimated a range of incidence with an extrapolated crude incidence of 39/100,000 persons/year in eastern Africa (*17*); an adjusted incidence of 284/100,000 person-years of observation in Kibera, Kenya (*3*); and an estimated incidence of 620/100,000 person-years in eastern sub-Saharan Africa (*8*). We found no direct comparison to clinical blood culture incidence rates available from Kenya or East Africa (*18*). The seroincidence rate we observed in this study is comparable to rates reported in other regions where typhoidal *Salmonella* is recognized as a public health concern; vaccination campaigns are targeting those populations. As for many infectious diseases in sub-Saharan Africa, limited surveillance data can reduce allocation of resources to address those problems. We demonstrated a substantially higher seroincidence of typhoidal *Salmonella* in western and coastal regions of Kenya than other areas in the country that might have an unrecognized higher level of exposure. Causes of higher seroincidence could be the limited availability and affordability of diagnostics, low sensitivity of culture, and subclinical infections.

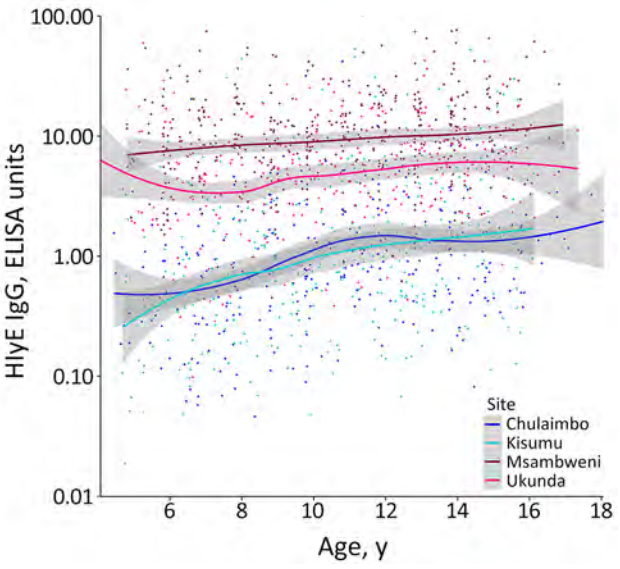

Figure 2. Antibody response by participant age and location in study of seroincidence rate of typhoidal *Salmonella* in children, Kenya, 2017–2018. Dots represent individual antibody responses, curves represent smoothed cumulative responses, and gray shading indicates 95% CIs.

Most typhoidal *Salmonella* studies evaluate febrile participants. Because patients can be exposed to *Salmonella* Typhi and Paratyphi without experiencing a symptomatic infection, the seroincidence rate in those studies will seem higher than in clinical studies because they included patients with subclinical infection otherwise not captured by clinical surveillance (*19*). Variable sensitivity in blood culture sampling and inoculum, especially in young children, could also cause false negative results. Furthermore, differences in health-seeking behavior can also account for delayed symptoms or missed typhoid cases in various communities (*20*–*22*).

In addition to estimating the population-level enteric fever seroincidence rate, we explored potential influence of established risk factors, including population density, SES, and water, sanitation, and hygiene measures (*23*,*24*). Consistent with previous studies, we found notable differences in seroincidence rates with water access, latrine use, and overall wealth. In the coastal region, we observed a trend toward a higher seroincidence rate of enteric fever associated with lower wealth, lower population density, and use of nonpiped water. In our study, we found higher enteric fever seroincidence rates in the coastal villages than in western villages. When evaluating the source of water, most nonpiped water was located in the coastal sites, which likely contributed to the higher levels of typhoidal *Salmonella* found in the coastal sites than the western sites. The coastal sites

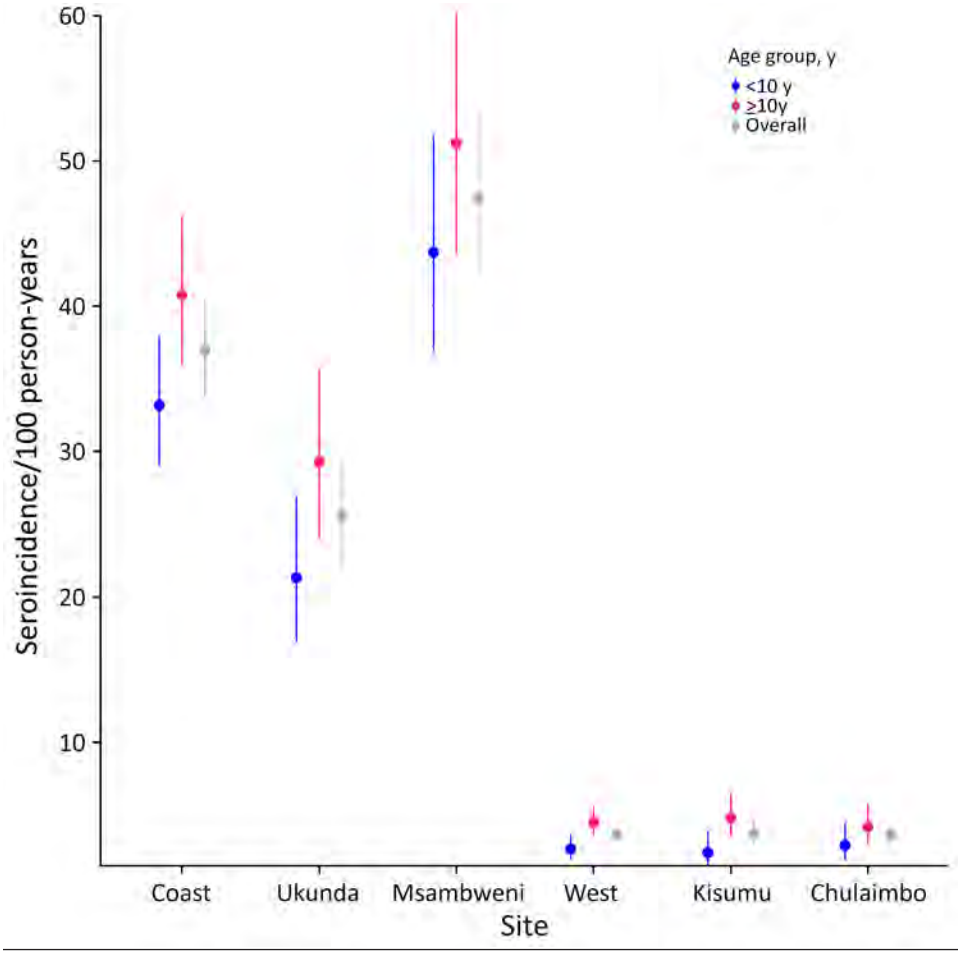

Figure 3. Seroincidence in study of typhoidal *Salmonella* in children, Kenya, 2017–2018. Typhoid seroincidence rate by region and study site is shown stratified by patient age. Dots represent medians; error bars indicate 95% CIs. Coast sites were Ukunda and Msambweni; west sites were Kisumu and Chulaimbo.

also have higher humidity and relative temperature and longer rainy seasons, which can be associated with foodborne and waterborne infections (*25*).

We also noted differences in seroincidence rates within the coastal sites and in comparison to the western sites. The less densely populated, less developed, and effectively rural site of Msambweni on the coast had the highest seroincidence rate, which deviates from studies in southern Asia and other parts of the world where denser populations have been associated with increased risk for infection. Many of those densely populated communities often do not have access to piped water, and residents live in housing with inadequate sanitation, which is different from our study sites (*26*). Msambweni had most of the participants of lowest SES from all 4 study sites and likely has multiple factors contributing to increased seroincidence rate, including lack of piped water, poor sanitation, and other environmental factors. Seasonal outbreaks or community sanitation leakages were possible but not reported during the study period. In contrast, we noted no major differences in the west between the urban center in Kisumu and its rural adjacent site, Chulaimbo. We attributed that finding to lower statistical power to detect a difference, given the low seroincidence rate overall in western sites; another possible cause is the difference in wealth index, population density, and environmental factors between the geographic sites. We noted a greater divide in calculated SES quartiles in the coastal region than in the west, where the distribution was closer, as was the calculated seroincidence rate. Last, the differing climate and susceptibility to flooding on the coast can also contribute to the higher seroincidence rate found in the coastal region in this study (*27,28*).

Our findings demonstrate that the risk for exposure and burden of typhoidal *Salmonella* is not homogenous and varies greatly both between regions and within populations in the same country. Previous studies have been performed in dense urban slums, which have specific factors that contribute to propagation of infection (*3,29*). When comparing urban and rural settings, the wide variation in living conditions, wealth, and access can influence exposure to typhoidal *Salmonella* pathogens. Our surveys did not capture the possibility of sanitation leakages, which

can contribute to typhoid exposure. Of note, no major outbreaks were reported during the study period.

The 2 main risk factors we explored in this study, water source and latrine access, were also included in the wealth index calculation and trended in the same direction as wealth, likely influencing the trend we identified. In addition, the original study (*10*) focused on mosquitoborne infections and did not include a comprehensive assessment of all the risk factors associated with enteric fever infection. For testing, HlyE is expressed by both *Salmonella* Typhi and *Salmonella* Paratyphi A; therefore, antibody responses to the antigen cannot distinguish between infections caused by these 2 pathogens (*2*). Although *Salmonella* Paratyphi A is a common cause of enteric fever in Asia, it is considered rare in Africa (*30*,*31*). Although HlyE is also present in the genomes of *Shigella* species and *Escherichia coli,* its expression during infection with those pathogens likely differs and may be repressed or disrupted in some lineages

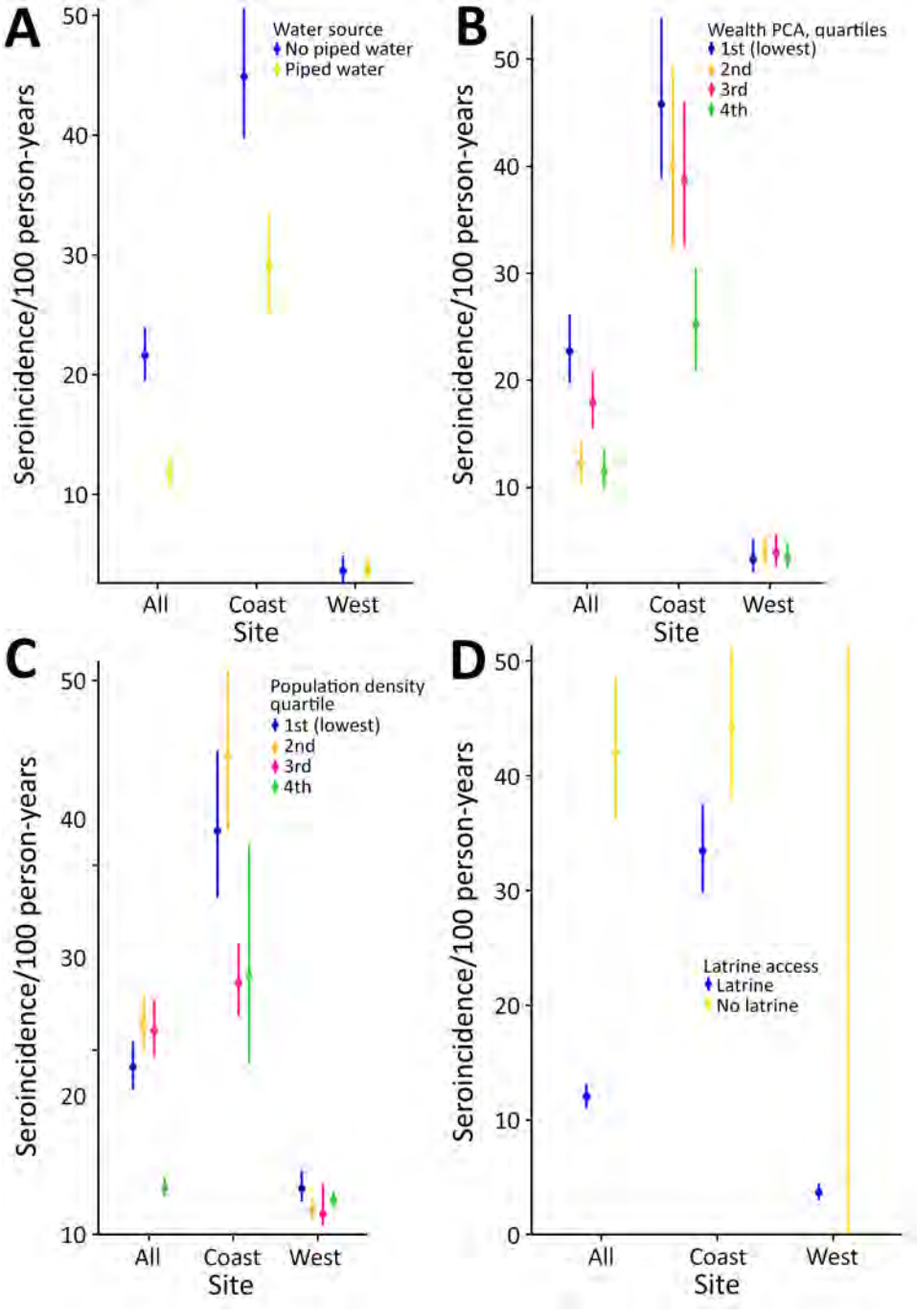

Figure 4. Typhoidal *Salmonella* seroincidence by site characteristics in study of typhoidal *Salmonella* in children, Kenya, 2017–2018. A) Seroincidence by water source. B) Seroincidence stratified by wealth. C) Seroincidence stratified by population density. D) Seroincidence by latrine type. Dots represent medians; error bars indicate 95% CIs. PCA, principal component analysis.

(*32*). The sample size might not be sufficient to comprehensively represent the greater regions across Kenya. In addition, although a sample size of 300–400 may be sufficient for calculating the seroincidence rate, those estimates are limited when stratifying by age and other typhoid-associated risk factors and should be explored further in a larger study. Furthermore, with random nonstratified sampling, we observed fewer children in the ≤5 years age group, which also can influence the overall seroincidence rate. Last, the samples were collected in 2017–2018; the seroincidence rate might have changed since that time given different seasons, climate change, drought/flooding, and other factors like the COVID-19 pandemic, which caused changes in movement and behavior. More detailed incidence studies are needed to improve incidence estimates to reveal the comprehensive burden of infection for implementation of public health measures and to determine if the burden remains high in Kenya.

Despite those limitations, our study demonstrates that the enteric fever seroincidence rate is high in Kenya, particularly in the coastal region, where incidence rates were comparable to other highly endemic areas for typhoid in Asia (e.g., Dhaka, Bangladesh) and >100-fold higher than estimates by blood culture surveillance. Our findings suggest there is a role for implementing typhoid conjugate vaccine to additional populations in coastal and western Kenya, in addition to the current practice of provide the vaccine to high-risk groups.

This article was preprinted at https://www.medrxiv.org/content/10.1101/2025.06.24.25330223v1.

The Bill & Melinda Gates Foundation (project no. INV-000572, principal investigator D.O.G.) and the National Institutes of Health (project no. R01AI134814, principal investigator R.C.C.; project no. R01AI102918, principal investigator A.D.L., project no. R21AI176416, principal investigator K.A.; and project no. K01TW012177, principal investigator K.A.) supported this work.

About the Author

Dr. Khan is a clinical assistant professor in the department of pediatrics and division of infectious diseases at Stanford University School of Medicine. His primary research interest is the epidemiology of mosquitoborne infections and febrile illnesses in children in limited resource settings, with a focus on identifying risk factors and mitigating measures in addition to appropriate diagnostics to reduce burden and improve diagnosis of mosquitoborne infections.

References

1. Marchello CS, Birkhold M, Crump JA. Complications and mortality of typhoid fever: a global systematic review and meta-analysis. J Infect. 2020;81:902–10. https://doi.org/10.1016/j.jinf.2020.10.030
2. Marks F, von Kalckreuth V, Aaby P, Adu-Sarkodie Y, El Tayeb MA, Ali M, et al. Incidence of invasive salmonella disease in sub-Saharan Africa: a multicentre population-based surveillance study. Lancet Glob Health. 2017;5:e310–23. https://doi.org/10.1016/S2214-109X(17)30022-0
3. Breiman RF, Cosmas L, Njuguna H, Audi A, Olack B, Ochieng JB, et al. Population-based incidence of typhoid fever in an urban informal settlement and a rural area in Kenya: implications for typhoid vaccine use in Africa. PLoS One. 2012;7:e29119. https://doi.org/10.1371/journal.pone.0029119
4. Mogasale V, Maskery B, Ochiai RL, Lee JS, Mogasale VV, Ramani E, et al. Burden of typhoid fever in low-income and middle-income countries: a systematic, literature-based update with risk-factor adjustment. Lancet Glob Health. 2014;2:e570–80. https://doi.org/10.1016/S2214-109X(14)70301-8
5. Mather RG, Hopkins H, Parry CM, Dittrich S. Redefining typhoid diagnosis: what would an improved test need to look like? BMJ Glob Health. 2019;4:e001831. https://doi.org/10.1136/bmjgh-2019-001831
6. Aiemjoy K, Seidman JC, Saha S, Munira SJ, Islam Sajib MS, Sium SMA, et al. Estimating typhoid incidence from community-based serosurveys: a multicohort study. Lancet Microbe. 2022;3:e578-e587. https://doi.org/10.1016/S2666-5247(22)00114-8
7. Andrews JR, Ryan ET. Diagnostics for invasive *Salmonella* infections: current challenges and future directions. Vaccine. 2015;33(Suppl 3):C8–15. https://doi.org/10.1016/j.vaccine.2015.02.030
8. Antillón M, Warren JL, Crawford FW, Weinberger DM, Kürüm E, Pak GD, et al. The burden of typhoid fever in low- and middle-income countries: a meta-regression approach. PLoS Negl Trop Dis. 2017;11:e0005376. https://doi.org/10.1371/journal.pntd.0005376
9. Marchello CS, Hong CY, Crump JA. Global typhoid fever incidence: a systematic review and meta-analysis. Clin Infect Dis. 2019;68(Suppl 2):S105–16. https://doi.org/10.1093/cid/ciy1094
10. Khan A, Bisanzio D, Mutuku F, Ndenga B, Grossi-Soyster EN, Jembe Z, et al. Spatiotemporal overlapping of dengue, chikungunya, and malaria infections in children in Kenya. BMC Infect Dis. 2023;23:183. https://doi.org/10.1186/s12879-023-08157-4
11. Teunis PFM, van Eijkeren JCH. Estimation of seroconversion rates for infectious diseases: effects of age and noise. Stat Med. 2020;39:2799–814. https://doi.org/10.1002/sim.8578
12. Teunis PFM, van Eijkeren JCH, de Graaf WF, Marinović AB, Kretzschmar MEE. Linking the seroresponse to infection to within-host heterogeneity in antibody production. Epidemics. 2016;16:33–9. https://doi.org/10.1016/j.epidem.2016.04.001
13. Teunis PFM, van Eijkeren JCH, Ang CW, van Duynhoven YTHP, Simonsen JB, Strid MA, et al. Biomarker dynamics: estimating infection rates from serological data. Stat Med. 2012;31:2240–8. https://doi.org/10.1002/sim.5322
14. Cortinovis I, Vella V, Ndiku J. Construction of a socio-economic index to facilitate analysis of health data in developing countries. Soc Sci Med. 1993;36:1087–97. https://doi.org/10.1016/0277-9536(93)90127-P

15. Greenacre M, Blasius J. Multiple correspondence analysis and related methods. New York: CRC Press; 2006.
16. Garrett DO, Longley AT, Aiemjoy K, Yousafzai MT, Hemlock C, Yu AT, et al. Incidence of typhoid and paratyphoid fever in Bangladesh, Nepal, and Pakistan: results of the Surveillance for Enteric Fever in Asia Project. Lancet Glob Health. 2022;10:e978–88. https://doi.org/10.1016/S2214-109X(22)00119-X
17. Crump JA, Luby SP, Mintz ED. The global burden of typhoid fever. Bull World Health Organ. 2004;82:346–53.
18. Murthy S, Hagedoorn NN, Faigan S, Rathan MD, Sharples KJ, Marchello CS, et al. Global typhoid fever incidence: an updated systematic review with meta-analysis. Lancet Infect Dis. 2025; 25:1347–62. https://doi.org/125:0.1016/S1473-3099(25)00359-7
19. Walker J, Russell P, Kermack L, Van TT, Thieu Nga TV, Mylona E, et al. Leveraging paired serology to estimate the incidence of typhoidal *Salmonella* infection in the STRATAA study. PLoS Negl Trop Dis. 2025;19: e0013612. https://doi.org/10.1371/journal.pntd.0013612
20. Nguyen M, Dzianach PA, Castle PECW, Rumisha SF, Rozier JA, Harris JR, et al. Trends in treatment-seeking for fever in children under five years old in 151 countries from 1990 to 2020. PLOS Glob Public Health. 2023;3:e0002134. https://doi.org/10.1371/journal.pgph.0002134
21. Abubakar A, Van Baar A, Fischer R, Bomu G, Gona JK, Newton CR. Socio-cultural determinants of health-seeking behaviour on the Kenyan coast: a qualitative study. PLoS One. 2013;8:e71998. https://doi.org/10.1371/journal.pone.0071998
22. Burton DC, Flannery B, Onyango B, Larson C, Alaii J, Zhang X, et al. Healthcare-seeking behaviour for common infectious disease-related illnesses in rural Kenya: a community-based house-to-house survey. J Health Popul Nutr. 2011;29:61–70. https://doi.org/10.3329/jhpn.v29i1.7567
23. Kim C, Goucher GR, Tadesse BT, Lee W, Abbas K, Kim J-H. Associations of water, sanitation, and hygiene with typhoid fever in case-control studies: a systematic review and meta-analysis. BMC Infect Dis. 2023;23:562. https://doi.org/10.1186/s12879-023-08452-0
24. Lee J-S, Mogasale VV, Mogasale V, Lee K. Geographical distribution of typhoid risk factors in low and middle income countries. BMC Infect Dis. 2016;16:732. https://doi.org/10.1186/s12879-016-2074-1
25. Guzman Herrador BR, de Blasio BF, MacDonald E, Nichols G, Sudre B, Vold L, et al. Analytical studies assessing the association between extreme precipitation or temperature and drinking water-related waterborne infections: a review. Environ Health. 2015;14:29. https://doi.org/10.1186/s12940-015-0014-y
26. Akullian A, Ng'eno E, Matheson AI, Cosmas L, Macharia D, Fields B, et al. Environmental transmission of typhoid fever in an urban slum. PLoS Negl Trop Dis. 2015;9:e0004212. https://doi.org/10.1371/journal.pntd.0004212
27. Awad DA, Masoud HA, Hamad A. Climate changes and food-borne pathogens: the impact on human health and mitigation strategy. Clim Change. 2024;177:92. https://doi.org/10.1007/s10584-024-03748-9
28. Nel J, Richards L. Climate change and impact on infectious diseases. Wits J Clin Med. 2022;4:129–34. https://doi.org/10.18772/26180197.2022.v4n3a1
29. Luby SP. Urban slums: a supportive ecosystem for typhoidal *Salmonellae*. J Infect Dis. 2018;218: S250–S254. https://doi.org/10.1093/infdis/jiy324
30. Arndt MB, Mosites EM, Tian M, Forouzanfar MH, Mokhdad AH, Meller M, et al. Estimating the burden of paratyphoid A in Asia and Africa. PLoS Negl Trop Dis. 2014;8:e2925. https://doi.org/10.1371/journal.pntd.0002925
31. Al-Emran HM, Eibach D, Krumkamp R, Ali M, Baker S, Biggs HM, et al. A multicountry molecular analysis of *Salmonella enterica* serovar Typhi with reduced susceptibility to ciprofloxacin in sub-Saharan Africa. Clin Infect Dis. 2016;62(Suppl 1):S42–6. https://doi.org/10.1093/cid/civ788
32. Hunt S, Green J, Artymiuk PJ. Hemolysin E (HlyE, ClyA, SheA) and related toxins. In: Anderluh G, Lakey J, editors. Proteins membrane binding and pore formation. New York: Springer; 2010. p. 116–26.

Address for correspondence: Aslam Khan, Stanford University School of Medicine, 453 Quarry Rd, Stanford, CA 94305-5119, USA; email: akhan1@stanford.edu

Environmental and Phylogenetic Investigations of *Aspergillus flavus* Outbreak Linked to Contaminated Building Materials, Denmark, 2025

Alexander Gewecke, Raphael Niklaus Sieber, Søren Hallstrøm, Marc Stegger, Barbara Kolarik, Jenny D. Knudsen, Birgitte Andersen, Astrid Hall, Nadja Hawwa Vissing, Maiken Cavling Arendrup

An *Aspergillus flavus* outbreak occurred in a tertiary hospital in Denmark. We compared environmental sampling methods, investigated the outbreak through short tandem-repeat genotyping, STR*Afla*, and analyzed isolate phylogeny using whole-genome sequencing. Paired sampling revealed that air sampling underestimated *A. flavus* burden (8 CFU/81 air samples vs. 585 CFU/81 surface samples), and culturing at 37°C was superior to 25°C (risk ratio 1.77; p<0.001). STR*Afla* (n = 145) confirmed clonality of the outbreak isolates. Active growth was identified in a kitchen inside the affected ward. Genetically related isolates were also found in the Department of Clinical Microbiology and in 4 unrelated wood-based building materials from retailers in Denmark. Phylogenetic analyses of 167 isolates supported introduction of *A. flavus* from building materials. We hypothesize that water damage enabled germination of dormant spores in precontaminated wood-based products. Our findings highlight a risk factor for outbreaks and should inform future hospital construction and infection prevention strategies.

Aspergillus flavus, the second leading cause of invasive aspergillosis (IA) worldwide, is an opportunistic mold that can cause severe infection, including IA, in immunocompromised patients (*1*). It predominates in Asia, the Middle East, and Africa because of its resilience in arid climates; however, because of climate change, its presence in the Northern hemisphere is expected to increase (*1*; N. van Rhijn, unpub. data, https://www.researchsquare.com/article/rs-6545782/v1). Hospital outbreaks mainly occur when airborne conidia are dispersed during construction work (*2*). The lower respiratory tract is usually the affected site of infection; in hematology patients, fatality rates are often high (*2*).

Renovations during 2017–2019 in a pediatric hematology ward at the largest tertiary hospital in Denmark likely led to infections in 6 patients by spreading conidia (*3*). Infections occurred despite amphotericin B prophylaxis, consistent with the intrinsic reduced susceptibility of *A. flavus*. Transition to posaconazole prophylaxis was implemented and prevented *A. flavus* in patients with adequate serum drug levels. In 2022–2023, we examined the genetic epidemiology of the outbreak using short tandem repeat (STR) genotyping, STR*Afla* (*4*,*5*). We confirmed isogeneity and linked 12 additional patients to the outbreak. Analysis of air samples also indicated the presence of *A. flavus* outbreak isolates in the ward, suggesting its undetected perseverance in the hospital over time. However, 8 more patients positive for outbreak-related *A. flavus* appeared during April 2023–January 2024; of those, 3 were from the outbreak ward floor and 5 were from other parts of the hospital, including a staff member in the Department of Clinical Microbiology (DCM).

In early 2024, a multidisciplinary team of specialists was formed to control the outbreak. In this study, we aimed to resolve the outbreak through optimizing environmental sampling to guide cleaning and source investigation and by using genome sequencing on a broad panel of *A. flavus* from the outbreak, the hospital environment, and epidemiologically unrelated patients and sites. We also used time-scaled phylogeny

Author affiliations: Statens Serum Institut, Copenhagen, Denmark (A. Gewecke, R.N. Sieber, S. Hallstrøm, M. Stegger, M.C. Arendrup); Harry Butler Institute, Murdoch University, Perth, Western Australia, Australia (M. Stegger); dansk MiljøAnalyse, Vedbæk, Denmark (B. Kolarik); Copenhagen University Hospital, Rigshospitalet, Copenhagen (J.D. Knudsen, A. Hall, N.H. Vissing, M.C. Arendrup); Aalborg University, Copenhagen (B. Andersen); University of Copenhagen, Copenhagen (M.C. Arendrup)

DOI: https://doi.org/10.3201/eid3203.251219

to understand the evolution of the outbreak isolates. Although the comparison of typing methodologies is not a novel approach in a clinical context (*6*–*10*), this study also applied an extensive genomics approach with time-scaled phylogeny to an ongoing *Aspergillus* outbreak. Leveraging phylogenetics delineated the evolution of isolates within an *A. flavus* population that inhabited the hospital environment and successfully pinpointed a plausible source of contamination, as well as an unexpected timing of introduction.

Materials and Methods

Environmental Sampling and Comparison of Sampling Strategies

We took air samples (1 m^3) using either a Microbio MB1 bioaerosol sampler (Cantium Scientific, https://www.cantiumscientific.com) onto 5 cm-diameter V8 agar contact plates (Bioneer A/S, https://bioneer.dk) or a MBASS30 V3 air sampler (Holbach, https://www.holbach.biz) onto 9-cm diameter V8 agar petri dishes (Bioneer A/S). We took surface samples using 5-cm diameter (25 cm^2) V8 agar contact plates (Bioneer A/S), preferably from infrequently cleaned surfaces (*11*). We incubated 1 set of contact plates and petri dishes at 25°C and read after 7 days and incubated the other set at 37°C and read after 3 days. Air sampling was nonaggressive because disturbing dust was unacceptable for hospital staff.

To assess *A. flavus* contamination and general fungal load, hospital sampling in March–June 2024 yielded 449 samples from 299 locations (in total). In March, we conducted environmental sampling at 41 predefined locations using V8 agar (*12*). At each location, we collected 4 samples (164 samples in total): 1 air sample incubated at 25 °C, 1 air sample incubated at 37 °C, 1 surface sample incubated at 25 °C, and 1 surface sample incubated at 37 °C. In addition, we investigated outdoor air controls and some sporadic surface samples (24 samples from 12 locations). Thus, in total, we collected 188 samples from 53 locations in the pediatric outbreak ward and outside the hospital. In April–June, we conducted another session focused on surface sampling and culturing at 37°C from the outbreak floor and collected 97 samples from 87 locations in both the pediatric and the adult hematology ward (Figure 1). That secondary sampling focused on areas that were most contaminated with *A. flavus* in the initial (paired) sampling session. Outside the outbreak floor, we took another 164 samples from 159 locations in high activity areas. We compared *A. flavus* CFU counts for paired samples in Rstudio using a χ^2 test (using table 2×2 function, R version 4.2.3, and the package *Publish*) (The R Project for Statistical Computing, https://www.r-project.org).

We verified active growth of *A. flavus* on materials using tape preparations, microscopy (*12*), and matrix-assisted laser desorption/ionization time-of-flight mass spectrometry for identification (*13*). We collected soil samples (n = 8) from the hospital surroundings near the outbreak-affected South complex using a method described elsewhere (*14*) and cultured them at 37°C. Four *A. flavus* isolates were previously isolated from wood-based building materials,

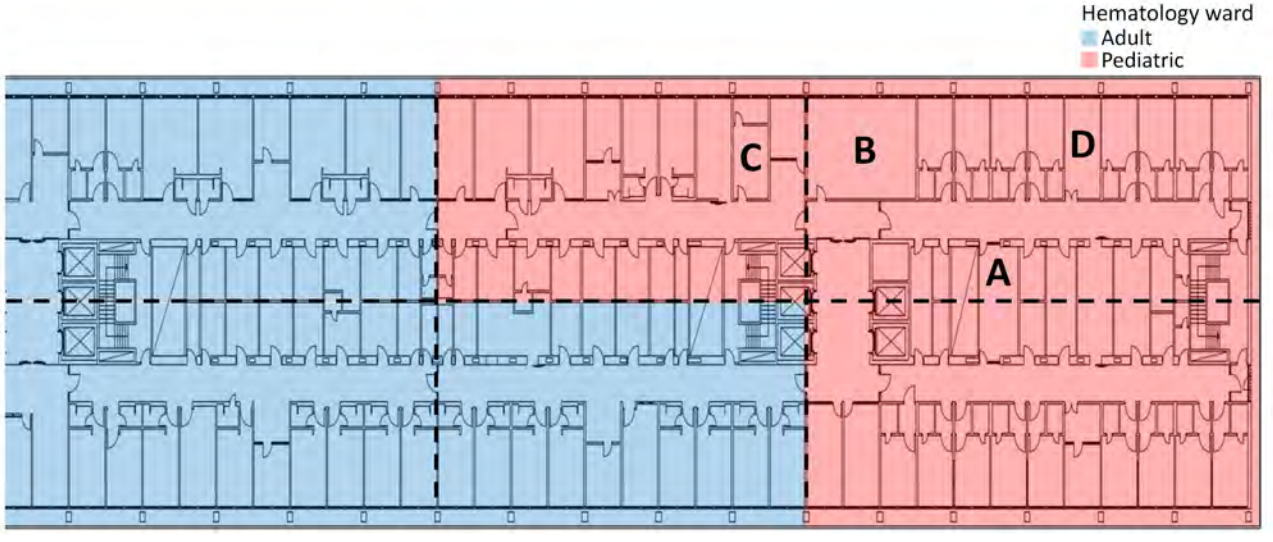

Figure 1. Floorplan of the outbreak floor in hospital South complex in study of environmental and phylogenetic investigations of *Aspergillus flavus* outbreak linked to contaminated building materials, Denmark, 2025. The hospital consists of 3 complexes: north, central, and south. The building is divided by corridors and staff rooms, with patient rooms facing the windows. Room A, staff meeting and lunchroom; room B, main kitchen; rooms C and D, staff offices. Figure created in BioRender (https://biorender.com/p56n130).

Table 1. Comparison of fungal yield for paired sampling of air and surfaces in study of environmental and phylogenetic investigations of *Aspergillus flavus* outbreak linked to contaminated building materials, Denmark, 2025*

	Air, n = 82				Surface, n = 82				
	25°C		37°C		25°C		37°C		
Identification	CFU (CFU/m^3)	Median (range)	CFU (CFU/m^3)	Median (range)	CFU (CFU/25 cm^2)	Median (range)	CFU (CFU/25 cm^2)	Median (range)	Total CFUs
Aspergillus	186 (4.5)	0.0 (0–28)	26 (0.6)	0.0 (0–13)	321 (7.8)	5.0 (0–55)	491 (12.0)	6.0 (0–70)	1,024
A. calidoustus	179 (4.4)	0.0 (0–28)	3 (0.1)	0.0 (0–1)	13 (0.3)	0.0 (0–4)	39 (1.0)	0.0 (0–27)	234
A. flavus	**3 (0.1)**	**0.0 (0–1)**	**5 (0.1)**	**0.0 (0–4)**	**236 (5.8)**	**2.0 (0–55)**	**349 (8.5)†**	**2.0 (0–63)**	**593**
A. fumigatus	2 (0.0)	0.0 (0–1)	18 (0.4)	0.0 (0–13)	1 (0.0)		41 (1.0)	0.0 (0–14)	62
A. niger	2 (0.0)	0.0 (0–1)	0 (0.0)		42 (1.0)	0.0 (0–23)	62 (1.5)	0.0 (0–34)	106
Aspergillus NI	0 (0.0)		0 (0.0)		29 (0.7)	0.0 (0–25)	0 (0.0)		29
Other fungi									
Alternaria	4 (0.1)	0.0 (0–3)	0 (0.0)		38 (0.9)	0.0 (0–6)	1 (0.0)		43
Aureobasidium	6 (0.1)	0.0 (0–2)	0 (0.0)		6 (0.1)	0.0 (0–6)	2 (0.0)	0.0 (0–1)	14
Cladosporium	154 (3.8)	2.0 (0–23)	0 (0.0)		131 (3.2)	1.0 (0–15)	0 (0.0)		285
Geotrichum	0 (0.0)		1 (0.0)		0 (0.0)		0 (0.0)		1
Mucorales	2 (0.0)	0.0 (0–1)	2 (0.0)	0.0 (0–1)	8 (0.2)	0.0 (0–1)	2 (0.0)	0.0 (0–1)	14
Penicillium	118 (2.9)	2.0 (0–20)	26 (0.6)	0.0 (0–10)	135 (3.3)	0.0 (0–33)	24 (0.6)	0.0 (0–19)	303
Molds NI	20 (0.5)	0.0 (0–16)	0 (0.0)		1 (0.0)		3 (0.1)	0.0 (0–2)	24
Growth NI	2 (0.0)	0.0 (0–1)	0 (0.0)		0 (0.0)		2 (0.0)	0.0 (0–2)	4
No growth	3		26		3		13		45
Fungi in total	492 (12.0)	9.0 (0–44)	55 (1.3)	0.0 (0–13)	640 (15.6)	13.0 (0–59)	525 (12.8)	6.0 (0–71)	1,712

*Samples were taken from 41 locations on the outbreak floor in March 2024 and cultured at 25°C or 37°C . Bolding highlights *A. flavus* findings. NI, not identified.
†p<0.001 for culturing surface samples at 37°C versus 25°C (*A. flavus*).

purchased from 2 retailers in Denmark, in an unrelated study of precontaminated materials (B. Andersen, unpub. data).

STR*Afla* of Environmental Isolates

We applied STR*Afla* genotyping on 145 *A. flavus* isolates as previously described (*4*,*5*). Of those, 33 isolates (24 from patients and 9 from air) were included in our previous study (*5*). We genotyped additional patient isolates (n = 11), hospital interior isolates (n = 87 [1 isolate per positive location]), soil isolates (n = 10), and building material isolates (n = 4).

Whole-Genome Sequencing of *A. flavus* Isolates

The dataset included 92 clinical and 17 environmental isolates from the outbreak hospital, 4 from unrelated wood-based materials, and 54 comparator isolates (167 isolates in total). All comparators, except 2, were previously STR*Afla* typed (*5*), and all originated either from hospital patients in Denmark who were not related to the outbreak or were control strains (4 UK-NEQAS and 2 ATCC 204304/200026 [CBS 128202] isolates).

We prepared sequencing libraries using a custom modified version of the DNA prep kit (Illumina, https://www.illumina.com) based on the Hackflex protocol (*15*) using 20 ng (2 ng/μL) genomic DNA as input and 25 μL of a 2× laboratory-made tagmentation buffer (20 mM Tris-HCl at pH 7.6), 20 mM MgCl2, and 10% (vol/vol) Propylene Carbonate (all Sigma-Aldrich, https://www.sigmaaldrich.com). We indexed the generated libraries with IDT for Illumina Unique Dual indexes and quantified them using the Quant-iT dsDNA HS Assay Kit (Thermo Fisher Scientific, https://www.thermofisher.com). We calculated molar concentrations using a standard conversion factor of 2 and pooled the samples at equimolar ratios. We assessed the quality of the final sequencing libraries by measuring concentration on a Qubit 3.0 fluorometer using the Qubit dsDNA HS quantification assay kit (Thermo Fisher Scientific) and by performing a fragment analysis using a TapeStation 4200 with the D5000 Screen Tape assay kit (Agilent, https://www.agilent.com). We sequenced quality checked final libraries on a NovaSeq (Illumina) using an S4 flowcell and 200-cycle reagent kit generating 2 × 100-bp paired-end reads.

We assessed quality and depth using NASP version 1.2.1 (*16*) and contamination screened using Kraken version 1.0 (*17*). We performed assembly with SPAdes version 3.11.1 (*18*) using the "–isolate" flag. We called single-nucleotide polymorphisms (SNPs) with NASP version 1.2.1 (*16*) aligned to NRRL 3357 (reference genome CBS128202, GenBank accession no. GCF_014117465) using BWA-MEM (H. Li, unpub. data, https://arxiv.org/abs/1303.3997v2) and GATK, requiring ≥10× depth and >90% unambiguous base calls. We removed recombination-prone regions using Gubbins version 2.3.4 (*19*) and inferred phylogenies with IQTREE version 2.0.3 (*20*) using the integrated model tester with ascertainment bias correction (-m TEST+ASC). Time-scaled phylogeny of

cluster 10 used core-genome SNPs with strain T21212 as reference. We used BEAST2 (https://www.beast2.org) with sample dates as tips, BEAST Model Test, a relaxed clock model, and coalescent exponential population, with Markov chain Monte Carlo lengths of 200 million. We inferred clusters using TreeCluster (*21*) with the Max Clade method at a threshold of 0.01 for the full dataset and 0.001 for the cluster 10 tree. Furthermore, we inferred STR*Afla* locus 2A ancestral state in R version 4.4.2 using the ace function from the package *ape* under an equal-rates model.

Results

Environmental Sampling

For initial sampling and comparison of strategies, paired sampling with culture on V8 agar yielded 1,712 fungal CFU, of which 775 were classical opportunistic species (including *Aspergillus flavus*, *A. fumigatus*, *A. niger*, and *Mucorales* spp.) and 593 were *A. flavus* specifically (Table 1, Figure 2). Surface sampling was more sensitive than air sampling overall (1,165 CFU [surface] vs. 547 CFU [air]), for the classical opportunistic species (731 CFU [surface] vs. 30 CFU [air]), and for *A. flavus* specifically (585 CFU [surface] vs. 8 CFU [air]) in the paired 81 air versus 81 surface samples. Culturing surface samples at 37°C increased *A. flavus* yield 1.77-fold (95% CI 1.57–1.99-fold; p<0.001). For air samples, the total CFU counts varied 9.2 fold at the 2 temperatures mainly because of notably fewer *A. calidoustus*, *Cladosporium*, and *Penicillium* spp. isolates when incubating at 37°C. Outdoor air controls grew *Cladosporium* and *Penicillium* spp. isolates but not *A. flavus* isolates.

We performed subsequent sampling during April–June 2024 with incubation at 37°C in 15 pediatric ward locations, which yielded a total of 324 *A. flavus* CFU (median 13.0 [range 0–58] CFU/25 cm²). Additional sampling above the ceiling gave 195 *A. flavus* CFU (median 4.0 [range 0–55] CFU/25 cm²). Samples beneath insulation sheets on the ceiling tiles were negative (Figure 3). In the adjacent adult hematology ward (Figure 1), we found 527 *A. flavus* CFU (median 1.0 [range 0–53] CFU/25 cm²). On 10 other floors, we collected 164 surface samples; we found *A. flavus* in 5 samples (33 CFU total); 29 were from a kitchen refrigerator top (central complex) and 4 were scattered elsewhere.

Peak *A. flavus* contamination was found in a combined staff meeting and lunchroom (room A), the main ward kitchen (room B), and staff offices (rooms C–D) (Figures 1–3), especially on less frequently cleaned surfaces. In November 2024, directed air samples suggested that the kitchenette base under the sink in room A was a source of contamination; yield was 1,500 CFU/m³. After dismantling, microscopy confirmed growth of *A. flavus* on a plywood cupboard (Figure 4).

STR*Afla* of Environmental Isolates

We genotyped a total of 145 *A. flavus* isolates using STR*Afla*, revealing 28 unique genotypes (Table 2). The dominant outbreak genotype, A, was identified in 19 isolates from 11 patients and 82/96 indoor hospital isolates and occurred exclusively on the outbreak floor, in both the adult and pediatric hematology wards (Table 2; Figure 1). In the adult ward specifically (Figure 1), 36/38 isolates shared genotype A, whereas 2 were different (Table 2). Eight isolates from 7 patients and 5 isolates from a contaminated DCM incubator shared genotype B, in which 1 of 9 markers (marker 2A) differed from that of genotype A by 1 repeat. Eight additional patient isolates shared 7–8 markers; genotype A displayed different marker

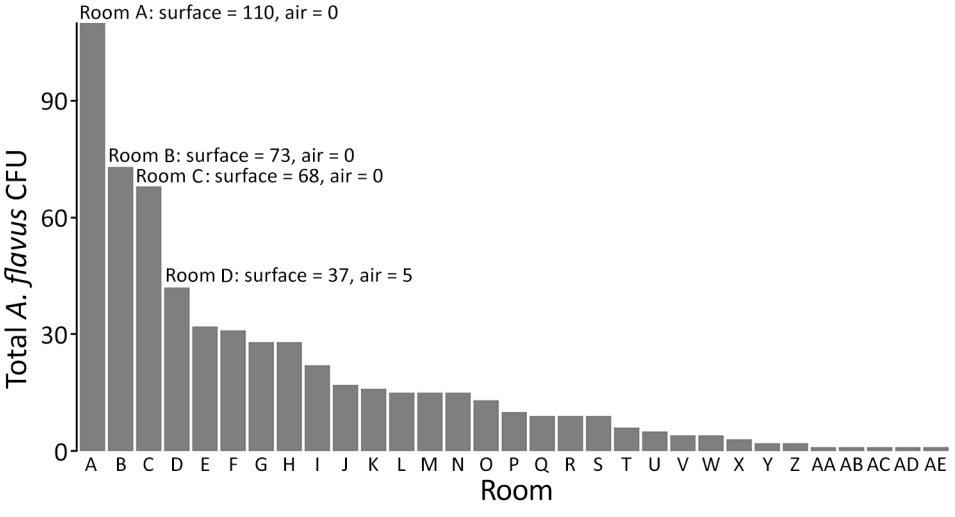

Figure 2. Distribution of *Aspergillus flavus* in hospital pediatric hemotology ward in study of environmental and phylogenetic investigations of *A. flavus* outbreak linked to contaminated building materials, Denmark, 2025. Bar chart displays total *A. flavus* CFU from paired samples in March 2024 (82 air samples and 82 surface samples incubated at 25°C or 37°C). Distribution in rooms of the ward shows varying concentration of spores with some hotspots of *A. flavus* contamination.

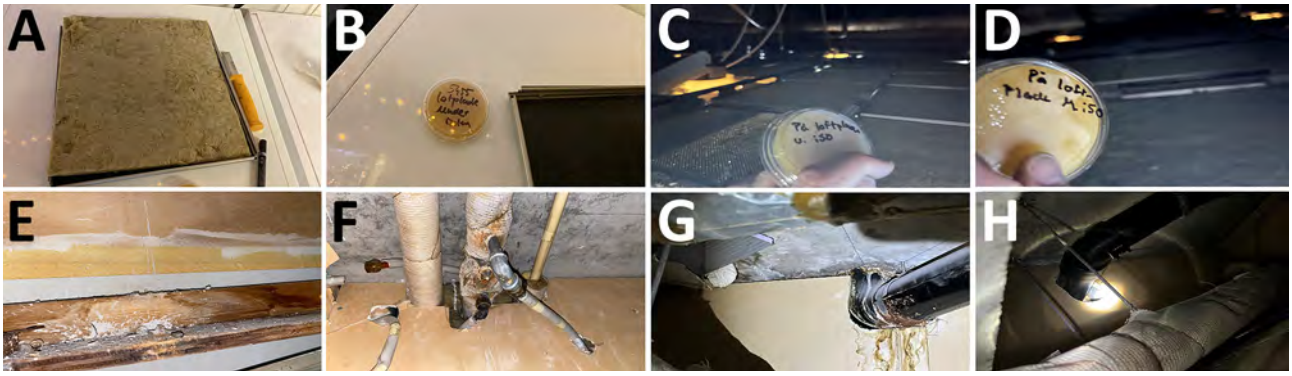

Figure 3. Examples of locations with dust accumulation above ceiling and large *Aspergillus flavus* contamination from hospital pediatric hemotology ward in study of environmental and phylogenetic investigations of *A. flavus* outbreak linked to contaminated building materials, Denmark, 2025. A) Ceiling tile from room A with 55 CFU/25 cm^2 *A. flavus* detected on top (none detected underneath); B) the same ceiling tile (black item) from room A with the insulation sheet (yellow mat) removed, where the surface had been covered and thus tested negative for *A. flavus*; C) area above ceiling in room B, 24 CFU/25 cm^2 (no rock wool); D) thick dust layer on inside of ceiling, room B; E) example of a water-damaged part of the wooden framing with mold-like growth above the suspended ceiling, 32 CFU/25 cm^2; F) 40 CFU/25 cm^2 on righthand pipe; G, H) pipes between rooms lacking sealing, which could possibly enable spore dispersal.

variations across the STR*Afla* panel (Table 2). Among the 82 hospital interior isolates with genotype A, 2 were from the water-damaged plywood cupboard in room A (Table 2; Figure 4). STR*Afla* of 4 outbreak-unrelated *A. flavus* isolates from wood-based panels (medium-density fiberboard, oriented strand board, and plywood) obtained from 2 retailers in Denmark and cultured outside this study, revealed partial similarity to genotype A with 5–8 of 9 shared markers (genotypes C, D, E) (Table 2). Remaining genotypes differed from the outbreak genotype A by ≥5 markers, as did soil isolates (Table 2).

Whole-Genome Sequencing–Based Population Analysis of *A. flavus* Isolates

A total of 167 isolates underwent whole-genome sequencing. We aligned reads to the reference genome and identified core-genome SNPs. After excluding recombination regions, we retained 303,560 SNPs in the reference chromosome for phylogenetic inference. This process produced a structured tree with distinct clusters separated by thousands of SNPs (Figure 5). Outbreak isolates grouped into cluster 10, which distinctly separated from others and showed minimal within-cluster variation indicating high genetic

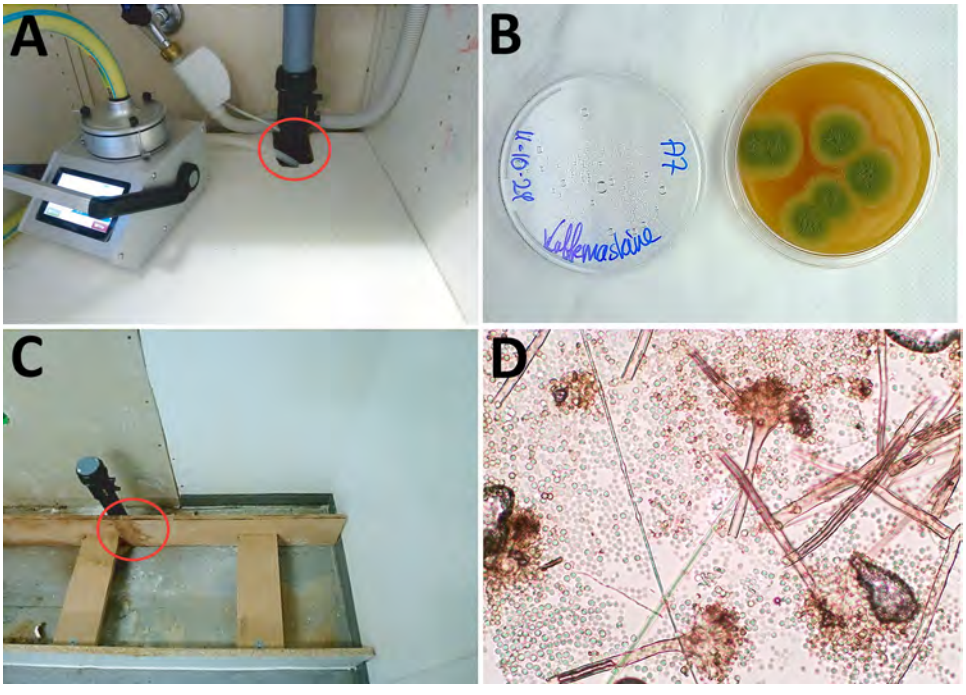

Figure 4. Testing materials from room A in hospital pediatric hemotology ward in study of environmental and phylogenetic investigations of *A. flavus* outbreak linked to contaminated building materials, Denmark, 2025. A) Directed air sampling under the kitchenette with a polyethylene tube (red circle). B) V8 contact plate from the top of the coffee machine showing *A. flavus* colonies after 3 days' incubation at 37°C. C) Discolored plywood (red circle) next to the drain after dismantling the cupboard. D) Tape preparation of the discolored area showing *A. flavus* stipes, heads, and spores.

similarity. All cluster 10 isolates originated from the hospital except for 4 building material isolates.

Using an internal outbreak draft genome as reference, resolution increased and enabled further analyses. In the cluster-specific tree (Figure 6), we retained 723 SNPs for time-scaled phylogenetic reconstruction. South complex and building material isolates were close, but the building material isolates clustered more basal alongside 2 isolates from patient 11 (infectious disease clinic). The last common ancestor of South complex and building material isolates likely dates to 2002 (95% highest posterior density [HPD] 1995–2008). South complex expansion occurred around 2017 (95% HPD 2015–2018). Isolates were distinct from the DCM isolates, which expanded around 2020 (95% HPD 2018–2021). A common ancestor to that monophyletic cluster dates back to ≈1990 (95% HPD 1975–2004).

Infectious disease clinic isolates were mainly from outpatients and considered noninfected. Those isolates displayed different STR*Afla* variants (Figure 6). Patients 6 and 11 were colonized and culture-positive twice. In both cases, the patients retained their original genotypes over a 1-year period. Isolates from patients 5, 8, 9, and 12–14 were regarded as plate contaminants because of growth outside the inoculation zone, lack of clinical signs, or both. European

Table 2. *Aspergillus flavus* genotypes found in 145 isolates in study of environmental and phylogenetic investigations of *Aspergillus flavus* outbreak linked to contaminated building materials, Denmark, 2025*

Source of isolate(s) (genotype)	No. isolates	STRA*fla*-markers									Comments
		2A	2B	2C	3A	3B	3C	4A	4B	4C	
Patients 1, 2, 4, 6, **9**, 10, 16, 17, 18, 20, 21 (genotype A)†	19	26	11	12	12	26	9	9	5	9	
Patient 21	3	26	11	12	12	25	9	9	5	9	
Patients **5**, 7 ,**12–14**, 15, 19 (genotype B)	8	25	11	12	12	26	9	9	5	9	
Patient 11	1	26	11	12	12	27	9	9	5	9	
Patient 11	1	27	11	12	12	27	9	9	5	9	
Patient **8**	1	26	11	14	12	26	9	9	5	9	
Patient 3	1	25	11	12	12	26	9	9	5	NA‡	
Patient 15	1	25	11	12	12	26	13	9	5	9	
Air samples (genotype A)†	9	26	11	12	12	26	9	9	5	9	Pediatric hematology ward
Plywood cupboard in room A§ (genotype A)†	2	26	11	12	12	26	9	9	5	9	Pediatric hematology ward
Vacuum cleaner bag (genotype A)†	2	26	11	12	12	26	9	9	5	9	Pediatric hematology ward
DCM laboratory incubator (genotype B)	5	25	11	12	12	26	9	9	5	9	
Hospital interior (genotype A)†	69	26	11	12	12	26	9	9	5	9	Adult/pediatric hematology ward
Hospital interior	1	62	11	12	9	20	9	7	12	10	Central complex
Hospital interior	1	40	12	11	8	13	4	7	7	9	South complex¶
Hospital interior	1	31	11	10	8	13	14	7	12	10	Adult hematology ward
Hospital interior	2	27	13	8	14	29	9	9	5	9	Central complex
Hospital interior	1	20	16	11	10	22	32	7	8	8	Pediatric hematology ward
Hospital interior	2	15	16	28	11	17	15	7	8	9	South complex¶
Hospital interior	1	14	11	10	8	22	9	7	12	10	Adult hematology ward
MDF (genotype C)	1	26	11	13	12	28	9	9	5	9	Retailer 1
MDF (genotype D)	1	NA‡	NA‡	NA‡	12	27	9	9	5	9	Retailer 2
OSB (genotype E)	1	26	11	12	12	27	9	9	5	9	Retailer 1
PW (genotype E)	1	26	11	12	12	27	9	9	5	9	Retailer 1
Soil-1a	1	15	7	22	16	12	16	9	5	8	
Soil-1b	1	15	7	23	17	13	5	9	5	8	
Soil-6a	1	15	11	12	8	30	14	8	7	10	
Soil-7a	1	16	7	11	19	6	5	7	5	8	
Soil-7b	1	30	11	11	8	24	15	7	7	10	
Soil-7c	1	15	7	21	18	12	11	10	5	8	
Soil-7d	1	28	11	11	8	20	9	7	12	10	
Soil-7e	1	29	11	11	8	23	15	7	7	10	
Soil-7f	1	16	7	33	14	6	11	17	5	8	
Soil-7g	1	39	11	10	8	45	9	7	12	10	
Total	145										

*Including 33 isolates compiled from Gewecke et al. (*6*). Patient numbers in bold indicate cases in which culture-plate contamination was assumed because of lack of symptoms, lack of statements in the medical records, or both. Gray shading indicates STRA*fla* marker overlaps with outbreak. MDF, medium-density fiberboard; OSB, oriented strand board; PW, plywood.
†Principal South complex outbreak cluster genotype A.
‡No STRA*fla* profile.
§Microscopy-confirmed growth of *A. flavus* on kitchen plywood cupboard in room A (see Figure 4).
¶South complex but different floor than outbreak ward.

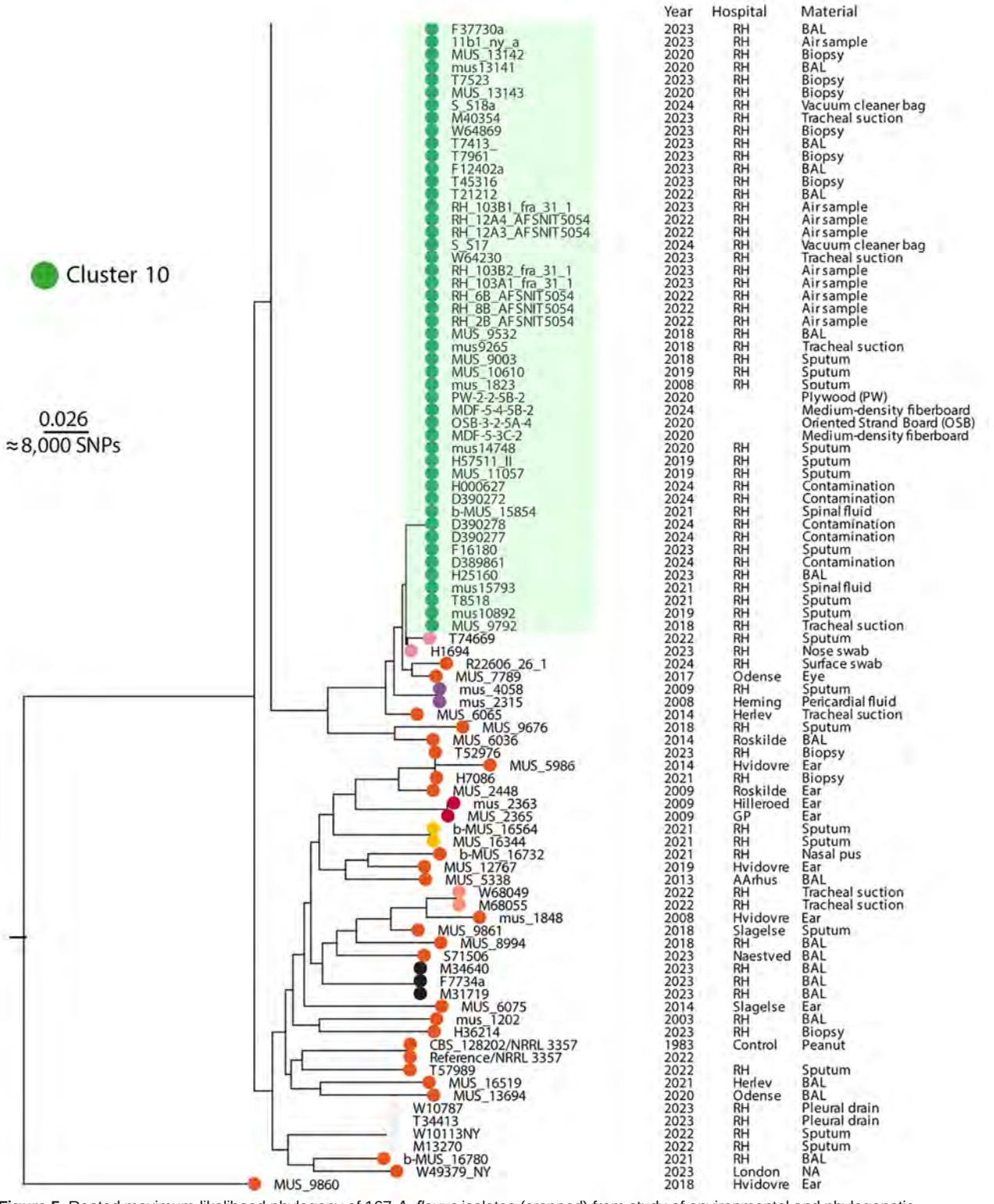

Figure 5. Rooted maximum-likelihood phylogeny of 167 *A. flavus* isolates (cropped) from study of environmental and phylogenetic investigations of *A. flavus* outbreak linked to contaminated building materials, Denmark, 2025. The tree shows clear distinction of several major clusters, including 1 monophyletic cluster 10 that contained all outbreak isolates. The tree was reconstructed based on 303,560 core-genome SNPs and rooted with MUS_9860 as outgroup. Scale bar indicates substitutions per site. Clusters were determined using TreeCluster (https://github.com/niemasd/TreeCluster). Full tree available in Appendix 1 (https://wwwnc.cdc.gov/EID/article/32/3/25-1219-App1.pdf). BAL, bronchoalveolar lavage; NA, not available (information on material source); RH, Rigshospitalet; SNP, single-nucleotide polymorphism.

Organisation for Research and Treatment of Cancer classification (into proven, probable, possible, or no infection) remains unverified (*22*).

Phylogenetic analysis also showed that STR*Afla* marker 2A was able to consistently differentiate South complex from DCM isolates (26 repeats for

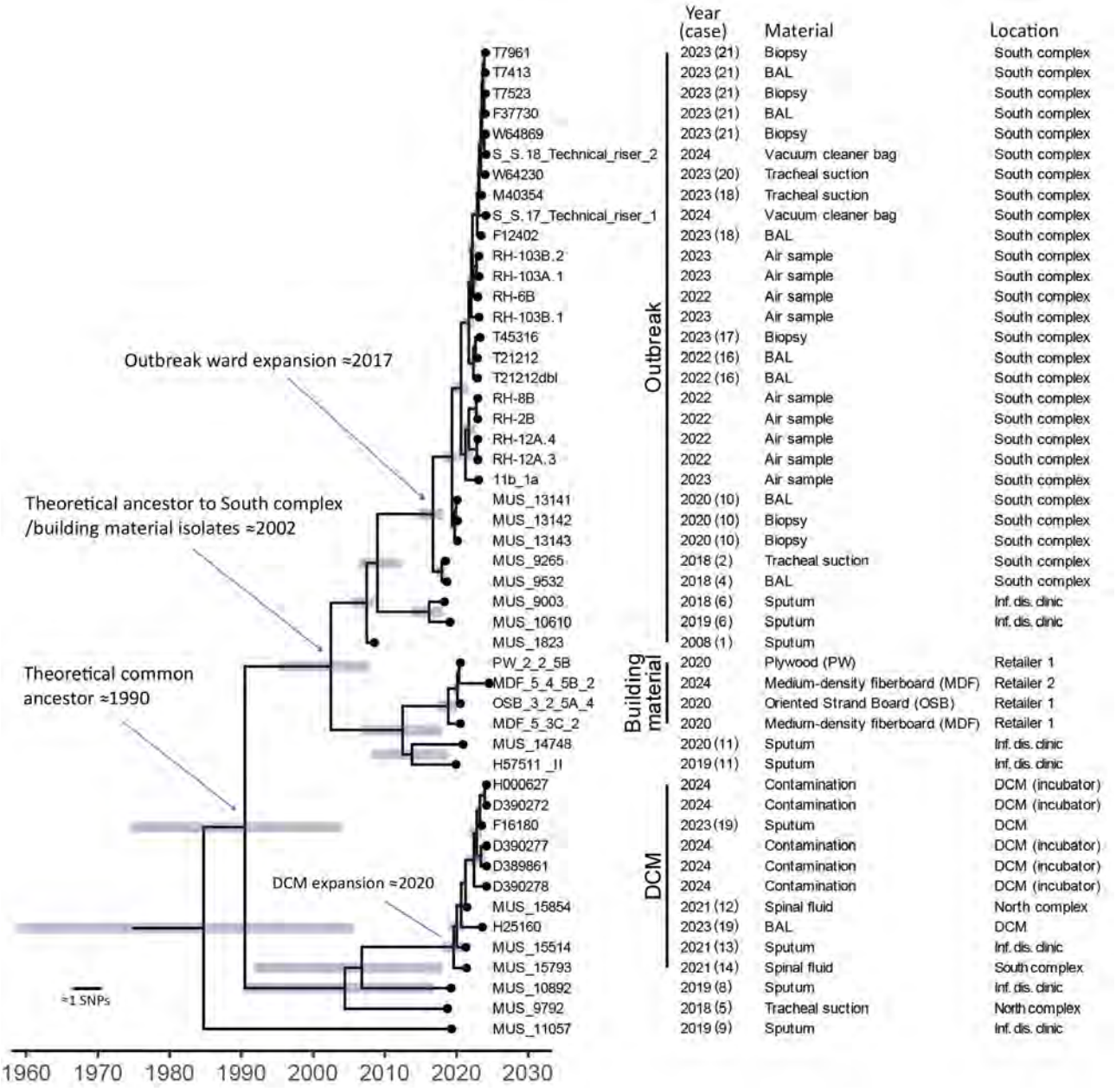

Figure 6. Time-scaled core-genome SNP-based phylogeny of cluster 10, which contained all outbreak isolates, in study of environmental and phylogenetic investigations of *A. flavus* outbreak linked to contaminated building materials, Denmark, 2025. Bars around internal nodes indicate the 95% highest posterior density (HPD) interval of the branching time. There is a distinct clustering of the South complex outbreak isolates (indicated as Outbreak), the isolates from building materials, and isolates from the DCM versus other quality control strains or strains from Denmark (Figure 4). Dating of ancestral nodes indicates that a common ancestor to the outbreak floor clonal expansion existed in the South complex around 2017 (95% HPD 2015–2018). The isolates from the outbreak floor are closely related with the building material isolates and share an inferred ancestor in 2002 (95% HPD 1995–2008). An expansion of a more recent ancestor occurred in the DCM around 2020 (95% HPD 2018–2021), detected as contamination in a laboratory incubator entailing an infection in ≥1 patient (case 19) and possibly also contamination of clinical samples (case 12, 13, 14) based on medical records. Earliest inferred ancestor to all outbreak isolates possibly existed around 1990 (95% HPD 1975–2004). The consensus tree was obtained using BEAST2 (https://www.beast2.org) on 723 core-tygenome SNPs called using an internal reference (T21212). *A. flavus* from patients 3, 7, and 15 were not available for sequencing. BAL, bronchoalveolar lavage; DCM, Department of Clinical Microbiology; inf. dis., infectious disease; SNP, single-nucleotide polymorphism.

South complex vs. 25 repeats for DCM isolates) (Table 2). The ancestral genotype of both were most likely genotype A with 26 repeats on the basis of an inferred ancestral state.

Discussion

This study highlights some of the challenges faced in an *Aspergillus* outbreak investigation, the importance of optimal sampling and identification strategies, and the valuable insights provided by modern typing and whole-genome sequencing techniques. Environmental sampling was challenging. Air sampling notably underestimated the overall burden of *A. flavus* on the outbreak floor, whereas in this investigation surface sampling proved notably more sensitive, not only for *A. flavus* but also for *A. fumigatus* and *A. niger*. Surface sampling established a contamination gradient across the outbreak floor (Figures 2, 3) and thus enabled the discovery of a plywood cupboard with microscopy-confirmed *A. flavus* growth (room A) (Figure 4). Phylogeny revealed a close link between the outbreak isolates and 4 *A. flavus* isolates from unused wood-based building materials sourced from 4 retailers in Denmark (Figure 6). Alongside confirmed in situ growth on 1 such material inside the ward (Figure 4), those findings suggest precontaminated building materials as a potential origin of the outbreak. On the basis of 95% HPD interval, a common ancestor to cluster 10 might have entered during initial hospital construction (≈1970s) or during later renovations. As previously speculated, the South complex isolates likely spread during ward renovations during 2017–2019 (*5*), coinciding with the outbreak onset, in accordance with this study's detection of clonal expansion in the South complex occurring at that time (Figure 6).

Consensus guidelines regarding how to perform and interpret *Aspergillus* hospital outbreak investigations are currently sparse and linked to air sampling. Ruiz-Camps et al. (*23*) recommended a limit of 0.5 fungal CFU/m^3 in HEPA-protected air and 25 CFU/m^3 in unprotected air but did not specify a culture temperature. Chang et al. (*24*) suggested limits of <5 *Aspergillus* CFU/m^3 in protective isolation areas and <0.1 *Aspergillus* CFU/m^3 in HEPA-filtered environments, along with a threshold of 15 fungal CFU/m^3 for gross colony counts. Moreover, culture at 37°C was recommended to favor growth of human pathogenic fungi (*24*). However, Morris et al. (*25*), using the same thresholds, advised culturing at 28°C. Those discrepancies are not trivial and may result in divergent risk assessment. Optimal growth conditions for *A. flavus* are 32°C–33°C, substrate water activity of 0.95, and pH 4–6.5 (*26*,*27*). However, it grows well at 37°C (*28*) and can grow at 20°C–40°C, substrate water activity of ≥0.80, and pH 4–9 (*26*,*27*). In addition, *A. flavus* can grow in a variety of substrates because of its abundant enzyme production (*11*). In our study, mean total fungal CFU counts varied 9-fold for paired air samples cultured at the 2 temperatures, mainly because of *A. calidoustus*, *Cladosporium*, and *Penicillium*, which dominated spore counts at 25°C but rarely cause infections. Perhaps even more concerning, air sampling was overall notably insensitive to detect *A. flavus*. Thus, surface sampling from infrequently cleaned sites is key for detection; this sampling substantially increased the yield of *A. flavus* (as well as of *A. fumigatus* and *A. niger*), in agreement with previous observations (*11*,*29*). Moreover, this study suggests incubation at 37°C to favor *A. flavus* (and other opportunistic molds) and to minimize overgrowth of irrelevant species, thereby avoiding difficulties in plate reading and underestimation of the *A. flavus* burden (Table 1). Finally, the dispersal of spores throughout the outbreak floor indicates that settled dust in less frequently cleaned areas might serve as satellite sources of spores with dust-mediated spread of *A. flavus* (*30*).

STR*Afla* typing identified the outbreak genotype A exclusively on the outbreak floor (Table 2) during the environmental sampling session March–June 2024. Closely related isolates came from 7 additional patients, a DCM incubator (5 isolates) (shared 8/9 markers, genotype B), and from wood-based materials (4 isolates) that shared 5–8/9 (genotypes C, D, E) STR*Afla* markers with the outbreak genotype A. Of note, individual STR*Af* markers in *A. fumigatus* might gain single-repeat variants over serial propagation in vivo and in vitro as a result of microevolution (*31*); thus, we initially regarded genotype A and B as identical and equally involved in the outbreak despite a 1-repeat difference (Table 2). However, genome-based phylogenetic analysis confirmed that degrees of isogeneity among *A. flavus,* observed through STR*Afla* typing were consistent. Single-repeat differences at 2A are likely to be genetically meaningful, and provided laboratories continuously use matching protocol parameters, interpretability in regards to single-repeat deviances should not be a concern (*32*). The relatively small variations in repeat counts in the genotypes of wood-based isolates might also reflect the evolutionary biology of STR sequences that possibly evolve through small, stepwise repeat changes over

time (*33*,*34*). Taken together, our results support STR*Afla*'s continued value as a sensitive and specific frontline screening tool for clinical outbreak investigations. Furthermore, those findings are consistent with those of other studies validating microsatellite assays in fungi through genome sequencing (*7*,*9*,*10*), although species-dependent variation in discriminatory power might exist.

Core-genome phylogeny revealed clusters across the isolate collection; cluster 10 (Figures 5, 6) distinctly separated from other clusters. Cluster 10 isolates only included isolates from the outbreak hospital, except those from building materials, supporting a localized outbreak. Minimal genetic diversity within cluster 10 indicated recent clonal expansion.

Bayesian time-scaled phylogeny identified 3 cluster 10 genetic variants: 1 in the South complex, 1 in external building materials (and patient 11 [Figure 6]), and 1 in the DCM. The variants were detected at different time points, but a common ancestor could date back to the 1970s, coinciding with the construction of the hospital (Figure 6).

Confirmed growth of the South complex variant on a plywood base in the outbreak ward suggests a link to precontaminated wood-based materials, also observed for other molds (*35*). The plywood was part of a kitchen installed in 2012, raising 2 possibilities: that periodic hospital renovations and occasional water damage promoted growth of already prevalent spores that persisted and evolved within the hospital environment, or that repeated introductions to the hospital occurred, possibly through precontaminated wood-based materials. The second is supported by almost genetically identical *A. flavus* isolates found in hospital-unrelated wood-based materials from retailers in Denmark, but that theory does not explain the finding of an outbreak isolate in a patient sample as early as 2008. If precontaminated materials were the original source, dormant *A. flavus* spores might have germinated after water damage (*36*). Wood-based materials can act as *Aspergillus* substrates (*11*), and strains phylogenetically related to the outbreak isolates grew on both plywood and oriented strand board (Table 2; Figure 4). Whether cluster 10 represents a genetically distinct subdivision of *A. flavus* or whether genome rearrangements (*37*), other alterations (*38*), or selective pressures (*7*,*38*) drove its hospital expansion remains unresolved. However, our findings raise concern related to the use of wood-based materials (and organic building materials in general) in hospital areas housing immunocompromised patients.

In conclusion, this study underscores the importance of comprehensive and correct environmental sampling and genomic analysis in *A. flavus* outbreaks. Our understanding of this outbreak was substantially enhanced by the use of phylogenetic analysis. Dormant spores of *A. flavus* had begun actively growing within the hospital environment, with settled dust acting as a reservoir for conidia. Phylogeny validated STR*Afla* typing as a sensitive and specific tool for frontline outbreak investigation. Crucially, time-scaled phylogeny linked the outbreak isolates to *A. flavus* isolated from colonized wood-based materials, implicating the hospital's original construction or subsequent renovations as the likely source of introduction. Our findings should be taken into consideration in planning for the material composition of future hospitals.

Acknowledgments

We thank Désiré Mageme Nahimana for substantial laboratory assistance.

Approval to conduct this study was granted by the Department for Data Protection and Information Security (DBIS) at Statens Serum Institut, J.nr. 22/01885, after institutional review. Publication permission of the data included in this article was granted by the Danish Data Protection Agency (case no. 2025-52-0173, doc. no. 687861). Both case documents will be provided upon request.

Fungal genome sequences generated in this study are available from the European Nucleotide Archive through the accession numbers provided in Appendix 2 (https://wwwnc.cdc.gov/EID/article/32/3/25-1219-App2.xlsx). Versions of Figures 5 and 6 were presented on a poster during the 12th Congress on Trends in Medical Mycology, September 19–22, 2025, Bilbao, Spain.

No funding was received for this study. M.C.A. has, over the past 5 years, received research grants/contract work (paid to the SSI) from Cidara, F2G, Gilead, and Scynexis, and speaker honoraria from Astellas, Chiesi, Gilead, and F2G. She is the current chairman of EUCAST-AFST.

AI (ChatGPT5) was used for grammatical improvement of the text.

About the Author

Dr. Gewecke is a PhD student in the Unit of Mycology at Statens Serum Institut, Copenhagen, Denmark. Under the supervision of M.C.A., he is researching *Aspergillus* outbreaks, including an *A. flavus* outbreak in a Copenhagen tertiary hospital, as part of his thesis.

References

1. Rudramurthy SM, Paul RA, Chakrabarti A, Mouton JW, Meis JF. Invasive aspergillosis by *Aspergillus flavus*: epidemiology, diagnosis, antifungal resistance, and management. J Fungi (Basel, Switzerland). 2019;5:55.
2. Vonberg R-P, Gastmeier P. Nosocomial aspergillosis in outbreak settings. J Hosp Infect. 2006;63:246–54. https://doi.org/10.1016/j.jhin.2006.02.014
3. Vissing NH, Lausen B, Hutchings Hoffmann M, Als-Nielsen B, Schmiegelow K, Helweg-Larsen J, et al. *Aspergillus flavus* infections in children with leukemia despite liposomal amphotericin-B prophylaxis. Pediatr Infect Dis J. 2021;40:749–52. https://doi.org/10.1097/INF.0000000000003189
4. Rudramurthy SM, de Valk HA, Chakrabarti A, Meis JF, Klaassen CH. High resolution genotyping of clinical *Aspergillus flavus* isolates from India using microsatellites. PLoS One. 2011;6:e16086. https://doi.org/10.1371/journal.pone.0016086
5. Gewecke A, Hare RK, Salgård C, Kyndi L, Høg M, Petersen G, et al. A single-source nosocomial outbreak of *Aspergillus flavus* uncovered by genotyping. Microbiol Spectr. 2024;12:e0027324.
6. Ballard E, Melchers WJG, Zoll J, Brown AJP, Verweij PE, Warris A. In-host microevolution of *Aspergillus fumigatus*: a phenotypic and genotypic analysis. Fungal Genet Biol. 2018;113:1–13. https://doi.org/10.1016/j.fgb.2018.02.003
7. Buil JB, Houbraken J, Reijers MH, Zoll J, Sanguinetti M, Meis JF, et al. Genetic and phenotypic characterization of in-host developed azole-resistant *Aspergillus flavus* isolates. J Fungi (Basel). 2021;7:164. https://doi.org/10.3390/jof7030164
8. Joste V, Delouis M, Mouhajir A, Gera Denis-Petit S, Moënne-Locoz P, Kernéis S, et al. Genomic investigation of an antifungal-resistant *Aspergillus fumigatus* outbreak in a French hospital. Med Mycol. 2025;63:myaf012. https://doi.org/10.1093/mmy/myaf012
9. Guinea J, Mezquita S, Gómez A, Padilla B, Zamora E, Sánchez-Luna M, et al. Whole genome sequencing confirms *Candida albicans* and *Candida parapsilosis* microsatellite sporadic and persistent clones causing outbreaks of candidemia in neonates. Med Mycol. 2021;60:myab068. https://doi.org/10.1093/mmy/myab068
10. Hiel SJP, Hendriks ACA, Eijkenboom JJA, Bosch T, Coolen JPM, Melchers WJG, et al. *Aspergillus* outbreak in an intensive care unit: source analysis with whole genome sequencing and short tandem repeats. J Fungi (Basel). 2024;10:51.
11. Loukou E, Jensen NF, Rohde L, Andersen B. Damp buildings: associated fungi and how to find them. J Fungi (Basel). 2024;10:108. https://doi.org/10.3390/jof10020108
12. Samson RA, Houbraken J, Thrane U, Frisvad JC, Andersen B; Westerdijk Fungal Biodiversity Institute. Food and indoor fungi. 2nd edition. Utrecht (the Netherlands): Westerdijk Fungal Biodiversity Institute; 2019.
13. Normand AC, Becker P, Gabriel F, Cassagne C, Accoceberry I, Gari-Toussaint M, et al. Validation of a new web application for identification of fungi by use of matrix-assisted laser desorption ionization–time of flight mass spectrometry. J Clin Microbiol. 2017;55:2661–70. https://doi.org/10.1128/JCM.00263-17
14. Arendrup MC, Hare RK, Jørgensen KM, Bollmann UE, Bech TB, Hansen CC, et al. Environmental hot spots and resistance-associated application practices for azole-resistant *Aspergillus fumigatus*, Denmark, 2020–2023. Emerg Infect Dis. 2024;30:1531–41. https://doi.org/10.3201/eid3008.240096
15. Gaio D, Anantanawat K, To J, Liu M, Monahan L, Darling AE. Hackflex: low-cost, high-throughput, Illumina Nextera Flex library construction. Microb Genom. 2022;8:000744.
16. Sahl JW, Lemmer D, Travis J, Schupp JM, Gillece JD, Aziz M, et al. NASP: an accurate, rapid method for the identification of SNPs in WGS datasets that supports flexible input and output formats. Microb Genom. 2016;2:e000074.
17. Wood DE, Salzberg SL. Kraken: ultrafast metagenomic sequence classification using exact alignments. Genome Biol. 2014;15:R46. https://doi.org/10.1186/gb-2014-15-3-r46
18. Bankevich A, Nurk S, Antipov D, Gurevich AA, Dvorkin M, Kulikov AS, et al. SPAdes: a new genome assembly algorithm and its applications to single-cell sequencing. J Comput Biol. 2012;19:455–77. https://doi.org/10.1089/cmb.2012.0021
19. Croucher NJ, Page AJ, Connor TR, Delaney AJ, Keane JA, Bentley SD, et al. Rapid phylogenetic analysis of large samples of recombinant bacterial whole genome sequences using Gubbins. Nucleic Acids Res. 2015;43:e15. https://doi.org/10.1093/nar/gku1196
20. Nguyen LT, Schmidt HA, von Haeseler A, Minh BQ. IQ-TREE: a fast and effective stochastic algorithm for estimating maximum-likelihood phylogenies. Mol Biol Evol. 2015;32:268–74. https://doi.org/10.1093/molbev/msu300
21. Balaban M, Moshiri N, Mai U, Jia X, Mirarab S. TreeCluster: clustering biological sequences using phylogenetic trees. PLoS One. 2019;14:e0221068. https://doi.org/10.1371/journal.pone.0221068
22. Peter Donnelly J, Chen SC, Kauffman CA, Steinbach WJ, Baddley JW, Verweij PE, et al.; Revision and update of the consensus definitions of invasive fungal disease from the European Organization for Research and Treatment of Cancer and the Mycoses Study Group Education and Research Consortium. Clin Infect Dis. 2020;71:1367–76. https://doi.org/10.1093/cid/ciz1008
23. Ruiz-Camps I, Aguado JM, Almirante B, Bouza E, Ferrer-Barbera CF, Len O, et al.; GEMICOMED (Medical Mycology Study Group of SEIMC). Guidelines for the prevention of invasive mould diseases caused by filamentous fungi by the Spanish Society of Infectious Diseases and Clinical Microbiology (SEIMC). Clin Microbiol Infect. 2011;17(Suppl 2):1–24. https://doi.org/10.1111/j.1469-0691.2011.03477.x
24. Chang CC, Ananda-Rajah M, Belcastro A, McMullan B, Reid A, Dempsey K, et al. Consensus guidelines for implementation of quality processes to prevent invasive fungal disease and enhanced surveillance measures during hospital building works, 2014. Intern Med J. 2014;44(12b):1389–97. https://doi.org/10.1111/imj.12601
25. Morris G, Kokki MH, Anderson K, Richardson MD. Sampling of *Aspergillus* spores in air. J Hosp Infect. 2000;44:81–92. https://doi.org/10.1053/jhin.1999.0688
26. Norlia M, Jinap S, Nor-Khaizura MAR, Radu S, John JM, Rahman MAH, et al. Modelling the effect of temperature and water activity on the growth rate of *Aspergillus flavus* and aflatoxin production in peanut meal extract agar. Int J Food Microbiol. 2020;335:108836. https://doi.org/10.1016/j.ijfoodmicro.2020.108836
27. Ponizovskaya VB, Rebrikova NL, Kachalkin AV, Antropova AB, Bilanenko EN, Mokeeva VL. Micromycetes as colonizers of mineral building materials in historic monuments and museums. Fungal Biol. 2019;123:290–306. https://doi.org/10.1016/j.funbio.2019.01.002

28. de Hoog GS, Guarro J, Gené J, Ahmed SA, Al-Hatmi AMS, Figueras MJ, et al. Atlas of clinical fungi. 4th edition [cited 2025 Nov 2]. https://www.atlasclinicalfungi.org
29. Heinemann S, Symoens F, Gordts B, Jannes H, Nolard N. Environmental investigations and molecular typing of *Aspergillus flavus* during an outbreak of postoperative infections. J Hosp Infect. 2004;57:149–55. https://doi.org/10.1016/j.jhin.2004.02.007
30. Arnow PM, Sadigh M, Costas C, Weil D, Chudy R. Endemic and epidemic aspergillosis associated with in-hospital replication of *Aspergillus* organisms. J Infect Dis. 1991;164:998–1002. https://doi.org/10.1093/infdis/164.5.998
31. de Groot T, Meis JF. Microsatellite stability in STR analysis *Aspergillus fumigatus* depends on number of repeat units. Front Cell Infect Microbiol. 2019;9:82. https://doi.org/10.3389/fcimb.2019.00082
32. de Valk HA, Meis JFGM, Klaassen CHW. Microsatellite based typing of *Aspergillus fumigatus*: strengths, pitfalls and solutions. J Microbiol Methods. 2007;69:268–72. https://doi.org/10.1016/j.mimet.2007.01.009
33. Jin L, Macaubas C, Hallmayer J, Kimura A, Mignot E. Mutation rate varies among alleles at a microsatellite locus: phylogenetic evidence. Proc Natl Acad Sci U S A. 1996;93:15285–8. https://doi.org/10.1073/pnas.93.26.15285
34. Islam MS, Callicott KA, Mutegi C, Bandyopadhyay R, Cotty PJ. *Aspergillus flavus* resident in Kenya: high genetic diversity in an ancient population primarily shaped by clonal reproduction and mutation-driven evolution. Fungal Ecol. 2018;35:20–33. https://doi.org/10.1016/j.funeco.2018.05.012
35. Andersen B, Dosen I, Lewinska AM, Nielsen KF. Pre-contamination of new gypsum wallboard with potentially harmful fungal species. Indoor Air. 2017;27:6–12. https://doi.org/10.1111/ina.12298
36. Vesper S, Wymer L, Cox D, Dewalt G. Populations of some molds in water-damaged homes may differ if the home was constructed with gypsum drywall compared to plaster. Sci Total Environ. 2016;562:446–50. https://doi.org/10.1016/j.scitotenv.2016.04.067
37. Kjærbølling I, Vesth T, Frisvad JC, Nybo JL, Theobald S, Kildgaard S, et al. A comparative genomics study of 23 *Aspergillus* species from section Flavi. Nat Commun. 2020;11:1106. https://doi.org/10.1038/s41467-019-14051-y
38. Morogovsky A, Handelman M, Abou Kandil A, Shadkchan Y, Osherov N. Horizontal gene transfer of triazole resistance in *Aspergillus fumigatus*. Microbiol Spectr. 2022;10:e0111222. https://doi.org/10.1128/spectrum.01112-22

Address for correspondence: Maiken Cavling Arendrup, Unit for Mycology building 45/112, Statens Serum Institut, Artillerivej 5, DK-2300 Copenhagen S, Denmark; email: maca@ssi.dk

etymologia revisited

Trichinella spiralis

[tri-kuh-neh′-luh spr-a′-luhs]

Trichinella is derived from the Greek words *trichos* (hair) and *ella* (diminutive); *spiralis* means spiral. In 1835, Richard Owen (1804–1892) and James Paget (1814–1899) described a spiral worm (*Trichina spiralis*)–lined sandy diaphragm of a cadaver. In 1895, Alcide Raillet (1852–1930) renamed it as *Trichinella spiralis* because *Trichina* was attributed to an insect in 1830. In 1859, Rudolf Virchow (1821–1902) described the life cycle. The genus includes many distinct species, several genotypes, and encapsulated and nonencapsulated clades based on the presence/absence of a collagen capsule.

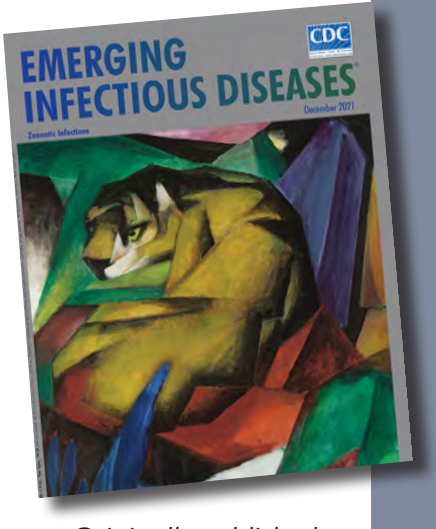

Originally published in December 2021

References

1. Campbell WC. History of trichinosis: Paget, Owens and the discovery of *Trichinella spiralis*. Bull Hist Med. 1979;53:520–52.
2. Centers for Disease Control and Prevention. Trichinellosis: general information [cited 2021 May 11]. https://www.cdc.gov/parasites/trichinellosis/gen_info/faqs.html
3. Gottstein B, Pozio E, Nöckler K. Epidemiology, diagnosis, treatment, and control of trichinellosis. Clin Microbiol Rev. 2009;22:127–45. https://doi.org/10.1128/CMR.00026-08
4. Observations on *Trichina spiralis*. Boston Med Surg J. 1860; 63:294–8. https://doi.org/10.1056/NEJM186011080631504
5. Zarlenga D, Thompson P, Pozio E. *Trichinella* species and genotypes. Res Vet Sci. 2020;133:289–96. https://doi.org/10.1016/j.rvsc.2020.08.012

https://wwwnc.cdc.gov/eid/article/27/12/et-2712_article

Tuberculosis before and during COVID-19 Pandemic, United States, 2010–2023

Pei-Jean I. Feng, Christina R. Phares, Robert Pratt, Julie L. Self

After a steady decline in tuberculosis (TB) during 2010–2019, the United States reported a sharp drop in 2020 and increases during 2021–2023. We assessed whether TB cases during 2020–2023 differed from what was expected in the absence of the COVID-19 pandemic. Using data from the Centers for Disease Control and Prevention National TB Surveillance System and Electronic Disease Notification system, we constructed Poisson regression models to predict frequencies of TB cases, persons receiving TB diagnosis within 1 year of arrival, and persons for whom postarrival TB follow-up was recommended on the basis of 2010–2019 trends. We observed lower than predicted TB cases (7,170 observed, 8,822 predicted), persons receiving diagnosis within 1 year of arrival (208 observed, 259 predicted), and persons with class B TB (4,827 observed, 7,169 predicted) in 2020. Migration changes and COVID-19–related factors likely contributed to the decrease in TB in 2020 and increases during 2021–2023.

In the United States, tuberculosis (TB) cases and incidence rates (cases/100,000 persons) declined steadily during 1992–2019 (*1*). During 2010–2019, both case counts and incidence rates decreased by an average of 3% per year. In 2020, concurrent with the onset of the COVID-19 pandemic, the United States reported 7,170 TB cases and an incidence rate of 2.2, representing a 19% decline in cases and 20% decline in incidence rate compared with 2019. The percentage decreases in TB case count and incidence rate from 2019 to 2020 were >6–8 times that of the yearly average from 2010–2019 (*1*). The drop in cases in 2020 was likely a result of multiple factors associated with the COVID-19 pandemic, including delayed diagnoses, changes in movement or travel of non–US-born persons to the United States (migration), and pandemic mitigation efforts (*2*).

Author affiliation: Centers for Disease Control and Prevention, Atlanta, Georgia, USA

DOI: https://doi.org/10.3201/eid3203.251459

Since 2001, most TB cases in the United States have occurred among persons born outside the United States (*1*). When stratified by the number of years since arrival, the highest percentage of TB diagnoses among non–US-born persons occurs in the first few years after arrival in the United States. In 2020, a total of 28% of cases among non–US-born persons were diagnosed within 5 years of arrival in the United States, compared with 30% in 2019 and a median of 32% during 2010–2018 (*1*).

TB cases and incidence rates have increased every year since 2020. TB cases increased by 10% from 2020 (n = 7,170) to 2021 (n = 7,866), 6% from 2021 to 2022 (n = 8,332), and 16% from 2022 to 2023 (n = 9,633). Similarly, TB incidence rate increased by 10% from 2020 (2.2 cases/100,000 persons) to 2021 (2.4 cases/100,000 persons), 6% from 2021 to 2022 (2.5 cases/100,000 persons), and 15% from 2022 to 2023 (2.9 cases/100,000 persons) (*1*).

We used multiple data sources to determine if the substantial drop in TB cases in 2020 was statistically different from what would have been expected had the COVID-19 pandemic not occurred and to examine possible factors that contributed to that drop and the subsequent increase in cases after 2020. The Centers for Disease Control and Prevention (CDC) reviewed this activity and deemed it not research. We conducted the study consistent with applicable federal law and CDC policy (*2*).

Materials and Methods

The 50 US states and the District of Columbia are required to report each new TB case to CDC's National Tuberculosis Surveillance System (NTSS) (*3*), using the Report of Verified Case of Tuberculosis (*4*). For our analysis, we obtained verified TB case counts from NTSS (*1*,*5*). We created a Poisson regression model to estimate annual TB case counts during 2010–2019, the years preceding the COVID-19 pandemic,

which we used to predict counterfactual annual case counts during the pandemic (2020–2023). We used the bootstrap method to obtain robust estimates of the predicted case counts and corresponding prediction intervals by running the Poisson model on 1,000 replicate datasets randomly sampled, with replacement, from the observed 2010–2019 case counts. The median of the 1,000 replicate predictions represents the bootstrap estimate of the predicted annual case count. The 2.5th and 97.5th percentiles represent the 95% prediction interval (PI), which accounts for the uncertainty from estimating the model and the variance of the projected case counts. We applied the bootstrap method to all models in our analysis.

The Poisson model consisted of predictors for case count year: the previous year's TB case count, which controls for autocorrelation and represents potential lag effects carried over from the previous year, and an offset variable to represent the US population from the US Census Bureau national population totals from 2023 (*6*). The offset variable accounted for population changes and enabled us to model rates, while maintaining the count structure of our data. We also stratified the Poisson model by origin of birth to examine if the association between COVID-19 and TB case counts differed among US-born persons and non–US-born persons. In NTSS, persons born in the United States, in US territories, or elsewhere to ≥1 US citizen parent were categorized as US-born. All other persons were categorized as non–US-born. We excluded persons with unknown origin of birth from the stratified analysis. We used annual US-born and non–US-born population estimates from the US Census Bureau American Community Survey (ACS) as offsets for the respective stratified Poisson models (*7*). Persons with a value for the citizenship status variable in ACS of not a citizen of the US or US citizen by naturalization were categorized non–US-born; all others were categorized as US-born (*8*).

To investigate the effect of migration-related factors on TB during the COVID-19 pandemic, we predicted the number of persons who received a TB diagnosis within 12 months of arrival to the United States (persons with first-year diagnoses) during 2020–2023 using a Poisson regression, based on 2010–2019 data, limited to non–US-born persons only. We determined the duration between arrival in the United States and diagnosis of TB by calculating the difference between the arrival date and the date the case was first reported to the health department. To control for autocorrelation, the model included predictors representing year of arrival to the United States and the number of persons with first-year diagnoses during the previous year. The offset variable for this model represented the annual number of non–US-born persons, regardless of legal status, who arrived in the United States, as reported by ACS (*7*). Because persons who arrive in the United States may later emigrate from the United States, the number of persons who report arriving during a particular year will decrease over time. We found that the reported number of persons who arrived in the United States in a particular year peaked in the 1-year ACS estimate of the following year. Therefore, we included the ACS estimates from the following year as the offset variable. We used that model to predict the number of persons with first-year diagnoses during 2020–2022. Because the peak number of persons who arrived in 2023 was not published at the time of our analysis, we predicted counts through 2022.

To further assess migration-related factors on TB during the pandemic, we analyzed health information reported to CDC's Electronic Disease Notification (EDN) system from overseas medical examinations of refugees, immigrants, and some parolees (*9*). Refugees are persons unable or unwilling to return to their country of nationality because of persecution or well-founded fear of persecution (*10*). Immigrants are foreign nationals with an immigrant visa who become lawful permanent residents upon admission to the United States (*12*). Parolees are persons granted parole into the United States for humanitarian reasons or substantial public benefit (*11*). An overseas medical examination, including screening for TB disease, is required for all refugees, all immigrants who apply for their immigrant visa from outside the United States, and some parolees; we collectively refer to those persons as persons screened overseas. Persons assigned a class B TB classification during the overseas evaluation are recommended to have a postarrival evaluation for TB (*13*). Class B TB classifications are assigned to persons who recently finished directly observed treatment for TB disease; have signs or symptoms or chest radiographs suggestive of TB disease, or have known HIV infection with negative sputum cultures and no clinical diagnosis of infectious TB disease; have extrapulmonary TB disease with a normal chest radiograph and negative sputum cultures; have a diagnosis of latent TB infection; or are contacts to infectious TB disease cases (*13*). We examined data from EDN to measure the effects of COVID-19 on the annual number of persons screened overseas who were assigned a class B TB classification (persons with class B TB). We created a Poisson model to predict the number of persons with class B TB during 2020–2023 on the basis of

Table 1. Demographic characteristics of all persons with tuberculosis disease reported to the National TB Surveillance System, United States, 2010–2023*

Characteristic	No. (%) persons	
	2010–2019	2020–2023
All	96,122	33,001
Sex		
M	58,544 (61)	20,337 (62)
F	37,567 (39)	12,653 (38)
Age group, y		
0–4	2,627 (3)	755 (2)
5–14	2,003 (2)	706 (2)
15–24	9,599 (10)	3,227 (10)
25–44	29,670 (31)	9,841 (30)
45–64	29,655 (31)	9,608 (29)
≥65	22,564 (23)	8,861 (27)
Race or ethnicity†		
American Indian or Alaska Native	1,185 (1)	387 (1)
Asian	31,665 (33)	11,066 (34)
Black or African American	20,814 (22)	5,850 (18)
White	13,129 (14)	3,401 (10)
Native Hawaiian or other Pacific Islander	896 (1)	532 (2)
Hispanic or Latino	27,610 (29)	10,909 (33)
Multiple race	586 (1)	549 (2)

*2010–2019 is the period before the COVID-19 pandemic; 2020–2023 is the period during the COVID-19 pandemic.
†Persons who identified as Hispanic or Latino were categorized as Hispanic, regardless of self-reported race. Persons who did not identify as Hispanic or Latino were categorized by self-reported race; if >1 race was reported, the person was categorized as multiple race.

prepandemic data, using year of arrival as the only predictor. We did not include a lag term because the number of persons with class B TB each year was not influenced by the previous year's number. We used the total number of refugees documented in EDN, along with the number of new arrivals obtaining lawful permanent resident status provided by the US Department of Homeland Security, as the offset variable for this model (*14*).

We conducted statistical analyses using SAS version 9.4 (SAS Institute, Inc, https://www.sas.com) and R statistical software version 4.4.2 (The R Project for Statistical Computing, https://www.r-project.org). We designated statistical significance at 5% ($\alpha \leq 0.05$). We considered as statistically significant any observed counts during 2020–2023 that fell outside the 95% PIs of the predicted counts.

Results

During 2010–2023, a total of 129,123 TB cases were reported to NTSS; of those, 96,122 cases were reported in 2010–2019, before the pandemic, and 33,001 cases in 2020–2023, during the pandemic (Table 1). The percentage of TB cases that occurred among US-born persons decreased from 33% (n = 32,083) during 2010–2019 to 26% (n = 8,599) during 2020–2023. The most common age group was 25–44 years among all persons across the prepandemic and pandemic periods: 29,670/96,122 (31%) persons during 2010–2019 and 9,841/33,001 (30%) persons during 2020–2023. The most common age group among US-born persons was 45–64 years, 11,256/32,083 (35%) persons during 2010–2019 and 2,501/8,599 (29%) persons during 2020–2023.

The most common age group among non–US-born persons was 25–44 years, 22,727/63,990 (36%) persons during 2010–2019 and 7,795/24,341 (32%) during 2020–2023) (Table 2). Among persons with

Table 2. Demographic characteristics of persons with tuberculosis disease reported to the National TB Surveillance System, by origin of birth, United States, 2010–2023*

Characteristic	US-born, no. (%) persons		Non–US-born, no. (%) persons	
	2010–2019	2020–2023	2010–2019	2020–2023
All	32,083	8,599	63,990	24,341
Sex				
M	20,668 (64)	5,384 (63)	37,839 (59)	14,914 (61)
F	11,414 (36)	3,213 (37)	26,142 (41)	9,421 (39)
Age group, y				
0–4	2,314 (7)	680 (8)	313 (0)	75 (0)
5–14	1,240 (4)	442 (5)	763 (1)	263 (1)
15–24	2,948 (9)	951 (11)	6,650 (10)	2,275 (9)
25–44	6,932 (22)	2,037 (24)	22,727 (36)	7,795 (32)
45–64	11,256 (35)	2,501 (29)	18,378 (29)	7,090 (29)
≥65	7,392 (23)	1,986 (23)	15,156 (24)	6,842 (28)
Race or ethnicity†				
American Indian or Alaska Native	1,176 (4)	382 (4)	9 (0)	5 (0)
Asian	1,331 (4)	442 (5)	30,325 (47)	10,614 (44)
Black or African American	12,148 (38)	2,892 (34)	8,664 (14)	2,953 (12)
White	10,254 (32)	2,351 (27)	2,871 (4)	1,043 (4)
Native Hawaiian or Other Pacific Islander	299 (1)	180 (2)	596 (1)	352 (1)
Hispanic or Latino	6,595 (21)	2,183 (25)	20,986 (33)	8,691 (36)
Multiple race	214 (1)	111 (1)	370 (1)	437 (2)

*2010–2019 is the period before the COVID-19 pandemic; 2020–2023 is the period during the COVID-19 pandemic.
†Persons who identified as Hispanic or Latino were categorized as Hispanic, regardless of self-reported race. Persons who did not identify as Hispanic or Latino were categorized by self-reported race; if >1 race was reported, the person was categorized as multiple race.

first-year diagnoses, 6,147 (67%) persons arrived in the United States during 2010–2019, before the onset of COVID-19, whereas 3,053 (33%) arrived during and after the pandemic, during 2020–2023 (Table 3). Similar to all non–US-born persons with TB, the most common age group in both periods among persons with first-year diagnoses was 25–44 years (2,425/6,147 [39%] during 2010–2019 and 1,413/3,053 [46%] during 2020–2023). The next most common age group was 15–24 years (1,390/6,147 [23%] during 2010–2019 and 674/3,053 [22%] during 2020–2023) (Table 3).

During 2010–2019, the number of persons with first-year diagnoses fluctuated from 522 to 708, representing an annual percentage change that ranged from −20% to 13% (Table 4). The number of persons with first-year diagnoses in 2020 was 60% lower than in 2019 (n = 208), followed by increases of 227% (n = 680) in 2021 and 70% (n = 1,159) in 2022. Prepandemic, the annual percentage change in the number of non–US-born persons arriving in the United States was −17% to 17% (Table 4). In 2020, the number of non–US-born persons who arrived in the United States decreased by 49% (n = 694,831) from 2019 (n = 1,369,247) before increasing by 110% (n = 1,456,907) in 2021 and 40% (n = 2,036,805) in 2022 (Table 4). The total number of persons with first-year diagnoses and the total number of non–US-born persons who arrived in the United States in 2023 were unavailable at the time of our analysis.

Of persons screened overseas, both before and during the pandemic, 4% were assigned class B TB classifications documented in EDN (Table 5). Before the pandemic, the annual number of persons with class B TB was 18,482–28,529; percentage change fluctuated from −19% to 19%. Compared with 2019, the number of persons with class B TB in 2020 decreased by 74% (n = 4,827), then increased by 129% (n = 11,056) in 2021, 80% (n = 19,905) in 2022, and 29% (n = 25,736) in 2023. During 2010–2019, the total number of persons screened overseas each year was 497,255–729,397. In 2020, the total decreased by 62% (n = 191,536) compared with 2019 (n = 497,255), before increasing by 104% (n = 391,138) in 2021, by 38% (n = 541,145) in 2022, and by 18% (n = 640,549) in 2023 (Table 5).

Table 3. Demographic characteristics of persons with first-year tuberculosis diagnoses as reported to the National TB Surveillance System, United States, 2010–2023*

Characteristic	No. (%) persons	
	2010–2019	2020–2023
All	6,147	3,053
Sex		
M	3,583 (58)	1,979 (65)
F	2,564 (42)	1,074 (35)
Age group, y		
0–4	174 (3)	41 (1)
5–14	276 (4)	99 (3)
15–24	1,390 (23)	674 (22)
25–44	2,425 (39)	1,413 (46)
45–64	1,073 (17)	482 (16)
≥65	809 (13)	344 (11)
Race or ethnicity†		
American Indian or Alaska Native	0	2 (0)
Asian	2,401 (39)	705 (23)
Black or African American	1,578 (26)	564 (18)
White	268 (4)	194 (6)
Native Hawaiian or Other Pacific Islander	55 (1)	28 (1)
Hispanic or Latino	1,751 (28)	1,469 (48)
Multiple race	60 (1)	20 (1)

*First-year diagnosis is a TB diagnosis within 12 months of arrival to the United States. 2010–2019 is the period before the COVID-19 pandemic; 2020–2023 is the period during the COVID-19 pandemic.
†Persons who identified as Hispanic or Latino were categorized as Hispanic, regardless of self-reported race. Persons who did not identify as Hispanic or Latino were categorized by self-reported race; if >1 race was reported, the person was categorized as multiple race.

Table 4. Percentage change in non–US-born persons with first-year diagnoses of tuberculosis reported to the National TB Surveillance System, by year of arrival, United States, 2010–2023*

Year of arrival	No. persons with first-year diagnoses	Total population†	Percentage change	
			Among persons with first-year diagnoses	Among total population
2010	663	1,158,774	Referent	Referent
2011	558	1,083,782	−15.8	−6.5
2012	631	1,212,664	13.1	11.9
2013	634	1,277,674	0.5	5.4
2014	637	1,494,121	0.5	16.9
2015	672	1,617,277	5.5	8.2
2016	708	1,746,695	5.4	8.0
2017	565	1,447,393	−20.2	−17.1
2018	557	1,341,551	−1.4	−7.3
2019	522	1,369,247	−6.3	2.1
2020	208	694,831	−60.2	−49.3
2021	680	1,456,907	226.9	109.7
2022	1,159	2,036,805	70.4	39.8

*Population consisted of persons not born in the United States, in US territories, or elsewhere to ≥1 US citizen parent who received a TB diagnosis within 12 months of arrival to the United States. Data for 2023 were not available at the time of analysis. NA, not available.
†Population data obtained from the American Community Survey (7).

Table 5. Percentage change in persons with class B TB reported to the Electronic Disease Notification system, by year of arrival, United States, 2010–2023*

Year of arrival	No. persons with class B TB	Total population†	Percentage change	
			Among persons with class B TB	Among total population
2010	24,763	574,672	Referent	Referent
2011	22,300	538,061	−9.9	−6.4
2012	26,045	570,436	16.8	6.0
2013	22,884	549,767	−12.1	−3.6
2014	22,059	563,993	−3.6	2.6
2015	24,145	630,993	9.5	11.9
2016	28,529	729,397	18.2	15.6
2017	23,820	604,016	−16.5	−17.2
2018	22,786	554,150	−4.3	−8.3
2019	18,482	497,255	−18.9	−10.3
2020	4,827	191,536	−73.9	−61.5
2021	11,056	391,138	129.0	104.2
2022	19,905	541,145	80.0	38.4
2023	25,736	640,549	29.3	18.4

*Population consisted of persons screened overseas before arrival who were recommended to have a postarrival evaluation for TB in the United States. TB, tuberculosis.
†Sum of population data obtained from the Centers for Disease Control and Prevention's Electronic Disease Notification system (*9*) and the US Department of Homeland Security Yearbook of Immigration Statistics (*15*).

On the basis of data reported to NTSS during 2010–2019, the number of TB cases reported in 2020 (n = 7,170) was significantly lower by 19% than the number predicted (8,822 [95% PI 8,560–9,034]) (Table 6; Appendix Figure 1, https://wwwnc.cdc.gov/EID/article/32/3/25-1459-App1.pdf). Among US-born persons, the number of observed cases in 2020 (n = 2,009) was 16% lower than the number predicted (2,384 [95% PI 2,200–2,513]) (Table 6; Figure 1). The number of cases reported among non–US-born persons (n = 5,151) was 18% lower than predicted (6,273 [95% PI 6,096–6,459]) (Table 6; Figure 2). Among all non–US-born persons who arrived in the United States in 2020, a total of 208 persons had first-year diagnoses, which was lower, but not significantly so, by 20% than the predicted count (n = 259 [95% PI 204–294]) (Table 6; Appendix Figure 2). The number of persons with Class B TB who moved to the United States in 2020 (n = 4,827), as documented in EDN, was significantly lower by 34% than what was predicted (7,169 [95% PI 6,705–7,582]) (Table 6; Appendix Figure 3).

The observed case count for both US-born and non–US-born persons increased every year during 2020–2023. In 2023, the observed overall case count (n = 9,633) was significantly higher than the predicted count (8,464 [95% PI 8,067–8,856]) by 14% (Tables 6, 7; Appendix Figure 1). The observed numbers of cases in 2023 (US-born, 2,293; non–US-born, 7,319) were also significantly higher than predicted for both the US-born (10%; 2,078 [95% PI 1,830–2,267]) and non–US-born (17%; 6,268 [95% PI 6,059–6,535]) populations (Tables 6, 7; Figures 1, 2). During 2020–2023, the total number of observed cases (n = 33,001) was 5% lower than the sum of predicted cases (n = 34,567) among all persons, 4% lower among US-born persons (observed, 8,599; predicted, 8,918), and 2% lower among non–US-born persons (observed, 24,341; predicted, 24,852) (Table 7).

Table 6. Observed and predicted frequencies of TB cases, persons with first-year diagnoses, and persons with class B TB, United States, 2020–2023*

Category	2020			2023		
	No. observed	No. predicted (95% PI†)	Percentage difference	No. observed	No. predicted (95% PI†)	Percentage difference
All persons‡	7,170	8,822 (8,560–9,034)	−18.7	9,633	8,464 (8,067–8,856)	13.8
US-born persons‡	2,009	2,384 (2,200–2,513)	−15.7	2,293	2,078 (1,830–2,267)	10.3
Non–US-born persons‡	5,151	6,273 (6,096–6,459)	−17.9	7,319	6,268 (6,059–6,535)	16.8
First-year diagnoses§	208	259 (204–294)	−19.7	NA	NA	NA
Persons with class B TB#	4,827	7,169 (6,705–7,582)	−32.7	25,736	22,953 (20,876–25,055)	12.1

*Data for TB cases and first-year diagnoses are from National TB Surveillance System; data for Class B TB are from CDC's Electronic Disease Notification system (*9*). First-year diagnoses are those of persons who received a diagnosis of TB disease within 12 months of arrival to the United States. Persons with Class B TB are those screened overseas before arrival who are recommended to have a postarrival evaluation for TB in the United States. NA, not available; TB, tuberculosis.
†Bootstrap prediction interval.
‡Predicted (counterfactual) frequencies for 2020 and 2023 were estimated from Poisson models using data from NTSS during 2010–2019 (*3*).
§Data for 2023 were not available at the time of analysis.
#Predicted frequencies for 2020 and 2023 were estimated from a Poisson model using data from EDN during 2010–2019 (*9*).

Table 7. Number of observed and predicted tuberculosis cases reported to the National TB Surveillance System, by origin of birth, United States, 2020–2023*

	All		US-born		Non–US-born	
Year	No. observed	No. predicted	No. observed	No. predicted	No. observed	No. predicted
2020	7,170	8,822	2,009	2,384	5,151	6,273
2021	7,866	8,703	2,170	2,278	5,676	6,168
2022	8,332	8,578	2,127	2,178	6,195	6,144
2023	9,633	8,464	2,293	2,078	7,319	6,268
Total	33,001	34,567	8,599	8,918	24,341	24,852

*Predicted (counterfactual) frequencies estimated from Poisson models of NTSS data with predictors representing the year the case was counted, the previous year's TB case count, and an offset representing the size of the US population from the US Census Bureau. Persons born in the United States, certain US territories, or elsewhere to ≥1 US citizen parent are categorized as US-born. All other persons are categorized as non–US-born. Persons with unknown origin of birth were excluded from the stratified analysis.

Discussion

In 2020, with the onset of COVID-19, the TB case count in the United States decreased by 19% compared with 2019 (Table 6). The observed case counts in 2020 among both US-born and non–US-born persons were each significantly lower than predicted by the Poisson model. Several COVID-19-related factors likely contributed to the significant decrease in TB cases in 2020.

Changes in migration likely contributed to the decrease in TB in 2020, because the number of non–US-born persons who entered the United States in 2020 decreased by about half compared with 2019 (*7*). In addition, DHS reported a 62% decrease in the number of new-arrival immigrants in 2020 compared with 2019 (*15*). EDN data also showed a decrease of >60% from 2019 to 2020 in the number of persons arriving in the United States who were screened overseas (Table 5). Fewer persons entered the country in 2020; the number of persons with first-year diagnoses also decreased (*1*). Changes in migration likely contributed to the significant decrease in cases in 2020 but do not fully explain it; we observed a decline in 2020 among US-born persons also.

COVID-19 mitigation strategies might have contributed to the drop in TB cases in 2020. For example, mandated or voluntary sheltering in place, use of masks, and physical distancing might have decreased the transmission of not only COVID-19 but also TB (*16*,*17*). Compliance with shelter-in-place mandates and fear of contracting COVID-19 might also have discouraged people from seeking healthcare (*18*). In

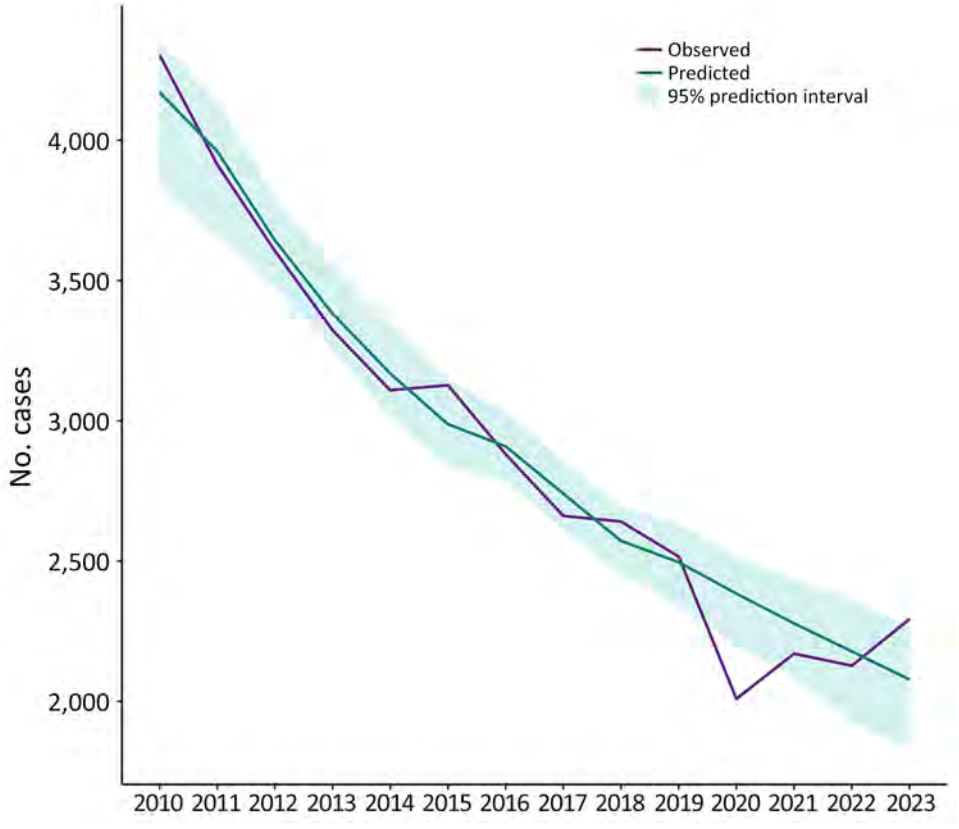

Figure 1. Observed and predicted tuberculosis cases among US-born persons reported to the National TB Surveillance System, United States, 2010–2023. US-born persons are those born in the United States, in US territories, or elsewhere to ≥1 US citizen parent.

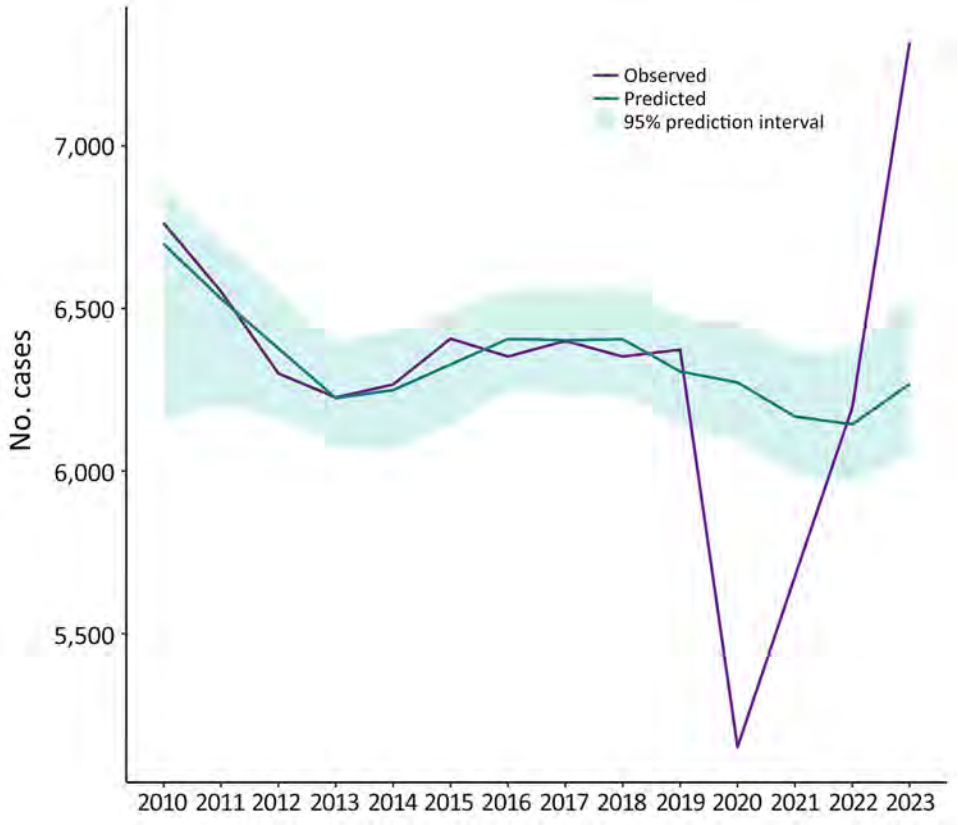

Figure 2. Observed and predicted tuberculosis cases among non–US-born persons reported to the National TB Surveillance System, United States, 2010–2023. Non–US-born persons are those who were not born in the United States, in US territories, or elsewhere to ≥1 US citizen parent.

a nationwide survey, 41% of adults reported having delayed or avoided medical care because of concerns about COVID-19 (*18*). In addition, by using health insurance claims data, researchers found that overall healthcare use decreased by 23% in March 2020 and by 52% in April 2020 (*19*). In San Francisco, California, USA, the city health department reported a substantial drop in persons seeking medical evaluations for signs and symptoms of TB disease after a legal order for shelter-in-place and a pause on routine medical appointments and elective surgery was issued in March 2020 (*20*).

The diversion of funds and staff away from TB programs and toward the COVID-19 response severely impaired the ability of TB programs to identify and diagnose TB, which likely contributed to a lower-than-expected case count in 2020. Activities such as testing, diagnosing and treating TB, conducting thorough and timely contact investigations, and prompt specimen turnaround time from laboratories were all disrupted (*21*). In April 2020, CDC reported that the deployment of TB program staff to COVID-19 activities had decreased the capacity of TB programs across the country to conduct essential TB-related activities. For example, 52% of TB programs saw a partial or high impact on the ability to diagnose and treat persons with TB disease and 64% saw a partial or high impact on the ability to conduct contact investigations for infectious TB cases (*22*).

Because identifying COVID-19 during the pandemic in emergency settings took priority, and because of the shared characteristics between COVID-19 and TB, such as the mode of transmission, risk factors, and respiratory manifestation, clinicians were likely to overlook the possibility of a TB diagnosis (*21*). Researchers found that during times of elevated COVID-19 incidence, clinicians in California had missed opportunities to diagnose TB disease in persons who sought care for respiratory symptoms by testing only for COVID-19 (*23*).

Since 2021, the number of TB cases in the United States has increased annually. In 2023, the TB case count (n = 9,633) surpassed the count in 2013 (n = 9,238). Similarly, the incidence rate of 2.9 in 2023 had not been reported so low since 2016 (*1*). The percentage increase in the number of persons with first-year diagnoses was >2 times the increase in the total number of non–US-born persons who arrived in the United States from 2020 to and 2021 and 1.8 times higher from 2021 to 2022. Those findings suggest not only that more non–US-born persons arrived in the United States after the onset of the COVID-19 pandemic in

2020 but also that the risk for TB among those persons might have been higher than among persons who arrived before the pandemic, evidenced by the continued increase in the percentage of non–US-born persons with first-year diagnoses (*1*,*7*,*15*). Public health entities could consider expanding prearrival screening to additional groups beyond those currently screened overseas.

COVID-19 mitigation strategies, the diversion of funds and staff from TB programs, and the priority of identifying COVID-19 in 2020 likely caused delayed diagnoses for many TB cases. Therefore, TB cases that occurred in 2020 might not have been identified until 2021 or later, which would have increased the case counts during 2021–2023. Furthermore, delayed diagnoses could have contributed to longer infectious periods, thereby increasing the probability of transmitting TB in the community (*24*).

Although the COVID-19 pandemic seems to have reversed the trend toward TB elimination observed before 2021, our data showed that the cumulative number of observed cases from 2021–2023 was still lower than predicted for that period among both US-born and non–US-born persons. That finding could indicate that the effect of the pandemic on TB in the United States was less pronounced than the year-to-year rise in cases would imply. However, continued attention toward TB elimination is warranted, especially because CDC provisionally reported a fourth consecutive year of increasing TB case counts in 2024 (*25*).

Surveillance data alone did not enable us to distinguish between increased transmission and delayed diagnoses. We could not calculate the exact duration between arrival in the United States and the time of diagnosis because the Report of Verified Case of Tuberculosis does not collect diagnosis date (*4*). Instead, we used the notification date to the health department as a proxy. Our analysis of persons with first-year diagnoses was limited to 2010–2022 because the data for persons who arrived in 2023 were not published at the time of our analysis. Also, we were unable to analyze the demographic characteristics of persons screened overseas because of incomplete EDN data in 2021 and 2022. No official agency counts the number of all persons who arrive in the United States annually, so we approximated the denominator to calculate incidence rate for persons with first-year diagnoses using ACS data, which provides estimates instead of counts.

Our analysis suggests that changes in migration and COVID-19–related factors contributed to both the sharp drop in TB cases in 2020 and the subsequent increase in cases from 2021–2023. In particular, the diversion of resources away from TB prevention and control toward COVID-19 mitigation efforts led to delayed TB diagnoses early in the pandemic, which contributed to the increase in cases after 2020. As time passes, the immediate effects associated with the COVID-19 pandemic will diminish. Changes in migration, however, will continue to influence TB in the United States. To resume progress toward TB elimination, renewed commitment in TB programs is essential to develop TB prevention and control strategies that can withstand challenges brought on by migration changes and future pandemics.

About the Author

Ms. Feng is an epidemiologist in the Surveillance, Epidemiology, and Outbreak Investigations Branch within the Division of Tuberculosis Elimination, National Center for HIV, Viral Hepatitis, STD, and TB Prevention, Centers for Disease Control and Prevention, Atlanta, Georgia, USA. Her primary research interests include TB surveillance, diagnostic testing, and the treatment of TB disease and latent TB infection.

References

1. Centers for Disease Control and Prevention. Reported tuberculosis in the United States, 2023 [cited 2024 Nov 18]. https://www.cdc.gov/tb-surveillance-report-2023/index.html
2. Filardo TD, Feng PJ, Pratt RH, Price SF, Self JL. Tuberculosis—United States, 2021. MMWR Morb Mortal Wkly Rep. 2022;71:441–6. https://doi.org/10.15585/mmwr.mm7112a1
3. Centers for Disease Control and Prevention. National Tuberculosis Surveillance System (NTSS). Atlanta: US Department of Health and Human Services; 2024.
4. Centers for Disease Control and Prevention. 2020 Report of Verified Case of Tuberculosis (RVCT) instruction manual. 2021[cited 2022 Feb 2]. https://www.cdc.gov/tb/media/pdfs/Report-of-Verified-Case-of-Tuberculosis-RVCT.pdf
5. Williams PM, Pratt RH, Walker WL, Price SF, Stewart RJ, Feng PI. Tuberculosis—United States, 2023. MMWR Morb Mortal Wkly Rep. 2024;73:265–70. https://doi.org/10.15585/mmwr.mm7312a4
6. United States Census Bureau. 2023 national population projections tables [cited 2024 Apr 11]. https://www.census.gov/data/tables/2023/demo/popproj/2023-summary-tables.html
7. United States Census Bureau. American Community Survey 1-year estimates public use microdata sample. 2024 [cited 2024 Sep 12]. https://data.census.gov/mdat
8. United States Census Bureau. American Community Survey 2023 1-year PUMS user guide and overview. 2024 [cited 2024 Oct 17]. https://www2.census.gov/programs-surveys/acs/tech_docs/pums/2023ACS_PUMS_User_Guide.pdf
9. Phares CR, Liu Y, Wang Z, Posey DL, Lee D, Jentes ES, et al. Disease surveillance among U.S.-bound immigrants

and refugees—Electronic Disease Notification System, United States, 2014–2019. MMWR Surveill Summ. 2022;71:1–21. https://doi.org/10.15585/mmwr.ss7102a1
10. Legal Information Institute. Title 8, Code §1101—definitions. [cited 2024 Jan 3]. https://www.law.cornell.edu/uscode/text/8/1101
11. Code of Federal Regulations. Public charge ground of inadmissibility. 87 C.F.R. 55636. Part 212 (2022).
12. Ward A. Office of Homeland Security statistics. U.S. lawful permanent residents: 2023. 2024 [cited 2024 Sep 30]. https://ohss.dhs.gov/sites/default/files/2024-09/2024_0906_plcy_lawful_permanent_residents_fy2023.pdf
13. Centers for Disease Control and Prevention. Tuberculosis. Technical instruction for panel physicians. [cited 2024 Nov 17]. https://www.cdc.gov/immigrant-refugee-health/hcp/panel-physicians/tuberculosis.html
14. Office of Homeland Security Statistics. Legal immigration and adjustment of status report. [cited 2024 May 7]. https://ohss.dhs.gov/topics/immigration/legal-immigration-and-adjustment-status-report
15. Office of Homeland Security Statistics. Yearbook 2023 [cited 2024 Sep 16]. https://ohss.dhs.gov/topics/immigration/yearbook/2023
16. Honein MA, Christie A, Rose DA, Brooks JT, Meaney-Delman D, Cohn A, et al.; CDC COVID-19 Response Team. Summary of guidance for public health strategies to address high levels of community transmission of SARS-CoV-2 and related deaths, December 2020. MMWR Morb Mortal Wkly Rep. 2020;69:1860–7. https://doi.org/10.15585/mmwr.mm6949e2
17. Jacobsen GD, Jacobsen KH. Statewide COVID-19 stay-at-home orders and population mobility in the United States. World Med Health Policy. 2020;12:347–56. https://doi.org/10.1002/wmh3.350
18. Czeisler MÉ, Marynak K, Clarke KEN, Salah Z, Shakya I, Thierry JM, et al. Delay or avoidance of medical care because of COVID-19-related concerns—United States, June 2020. MMWR Morb Mortal Wkly Rep. 2020;69:1250–7. https://doi.org/10.15585/mmwr.mm6936a4
19. Whaley CM, Pera MF, Cantor J, Chang J, Velasco J, Hagg HK, et al. Changes in health services use among commercially insured US populations during the COVID-19 pandemic. JAMA Netw Open. 2020;3:e2024984. https://doi.org/10.1001/jamanetworkopen.2020.24984
20. Louie JK, Reid M, Stella J, Agraz-Lara R, Graves S, Chen L, et al. A decrease in tuberculosis evaluations and diagnoses during the COVID-19 pandemic. Int J Tuberc Lung Dis. 2020;24:860–2. https://doi.org/10.5588/ijtld.20.0364
21. Cioboata R, Biciusca V, Olteanu M, Vasile CM. COVID-19 and tuberculosis: unveiling the dual threat and shared solutions perspective. J Clin Med. 2023;12:4784. https://doi.org/10.3390/jcm12144784
22. Cronin AM, Railey S, Fortune D, Wegener DH, Davis JB. Notes from the field: effects of the COVID-19 response on tuberculosis prevention and control efforts—United States, March–April 2020. MMWR Morb Mortal Wkly Rep. 2020;69:971–2. https://doi.org/10.15585/mmwr.mm6929a4
23. Han E, Nabity SA, Dasgupta-Tsinikas S, Guevara RE, Moore M, Kadakia A, et al. Tuberculosis diagnostic delays and treatment outcomes among patients with COVID-19, California, USA, 2020. Emerg Infect Dis. 2024;30:136–40. https://doi.org/10.3201/eid3001.230924
24. Jones AJ, Jones-López EC, Butler-Wu SM, Wilson ML, Rodman J, Flors L, et al. Impact of COVID-19 on diagnosis and testing for TB in a high-resource, low-burden setting. Int J Tuberc Lung Dis. 2022;26:888–90. https://doi.org/10.5588/ijtld.22.0132
25. Centers for Disease Control and Prevention. Provisional 2024 tuberculosis data, United States. [cited 2025 Mar 12]. https://www.cdc.gov/tb-data/2024-provisional/index.html

Address for correspondence: P. Feng, Centers for Disease Control and Prevention, 1600 Clifton Rd NE, Mailstop H24-3, Atlanta, GA 30329-4018 USA, email: pfeng@cdc.gov

Rethinking Leptospirosis Prevention, the Philippines

Ryan V. Labana

Leptospirosis, the disease caused by infection with *Leptospira* spp. bacteria, remains a recurring public health challenge in the Philippines, particularly during monsoon floods and typhoon seasons. Despite responsive measures, such as Code White Alerts, standardized treatment protocols, and postflood prophylaxis, cases and associated deaths persist, emphasizing the limitations of reactive strategies. Structural challenges in flood control, urban sanitation, and rodent management hinder long-term prevention. This policy review applies a systems thinking approach to integrate national programs with community-led interventions, recognizing the interlinked roles of environmental management, behavioral change, and grassroots surveillance. Low-cost, context-sensitive actions, such as community drainage clearing, shared protective gear, local rodent-proofing, and barangay-level reporting, can address immediate risks while reinforcing structural initiatives. Embedding those actions within a feedback loop between local actions and national policies fosters resilience, reduces disease incidence, and shifts the paradigm from reactive response to sustainable prevention.

The Philippines usually encounters leptospirosis outbreaks weeks after monsoon floods. In 2025, the Department of Health (DOH) recorded 3,037 cases during January–July; 1,114 of those cases occurred 1 week after the rainy season officially began on June 2. During June 8–August 7, a total of 2,396 verified hospital reports were recorded nationwide. Metro Manila bore the brunt of the impact, and several tertiary hospitals reported strain on capacity caused by the sudden increase in leptospirosis cases. The looming threat of further rainfall could lead to new infections, highlighting the urgent need for early consultation for fever, myalgia, jaundice, and other symptoms after exposure to floodwater (*1*–*4*).

The spikes in leptospirosis cases during typhoon seasons in the Philippines have already been observed in the past several years. For example, Tropical Storm Washi (locally known as Sendong) in December 2011 triggered a poststorm outbreak of leptospirosis. That outbreak resulted in >400 infections and 22 deaths shortly after the floods subsided (*5*). In September 2009, Typhoon Ondoy (Ketsana) caused widespread flooding across Metro Manila, leading to 2,089 leptospirosis cases and 162 deaths; although that event predates 2012, it established a troubling precedent for disease risk tied to typhoons (*6*).

Epidemiologic evidence shows that leptospirosis hospital admissions typically peak ≈2 weeks after periods of intense rain. However, once the variable of flooding is factored in, the direct rain–leptospirosis association weakens, highlighting flooding itself as the critical driver of transmission (*7*). Flooding increases human contact with water and soil contaminated by the urine of infected rats, which serve as the main reservoirs of *Leptospira* spp. bacteria, the causative agent of leptospirosis (*4*). Case–control studies confirm that contact with floodwater is a significant risk factor; 1 meta-analysis indicated an odds ratio of 2.19 (95% CI 1.48–3.24) for leptospirosis among persons exposed to flooding (*8*). In urban settings, particularly in densely populated slum areas with poor sanitation infrastructure, flood events drastically increase exposure risk for leptospirosis outbreaks (*9*). The consistent pattern across multiple years underscores how every typhoon season, from 2012 on, is a dangerous period for potential leptospirosis outbreaks, particularly in flood-prone urban areas where exposure to *Leptospira*-contaminated water is frequent.

The goal of this policy review is to reframe leptospirosis prevention in the Philippines. By using a systems thinking approach, we examined current national and local interventions to identify strategic leverage points for improvement. Our findings highlight the importance of integrating community-led actions into existing national programs to strengthen feasibility and impact. We advocate for a participatory governance approach that links grassroots engagement with national and local policy, infrastructure,

Author affiliation: Polytechnic University of the Philippines, Manila, the Philippines

DOI: https://doi.org/10.3201/eid3203.251250

and research toward a more adaptive and resilient framework for leptospirosis control.

When Interventions Fall Short—Flood Control Controversies, Misguided Education Campaigns, and the Struggle against Leptospirosis

Various interventions against leptospirosis exist in the Philippines. They are mapped in this policy review according to feasibility and potential impact, highlighting where existing strategies stand and where improvements are most needed. We summarize the impact–feasibility matrix of leptospirosis interventions in the Philippines (Figure 1).

High Impact, High Feasibility Interventions

Health policy coordination, especially during a disease outbreak, is a crucial measure to ensure that leptospirosis cases are addressed promptly. The government implements Code White Alerts during peak risk periods. This alert system is used by DOH to enhance the readiness of hospitals and health facilities while they remain on standby for potential case surges. The announcement of a Code White Alert is communicated through press releases and regional and local rollouts. DOH, through its Regional Epidemiology and Surveillance Units, actively tracks and reports cases, whereas local government units collaborate with DOH on real-time data reporting and flood-season mapping to guide targeted interventions. Those programs are crucial in reducing disease severity, preventing fatalities, and ensuring timely clinical care for diagnosed patients, helping them avoid further complications (*10*,*11*). The interventions have high feasibility and high impact in the Philippines.

High Feasibility, Low Impact Interventions

In the Philippines, the onset of typhoons and monsoon floods often triggers a surge in information, education, and communication (IEC) materials on leptospirosis from government agencies, local government units, universities, and nongovernment organizations; one such IEC material, posted on social media, informed the public about the transmission cycle of *Leptospira* and preventive and control measures (Appendix, https://wwwnc.cdc.gov/EID/article/32/3/25-1250-App1.pdf). That IEC material and other IEC materials, typically focus on ideal preventive actions such as avoiding wading in floodwater, wearing protective boots and gloves, washing with soap after exposure, and seeking early medical care if symptomatic. Although such advisories are medically sound, they often fail to account for the lived realities of urban flood-prone communities. In low-income settlements, many residents have no choice but to wade through floodwaters to evacuate, retrieve belongings, commute to work, or access basic needs. High flood levels make the use of boots impractical. Similarly, hygiene recommendations such as thorough washing with soap and clean water are challenging when water supplies are disrupted and soap is a low priority in emergencies. Messages about rodent control and drainage maintenance may also be irrelevant in the immediate aftermath of a disaster, when survival and shelter take precedence over

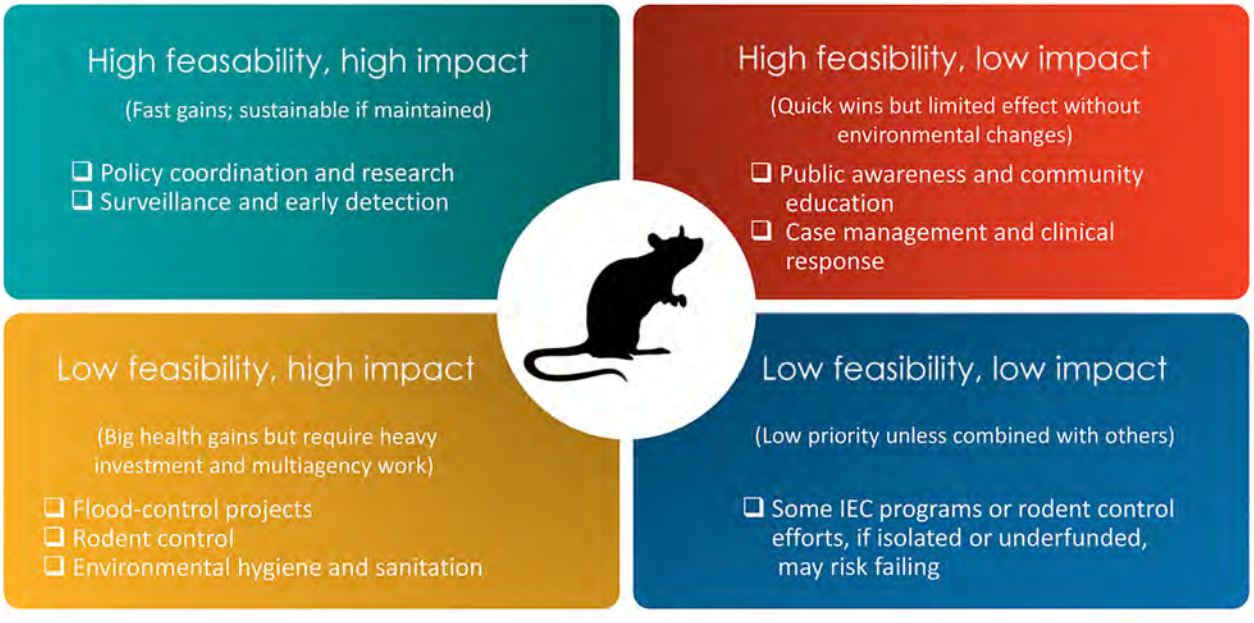

Figure 1. Impact–feasibility matrix of leptospirosis interventions, the Philippines. IEC, information, education, and communication.

environmental interventions. The mismatch between the prescriptive tone of IEC materials and vulnerable communities' structural constraints may reduce the credibility and impact of public health messaging. To be effective, leptospirosis prevention campaigns must move beyond one-size-fits-all advice and integrate context-sensitive strategies, such as guidance for unavoidable exposure, accessible postexposure prophylaxis, and community-based flood safety measures, that reflect the realities on the ground.

For case management and clinical response, standardized Clinical Practice Guidelines developed by DOH with professional medical societies ensure uniform diagnosis and treatment protocols across health facilities (*12*). Benefit packages for leptospirosis, implemented by the Philippine Health Insurance Corporation (PhilHealth), help ease the financial burden on affected patients and support the cost of care by covering expenses related to hospital confinement, laboratory tests, and medications (*13*). The government also deploys medical missions and provides postflood doxycycline prophylaxis to high-risk persons in flood-affected areas. However, when those measures are activated, persons have already been exposed and infected, meaning the burden on the healthcare system and communities remains high.

Educational campaigns with structural constraints do not substantially help in reducing leptospirosis prevalence. On the other hand, case management and clinical response minimize fatalities and severe cases, but do not necessarily ease the burden on the healthcare system. Thus, both are feasible in the Philippines, but both have a low impact.

Low Feasibility, High Impact Interventions

Flooding, as a major risk factor of leptospirosis outbreaks, requires mitigation, including national flood-control projects. Flood control in the Philippines, particularly in urban communities like Metro Manila, faces chronic challenges from rapid, unplanned urbanization, inadequate infrastructure, and governance issues. Informal settlements along rivers and drainage systems obstruct waterways, whereas aging pumping stations and silted floodways like the Manggahan Floodway in Pasig City struggle to cope with intense rainfall and typhoon-induced surges.

Major projects intended to address these problems often have been marred by controversy. In a city in the Visayas region, for example, nearly 4 billion Philippine pesos' worth of flood-control projects were reported in 2025 as incomplete, poorly built, or entirely missing. National audits have long indicated that many flood-control budgets are lost to graft, leading to stalled or substandard infrastructure (*14*,*15*). The head of government raised allegations of corruption and mismanagement from the executive and legislative branches, prompting nationwide investigations into several of those projects (*16*).

In a different aspect, Laguna Lakeshore Expressway–Dike, another flood-control project, has faced opposition from some environmentalists and fisherfolk because of concerns about displacement, ecologic damage, and inequitable benefits (*17*). Similarly, the proposed Pasig River Expressway drew criticism for threatening heritage areas, worsening urban heat, and potentially increasing flood risk by reducing river buffer zones (*18*). Even long-standing flood-control structures like the Manggahan Floodway have had unintended consequences, such as aggravating flooding in downstream communities around Laguna de Bay because of siltation and pollution (*19*). Such controversies hamper engineering capacity, transparent governance, inclusive urban planning, and sustained maintenance, making the affected areas vulnerable to recurring, often catastrophic floods.

Although the flood-control projects in the Philippines are not yet adequately managed, other interventions also must be considered. Rat-catching campaigns in the Philippines have long been promoted to reduce leptospirosis and other rodentborne zoonotic diseases, particularly in flood-prone urban and agricultural areas where human–rat contact is frequent (*20*,*21*). However, their long-term effectiveness is challenged by the biology of rats, which have exceptionally high reproductive potential. Many common rat species, such as *Rattus norvegicus* and *Rattus rattus*, reach sexual maturity in as little as 3 months, and female rats can conceive again within weeks after giving birth. Because each litter may produce 6–12 offspring and multiple litters can occur annually, rat populations can rebound quickly even after intensive control efforts (*22*,*23*). This rapid turnover means that without sustained, integrated control, combining environmental sanitation, secure food storage, habitat destruction, and public health education, rat-catching alone offers only temporary relief. The importance of sustained, integrated control cannot be overstated, given that it is the key to long-term prevention and control of leptospirosis transmission, particularly after flooding events when contaminated water is widespread.

Environmental hygiene, an approach that can be integrated with rat-catching, also faces substantial challenges in urban communities, especially in low-income areas of the Philippines. Many urban low-income families live in informal settlements where

water access is limited to shared or purchased sources, often of questionable quality (*24*). Housing frequently does not meet the family's needs, being makeshift, overcrowded, and vulnerable to flooding, creating ideal habitats for rats and other disease vectors (*25*). Waste-management systems are inconsistent or absent, accumulating garbage in streets and waterways, attracting rodents, and exacerbating flooding. Toilet facilities, if present, often are shared by multiple households and may lack proper sewage connections, resulting in environmental contamination that increases the risk for leptospirosis and other zoonotic diseases (*26*). Those constraints mean that, even when communities engage in rat-catching activities, unhygienic environmental conditions continually undermine disease-control efforts, making sustainable prevention difficult without broader improvements in urban infrastructure and social services.

Flood control, rodent control, and environmental hygiene and sanitation are key interventions for mitigating leptospirosis cases and preventing outbreaks. Their collective impact is considerable because they directly disrupt the transmission cycle of *Leptospira* bacteria. However, because of poverty, corruption, and a lack of political will, the feasibility of these essential interventions remains low in the country.

Low Feasibility, Low Impact Interventions

Some interventions are challenging to implement and yield minimal benefits when executed. For example, developing targeted educational materials for leptospirosis prevention can be challenging because of the diverse and complex social structures across Philippine communities. Cultural variations, language barriers, and differing levels of health literacy make designing messages that resonate effectively with all audiences difficult. In addition, when targeted educational materials are used in isolation, they cannot produce a high impact on reducing leptospirosis transmission. This limitation also applies to rodent control, which will remain ineffective without the integration of improved environmental hygiene and sanitation.

The limited effectiveness of isolated, reactive interventions highlights the importance of prioritizing preventive, integrated strategies over responses. Preventive measures, such as effective flood control, rodent population management, improved urban sanitation, access to protective equipment, and health education before flood events, address the root causes of leptospirosis transmission. Unlike responsive measures, which are reactive and resource-intensive, preventive strategies can reduce exposure risk, lower the incidence of infection, and minimize the need for costly hospitalization and emergency care. In the long term, prioritizing prevention saves lives, alleviates pressure on the healthcare system, conserves public funds, and fosters healthier, more resilient communities.

Rethinking Leptospirosis Prevention through Systems Thinking

National and regional interventions against leptospirosis in the Philippines are often costly, long-term, and dependent on government agencies and multisectoral collaboration. Through use of the impact-feasibility matrix discussed in this policy review, various interventions should be strategically deployed to achieve better outcomes. We used a systems thinking approach, mapping various interventions against leptospirosis to guide and support decision-making for curbing leptospirosis cases in the Philippines (Figure 2).

The systems thinking map (Figure 2) provides a holistic view of how different interventions are interconnected to improve leptospirosis prevention outcomes. At the core of the system are leverage points. They represent critical areas of interventions that have both high impact and high feasibility in the Philippine context. Those areas include policy coordination, surveillance, early detection, and research, all of which strengthen the foundation of leptospirosis management in the country. Surrounding those areas are interventions with moderate impact, such as clinical response, case management, public awareness, and community education, which act as an operational amplifier. That operational amplifier enhances the system's ability to reduce disease transmission and severity through informed communities and effective healthcare delivery. Meanwhile, flood-control projects, hygiene and sanitation, and rodent control have high impact but are less feasible measures that demand long-term investment and intersectoral collaboration to sustainably reduce environmental risks. Those interventions must be integrated as part of the leverage points for better outcomes. Furthermore, fragmented IEC and underfunded rodent control, which both exist in the Philippines, are considered weak and low-impact components. They require merging and capacity strengthening to become more effective. The map (Figure 2) also illustrates that a successful leptospirosis-prevention strategy depends on reinforcing these interconnected elements.

Community-Led Approach in Mitigating Leptospirosis Cases in Small Communities

Addressing leptospirosis in the Philippines remains a big challenge because of its massive cost in controlling its main drivers: flooding, poor environmental hygiene, and poor sanitation. As a quick-fix solution,

with potential to become a sustainable response, community-led interventions can be implemented. Integrating community-led interventions against leptospirosis offers a practical, low-cost, and context-sensitive approach, and it complements national and regional strategies (Figure 3). Such initiatives empower residents to act as the first line of defense, tackling risk factors directly in their environments. Environmental and floodwater management measures, such as monthly drainage-clearing days, DIY flood barriers using sandbags or bamboo, and household-level water diversion, reduce floodwater stagnation and limit contact with contaminated water. Rodent population control activities, including community rat-trapping drives, rodentproof food storage from recycled materials, and supervised garbage disposal systems, target one of the primary reservoirs of *Leptospira* bacteria.

Behavior changes and risk reduction strategies such as boot banks in areas with minimal flooding for shared protective gear, flood buddy systems for mutual safety checks, and local IEC patrols ensure that information and preventive measures reach residents during critical periods. Local surveillance and early detection enhance responsiveness through barangay (the smallest administrative division in the Philippines) case watch boards, regular health check days, and rapid reporting networks using SMS or social media to alert local health workers of suspected cases. Local production and distribution of protective and cleaning materials strengthen preparedness; soap-making workshops, DIY disinfectant production, and low-cost water filtration kits provide communities with essential tools even when external supplies are delayed.

Interventions embedded within a systems thinking framework become part of a feedback loop that connects grassroots actions to national policy. Community-driven measures address immediate, localized risks, whereas national-scale programs provide structural support such as infrastructure upgrades, health system readiness, and formal surveillance.

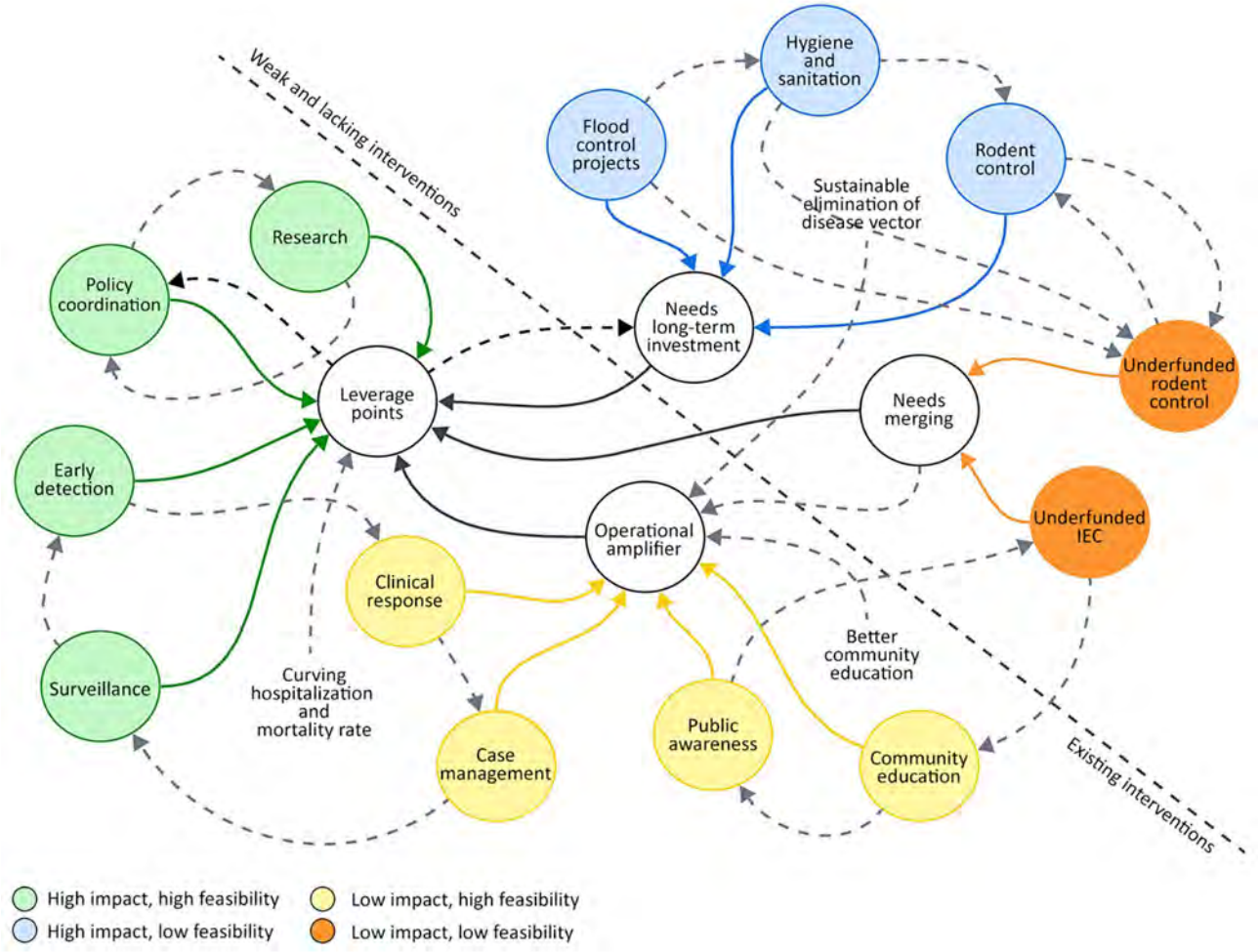

Figure 2. Systems thinking framework linking national strategies for leptospirosis prevention, the Philippines. IEC, information, education, and communication.

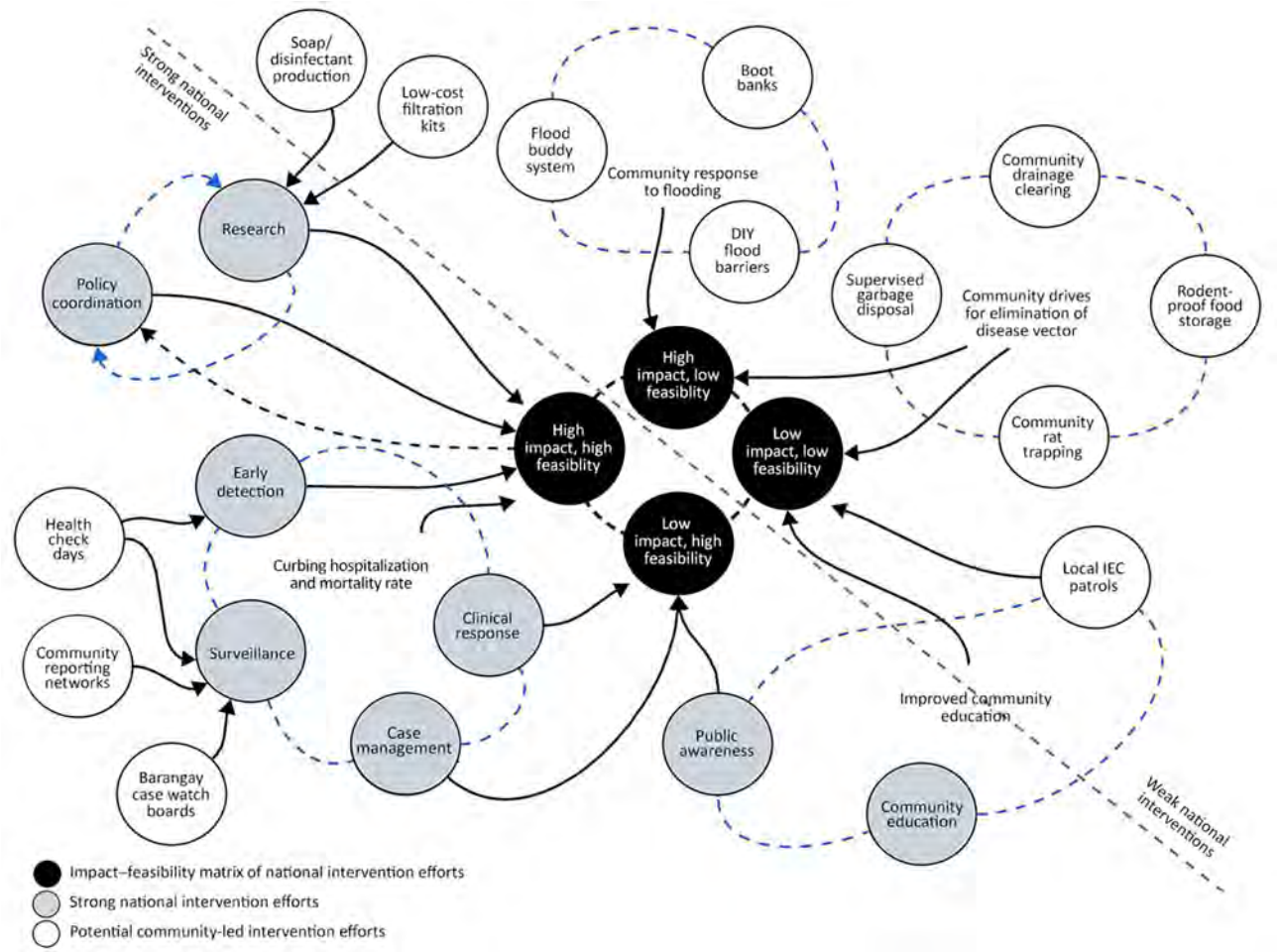

Figure 3. Reframing leptospirosis interventions from national scope into community-led interventions, the Philippines. IEC, information, education, and communication.

That integration ensures that prevention is not solely dependent on costly, long-term government projects but is reinforced by sustained, everyday action at the community level, making leptospirosis control more adaptive, resilient, and sustainable over time.

Conclusions

Leptospirosis prevention in the Philippines needs a shift from reactive responses to proactive, community-driven interventions. Integrating local, low-cost interventions within a systems thinking framework complements national programs and fosters sustainability. Some of those local interventions include community drainage clearing operations, rodent control, and grassroots surveillance. Linking community action with national and local policy coordination, research productions, and infrastructure investment creates reinforcing feedback loops that enhance resilience and reduce disease prevalence. Through this integrated approach, leptospirosis interventions become more adaptive, participatory, and effective in protecting vulnerable communities.

Acknowledgments

The author acknowledges Leptospirosis Awareness, Warning, and Action–Philippines, an organization of One Health researchers in the Philippines, as a source of inspiration in writing this policy review.

The author used EditGPT (https://editgpt.app) for correcting grammar issues.

About the Author

Mr. Labana is the chief of the Center for Health Sciences at the Research Institute for Science and Technology and an associate professor in the Department of Biology, College of Science, Polytechnic University of the Philippines, Manila. His primary research interests include parasitology, zoonotic diseases, and One Health approaches to emerging infectious diseases.

References

1. Limos A. DOH: leptospirosis cases on the rise. The Mailia Times. 2025 Aug 3 [cited 2025 Aug 5]. https://www.manilatimes.net/2025/08/03/news/national/doh-leptospirosis-cases-on-the-rise/2161114
2. Montemayor MT. DOH reminds the public anew of leptospirosis risk amid rainy season. Philippine News Agency. 2025 Aug 5 [cited 2025 Aug 5]. https://www.pna.gov.ph/articles/1255851
3. Herriman R. Philippines records more than 1,100 leptospirosis since June 8. 2025. Outbreak News Today. 2025 Aug 3 [cited 2025 Aug 5]. https://outbreaknewstoday.substack.com/p/philippines-records-more-than-1100
4. Sandoval KL, Cada KJS, Dimasin RVD, Labana RV. A One Health approach to the prevention, control, and management of leptospirosis: a scoping review. Discov Public Health. 2025;22:1–18. https://doi.org/10.1186/s12982-025-00489-7
5. Petley D. The Philippine tropical storm Washi (Sendong) disaster may have been due to the collapse of landslide dams. 2011 Dec 11 [cited 2025 Aug 5]. https://blogs.agu.org/landslideblog/2011/12/24/the-philippine-tropical-storm-washi-sendong-disaster-may-have-been-due-to-the-collapse-of-landslide-dams
6. Davies R. Floods in Philippines. Floodlist. 2013 Apr 30 [cited 2025 Aug 5]. https://floodlist.com/asia/philippines-2009
7. Matsushita N, Ng CFS, Kim Y, Suzuki M, Saito N, Ariyoshi K, et al. The non-linear and lagged short-term relationship between rainfall and leptospirosis and the intermediate role of floods in the Philippines. PLoS Negl Trop Dis. 2018;12:e0006331. https://doi.org/10.1371/journal.pntd.0006331
8. Naing C, Reid SA, Aye SN, Htet NH, Ambu S. Risk factors for human leptospirosis following flooding: a meta-analysis of observational studies. PLoS One. 2019;14:e0217643. https://doi.org/10.1371/journal.pone.0217643
9. Escobar Carías MS, Johnston DW, Knott R, Sweeney R. Flood disasters and health among the urban poor. Health Econ. 2022;31:2072–89. https://doi.org/10.1002/hec.4566
10. Philippine Information Agency. All public hospitals, health facilities on 'Code White' Alert. 2025 Apr 16 [cited 2025 Aug 5]. https://pia.gov.ph/news/all-public-hospitals-health-facilities-on-code-white-alert
11. Union of Local Authorities of the Philippines. The 2020 revised implementing rules and regulations of Republic Act no. 11332, or the Mandatory Reporting of Notifiable Diseases and Health Events of Public Health Concern Act [cited 2025 Aug 5]. https://ulap.net.ph/ulap-news/advisories/566-revised-implementing-rules-and-regulations-irr-of-ra-no-11332.html
12. Republic of the Philippines Department of Health. Compendium of DOH-approved clinical practice guidelines [cited 2025 Aug 5]. https://doh.gov.ph/dpcb/doh-approved-cpg
13. Philippine Information Agency. PhilHealth covers dengue, leptospirosis treatment amid flooding. 2025 Jul 24 [cited 2025 Aug 5]. https://pia.gov.ph/news/philhealth-covers-dengue-leptospirosis-treatment-amid-flooding
14. Pabico Lalu G. Mayors call for probe of companies in flood control projects. 2025 Aug 14 [cited 2026 Feb 26]. https://newsinfo.inquirer.net/2095554/mayors-call-for-probe-of-companies-in-flood-control-projects
15. Capstone-Intel Corporation. Former anti-graft chief seeks audit of P245 billion flood control projects amid Metro's massive flooding. 2023 [cited 2025 Aug 5]. https://www.capstone-intel.com/former-anti-graft-chief-seeks-audit-of-p245-billion-flood-control-projects-amid-metros-massive-flooding
16. Romero A. Marcos orders probe of flood control projects. 2025 Jul 29 [cited 2025 Nov 9]. https://www.philstar.com/headlines/2025/07/29/2461542/marcos-orders-probe-flood-control-projects
17. Public-Private Partnership Center of the Philippines. The Laguna Lakeshore Expressway Dike: building infrastructure to rebuild lives. 2015 Sep 3 [cited 2025 Aug 5]. https://ppp.gov.ph/press_releases/the-laguna-lakeshore-expressway-dike-building-infrastructure-to-rebuild-lives
18. Cabico GK. Planned Pasig River expressway may just make traffic, pollution worse—groups. 2021 Jul 19 [cited 2025 Aug 5]. https://www.philstar.com/nation/2021/07/19/2113577/planned-pasig-river-expressway-may-just-make-traffic-pollution-worse-groups
19. Alvarez MK, Cardenas K. Evicting slums, 'building back better': resiliency revanchism and disaster risk management in Manila. Int J Urban Reg Res. 2019;43:227–49. https://doi.org/10.1111/1468-2427.12757
20. Dumalao A. Baguio relaunches rat hunting campaign to fight spread of leptospirosis. 2024 May 27 [cited 2025 Aug 5]. https://www.philstar.com/nation/2024/05/27/2358363/baguio-relaunches-rat-hunting-campaign-fight-spread-leptospirosis
21. Fernandez E. Tacurong rolls out 'cash for rats' program amid infestation. 2022 Jun 3 [cited 2025 Aug 5]. https://www.pna.gov.ph/articles/1175828
22. Kohn DF, Clifford CB. Biology and diseases of rats. In: Fox JG, Anderson LC, Loew FM, Quimby FW, editors. Laboratory animal medicine. Second edition. New York: Academic Press; 2007. p. 121–65 [cited 2025 Aug 5]. https://doi.org/10.1016/B978-012263951-7/50007-7
23. Quesenberry KE, Boschert KR. Breeding and reproduction of rats. 2024 Sep [cited 2025 Aug 5]. https://www.msdvetmanual.com/all-other-pets/rats/breeding-and-reproduction-of-rats
24. Hussain N, Chaves C. Securing water for all is urgent, but impossible if we ignore housing inequalities. New Security Beat. 2021 Sep 13 [cited 2025 Aug 5]. https://www.newsecuritybeat.org/2021/09/securing-water-urgent-impossible-ignore-housing-inequalities
25. Tan R. Reforming housing for the poor in the Philippines. East Asia Forum. 2010 Mar 27 [cited 2025 Aug 5]. https://eastasiaforum.org/2010/03/27/reforming-housing-for-the-poor-in-the-philippines
26. Purwar D, Sliuzas R, Flacke J. Assessment of cascading effects of typhoons on water and sanitation services: a case study of informal settlements in Malabon, Philippines. Int J Disaster Risk Reduct. 2020;51:101755. https://doi.org/10.1016/j.ijdrr.2020.101755

Address for correspondence: Ryan V. Labana, Polytechnic University of the Philippines, Mabini Campus, Anonas Street, Sta. Mesa, Manila 1016, Philippines; email: rvlabana@pup.edu.ph

Optimal Specimens and Lesions for Mpox Diagnosis Using Real-Time PCR, South Korea

Dong-Min Kim, Munawir Muhammad, Jin Won Kim, Choon-Mee Kim, Jun-Won Seo, Da Young Kim, Na Ra Yun, Beomgi Lee, Minji Lee, Jeong Hyun Lee, Myung-Min Choi, Yoon-Seok Chung

We analyzed 612 specimens from 135 patients with monkeypox virus clade IIb in South Korea by using real-time PCR. Crusted and anogenital skin lesions and rectal swab specimens demonstrated the highest positivity rates. Viral loads varied by lesion type, anatomic site, and time since symptom onset, supporting our specimen selection for clade IIb detection.

Mpox, a zoonotic disease caused by the monkeypox virus (MPXV), a member of the genus *Orthopoxvirus*, was first reported in South Korea in 2022 and initially involved imported cases and a hospital-acquired infection (*1*,*2*). A local outbreak began in April 2022 and peaked in late April to early May 2023, largely affecting young adult men (mostly men who have sex with men); most transmission events were linked to sexual contact (*2*,*3*,*4*). Genomic analysis revealed that circulating strains in 2023 belonged to MPXV clade IIb, with the B.1.3 lineage predominating (*4*).

As the outbreak evolved, understanding the MPXV transmission dynamics and diagnostic accuracy became increasingly crucial. Although mpox is primarily transmitted by symptomatic persons, presymptomatic transmission occurring 1–4 days before symptom onset has been reported (*5*). Accurate diagnosis relies on appropriate specimen selection and timing of sample collection. However, relatively few studies have systematically compared viral loads across specimen types, and we did not find published studies that comprehensively evaluated differences between anogenital and nonanogenital skin lesions. To address those gaps, we assessed MPXV viral loads and positivity rates in South Korea by specimen type and time since symptom onset by using real-time quantitative PCR (qPCR).

Author affiliations: Chosun University College of Medicine, Gwang-Ju, South Korea (D.-M. Kim, M. Muhammad, C.-M. Kim, J.-W. Seo, D.Y. Kim, N.R. Yun, B. Lee); Hasanuddin University, Makassar, Indonesia (M. Muhammad); Korea Disease Control and Prevention Agency, Cheongju, South Korea (J.W. Kim, M. Lee, J.H. Lee, M.-M. Choi, Y.-S. Chung)

DOI: https://doi.org/10.3201/eid3203.250582

The Study

We conducted a retrospective observational study to analyze demographic characteristics, symptom onset, specimen types, qPCR results, and cycle threshold (Ct) values of suspected MPXV cases in South Korea referred to the Korea Disease Control and Prevention Agency (KDCA). Clinical specimens were collected by trained healthcare personnel and included skin lesions, upper respiratory tract swab specimens, blood, and rectal swab specimens. We categorized skin lesions by type (crusted, vesicular, papular, pustular, or unknown) and site (anogenital, nonanogenital, or unknown), including the anus, perineum, penis, and vulva. We grouped samples by days since symptom onset (0–1, 2–3, 4–10, and >10 days). We considered Ct values $\geq$40 or undetectable negative and Ct values <40 positive.

We extracted viral DNA from 200 μL of clinical specimens by using the QIAamp Blood Mini Kit (QIAGEN, https://www.qiagen.com) following the manufacturer's protocol. qPCR targeted F3L and A39R genes by using the following primers and probes: F3L forward 5′-CATCTATTATAGCATCAGCATCAGA-3′, reverse 5′-GATACTCCTCCTCGTTGGTCTAC-3′, probe 5′-FAM-TGTAGGCCGTGTATCAGCATCCATT-IBFQ-3′; A39R forward 5′-TGGGATAACGAATCCAATGTCA-3′, reverse 5′-GCGTGCTTCCAGCAACACT-3′, probe 5′-FAM-AGCGCCTAGCACAGAACACATTTACGA-IBFQ-3′.

For group comparisons, we used χ^2 or Fisher exact test for categorical variables and the Kruskal-Wallis test or analysis of variance for Ct value comparisons. We conducted analyses by using SPSS Statistics

29.0.10 (IBM, https://www.ibm.com) and GraphPad Prism version 8 (https://www.graphpad.com). This study was approved by the KDCA Institutional Review Board (approval no. 2020-03-01-P-A), which waived written informed consent.

During August 28, 2022–October 3, 2023, the KDCA received 1,668 specimens from 379 patients with suspected mpox. After we excluded 244 patients (1,056 specimens) because of missing clinical data (999 samples from 231 patients) and unclear onset times (57 samples from 13 patients), we analyzed 612 specimens from 135 patients. Most (97.7%) patients were men. Median patient age was 31.7 (interquartile range [IQR] 27.7–37.1) years, and median collection time was 6 (IQR 2.0–8.0) days after onset. Specimens were 362 skin lesions, 109 upper respiratory tract swab specimens, 135 blood samples, and 6 rectal swab specimens; 445 samples were PCR-positive.

MPXV DNA was more frequently detected from skin lesions (92.8%, n = 336/362) and rectal swab specimens (100%, n = 6/6) than from upper respiratory tract (68.8%, n = 75/109) and blood samples (28.2%, n = 38/135) (Table 1; Appendix Figure 1, http://wwwnc.cdc.gov/EID/article/32/3/25-0582-App1.pdf). Median Ct values were significantly lower for skin lesions (median 22.01, IQR 19.25–28.19) and rectal swab specimens (median 20.19, IQR 18.85–24.23) than in the upper respiratory tract (median 33.61, IQR 29.09–40.00) and blood samples (median 40.00, IQR 38.61–40.00; p<0.001); we found no significant difference between skin lesions and rectal swab specimens (p = 0.36) (Table 1; Figure 1). Among skin lesions, crusted types demonstrated the highest positivity rate (93.3%, n = 70/75) and the lowest median Ct value (median 20.63, IQR 18.30–24.48), significantly lower than for other lesion types (median 23.33, IQR 19.74–30.00; p<0.001).

Table 1. Mpox specimen types and Ct values of 135 confirmed patient samples acquired from the Korea Disease Control and Prevention Agency when a suspected mpox patient visited the hospital, South Korea, 2022–2023*

	Samples			Ct values					Median (IQR) days after symptom onset
Specimen type	Total	No. (%) positive	χ^2	Mean (SD)	Median (95% CI)	25th percentile	75th percentile	p value	
All skin lesions	362	336 (92.82)		24.41 (6.90)	22.01 (21.55–22.87)	19.25	28.19		6 (2.00–8.00)
Type									
Crust	75	70 (93.33)	0.2965	22.51 (6.52)	20.63 (19.59–21.76)	18.30	24.48	<0.0001	7.00 (2.00–13.00)
Other	260	239 (91.92)		25.32 (7.02)	23.33 (22.11–24.6)	19.74	30.00		5.00 (2.00–7.00)
Unknown	27	27 (100)		20.9 (4.20)	19.85 (19.17–21.74)	18.87	21.85		7.00 (5.00–10.00)
Site									
Anogenital	74	72 (97.30)	0.1142	22.58 (6.15)	20.78 (19.71–22.06)	17.91	25.65	0.0178	6.00 (3.00–7.25)
Other	116	109 (93.97)		25.14 (6.91)	22.82 (21.51–24.91)	19.91	29.94		5.00 (2.25–7.75)
Unknown	172	155 (90.12)		24.7 (7.10)	22.51 (21.16–24.25)	19.47	28.71		6.00 (1.00–8.00)
Nationality									
South Korea	338	314 (92.90)	0.8154	24.24 (6.84)	21.87 (21.66–22.77)	19.24	27.7	0.2068	
Other Asian	21	19 (90.50)		26.57 (7.47)	25.00 (20.85–30.25)	20.75	30.46		
Western countries	3	3 (100)		28.32 (8.42)	30.39 (19.06–35.52)	19.06	35.52		
Sample location									
Upper respiratory tract	109	75 (68.81)	0.5564	33.29 (6.05)	33.61 (32.52–35.24)	29.09	40	0.3505	5.00 (2.00–8.00)
Nasopharynx	4	2 (50)		36.53 (4.13)	37.14 (31.84–40.00)	32.45	40		5.00 (0.75–7.75)
Oropharynx	28	18 (64.29)		34.35 (5.11)	34.37 (31.22–40.00)	29.78	40		3.00 (0.00–8.00)
Unknown	77	55 (71.43)		32.74 (6.39)	33.16 (31.44–35.24)	27.56	40		6.00 (3.00–8.00)
Blood	135	38 (28.19)	NA	38.75 (2.56)	40.00 (40.00–40.00)	38.61	40.00	NA	5.00 (3.00–7.00)
Rectal swab	6	6 (100)	NA	21.68 (4.708)	20.19 (17.61–30.82)	18.85	24.23	NA	5.00 (1.50–12.25)

*Ct, cycle threshold; IQR, interquartile range; NA, not available.

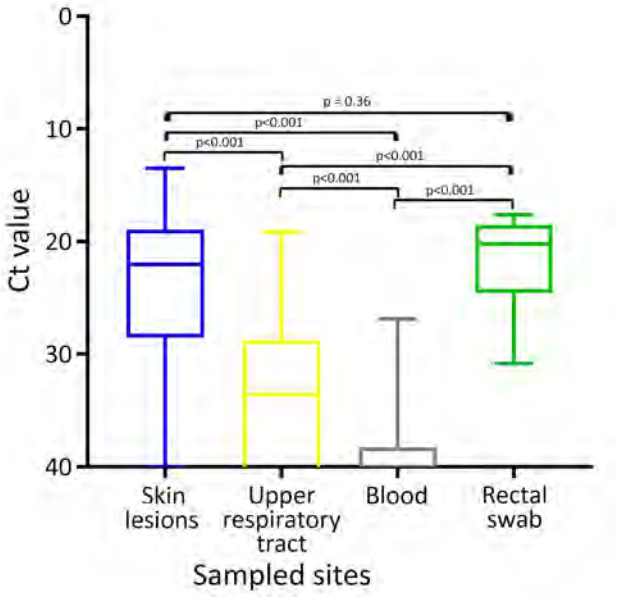

Figure 1. Comparison of Ct values of real-time PCR by lesion and time point after symptom onset in patients with mpox, South Korea, 2022–2023. Horizontal lines within boxes represent medians, box tops and bottoms represent interquartile ranges, and error bars represent minimum and maximum values. Ct, cycle threshold.

Anogenital lesions had lower Ct values (median 20.78, IQR 17.91–25.65) than lesions at other sites (median 22.82, IQR 19.91–29.94; p = 0.018). Positivity rates (p = 0.556) and Ct values (p = 0.351) did not differ significantly between oropharyngeal and nasopharyngeal specimens; however, oropharyngeal samples tended toward higher positivity (64.3%) and lower Ct values (median 34.37, IQR 29.78–40.00) compared with nasopharyngeal samples (50.0%, n = 2/4; median Ct 37.14, IQR 32.45–40.00), despite the limited sample size.

Positivity and Ct values varied over time after symptom onset (Table 2; Figure 2). The Ct values of the skin lesions changed significantly (p<0.001), whereas positivity remained high (≈90%) for up to 60 days (p = 0.142). Upper respiratory tract specimens showed no significant changes in positivity (p = 0.738) or Ct values (p = 0.369), with peak positivity (75%) on day 1, lasting until day 30. Blood samples had low positivity (28.2%) and no substatial variation over time, peaking in the first 3 days (32%), and were detectable for ≈20 days.

Mpox is primarily transmitted through direct contact with body fluids, respiratory droplets, or contaminated surfaces (*6*). Increasing evidence indicates that sexual contact is the dominant transmission route during outbreaks, particularly among men who have sex with men (*7*). This evidence is supported by frequent anogenital lesions and the detection of culturable viruses in saliva, the nasopharynx, and semen (*7*). The high positivity and low Ct values observed in anogenital lesions in our study further support these findings.

After inoculation, MPXV replicates in the skin, spreads to the lymph nodes, and causes viremia and systemic dissemination (*8*). Skin lesions progress through macules, papules, vesicles or pustules, and crusts (*6*). Crusted lesions have historically been regarded as less infectious, but accumulating evidence indicates that viral DNA and infectious virus might persist until crust detachment (*9*,*10*). Consistent with that persistence of infectious virus, we observed high MPXV DNA levels in crusted lesions, indicating its potential infectivity. MPXV also demonstrates strong tropism for keratinocytes. Skin specimens, particularly anogenital lesions and rectal swab specimens, exhibit higher viral loads than blood or respiratory specimens, underscoring

Table 2. Comparison of the positivity rate and Ct value of real-time PCR at the time point of each specimen after symptom onset in patients with mpox, South Korea, 2022–2023*

	Days since symptom onset									
	0–1		2–3		4–10		10			
Specimen type	No. (%) positive	Median (IQR) Ct	No. (%) positive	Median (IQR) Ct	No. (%) positive	Median (IQR) Ct	No. (%) positive	Median (IQR) Ct	χ^2	p value
Skin lesion, n = 362	67/76 (88.2)	27.38 (21.9–34.8)	47/48 (97.9)	21.41 (19.5–25.0)	177/188 (94.2)	21.7 (18.8–27.4)	45/50 (90.0)	20.18 (17.8–24.0)	0.1421	<0.0001
Upper respiratory tract, n = 109	18/24 (75.0)	33.47 (28.2–39.2)	10/15 (66.7)	34.34 (30.5–40.0)	37/57 (64.9)	33.9 (29.2–40.0)	10/13 (76.9)	30.98 (25.0–37.2)	0.7380	0.3689
Blood, n = 135	8/25 (32.0)	40 (36.9–40)	8/22 (36.4)	40 (38.0–40)	18/74 (24.3)	40 (39.84–40)	4/14 (28.6)	40 (36.6–40)	0.6930	0.7635
Rectal swab, n = 6	1/1 (100)	20.54 (20.5–20.5)	2/2 (100)	18.7 (17.6–19.8)	1/1 (100)	22.0 (22.0–22.0)	2/2 (100)	26.43 (22.0–30.8)	NA	0.1778

*Denominators indicate no. specimens tested on those days. χ^2 value is of positivity rate; p value is of Ct. Ct, cycle threshold; IQR, interquartile range; NA, not available.

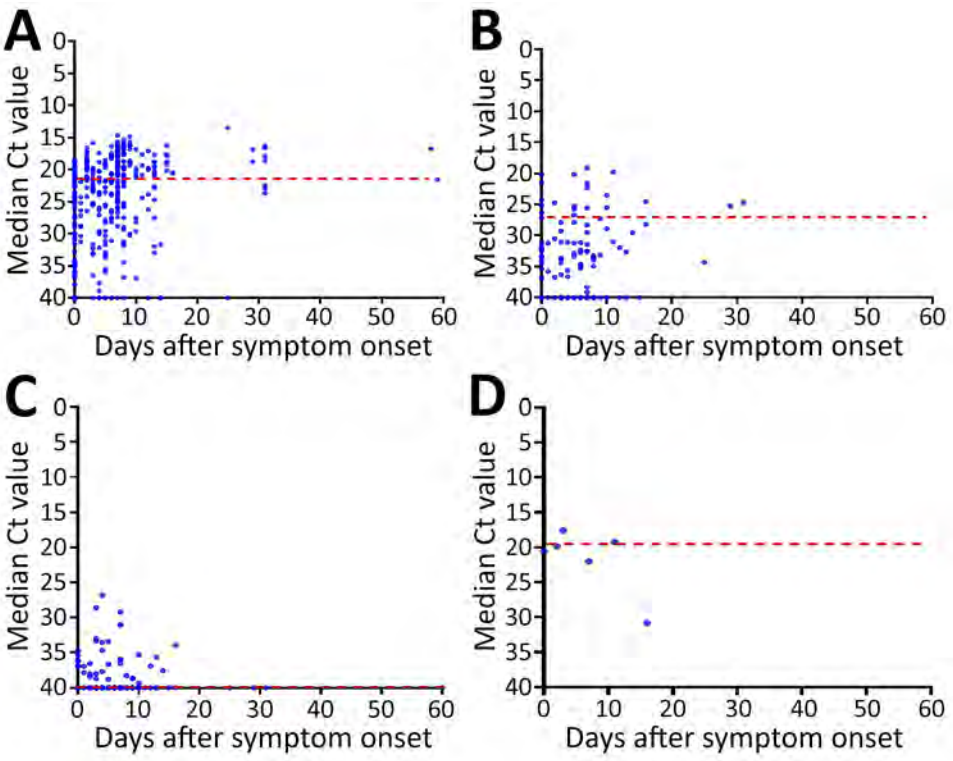

Figure 2. Monkeypox viral loads given as Ct values in patients with mpox, according to sampled sites and time of onset, South Korea, 2022–2023. Blue dots indicate Ct results for each sample. Red dashed lines represent median values. Ct, cycle threshold.

the central role of the skin in viral replication and direct contact transmission (*11*,*12*).

Ct values in skin lesions decreased significantly over time, consistent with reports from China demonstrating high viral DNA detection for up to 3 weeks (*13*). Upper respiratory tract samples peaked in positivity 1 day after symptom onset and then declined, similar to the oropharyngeal patterns reported in China (*13*). Blood samples demonstrated low positivity, which increased slightly in the first 3 days and then declined, consistent with reports of plasma and serum viral DNA peaking before day 10 (*13*). Our findings support evidence that skin and rectal swab specimens yield higher viral loads than blood or respiratory swab specimens (*14*,*15*).

The limitations of our study include incomplete clinical data and a small number of rectal swabs. For many patients, we relied on referral records that lacked detailed lesion or location data. Prospective studies are necessary to clarify the links between symptoms, severity, duration, and outcomes.

Conclusions

Our study of MPXV clade IIb infection during the 2022–2023 outbreak in South Korea found that crusted and anogenital skin lesions and rectal swab specimens demonstrated the highest PCR positivity rates, followed by upper respiratory tract and blood samples. Peak positivity occurred around day 1 in respiratory specimens and on day 3 in blood. The Ct values differed significantly by lesion type and anatomic location, highlighting the importance of targeted specimen collection and the appropriate sampling timing in MPXV clade IIb infection.

This study was supported by research fund from Chosun University, 2024 (to D.-M.K.).

About the Author

Dr. Kim is a professor in the Department of Internal Medicine of Chosun University Hospital and Chosun University College of Medicine, Korea. His research interests include emerging infectious diseases, particularly vectorborne diseases.

References

1. Shim M, Cho SH, Lee SE, Kim T. Epidemiological characteristics and risk factors of suspected and confirmed mpox cases during the 2022–2023 epidemic in the Capital Region, Korea. Epidemiol Health. 2024;46:e2024092. https://doi.org/10.4178/epih.e2024092
2. Kim T, Park E, Eun JS, Lee EY, Mun JW, Choi Y, et al. Detecting mpox infection in the early epidemic: an epidemiologic investigation of the third and fourth cases in Korea. Epidemiol Health. 2023;45:e2023040. https://doi.org/10.4178/epih.e2023040
3. Kwon SL, Song M, Lee W, Shin J, Lee SY, Yeo SG, et al. First nationwide mpox vaccination program in the Republic of Korea: implications for an enhanced public health response. J Korean Med Sci. 2024;39:e235. https://doi.org/10.3346/jkms.2024.39.e235

4. Choi CH, Lee M, Lee SE, Kim JW, Shin H, Choi MM, et al. Genomic analysis of monkeypox virus during the 2023 epidemic in Korea. J Korean Med Sci. 2024;39:e165. https://doi.org/10.3346/jkms.2024.39.e165
5. Rossotti R, Calzavara D, Cernuschi M, D'Amico F, De Bona A, Repossi R, et al. Detection of asymptomatic mpox carriers among high-risk men who have sex with men: a prospective analysis. Pathogens. 2023;12:798. https://doi.org/10.3390/pathogens12060798
6. Jezek Z, Grab B, Szczeniowski MV, Paluku KM, Mutombo M. Human monkeypox: secondary attack rates. Bull World Health Organ. 1988;66:465–70.
7. Pan D, Nazareth J, Sze S, Martin CA, Decker J, Fletcher E, et al. Transmission of monkeypox/mpox virus: a narrative review of environmental, viral, host, and population factors in relation to the 2022 international outbreak. J Med Virol. 2023;95:e28534. https://doi.org/10.1002/jmv.28534
8. Niu L, Liang D, Ling Q, Zhang J, Li Z, Zhang D, et al. Insights into monkeypox pathophysiology, global prevalence, clinical manifestation and treatments. Front Immunol. 2023;14:1132250. https://doi.org/10.3389/fimmu.2023.1132250
9. Ng OT, Lee V, Marimuthu K, Vasoo S, Chan G, Lin RTP, et al. A case of imported monkeypox in Singapore. Lancet Infect Dis. 2019;19:1166. https://doi.org/10.1016/S1473-3099(19)30537-7
10. Ouafi M, Regueme A, Alcaraz I, Riviere P, Bazus H, Salmon-Rousseau A, et al. Oropharyngeal samples versus lesion specimens at diagnosis in patients infected with monkeypox virus in Northern France. J Med Virol. 2023;95:e28276. https://doi.org/10.1002/jmv.28276
11. Li P, Pachis ST, Xu G, Schraauwen R, Incitti R, de Vries AC, et al. Mpox virus infection and drug treatment modelled in human skin organoids. Nat Microbiol. 2023;8:2067–79. https://doi.org/10.1038/s41564-023-01489-6
12. Yang S, Xia C, Zhang Y, Shen Y, Xia C, Lu Y, et al. Clinical features and viral load variations of mpox: a retrospective study in Chongqing, China. BMC Infect Dis. 2024;24:641. https://doi.org/10.1186/s12879-024-09537-0
13. Guo L, Song R, Zhang Q, Li D, Chen L, Fang M, et al. Profiling of viral load, antibody and inflammatory response of people with monkeypox during hospitalization: a prospective longitudinal cohort study in China. EBioMedicine. 2024;106:105254. https://doi.org/10.1016/j.ebiom.2024.105254
14. Hasso M, Perusini S, Eshaghi A, Tang E, Olsha R, Zhang H, et al. Monkeypox virus detection in different clinical specimen types. Emerg Infect Dis. 2022;28:2513–5. https://doi.org/10.3201/eid2812.221160
15. Cordeiro R, Pelerito A, de Carvalho IL, Lopo S, Neves R, Rocha R, et al. An overview of monkeypox virus detection in different clinical samples and analysis of temporal viral load dynamics. J Med Virol. 2024;96:e70104. https://doi.org/10.1002/jmv.70104

Address for correspondence: Yoon-Seok Chung, Korea Disease Control and Prevention Agency, Cheongju 28159, South Korea; email: rollstone93@korea.kr

etymologia revisited

Petri Dish

[pe'tre 'dish]

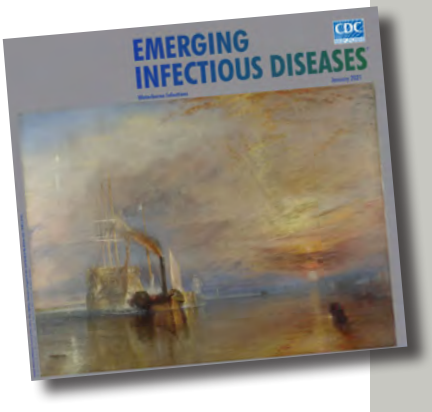

Originally published in January 2021

The Petri dish is named after the German inventor and bacteriologist Julius Richard Petri (1852–1921). In 1887, as an assistant to fellow German physician and pioneering microbiologist Robert Koch (1843–1910), Petri published a paper titled "A minor modification of the plating technique of Koch." This seemingly modest improvement (a slightly larger glass lid), Petri explained, reduced contamination from airborne germs in comparison with Koch's bell jar.

References

1 Central Sheet for Bacteriology and Parasite Science [in German]. Biodiversity Heritage Library. Volume 1, 1887 [cited 2020 Aug 25]. https://www.biodiversitylibrary.org/item/210666#page/313/mode/1up
2. Petri JR. A minor modification of the plating technique of Koch [in German]. Cent für Bacteriol und Parasitenkd. 1887;1:279–80.
3. Shama G. The "Petri" dish: a case of simultaneous invention in bacteriology. Endeavour. 2019;43:11–6. DOIExternal
4. The big story: the Petri dish. The Biomedical Scientist. Institute of Biomedical Science [cited 2020 Aug 25]. https://thebiomedicalscientist.net/science/big-story-petri-dish

https://wwwnc.cdc.gov/eid/article/27/1/et-2701_article

Tuberculosis after TB Preventive Therapy in Persons Living with HIV Recently Initiating Antiretroviral Therapy, Mozambique

Lindsay Templin, Yagna Varajidas, Durval Respeito, Pereira Zindoga, Debora Weiss, Alexandre Nguimfack, Eudoxia Filipe, Arlete Mahumane, Maria Inês Tomo de Deus, José Mizela, Sonia Chilundo, Bruno Simoes, Aleny Couto, Ishani Pathmanathan, Emilio Dirlikov, Benedita José

We investigated tuberculosis (TB) diagnoses among persons living with HIV recently initiated on antiretroviral therapy in Mozambique during 2021–2024 (N = 341,844). TB diagnosis rates were lower among those who completed TB preventive therapy (3.1/1,000 person-years) compared with those who had an incomplete course (11.0/1,000 person-years) or did not start (21.6/1,000 person-years).

Tuberculosis (TB) remains the leading cause of illness and death among persons living with HIV (PLHIV) (*1*,*2*). In 2024, among ≈40.8 million PLHIV globally (*3*), there were ≈620,000 TB cases and ≈150,000 TB-related deaths (*4*). For PLHIV, HIV antiretroviral therapy (ART) and TB preventive therapy (TPT) reduce TB incidence and contribute to reduced TB deaths (*5*). TPT should be administered to all PLHIV ≥12 months of age who have no symptoms of active TB (*2*).

In 2024, there were ≈2.5 million PLHIV in Mozambique; of those, 86% were on ART (*6*). Among all PLHIV were ≈29,000 incident TB cases and ≈5,600 TB-related deaths (*4*). Since 2007, Mozambique has greatly expanded TPT among PLHIV, reaching TPT coverage of 89% by March 2024 (D. Respeito et al., unpub. data, https://doi.org/10.1101/2024.11.25.2431776). During 2007–2023, TPT consisted primarily of a 6-month course of isoniazid (INH); in May 2023, a 3-month course of 12 (1/wk) doses of isoniazid and rifapentine (3HP) was introduced in the southern region.

In this study, we aimed to determine the effect of TPT among PLHIV in Mozambique newly initiating ART by TPT completion status using a national data warehouse. We obtained ethics approval from the Mozambique National Bioethics Committee for Health. This activity was deemed research not involving human subjects by the US Centers for Disease Control and Prevention.

The Study

We retrospectively studied all PLHIV who initiated ART during 2021–2022, using data from Mozambique's national ART data warehouse, MozART (Appendix, https://wwwnc.cdc.gov/EID/article/32/3/25-1349-App1.pdf); as of December 2024, the warehouse contained deidentified clinical-encounter data from 620 facilities and 1.6 million PLHIV on ART. We excluded PLHIV with previous TB treatment or TB diagnosis within 90 days of ART initiation; we also excluded those without a documented HIV viral load test within 2 years or ART pickup within 3 months of ART initiation, as a proxy for non-engagement in care.

The outcome of interest was any TB diagnosis within 2 years of ART initiation, as documented in medical records or by enrollment in the TB service ward. The primary independent variable was TPT completion, categorized as did not start TPT, incomplete TPT (<170 days for INH; <80 days for 3HP),

Author affiliations: US Centers for Disease Control and Prevention, Maputo, Mozambique (L. Templin, Y. Varajidas, D. Respeito, A. Nguimfack, A. Mahumane, M. Tomo de Deus, J. Mizela, S. Chilundo, I. Pathmanathan, E. Dirlikov); US Agency for International Development, Maputo (P. Zindoga); Ministry of Health Mozambique, Maputo (E. Filipe, B. Simoes, A. Couto, B. José); US Centers for Disease Control and Prevention, Atlanta, Georgia, USA (D. Weiss)

DOI: https://doi.org/10.3201/eid3203.251349

and completed TPT (≥170 days for INH; ≥80 days for 3HP). Control variables were age at ART initiation (<15, 15–49, ≥50 years); sex; facility setting (urban/rural) and region; most recent CD4 count (<200 cells/mm^3, ≥200 cells/mm^3) and World Health Organization (WHO) clinical stage (I–IV) at ART initiation; and most recent HIV viral load result (suppressed, <1,000 copies/mL; unsuppressed, ≥1,000 copies/mL) before or after TB diagnosis or <24 months on ART and time of TPT initiation (at ART start or delayed).

We used Poisson regression with generalized estimating equations to calculate incidence rate ratios (IRRs) and to account for potential correlation between observations within health facilities. We used IRRs to compare completion categories. We calculated incidence of diagnosed TB as the number of PLHIV with TB diagnosis per total person-years divided by 1,000.

During 2021–2022, a total of 505,098 PLHIV were newly initiated on ART; of those, 28,498 (5.6%) were <15 years of age. We included a total of 341,844 (67.7%) in the analysis; 215,357 (63%) were female and 126,487 (37%) male, median age was 30.0 (interquartile range [IQR] 24–39) years, and 82,418 (24%) received ART in the Southern Region (Table 1). Of the 163,254 PLHIV excluded from the analysis, 120,555 (23.9%) did not have a registered viral load, 28,620 (5.7%) did not have an ART pickup within 30 days of

Table 1. Characteristics of persons newly diagnosed with HIV in study of TB in persons living with HIV initiating ART, Mozambique, 2021–2024*

Characteristic	No TB diagnosis, n = 338,717	TB diagnosis, n = 3,127	Total, N = 341,844
Age, y, median (IQR)	30 (24–39)	35 (26–43)	30 (24–39)
Age group, y			
<15	17,939 (5.3)	298 (9.5)	18,237 (5.3)
15–49	293,225 (87)	2,352 (75)	295,577 (86)
≥50	27,553 (8.1)	477 (15)	28,030 (8.2)
Sex			
F	213,804 (63)	1,553 (50)	215,357 (63)
M	124,913 (37)	1,574 (50)	126,487 (37)
Geographic region†			
Central	153,268 (45)	1,295 (41)	154,563 (45)
Northern	104,067 (31)	796 (25)	104,863 (31)
Southern	81,382 (24)	1,036 (33)	82,418 (24)
Last viral load result‡			
Suppressed	312,197 (92)	2,603 (83)	314,800 (92)
Unsuppressed	26,520 (7.8)	524 (17)	27,044 (7.9)
CD4 result			
<200 cells/mm^3	8,842 (2.6)	326 (10)	9,168 (2.7)
≥200 cells/mm^3	38,868 (11)	550 (18)	39,418 (12)
Not tested	291,007 (86)	2,251 (72)	293,258 (86)
TPT initiation and completion			
Complete	265,427 (78)	1,550 (50)	266,977 (78)
Incomplete	67,248 (20)	1,346 (43)	68,594 (20)
Not started	6,042 (1.8)	231 (7.4)	6,273 (1.8)
TPT type			
3HP	17,659 (5.2)	224 (7.2)	17,883 (5.2)
Isoniazid	315,016 (93)	2,672 (85)	317,688 (93)
No TPT	6,042 (1.8)	231 (7.4)	6,273 (1.8)
Started TPT within 30 d of ART initiation			
Delayed TPT start	22,805 (6.7)	327 (10)	23,132 (6.8)
Not started	6,042 (1.8)	231 (7.4)	6,273 (1.8)
TPT at ART start	309,870 (91)	2,569 (82)	312,439 (91)
WHO status at initiation			
Not recorded	5,733 (1.7)	63 (2.0)	5,796 (1.7)
Stage I	275,880 (81)	2,117 (68)	277,997 (81)
Stage II	41,366 (12)	551 (18)	41,917 (12)
Stage III	13,408 (4.0)	345 (11)	13,753 (4.0)
Stage IV	2,330 (0.7)	51 (1.6)	2,381 (0.7)
Health facility setting			
Rural	208,149 (61)	1,749 (56)	209,898 (61)
Urban	130,568 (39)	1,378 (44)	131,946 (39)

*Values are no. (%) except as indicated. ART, antiretroviral therapy; IQR, interquartile range; TPT, TB preventive therapy; WHO, World Health Organization; 3HP, 3-month course of 12 (1/wk) doses of isoniazid and rifapentine.
†Mozambique's 11 provinces are categorized into 3 regions: Central (Sofala, Manica, Tete, Zambezia), Northern (Nampula, Niassa, Cabo Delgado), and Southern (Maputo City, Maputo, Gaza, Inhambane).
‡Suppressed, <1,000 copies/mL; unsuppressed, ≥1,000 copies/mL.

Table 2. Incidence of TB among persons living with HIV newly initiated on ART after 2 years of follow-up, Mozambique, 2021–2024*

Characteristic	No. TB positive	Person-years	Incidence (95% CI)	Univariate analysis		Multivariate analysis	
				IRR (95% CI)	p value	IRR (95% CI)	p value
TPT completion status							
Complete	1,550	492,835	3.1 (3.0–3.3)	Referent		Referent	
Incomplete	1,346	122,675	11.0 (10.4–11.6)	3.5 (3.2–3.8)	<0.001	3.83 (3.5–4.2)	<0.001
Not started	231	10,705	21.6 (18.9–24.5)	6.9 (5.7–8.3)	<0.001	5.25 (4.4–6.3)	<0.001
Sex							
F	1,553	393,961	3.9 (3.7–4.1)	Referent		Referent	
M	1,574	232,254	6.8 (6.4–7.1)	1.7 (1.6–1.9)	<0.001	1.56 (1.4–1.7)	<0.001
Viral load result†							
Suppressed	2,603	579,825	4.5 (4.3–4.7)	Referent		Referent	
Unsuppressed	524	46,390	11.3 (10.3–12.3)	2.5 (2.3–2.8)	<0.001	2.28 (2.0–2.5)	<0.001
Age group							
15–49	2,352	541,281	4.3 (4.2–4.5)	Referent		Referent	
>50	477	52,035	9.2 (8.4–10.0)	2.1 (1.9–2.4)	<0.001	1.55 (1.4–1.8)	<0.001
<15	298	32,899	9.1 (8.1–10.1)	2.1 (1.8–2.4)	<0.001	1.76 (1.6–2.0)	<0.001
TPT regimen‡							
Isoniazid	2,672	583,015	4.6 (4.4–4.8)	Referent			
3HP	224	32,495	6.9 (6.0–7.9)	1.5 (1.2–1.8)	<0.001		
No TPT	231	10,705	21.6 (18.9–24.5)	4.7 (3.9–5.6)	<0.001		
Health facility setting							
Rural	1,749	392,126	4.5 (4.3–4.7)	Referent		Referent	
Urban	1,378	234,089	5.9 (5.6–6.2)	1.3 (1.1–1.5)	<0.001	1.21 (1.1–1.4)	<0.001
Region§							
Northern	796	185,636	4.3 (4.0–4.6)	Referent		Referent	
Central	1,295	289,951	4.5 (4.2–4.7)	1.0 (0.9–1.3)	0.67	0.84 (0.7–1.0)	0.02
Southern	1,036	150,628	6.9 (6.5–7.3)	1.6 (1.4–1.9)	<0.001	1.51 (1.3–1.8)	<0.001
Latest CD4 result							
>200 cells/mm^3	550	72,187	7.6 (7.0–8.3)	Referent		Referent	
<200 cells/mm^3	326	16,597	19.6 (17.6–21.9)	2.6 (2.2–3.0)	<0.001	2.11 (1.8–2.5)	<0.001
Not tested	2,251	537,431	4.2 (4.0–4.4)	0.5 (0.5–0.6)	<0.001	0.58 (0.5-0.7)	<0.001
WHO staging status at ART start							
Stage I	2,117	509,232	4.2 (4.0–4.3)	Referent		Referent	
Stage II	551	77,186	7.1 (6.6–7.8)	1.7 (1.5–1.9)	<0.001	1.61 (1.5–1.8)	<0.001
Stage III	345	24,948	13.8 (12.4–15.4)	3.3 (3.0–3.8)	<0.001	2.62 (2.3–3.0)	<0.001
Stage IV	51	4,201	12.1 (9.0–16.0)	2.9 (2.3–3.8)	<0.001	1.89 (1.5–2.4)	<0.001
Not recorded	63	10,649	5.9 (4.5–7.6)	1.4 (1.1–1.9)	0.01	1.29 (1.0–1.7)	0.06
Started TPT within 30 d of ART initiation‡							
TPT at ART start	2,569	572,983	4.5 (4.3–4.7)	Referent			
Delayed TPT start	327	42,527	7.7 (6.9–8.9)	1.7 (1.5–1.9)	<0.001		
Not started	231	10,705	21.6 (18.9–24.5)	4.8 4.0–5.8)	<0.001		

*Incidence is cases/1,000 person-years. IRR, incidence rate ratio, TPT, TB prevention therapy, 3HP, 3-month course of 12 (1/wk) doses of isoniazid and rifapentine.
†Suppressed, <1,000 copies/mL; unsuppressed, ≥1,000 copies/mL.
‡Variable not included in multivariate analysis.
§Mozambique's 11 provinces are categorized into 3 regions: Central (Sofala, Manica, Tete, Zambezia), Northern (Nampula, Niassa, Cabo Delgado), and Southern (Maputo City, Maputo, Gaza, Inhambane).

ART initiation, and 14,079 (2.8%) received their diagnosis before initiating ART.

Of 341,844 PLHIV analyzed, 266,977 (78%) completed TPT, 68,594 (20%) had incomplete TPT, and 6,273 (1.8%) did not start TPT (Table 1). Incidence of diagnosed TB was 5.0/1,000 person-years. Compared with those who completed TPT (3.1/1,000 person-years), diagnosed TB was higher among PLHIV who did not start TPT (21.6/1,000 person-years; IRR 6.9 [95% CI 5.7–8.3]) and those with incomplete TPT (11.0/1,000 person-years; IRR 3.5 [95% CI 3.2–3.8]) (Table 2).

Median time between ART initiation and TB diagnosis was shortest for PLHIV who did not start TPT (182 [IQR 118–323] days), followed by those with incomplete TPT (216 [IQR 141–408] days) and those who completed TPT (418 IQR 294–560] days). Among those who completed TPT, diagnosed TB was higher in male PLHIV (IRR 1.5 [95% CI 1.4–1.7]), younger and older age groups (<15 years, IRR 1.5 [95% CI 1.4–1.7]; ≥50 years, IRR 1.7 [95% CI 1.5–2.0]), and in the Southern Region (IRR 1.6 [95% CI 1.3–1.9]) (Table 3). Other risk factors were unsuppressed viral load (IRR 2.3 [95% CI 2.0–2.7]), CD4 count <200 cells/mm^3 (IRR 1.9 [95% CI 1.5–2.3]), and WHO clinical stage II–IV at ART initiation (stage II, IRR 1.6 [95% CI 1.3–1.8]; stage III, IRR 2.5 [95% CI 2.1–2.9]; stage IV, IRR 1.7 [95% CI 1.1–2.7]).

Conclusions

In Mozambique, TPT was associated with reduced incidence of TB disease among PLHIV, including

among those with incomplete TPT. TPT likely averted TB among PLHIV, potentially saving lives and reducing costs to the health system. Despite that success, certain groups had an elevated risk of developing TB disease, even after TPT completion: men, younger and older PLHIV, and those with poor clinical status at ART initiation (unsuppressed HIV viral load, WHO clinical stages II–IV, and low CD4 count). Our findings are consistent with studies on TB incidence after TPT among PLHIV in sub-Saharan Africa (*7*,*8*). In addition, PLHIV in the Southern Region had elevated incidence, which aligns with higher overall TB incidence rates in the region; it might also reflect regional differences in TB services, including TB case detection (*9*; D. Respeito et al.).

PLHIV who completed TPT had a longer median time to TB diagnosis than did those who did not complete TPT. Our results aligned with similar studies in sub-Saharan Africa and India (*10*–*12*). Because TB diagnosis among those completing TPT occurred ≈14 months after ART initiation, a second course of TPT after a year could be beneficial, particularly among groups with elevated incidence. However, a recent randomized controlled trial did not find additional benefit from a repeat course of 3HP in Ethiopia, Mozambique, and South Africa (*2*,*13*). There is insufficient evidence for additional courses of TPT for PLHIV who completed TPT without new TB exposures (*2*).

Our findings are strengthened by data from a large national patient cohort containing 85% of PLHIV on ART. However, routine data are prone to quality concerns (i.e., data entry errors, poor completion of clinical tools); continual quality assurance activities and rigorous study exclusion criteria helped mitigate potential data-quality bias. We analyzed available programmatic data, which did not include other variables affecting TB (e.g., underlying conditions, body mass index). Misclassification could have occurred, given reliance on PLHIV self-reporting as newly initiated on ART and data cleaning assumptions.

Table 3. Incidence of TB among PLHIV newly initiated on ART who completed TPT, Mozambique, 2021–2024*

Characteristic	TB positive	Person-years	Incidence rate (95% CI)	Univariate analysis		Multivariate analysis	
				IRR (95% CI)	p value	IRR (95% CI)	p value
Sex							
F	803	313,190	2.6 (2.4–2.7)	Referent		Referent	
M	747	179,645	4.2 (3.9–4.5)	1.6 (1.5–1.8)	<0.001	1.54 (1.4–1.7)	<0.001
Viral load result†							
Suppressed	1,316	458,416	2.9 (2.7–3.0)	Referent		Referent	
Unsuppressed	234	34,419	6.8 (6.0–7.7)	2.4 (2–2.7)	<0.001	2.35 (2–2.7)	<0.001
Age group							
15–49	1,197	427,626	2.8 (2.6–3.0)	Referent		Referent	
<15	118	23,783	5.0 (4.1–5.9)	1.8 (1.5–2.2)	<0.001	1.50 (1.2–1.8)	<0.001
≥50	235	41,425	5.7 (5.0–6.4)	2.0 (1.7–2.3)	<0.001	1.72 (1.5–2)	<0.001
TPT regimen							
Isoniazid	1,371	461,601	3.0 (2.8–3.1)	Referent		Referent	
3HP	179	31,234	5.7 (4.9–6.6)	1.9 (1.6–2.3)	<0.001	1.07 (0.9–1.3)	0.54
Health facility setting							
Rural	872	305,777	2.9 (2.7–3)	Referent		Referent	
Urban	678	187,058	3.6 (3.4–3.9)	1.3 (1.1–1.5)	<0.001	1.12 (1–1.3)	0.14
Region‡							
Northern	416	159,095	2.6 (2.4–2.9)	Referent		Referent	
Central	533	205,089	2.6 (2.4–2.8)	1.0 (0.8–1.2)	0.95	1.05 (0.9–1.3)	0.60
Southern	601	128,651	4.7 (4.3–5.1)	1.8 (1.5–2.1)	<0.001	1.58 (1.3–1.9)	<0.001
Latest CD4 result							
≥200 cells/mm3	301	58,421	5.2 (4.6–5.8)	Referent		Referent	
<200 cells/mm3	160	13,622	11.7 (10–13.7)	2.3 (1.9–2.8)	<0.001	1.87 (1.5–2.3)	<0.001
Not Tested	1,089	420,792	2.6 (2.4–2.7)	0.5 (0.4–0.6)	<0.001	0.57 (0.5–0.7)	<0.001
WHO staging status at ART start							
Stage I	1,105	403,014	2.7 (2.6–2.9)	Referent		Referent	
Stage II	268	60,760	4.4 (3.9–5)	1.6 (1.4–1.9)	<0.001	1.55 (1.3–1.8)	<0.001
Stage III	131	18,502	7.1 (5.9–8.4)	2.6 (2.2–3.1)	<0.001	2.46 (2.1–2.9)	<0.001
Stage IV	18	2,993	6.0 (3.6–9.5)	2.2 (1.4–3.5)	<0.001	1.70 (1.1–2.7)	<0.001
Not recorded	28	7,566	3.7 (2.5–5.3)	1.3 (0.9–2)	0.13	1.41 (1–2.1)	0.08
Started TPT within 30 d of ART initiation							
TPT at ART start	1,446	466,832	3.1 (2.9–3.3)	Referent		Referent	
Delayed TPT start	104	26,003	4.0 (3.3–4.8)	1.3 (1.1–1.6)	<0.001	1.02 (0.8–1.2)	0.88

*Incidence is cases/1,000 person-years. IRR, incidence rate ratio, TPT, TB prevention therapy, 3HP, 3-month course of 12 (1/wk) doses of isoniazid and rifapentine.
†Suppressed, <1,000 copies/mL; unsuppressed, ≥1,000 copies/mL.
‡Mozambique's 11 provinces are categorized into 3 regions: Central (Sofala, Manica, Tete, Zambezia), Northern (Nampula, Niassa, Cabo Delgado), and Southern (Maputo City, Maputo, Gaza, Inhambane).

Despite those limitations, our study shows high concordance with other studies analyzing the effectiveness of TPT among PLHIV (*14*) and underscores the value of using a national data warehouse for analyzing programmatic outcomes.

In summary, TPT was associated with reduced TB incidence among PLHIV in Mozambique, including those who had not completed TPT. Improving TPT initiation and completion, along with focusing on men, younger and older PLHIV, and those with poor clinical status at ART initiation, could further reduce TB incidence.

Acknowledgments

We thank Irénio Gaspar, Rommel Bain, and Roberta Horth.

About the Author

Ms. Templin is an epidemiologist for the US Centers for Disease Control and Prevention based in Mozambique. She supports the analytical needs of the HIV/TB program to inform program improvement and strategic planning.

References

1. Gupta RK, Lucas SB, Fielding KL, Lawn SD. Prevalence of tuberculosis in post-mortem studies of HIV-infected adults and children in resource-limited settings. AIDS. 2015;29:1987–2002. https://doi.org/10.1097/QAD.0000000000000802
2. World Health Organization. WHO consolidated guidelines on tuberculosis. Module 6: tuberculosis and comorbidities: Geneva: The Organization; 2024.
3. UNAIDS. The urgency of now: AIDS at a crossroads. 2024 global AIDS update. 2025 [cited 2025 Jul 23]. https://www.unaids.org/sites/default/files/media_asset/2024-unaids-global-aids-update_en.pdf
4. World Health Organization. Global tuberculosis report. Geneva: The Organization; 2025
5. Suthar AB, Lawn SD, del Amo J, Getahun H, Dye C, Sculier D, et al. Antiretroviral therapy for prevention of tuberculosis in adults with HIV: a systematic review and meta-analysis. PLoS Med. 2012;9:e1001270. https://doi.org/10.1371/journal.pmed.1001270
6. UNAIDS. Mozambique country data. 2024 [cited 2025 Jul 23]. https://www.unaids.org/en/regionscountries/countries/mozambique
7. Turinawe G, Asaasira D, Kajumba MB, Mugumya I, Walusimbi D, Tebagalika FZ, et al. Active tuberculosis disease among people living with HIV on ART who completed tuberculosis preventive therapy at three public hospitals in Uganda. PLoS One. 2024;19:e0313284. https://doi.org/10.1371/journal.pone.0313284
8. Sabasaba A, Mwambi H, Somi G, Ramadhani A, Mahande MJ. Effect of isoniazid preventive therapy on tuberculosis incidence and associated risk factors among HIV infected adults in Tanzania: a retrospective cohort study. BMC Infect Dis. 2019;19:62. https://doi.org/10.1186/s12879-019-3696-x
9. Cuboia N, Amaro M, Manhiça I, Reis-Pardal J, Zindoga P, Pfumo-Cuboia I, et al. Tuberculosis incidence among children under five years of age in Mozambique: spatial distribution and predictors in a nationwide Bayesian disease mapping study. Scientific African. 2025;28:e02757.
10. Agarwal R, Nyendak M, Chava N, Allam RR, Moonan PK, Sriram CS, et al. Long-term protection from TB preventive treatment among people with HIV in a high-burden tuberculosis setting: an observational cohort study from India. Clin Infect Dis. 2025;81:970–9. https://doi.org/10.1093/cid/ciaf322
11. Kazibwe A, Oryokot B, Mugenyi L, Kagimu D, Oluka AI, Kato D, et al. Incidence of tuberculosis among PLHIV on antiretroviral therapy who initiated isoniazid preventive therapy: a multi-center retrospective cohort study. PLoS One. 2022;17:e0266285. https://doi.org/10.1371/journal.pone.0266285
12. Semu M, Fenta TG, Medhin G, Assefa D. Effectiveness of isoniazid preventative therapy in reducing incidence of active tuberculosis among people living with HIV/AIDS in public health facilities of Addis Ababa, Ethiopia: a historical cohort study. BMC Infect Dis. 2017;17:5. https://doi.org/10.1186/s12879-016-2109-7
13. Churchyard G, Cárdenas V, Chihota V, Mngadi K, Sebe M, Brumskine W, et al.; WHIP3TB Study Team. Annual tuberculosis preventive therapy for persons with HIV infection. Ann Intern Med. 2021;174:1367–76. https://doi.org/10.7326/M20-7577
14. Silva Júnior JNB, Leal GDC, Ferreira QR, Andrade LKA, Ballestero JGA, Santos VS, et al. Effectiveness of tuberculosis preventive treatment on disease incidence among people living with HIV/AIDS: A systematic review and meta-analysis. PLoS One. 2025;20:e0330208. https://doi.org/10.1371/journal.pone.0330208

Address for correspondence: Lindsay Templin, Centers for Disease Control and Prevention, 1600 Clifton Rd, Mailstop H21-10, Atlanta, GA 30329-4018, USA; email: xxz4@cdc.gov

Emerging Endemic Area for Blastomycosis, New York, USA, 2000–2024

Laura E. Ramirez, Christian Kostowniak, Jessica Kumar, Sudha Chaturvedi, Ananthakrishnan Ramani, Amit Chopra

Blastomycosis is not yet considered endemic in upstate New York, USA; however, cases have increased during the past decade. We performed a retrospective study of 54 laboratory-confirmed cases reported during 2000–2024. Our results demonstrate an increase in incidence over time, indicating that this region represents an emerging endemic area.

The fungal infection blastomycosis had not been considered endemic to upstate New York, USA, but an increase in cases has been seen during the past decade (*1*,*2*), such that it could be an emerging endemic area (*3*). Despite increased efforts to raise awareness, this disease is not reportable in the state of New York. Because of the lack of recognition of blastomycosis as an emerging infection, diagnosis and treatment are often delayed (*3*). We conducted a retrospective study of patients with blastomycosis in this region, aiming to describe the epidemiologic characteristics and geographic distribution and to raise awareness of this disease.

The Study

We retrospectively reviewed patients with diagnosed blastomycosis who were either hospitalized or managed in infectious disease clinics in Albany, New York, USA, during January 2000–December 2024. We identified patients with confirmed blastomycosis by reviewing pathology records, microbiology records, or both, through an electronic medical record system. We defined a confirmed case as a positive *Blastomycosis* spp. result for ≥1 of the following tests: real-time PCR, positive culture, or histopathology and cytopathology findings consistent with the diagnosis (*4*,*5*). Real-time PCR was performed on clinical specimens obtained directly from patients, including tissue biopsy specimens, bronchoalveolar lavage fluid, and sputum. The PCR used in this study was developed by the laboratory of the New York State Department of Health's Wadsworth Center from BAD1 *Blastomyces* spp. with high sensitivity and specificity (*2*). The test has undergone the Clinical Laboratory Evaluation Program of the New York State Department of Health.

We calculated incidence of blastomycosis over 24 years. We used Tableau Desktop 2025.1.1 (Tableau, https://www.tableau.com) to generate a geographic map to visualize the incidence distribution across the affected regions using postal (ZIP) codes. We classified patients as having either isolated pulmonary infection or disseminated infection (involving ≥1 organ or any organ other than the lung). We compiled clinical characteristics, radiologic features, diagnostic methods, and treatment for both groups.

We identified 54 patients with a confirmed blastomycosis diagnosis during the study period (Table 1). Most (87%, n = 47) patients were hospitalized, but 7 (13%) patients were managed as outpatients. Nearly all cases were initially misdiagnosed, most commonly with community-acquired pneumonia or malignancy. More than half (57%) of patients had no identifiable underlying conditions (Table 1).

The most common diagnostic method for specimen collection was biopsy, performed in 42 (82%) patients. Biopsy was performed in 25/28 (89%) patients with disseminated infection and 17/23 (71%) patients with pulmonary infection. The most commonly biopsied organ was the lung (56%), followed by skin (25%) and bone (17%). Real-time PCR was used in 39 (78%)

Author affiliations: Albany Medical College, Albany, New York, USA (L.E. Ramirez, C. Kostowniak, J. Kumar, A. Ramani, A. Chopra); College of Integrated Health Sciences, State University of New York, Albany (J. Kumar); New York State Department of Health, Albany (J. Kumar); Wadsworth Center Mycology Laboratory, New York State Department of Health, Albany (S. Chaturvedi)

DOI: https://doi.org/10.3201/eid3203.251306

cases, culture in 29 (58%) cases, and histopathology/cytopathology in 13 (26%) cases. Only in 13/50 (24%) cases was PCR the sole method of diagnosis. More than 1 diagnostic method was used in 52% of cases (Table 2).

Most (96%) patients were residents of upstate New York, and 85% of those lived in counties within the Capital District region around Albany (Appendix Figure, https://wwwnc.cdc.gov/EID/article/32/3/25-1306.pdf). No patients reported travel to known endemic areas. We mapped the geographic distribution of cases along the Mohawk River (Figure 1). The number of reported blastomycosis cases rose substantially during the study years, but the most pronounced rise occurred in 2024, which represented 24% (13/54) of total cases (Figure 2). Those cases were distributed over multiple counties in the region and not concentrated in 1 area.

Disseminated infection was present in 54% of patients; the other 46% had isolated pulmonary involvement. We compared the clinical characteristics, radiologic features, diagnostic methods, and treatments for those 2 groups (Table 2) and found no noticeable differences. We did not perform statistical analyses for the comparison of the 2 groups because of the small sample sizes.

The results from this study demonstrate the recent increase in the incidence of blastomycosis cases in upstate New York. Many patients resided near the Mohawk River Valley area, highlighting the disease's rising incidence in that region. None of the patients in this study had documented travel history to known endemic areas, implying that the infection was acquired locally. That increasing trend might be the result of climate change causing a more favorable environment for the growth or sporulation of *Blastomyces* species. Previous studies have suggested that a global increase in temperature and rainfall has played a key role in the rising number of blastomycosis cases and its spread to nonendemic areas, given that the fungus thrives in moist and warm environments (*6*,*7*). Similarly, temperatures and precipitation in upstate New York have risen over the years (*8*), contributing to a more favorable environment for *Blastomyces* spp. growth. Another factor that might have contributed to the increasing trend is increased disease detection with PCR, which has high sensitivity and specificity for *Blastomyces* spp. (*9*).

Historically, blastomycosis was recognized as endemic in parts of North America, particularly in regions surrounding the Ohio and Mississippi River Valleys and the Great Lakes (*10*). The infectious etiology in this study follows a similar pattern, with a high incidence of cases reported in areas along the Mohawk River (Figure 1). Currently, only 5 US states require reporting blastomycosis to the health department: Arkansas, Louisiana, Michigan, Minnesota, and Wisconsin (*11*). The cases described in this study reflect a single medical center, suggesting that the data are probably a fraction of the actual disease burden in the region and that the true incidence might exceed official estimates. In 2017, the Centers for Disease Control and Prevention, alerted by the New York State Department of Health, reported an increase in blastomycosis incidence in the Capital District region among patients with no travel history to endemic areas (*12*). Other studies have provided evidence of the increasing blastomycosis incidence, suggesting that upstate New York could be an emerging endemic region (*3*,*13*,*14*).

Diagnosis of blastomycosis requires a high index of clinical suspicion, particularly in patients with pulmonary infections and extrapulmonary lesions. Such

Table 1. Demographic characteristics and underlying conditions for 54 patients with laboratory-confirmed blastomycosis reported in Albany, New York, USA, 2000–2024*

Characteristics	Value
Mean age ± SD, y	43 ± 18
Median age, y (range)	42 (4–78)
Sex	
F	12 (22)
M	42 (78)
Average BMI ± SD	27 ± 6
Median BMI (range)	26 (16.9–39.7)
Race	
Caucasian	37 (69)
African American	9 (17)
Asian	2 (4)
Other	6 (11)
Underlying conditions	
Chronic lung disease	10 (19)
Diabetes mellitus	9 (17)
Cardiovascular disease	4 (7)
Malignancy	4 (7)
Immunosuppression	2 (4)
Organ transplant	1 (2)
HIV	1 (2)
Kidney disease and failure	2 (4)
Pregnancy	1 (2)
None identified	31 (57)
Tobacco use	30 (55)
Marijuana use	9 (15)
Preliminary diagnoses, n = 46	
Community-acquired pneumonia	14 (30)
Malignancy	12 (26)
Skin and soft tissue infection	5 (11)
Osteomyelitis	4 (9)
Bacterial and viral infection	3 (7)
Tuberculosis	1 (2)
Blastomycosis	1 (2)
Other	6 (13)

*Values are no. (%) except as indicated. Categories are not mutually exclusive, so totals may sum to >100%.

Table 2. Diagnostic evaluation and treatment patterns for patients with isolated and disseminated laboratory-confirmed blastomycosis reported in Albany, New York, USA, 2000–2024*

Characteristics	Isolated pulmonary	Disseminated	Total
Mean age ± SD, y	45 ± 17	40 ± 19	43 ± 18
Sex	n = 24	n = 28	n = 52
F	7 (29)	4 (14)	11 (21)
M	17 (71)	24 (86)	41 (79)
Method of specimen collection	n = 23	n = 28	n = 51
Biopsy	17 (71)	25 (89)	42 (82)
Bronchioalveolar lavage	14 (58)	3 (11)	17 (32)
Sputum	2 (8)	1 (4)	3 (6)
Lumbar puncture	0	3 (11)	3 (6)
Methods of establishing diagnosis	n = 22	n = 28	n = 50
Real-time PCR	17 (77)	22 (79)	39 (78)
Culture	12 (55)	17 (61)	29 (58)
Histopathology and cytopathology	6 (27)	7 (25)	13 (26)
Computed tomography chest characteristics	n = 24	n = 12	n = 36
Mass	8 (33)	5 (42)	13 (36)
Lobar consolidation	9 (38)	3 (25)	12 (33)
Nodular	7 (29)	4 (33)	11 (31)
Pleural effusion	3 (13)	3 (25)	6 (17)
Mediastinal lymphadenopathy	2 (8)	2 (17)	4 (11)
Cavity	3 (13)	0	3 (8)
Miliary	1 (4)	1 (8)	2 (6)
Treatment	n = 19	n = 21	n = 40
Itraconazole only	13 (68)	11 (53)	24 (60)
Amphotericin B followed by itraconazole	4 (21)	6 (29)	11 (28)
Amphotericin B only	2 (11)	2 (10)	4 (10)
Fluconazole	0	2 (10)	2 (5)
Voriconazole	1 (5)	0	1 (3)
Length of treatment, n = 31	n = 15	n = 16	n = 31
6 mo	7 (47)	1 (6)	8 (26)
9 mo	0	1 (6)	1 (3)
12 mo	8 (53)	14 (88)	22 (71)
Death	1 (2)	2 (4)	3 (6)
Total	24 (46)	28 (54)	52

*Values are no. (%) except as indicated. Categories are not mutually exclusive, so totals may sum to >100%. Data were not available for all variables for every patient; therefore, denominators vary by category. Percentages are calculated by using the number of patients with available data for each variable.

patients often have no notable underlying conditions. Given that nearly all patients in this cohort initially had misdiagnoses and that New York is not currently considered an endemic region, most patients experienced a delay in diagnosis and appropriate treatment.

The first limitation of this study was its single-center retrospective nature, which limits the generalizability of our results and creates the need for further studies with a broader sample of the population. Second, asymptomatic patients were less likely to seek

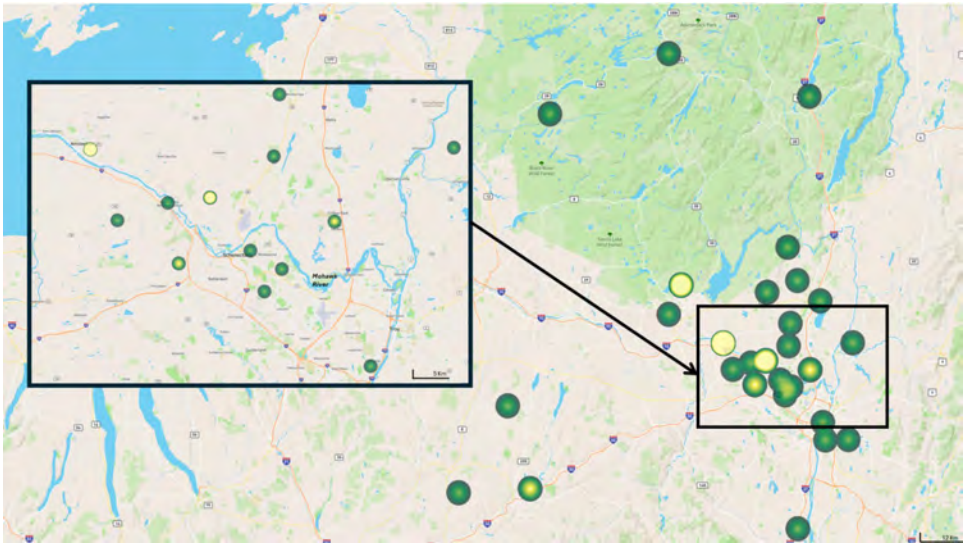

Figure 1. Geographic distribution of blastomycosis cases in upstate New York, USA, 2000–2024. Yellow shading indicates a higher number of cases associated with that postal (ZIP) code. A higher concentration of cases is observed in regions near the Mohawk River (inset), suggesting a potential area of increased endemicity.

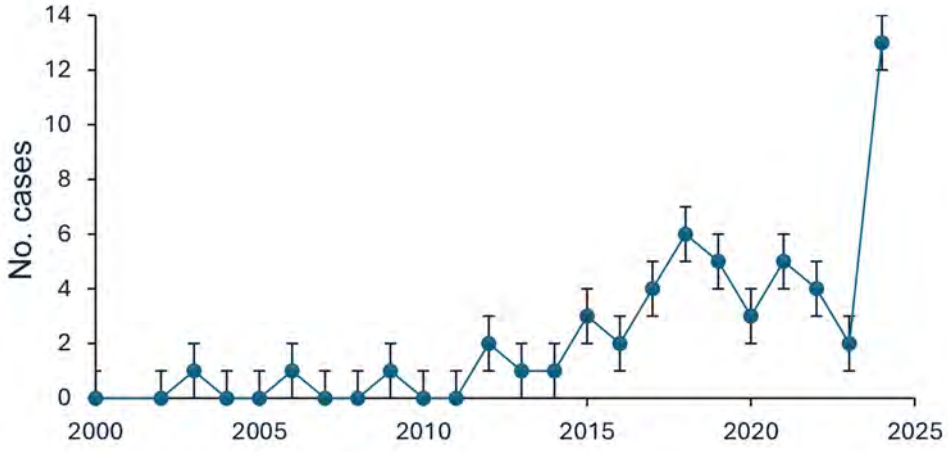

Figure 2. Annual number of blastomycosis cases diagnosed at Albany Medical Center, Albany, New York, USA, 2000–2024. Case numbers remained stable during 2000–2014, then markedly increased during 2015–2024. Error bars indicate SE.

medical care and were thus omitted. Third, PCR testing was performed on samples from many patients, but PCR is not widely available at other hospitals. However, in many cases, results were also confirmed by culture results. Fourth, some patients did not have comprehensive clinical and diagnostic data available for a thorough analysis. Last, some patients might have received treatment at a different medical center and were not captured in this analysis. Therefore, the cases we report do not represent the true incidence of cases in the community, although results were validated with the state public health laboratory at the Wadsworth Center.

Conclusions

Despite the limitations, our results strongly indicate that upstate New York represents a new emerging endemic area for blastomycosis. Therefore, we recommended that this disease be made reportable to the state's health departments. Physicians in this region should consider blastomycosis when pulmonary symptoms are accompanied by cutaneous findings, potentially reducing initial misdiagnoses and treatment delays.

The Albany Medical College Institutional Review Board determined that the study was exempt from further review because the database used was exclusively deidentified.

All authors contributed equally to the conception, drafting, and review of this case report. Each author has approved the final version for submission.

About the Author

Ms. Ramirez is third-year medical student at Albany Medical College, Albany, New York. Her research interests are infectious disease and pulmonology.

References

1. McDonald R, Dufort E, Jackson BR, Tobin EH, Newman A, Benedict K, et al. Notes from the field: blastomycosis cases occurring outside of region with known endemicity—New York, 2007–2017. MMWR Morb Mortal Wkly Rep. 2018;67:1077–8. https://doi.org/10.15585/mmwr.mm6738a8
2. Kaplan M, Zhu Y, Kus JV, McTaggart L, Chaturvedi V, Chaturvedi S. Development of a duplex real-time PCR assay for the differentiation of Blastomyces dermatitidis and *Blastomyces gilchristii* and a retrospective analysis of culture and primary specimens from blastomycosis cases from New York (2005 to 2019). J Clin Microbiol. 2021;59:e02078–20. https://doi.org/10.1128/JCM.02078-20
3. Austin A, Tobin E, Judson MA, Hage CA, Hu K, Epelbaum O, et al. Blastomycosis in the Capital District of New York State: a newly identified emerging endemic area. Am J Med. 2021;134:e101–8. https://doi.org/10.1016/j.amjmed.2020.09.017
4. Sidamonidze K, Peck MK, Perez M, Baumgardner D, Smith G, Chaturvedi V, et al. Real-time PCR assay for identification of *Blastomyces dermatitidis* in culture and in tissue. J Clin Microbiol. 2012;50:1783–6. https://doi.org/10.1128/JCM.00310-12
5. Linder KA, Kauffman CA. Current and new perspectives in the diagnosis of blastomycosis and histoplasmosis. J Fungi (Basel). 2020;7:12. https://doi.org/10.3390/jof7010012
6. Bonifaz A, García-Salazar E, Frías-De-León MG. Climate change exacerbating fungal disease disparities. Curr Fungal Infect Rep. 2024;18:1–12. https://doi.org/10.1007/s12281-023-00479-9
7. Khadilkar A, Waddell L, Acheson ES, Ogden NH. Perspectives on blastomycosis in Canada in the face of climate change. Can Commun Dis Rep. 2024;50:400–11. https://doi.org/10.14745/ccdr.v50i11a04
8. Goff C, Amarakoon S, Curtis D, Stevens A. New York State climate impacts assessment. Chapter 01: introduction. Ann N Y Acad Sci. 2024;1542:67–90. https://doi.org/10.1111/nyas.15202
9. Saravanababu T, Elsayed S, Gupta R, Delport J, Rahimi Shahmirzadi M, AlMutawa F. Diagnosing blastomycosis: a review of laboratory methods and clinical utility. J Fungi (Basel). 2025;11:589. https://doi.org/10.3390/jof11080589
10. Benedict K, Roy M, Chiller T, Davis JP. Epidemiologic and ecologic features of blastomycosis: A review. Curr Fungal Infect Rep. 2012;6:327–35. https://doi.org/10.1007/s12281-012-0110-1

11. Benedict K, Gibbons-Burgener S, Kocharian A, Ireland M, Rothfeldt L, Christophe N, et al. Blastomycosis surveillance in 5 states, United States, 1987–2018. Emerg Infect Dis. 2021;27:999–1006. https://doi.org/10.3201/eid2704.204078
12. McDonald R, Dufort E, Jackson BR, Tobin EH, Newman A, Benedict K, et al. Notes from the field: blastomycosis cases occurring outside of regions with known endemicity—New York, 2007–2017. MMWR Morb Mortal Wkly Rep. 2018;67:1077–8. https://doi.org/10.15585/mmwr.mm6738a8
13. Bethuel NW, Siddiqui N, Edmonds L. Pulmonary blastomycosis in rural Upstate New York: a case series and review of literature. Ann Thorac Med. 2020;15:174–8. https://doi.org/10.4103/atm.ATM_86_20
14. Ramirez LE, Foyt AK, Darwish N, Foulke L, Kostowniak C, Chopra A. A rare case of miliary blastomycosis. Respir Med Case Rep. 2025;55:102203. https://doi.org/10.1016/j.rmcr.2025.102203

Address for correspondence: Laura E. Ramirez, Albany Medical College, 43 New Scotland Ave, Albany, NY 12208-3479, USA; email: ramirel@amc.edu

Home-Based Monitoring of Treatment-Related Adverse Events during Drug-Resistant Tuberculosis Treatment, India, 2020–2024

Minal Ahson, Daksha Shah, Sampada Bhide, Rajesh Deshmukh, Jonathan P. Smith, Smita Waghmare, Satish Kaipilyawar, Varsha Puri, Dilip K. Khetade, Vijay Yeldandi, Anand Date, Patrick K. Moonan,[1] Christine S. Ho[1]

We investigated home-based outreach and point-of-care diagnostic tools for monitoring adverse events among persons treated for drug-resistant tuberculosis in Dharavi, India. Of 974 persons treated, 518 (53%) reported 1,410 adverse events, 126/477 (26%) required regimen change, and 83% of patients completed therapy. Home-based adverse event monitoring can help improve tuberculosis treatment adherence.

India contributes 25% of the tuberculosis (TB) burden and 32% of drug-resistant TB (DR TB) cases worldwide (*1*). DR TB in Mumbai ranks among the highest globally (*2*). Within Mumbai, Dharavi is one of the world's largest informal settlements, housing >1 million persons in 0.8 square miles and supporting ≈15,000 small factories employing >250,000 persons (*3*).

Completing DR TB treatment in Dharavi remains challenging because many patients are migrants who lack stable family support during treatment (*4*). DR TB treatment regimens are prolonged and rely on second-line drugs, which are more toxic than those used for drug-susceptible TB. Drug-related adverse events are common during DR TB treatment and complicate clinical management (*5*). Consequently, DR TB is associated with higher relapse and mortality rates (*1*).

The development of shorter, more tolerable DR TB regimens offers opportunities to improve and decentralize care. However, data on drug-specific adverse events in community-based programs remain limited despite global recommendations for active monitoring (*6*). We evaluated a home-based adverse event monitoring system implemented in Dharavi to assess patient adherence to treatment regimens and feasibility of such programs in resource-limited settings.

The Study

The End DRTB in Dharavi project included a series of programmatic interventions aimed at improving treatment adherence and outcomes among patients with DR TB in that area (*7*). In brief, all adult (≥18 years of age) DR TB patients within Dharavi who initiated government-supported treatment during December 2020–June 2022 were eligible for inclusion. The project prospectively enrolled TB patients who initiated treatment for multiple phenotypic drug-resistance patterns, including monoresistant (i.e., resistance to 1 first-line drug), polyresistant (i.e., resistance ≥2 first-line drugs but not to both isoniazid and rifampin), multidrug-resistant (MDR; i.e., resistance to at least isoniazid and rifampin), and extensively drug-resistant (XDR; i.e., MDR and resistance to any fluoroquinolone and a second-line injectable drug [SLID]). All participants received drug-susceptibility guided treatment, according to national guidelines (*8*). Urban Health Centre (UHC) Dharavi provided baseline testing to assess toxicity, including audiometry, electrocardiogram (ECG), visual acuity and Snellen tests, and comprehensive metabolic blood panels for pretreatment evaluation. We provided point-of-care, tablet-based audiometry (Shoebox, https://www.shoebox.md) and electrocardiogram

Author affiliations: Centers for Disease Control and Prevention, Atlanta, Georgia, USA (M. Ahson, J.P. Smith, A. Date, P.K. Moonan, C.S. Ho); Brihanmumbai Municipal Corporation, Mumbai, India (D. Shah, V. Puri, D.K. Khetade); Society for Health Allied Research and Education, Hyderabad, India (S. Bhide, S. Waghmare, S. Kaipilyawar, V. Yeldandi); US Centers for Disease Control and Prevention, Mumbai (R. Deshmukh)

DOI: https://doi.org/10.3201/eid3203.251893

[1]These authors contributed equally to this article.

(SmartHeart, https://www.getsmartheart.com) tests to expedite pretreatment evaluation and reduce travel requirements for testing. Trained field coordinators subsequently recorded clinical adverse events during monthly home visits by using a standardized screening and referral questionnaire (Appendix Figure, https://wwwnc.cdc.gov/EID/article/32/3/25-1893-App1.pdf), audiometry, and electrocardiogram testing, following a previously described predetermined schedule (*7*).

We categorized adverse events as mild, moderate, or severe. Severe adverse events resulted in hospitalization, persistent disability, a life-threatening condition, or death and required clinical intervention to prevent or manage those outcomes (*7*). Moderate adverse events required clinical intervention, symptomatic treatment, or treatment modification but not hospitalization, and mild adverse events did not require clinical intervention or treatment modification. We referred patients reporting any adverse event to the nearest medical officer for evaluation, per standard guidelines (*8*), and referred patients with abnormal audiometry or ECG findings or any severe adverse event to a tertiary care facility or the UHC chest physician for further management and any necessary treatment regimen modifications.

Our primary outcomes were occurrence and timing of any clinically relevant adverse event or abnormality (audiometric, cardiac, optic, or metabolic) during DR TB treatment. We excluded from analysis adverse events that were reported at baseline, before the medication regimen began. We counted adverse events reported at consecutive visits as a single event unless severity increased and considered nonconsecutive episodes separate events. Because hearing loss is generally irreversible, we classified it as a nonrecurring event but recorded any worsening (*9*).

We used frequencies and proportions to describe new adverse events during treatment, stratified by regimen and antimicrobial drugs. We assessed group differences by using χ^2 or Monte Carlo simulation methods, as appropriate. We analyzed time to first event by using cumulative incidence function with Gray's method, accounting for competing risks,

Table. Frequency, severity, and treatment modification of reported adverse events during home-based monitoring of drug-resistant tuberculosis treatment, Dharavi, Mumbai, India, 2020–June 2024*

Adverse event†	Total	Severity			Required treatment modification
		Mild	Moderate	Severe	
Neurologic	292 (21)	86 (29)	203 (70)	3 (1)	52 (18)
Tingling, pain, or numbness in hands or feet	148 (11)	48 (32)	99 (67)	1 (1)	34 (23)
Visual disturbances	54 (4)	15 (28)	39 (72)	0	12 (22)
Headache	34 (3)	7 (21)	26 (76)	1 (3)	3 (9)
Dizziness	27 (2)	8 (30)	19 (70)	0	0
Hearing loss	16 (1)	1 (6)	15 (94)	0	1 (6)
Ringing in ears	12 (1)	7 (58)	5 (42)	0	2 (17)
Seizure	1 (<1)	0	0	1 (100)	0
Gastrointestinal	309 (22)	123 (40)	175 (57)	11 (4)	12 (4)
Nausea, vomiting	163 (12)	79 (48)	80 (49)	4 (3)	6 (4)
Loss of appetite	68 (5)	24 (35)	43 (63)	1 (2)	3 (4)
Abdominal pain	51 (4)	13 (25)	33 (65)	5 (10)	2 (4)
Diarrhea	13 (1)	3 (23)	10 (77)	0	1 (8)
Constipation	8 (<1)	2 (25)	6 (75)	0	0
Difficulty urinating	4 (<1)	1 (25)	2 (50)	1 (25)	0
Yellowish discoloration of skin and eyes	2 (<1)	1 (50)	1 (50)	0	0
Musculoskeletal	174 (12)	66 (38)	108 (62)	0	23 (13)
Joint pain	168 (12)	65 (39)	103 (61)	0	22 (13)
Neck, face swelling	6 (<1)	1 (17)	5 (83)	0	1 (17)
Behavioral	48 (4)	18 (38)	26 (54)	4 (8)	10 (21)
Psychosis	10 (1)	6 (60)	4 (40)	0	2 (20)
Changes in behavior	18 (1)	6 (33)	11 (61)	1 (6)	5 (28)
Sleep disturbances	8 (<1)	3 (38)	5 (62)	0	1 (13)
Depression or suicidal ideation	12 (1)	3 (25)	6 (50)	3 (25)	2 (17)
Dermatologic	37 (3)	21 (57)	16 (43)	0	3 (8)
Skin rash or itching	37 (3)	21 (57)	16 (43)	0	3 (8)
Cardiologic	99 (7)	28 (28)	66 (67)	5 (5)	5 (5)
Abnormal electrocardiogram	39 (3)	20 (51)	19 (49)	0	0
Fatigue	38 (3)	4 (11)	31 (82)	3 (8)	3 (8)
Palpitations	22 (2)	4 (18)	16 (73)	2 (9)	2 (9)
Other, unspecified	451 (32)	139 (31)	284 (63)	28 (6)	21 (5)
Total	1,410	481 (34)	878 (62)	51 (4)	126 (9)

*Values are no. (%).
†Patients could experience multiple events.

including death, loss to follow-up, treatment discontinuation, and transfers out of the service area. We estimated subdistribution hazard ratios and 95% CIs by using the Fine-Gray model with weighted Cox regression. This activity was approved by the Brihanmumbai Mumbai Corporation and the US Centers for Disease Control and Prevention and was determined to be nonresearch.

Among 974 DR TB patients, 880 (90%) started MDR TB treatment, 51 (5%) started monoresistant TB treatment, 38 (4%) started XDR TB treatment, and 5 (<1%) started polyresistant TB regimens (Appendix Table). Overall, 518 (53%) patients reported a total of 1,410 discrete adverse events, the most frequent of which were gastrointestinal (22%), neurologic (21%), and musculoskeletal (12%) events (Table). Most (96%, n = 1,359) events were mild or moderate; 38 (7%) patients experienced 51 (4%) severe events. Participants receiving MDR TB regimens were more likely (55%) to report ≥1 adverse event than those who received monoresistant or polyresistant (41%) or XDR TB regimens (40%) (p = 0.04), none of which included SLIDs. Participants on a regimen containing SLIDs were almost 4 times as likely to report an adverse event compared with those not using SLIDs (hazard ratio 3.87 [95% CI 3.14–4.77]) (Figure). Of patients who received SLIDs, 206 (89%) completed treatment. Overall, 805 (83%) patients completed TB treatment.

Treatment modification data were available for 477 (92%) patients who reported an adverse event. Among those, 126 (26%) reported ≥1 regimen change attributable to their event, and 57 (45%) regimen changes occurred at first adverse event. Two patients developed clinically apparent jaundice, corroborated by elevated hepatic transaminase and bilirubin levels; both required treatment regimen modification. Thirty-nine (3%) patients had abnormal ECG findings and were referred to UHC chest physicians for further evaluation; none required treatment regimen modification. Among 233 patients receiving SLIDs, 219 (94%) had baseline audiometric screening, and 173 (79%) had abnormal follow-up results. Of those, 100 (58%) were evaluated by an otolaryngologist or audiology subspecialist, and 14 (14%) discontinued SLIDs after assessment. Regimen changes enabled patients to continue treatment safely and did not necessarily result in treatment interruption or discontinuation. Our findings aligned with results from an individual patient data meta-analysis on MDR TB, which demonstrated poorer outcomes among patients treated with kanamycin or capreomycin SLIDs (*10*).

Conclusions

This home-based monitoring model coincided with sustained care engagement and adherence; 83% of patients completed therapy in Dharavi, compared with ≈1 in 3 before implementation of this model (*7*). Even among patients on SLID-containing regimens, the group with the most adverse events, 89% completed treatment. Although not a causal evaluation, our findings suggest that routine adverse event monitoring, detection, and timely management supported

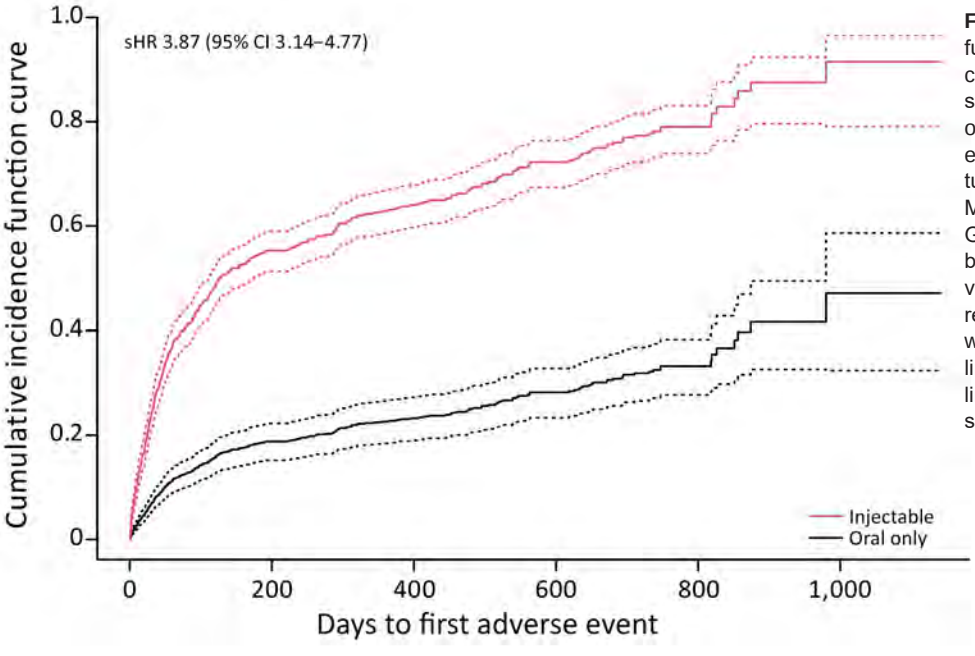

Figure. Cumulative incidence function curves of time to first clinical adverse events in a study of home-based monitoring of treatment-related adverse events during drug-resistant tuberculosis treatment, Dharavi, Mumbai, India, 2020–2024. Graphs compare reactions between patients with injectable versus noninjectable treatment regimens among patients with drug-resistant TB. Solid lines indicate medians; dotted lines indicate 95% CIs. sHR, subdistribution hazard ratio.

improved treatment adherence and completion. SLIDs have been downgraded in national guidelines (*7*), but several factors highlight the need to reassess their role in TB treatment. Those factors include rising bedaquiline resistance; challenges accessing bedaquiline, pretomanid, linezolid, and moxifloxacin–based regimens; frequent linezolid toxicity; and limited access to drug-susceptibility testing (*11*,*12*). Given their high resistance threshold, SLIDs might remain useful when judiciously applied. Emerging evidence that 2 early high-dose amikacin doses can reduce initial resistance without added short-term toxicity (*13*) supports a limited transitional role for SLIDs within evolving all-oral, patient-centered treatment models.

In conclusion, sustained investments in local capacity and integration of patient-centered monitoring within national TB programs are essential to achieving global End TB targets (*14*). We found that active home-based monitoring for adverse events and use of point-of-care diagnostic tools were feasible and effective in this high-burden, resource-constrained setting. That approach improved early detection and management of drug-related toxicities and sustained engagement in care and adherence among patients with DR TB. Implementation of decentralized adverse event surveillance and mobile health technologies can strengthen pharmacovigilance and improve treatment outcomes in similar high-density, informal settlements.

Acknowledgments

We thank Central TB Division, Government of India, and State National Tuberculosis Elimination Programme (NTEP) Maharashtra for providing and ensuring uninterrupted supply of medicines. We thank Brihanmumbai Municipal Corporation NTEP (Santosh Gaikwad, Harshal Pagare, Narendra Sutar) and Dadar NTEP team (Sandeep Ghuge, Bhimrao Shinde, Jayshree Salvi, Bharat Gaikwad, Manisha Palande, Laxmi Salvdi, Shila Sable, Amol Kambli, Chetan Patil, Seema Dhuri) for support with pretreatment evaluation, treatment initiation, and clinical management of adverse events. We thank Society for Health Allied Research and Education (SHARE) India team (Nikunj Fofani, Jaya Nair, Swapnali Ambekar, Darshana Bangera, Komal Chavan, Padmaja Chavan, Priyanka Kawade, Siddhesh Khetale, Vilas Vitthal Naik, Asha Manoj Pawar, Vishal Sakpal, Shabnam Shaikh, Deepali Shirke, Shashikant Tambe) for support with field visits, referral and outcome reporting, data collection, and data analysis.

This project was partially supported by the President's Emergency Plan for AIDS Relief (PEPFAR) through the US Centers for Disease Control and Prevention under the terms of cooperative agreement no. NU2GGH002312. This project followed all US federal regulations, including 45 C.F.R. part 46, 21 C.F.R. part 56; 42 U.S.C. Sect. 241(d); 5 U.S.C. Sect. 552a; 44 U.S.C. Sect. 3501 et seq.

About the Author

Dr. Ahson is a medical officer and former epidemic intelligence service officer for the Global Tuberculosis Branch in the Division of Global HIV and Tuberculosis, Global Health Center, US Centers for Disease Control and Prevention. Her work is focused on programmatic and technical support for TB programs to prevent, diagnose, and treat TB.

References

1. World Health Organization. Global tuberculosis report 2025 [cited 2025 Nov 19]. https://www.who.int/teams/global-programme-on-tuberculosis-and-lung-health/tb-reports/global-tuberculosis-report-2025
2. D'souza DT, Mistry NF, Vira TS, Dholakia Y, Hoffner S, Pasvol G, et al. High levels of multidrug resistant tuberculosis in new and treatment-failure patients from the Revised National Tuberculosis Control Programme in an urban metropolis (Mumbai) in western India. BMC Public Health. 2009;9:211. https://doi.org/10.1186/1471-2458-9-211
3. Dey S, Iulo LD. The circular economy of Dharavi: making building materials from waste. Enquiry. ENQ the ARCC J Archit Res. 2021;18:4–28. https://doi.org/10.17831/enqarcc.v18i2.1099
4. Eyre L. The shanty towns of central Bombay. Urban Geogr. 1990;11:130–52. https://doi.org/10.2747/0272-3638.11.2.130
5. World Health Organization. Active tuberculosis drug-safety monitoring and management (aDSM): framework for implementation [cited 2025 Oct 10]. https://www.who.int/publications/i/item/WHO-HTM-TB-2015.28
6. Munro SA, Lewin SA, Smith HJ, Engel ME, Fretheim A, Volmink J. Patient adherence to tuberculosis treatment: a systematic review of qualitative research. PLoS Med. 2007;4:e238. https://doi.org/10.1371/journal.pmed.0040238
7. Gomare MD, Bhide S, Deshmukh R, Kaipilyawar S, Puri V, Moonan PK, et al. Retaining patients with drug-resistant tuberculosis on treatment during the COVID-19 pandemic—Dharavi, Mumbai, India, 2020–2022. MMWR Morb Mortal Wkly Rep. 2023;72:304–8. https://doi.org/10.15585/mmwr.mm7212a2
8. National Tuberculosis Elimination Programme (India). Guidelines for programmatic management of drug-resistant tuberculosis in India. New Delhi: Ministry of Health and Family Welfare, Government of India; 2024.
9. Fausti SA, Henry JA, Schaffer HI, Olson DJ, Frey RH, McDonald WJ. High-frequency audiometric monitoring for early detection of aminoglycoside ototoxicity. J Infect Dis. 1992;165:1026–32. https://doi.org/10.1093/infdis/165.6.1026
10. Ahmad N, Ahuja SD, Akkerman OW, Alffenaar JC, Anderson LF, Baghaei P, et al.; Collaborative Group for the Meta-Analysis of Individual Patient Data in MDR-TB treatment–2017. Treatment correlates of successful outcomes in pulmonary multidrug-resistant tuberculosis: an individual

patient data meta-analysis. Lancet. 2018;392:821–34. https://doi.org/10.1016/S0140-6736(18)31644-1
11. Günther G, Mhuulu L, Diergaardt A, Dreyer V, Moses M, Anyolo K, et al. Bedaquiline resistance after effective treatment of multidrug-resistant tuberculosis, Namibia. Emerg Infect Dis. 2024;30:568–71. https://doi.org/10.3201/eid3003.240134
12. Hasan T, Medcalf E, Nyang'wa BT, Egizi E, Berry C, Dodd M, et al. The safety and tolerability of linezolid in novel short-course regimens containing bedaquiline, pretomanid, and linezolid to treat rifampicin-resistant tuberculosis: an individual patient data meta-analysis. Clin Infect Dis. 2024;78:730–41. https://doi.org/10.1093/cid/ciad653
13. Snobre J, Gasana J, Decroo T, Mucyo Y, Jacobs BKM, Rigouts L, et al. High-dose amikacin in the first week of all-oral rifampicin-resistant TB treatment is safe: a single-arm trial. IJTLD Open. 2025;2:655–61. https://doi.org/10.5588/ijtldopen.25.0120
14. Surie D, Sathyanarayanan MK, Lavanya J, Smith JP, Shanmugam SK, Tamilzhalagan S, et al. Long-term follow-up of persons diagnosed with multidrug-resistant TB in Chennai, India, 2013–2020. Int J Tuberc Lung Dis. 2024;28:54–6. https://doi.org/10.5588/ijtld.23.0272

Address for correspondence: Christine Ho, Centers for Disease Control and Prevention, 1600 Clifton Rd NE, Mailstop E4, Atlanta, GA 30329-4018, USA; email: gtb9@cdc.gov

Rapid Interventions to Limit Outbreak of Invasive *Streptococcus pneumoniae* in Correctional Facility, North Carolina, USA, 2024

Camden D. Gowler, Emma Doran, Niketa D. Williams, Justin P. Albertson, Ty Lautenschlager, Sopio Chochua, Ryan Gierke, Arthur Campbell, Miwako Kobayashi, Aaron Fleischauer, Erica Wilson

A *Streptococcus pneumoniae* serotype 4 outbreak in a North Carolina correctional facility resulted in 14 cases (8 suspected, 1 probable, and 5 confirmed). After implementation of movement restrictions and vaccination with 23-valent pneumococcal polysaccharide vaccine, new cases ceased. Serotype 4 presence in this setting raises challenges for an effective vaccination strategy.

Streptococcus pneumoniae (pneumococcus) is a leading bacterial cause of community-acquired pneumonia in the United States (*1*). Although infrequent, pneumococcus can also cause invasive pneumococcal disease (IPD), an infection in a normally sterile site (i.e., blood, cerebrospinal fluid, or bone or joint space) (*2*). Young children, persons with certain underlying conditions or risk factors (e.g., chronic heart, liver, or lung disease; HIV infection; cigarette smoking), and older adults are at increased risk for IPD (*1*).

IPD outbreaks can occur in congregate settings, such as nursing homes or correctional facilities (i.e., jails and prisons), and result in substantial illness and death (*3*,*4*). Close living quarters increase risk for pneumococcal transmission. Effective vaccines against IPD are available (*5*); however, pneumococcal vaccines confer protection only to the specific *S. pneumoniae* serotypes contained in vaccines (*5*). That limitation poses a challenge to timely use of vaccines for containing outbreaks because delays in determining pneumococcal serotypes often occur. Emergence of serotype 4 IPD cases among certain adult populations might further complicate vaccine product selection (*6*,*7*). Newer pneumococcal conjugate vaccines (PCVs) cover more serotypes, but the 21-valent PCV (PCV21) that was most recently recommended for adults in 2024 (*5*) does not contain serotype 4, whereas other recommended pneumococcal vaccines do. As of 2023, serotype 4 was uncommon in the southeastern United States, according to available data from the Centers for Disease Control and Prevention (CDC) Active Bacterial Core surveillance (*8*).

On June 26, 2024, the North Carolina Division of Public Health was informed of multiple pneumonia and pneumococcal disease cases at a minimum custody correctional facility in North Carolina, USA. We conducted an investigation to characterize cases identified within the facility during June 14–July 30, 2024, and to determine intervention strategies.

The Investigation

We classified cases into 3 categories: suspected, probable, and confirmed (Appendix, https://wwwnc.cdc.gov/EID/article/32/3/25-0789-App1.pdf). Suspected cases were defined as new-onset respiratory symptoms necessitating antibiotic treatment but without laboratory-confirmed pneumococcal infection. Probable cases were defined as radiograph-confirmed pneumonia or clinical or laboratory signs of sterile site infection (e.g., sepsis) without pneumococcal detection. Confirmed cases were defined as culture-confirmed *S. pneumoniae* from a normally sterile site. Pneumococcal isolates were sent to CDC for serotyping and to assess genetic relatedness by single-nucleotide polymorphism analysis. This

Author affiliations: Centers for Disease Control and Prevention, Atlanta, Georgia, USA (C.D. Gowler, S. Chochua, R. Gierke, M. Kobayashi, A. Fleischauer); North Carolina Department of Health and Human Services, Raleigh, North Carolina, USA (C.D. Gowler, E. Doran, N.D. Williams, J.P. Albertson, T. Lautenschlager, A. Fleischauer, E. Wilson); North Carolina Department of Adult Correction, Raleigh (A. Campbell)

DOI: https://doi.org/10.3201/eid3203.250789

activity was reviewed by CDC, deemed not research, and was conducted consistent with applicable federal law and CDC policy (see, e.g., 45 C.F.R. part 46.102(l)(2), 21 C.F.R. part 56; 42 U.S.C. §241(d); 5 U.S.C. §552a; 44 U.S.C. §3501 et seq.).

We identified 14 cases (8 suspected, 1 probable, and 5 confirmed) among 267 incarcerated persons (Table; Figure). Persons with suspected cases had mild respiratory symptoms (i.e., cough); those with probable and confirmed cases had more severe signs and symptoms (Table). All persons with confirmed and probable cases were hospitalized, and all survived (Table). Median age at illness onset was 51 (range 29–68) years. Most (79%, n = 11) cases, including all confirmed and probable cases, occurred among Black men. Among confirmed and probable cases, 4 (67%) of 6 occurred among current or former smokers. Most (79%, n = 11) cases occurred among persons with occupations while incarcerated, either within the facility (e.g., kitchen or custodial staff) or as part of work-release (e.g., nearby poultry plant). We abstracted pneumococcal vaccination statuses for patients from medical records and compared those records with the North Carolina Immunization Registry. No patient had a documented pneumococcal vaccination history.

All incarcerated persons and facility staff were offered prophylactic vaccination with 23-valent pneumococcal polysaccharide vaccine (PPSV23); PPSV23 was most readily available for purchase in sufficient quantities. On July 1, 2024, five days after the outbreak was reported, multiple staff and 157 (59%) incarcerated persons received PPSV23. Postexposure antibiotic prophylaxis was not offered, but symptomatic persons received empiric antibiotic treatment with azithromycin. Work-release and movement within the correctional facility were restricted from June 26 through July 8, 2024. No additional cases were reported after June 26, 2024.

Pneumococcal isolates from laboratory-confirmed cases were all serotype 4, multilocus sequence type (ST) 695. The average core-genome single-nucleotide polymorphism difference was 10, indicating isolates were closely related. All 5 isolates were pansusceptible to relevant antibiotics (penicillin, amoxicillin, cefotaxime, ceftriaxone, cefuroxime, meropenem, vancomycin, erythromycin, tetracycline, doxycycline, levofloxacin, trimethoprim/sulfamethoxazole, chloramphenicol, rifampin, clindamycin, quinupristin/dalfopristin, and linezolid) on the basis of whole-genome sequencing predictions (*9*).

This IPD serotype 4 outbreak occurred in a correctional facility located in a geographic area where serotype 4 is considered to be uncommon. IPD outbreaks in congregate settings, such as correctional facilities, remain a public health concern. Rapid detection of the outbreak and timely interventions were aided

Table. Demographics and risk factors of pneumococcal infections by case classification among patients in correctional facility, North Carolina, USA, June 14–July 30, 2024*

Category	Confirmed	Probable	Suspected
Total no. cases	5	1	8
Median patient age, y (range)	42 (39–62)	29 (NA)	54.5 (30–68)
Race			
Black or African American	5 (100)	1 (100)	5 (62.5)
White	0	0	3 (37.5)
Work status			
None	1 (20)	0	2 (25)
Poultry plant	2 (40)	0	1 (12.5)
Other work†	2 (40)	1 (100)	5 (62.5)
Current	2 (40)	0	NA
Smoking status‡			
Former	2 (40)	0	NA
Never	1 (20)	1 (100)	NA
Select signs and symptoms			
Fever	2 (40)	1 (100)	0
Cough	4 (80)	1 (100)	8 (100)
Radiograph-confirmed pneumonia	5 (100)	1 (100)	0
Clinical signs of sepsis	4 (80)	1 (100)	0
Lumbar puncture–confirmed meningitis	1 (20)	0	0
Testing and treatment			
Treated with antibiotics§	5 (100)	1 (100)	8 (100)
Positive culture from normally sterile site	5 (100)	0	0
Hospitalized	5 (100)	1 (100)	0

*Values are no. (%) except as indicated. NA, not applicable.
†Other work includes custodial staff, kitchen, and municipal worker (any job except at the poultry plant), some of which occurred outside the correctional facility.
‡Smoking status was determined by medical record review. Records were only available to sufficiently review confirmed and probable cases.
§Empiric treatment with antibiotics only. Postexposure antibiotic prophylaxis was not administered, but providers might have had a higher suspicion of pneumococcal disease after the outbreak began.

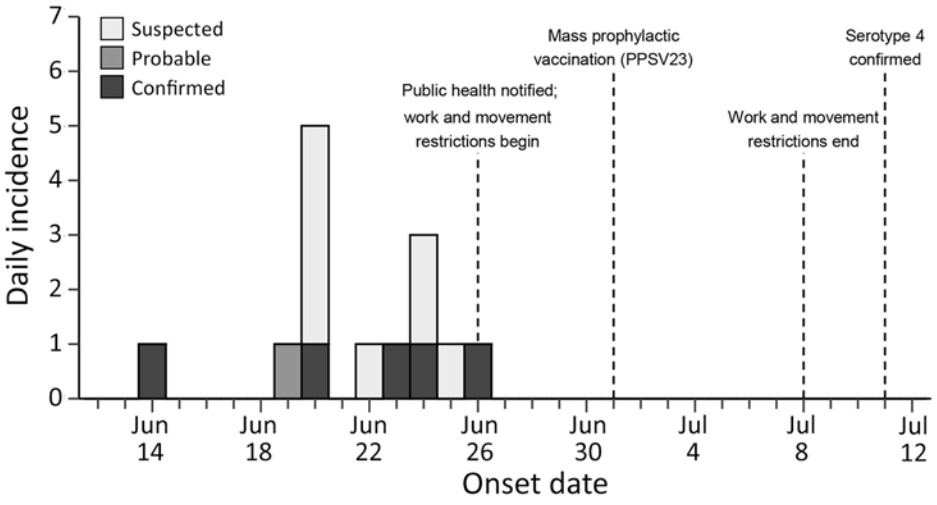

Figure. Incidence of pneumococcal disease by day and case classification among patients in correctional facility, North Carolina, USA, June 14–July 30, 2024. Vertical dashed lines and labels denote key events during the public health investigation and response. PPSV23, 23-valent pneumococcal polysaccharide vaccine.

by collection of bacterial cultures. In this outbreak, before serotyping results were available, public health officials chose PPSV23 on the basis of availability; fortunately, that vaccine covered the outbreak strain (serotype 4).

Historically, serotype 4 IPD cases declined across all ages after routine pneumococcal conjugate vaccine (PCV) use in children began in 2000 (*10*). Since 2013, serotype 4 IPD cases in the western United States have increased among adults; clusters of IPD cases were observed among persons experiencing homelessness and among adults with underlying conditions or risk factors, including injection drug use (*8*,*9*). The increase in serotype 4 invasive IPD in the western United States has been associated with lineages ST10172, ST244, and ST695, with ST10172 identified as most prevalent (*7*). Recent CDC Active Bacterial Core surveillance data indicate a notable decline in the serotype 4/ST695 prevalence since 2015 (CDC, unpub. data), largely supplanted by ST10172.

This outbreak response underscores continued risk for IPD outbreaks within correctional facilities, where close quarters and underlying risk factors for IPD (e.g., history of cigarette smoking or chronic medical conditions) can be common (*3*,*10*,*11*). Although public health studies of correctional facilities are limited (*12*), the most recently described US correctional facility IPD outbreak occurred in an Alabama state prison in 2018 but was caused by serotype 12F (*3*).

Conclusions

Assessing large, mobile populations, such as the population of the United States, for asymptomatic carriage of *S. pneumoniae* serotypes is difficult because of the large number of persons required to test; a study in Europe reported prevalence among adult men is ≈3.7% (*13*). Our report indicates serotype 4 IPD clusters are not geographically restricted to the western United States. Given the potential increased risk in correctional facilities, coupled with the absence of documented pneumococcal vaccination among persons in this outbreak, officials might consider serotyping IPD to guide choice of vaccine in similar outbreaks.

In addition to work-release and movement restrictions, a primary public health intervention in this response was prophylactic vaccination with PPSV23. Antibiotic prophylaxis was not administered because determining close contacts for prophylaxis would have been logistically challenging and could have included >200 incarcerated persons. Prophylactic vaccination with PPSV23 appeared successful; rollout was fast and covered the outbreak strain (serotype 4), and no cases were documented after vaccination in the correctional facility. Although conjugate vaccines (PCV15, PCV20, PCV21) are more immunogenic than polysaccharide vaccines (PPSV23), timely administration of PPSV23 might have prevented additional serotype 4 IPD cases.

Without serotype results, public health officials might have opted to use PCV21, had it been available. Compared with other vaccines, PCV21 is thought to cover more circulating serotypes in the eastern United States, and surveillance data did not indicate a high probability of serotype 4 causing an outbreak in North Carolina (*14*). Serotyping may be obtained through state public health laboratories or CDC, subject to availability. Rapid serotyping of pneumococcal cases can inform vaccine selection in managing IPD within specific environments, including correctional facilities.

About the Author

Dr. Gowler is a communicable disease epidemiologist at the Chicago Department of Public Health and previously worked as an Epidemic Intelligence Service Officer with the Centers for Disease Control and Prevention, assigned to the North Carolina Department of Health and Human Services. His research interests include infectious diseases, disease surveillance, and mathematical modeling.

References

1. Gierke R, Wodi AP, Kobayashi M. Pneumococcal disease. In: Centers for Disease Control and Prevention. Epidemiology and prevention of vaccine-preventable diseases, 14th edition. 2021 [cited 2025 May 1]. https://www.cdc.gov/pinkbook/hcp/table-of-contents/chapter-17-pneumococcal-disease.html
2. Weiser JN, Ferreira DM, Paton JC. *Streptococcus pneumoniae*: transmission, colonization and invasion. Nat Rev Microbiol. 2018;16:355–67. https://doi.org/10.1038/s41579-018-0001-8
3. Sanchez GV, Bourne CL, Davidson SL, Ellis M, Feldstein LR, Fay K, et al. Pneumococcal disease outbreak at a state prison, Alabama, USA, September 1–October 10, 2018. Emerg Infect Dis. 2021;27:1949–52. https://doi.org/10.3201/eid2707.203678
4. Hoge CW, Reichler MR, Dominguez EA, Bremer JC, Mastro TD, Hendricks KA, et al. An epidemic of pneumococcal disease in an overcrowded, inadequately ventilated jail. N Engl J Med. 1994;331:643–8. https://doi.org/10.1056/NEJM199409083311004
5. Kobayashi M, Leidner AJ, Gierke R, Farrar JL, Morgan RL, Campos-Outcalt D, et al. Use of 21-valent pneumococcal conjugate vaccine among U.S. adults: recommendations of the Advisory Committee on Immunization Practices—United States, 2024. MMWR Morb Mortal Wkly Rep. 2024;73:793–8. https://doi.org/10.15585/mmwr.mm7336a3
6. Kobayashi M, Leidner AJ, Gierke R, Xing W, Accorsi E, Moro P, et al. Expanded recommendations for use of pneumococcal conjugate vaccines among adults aged ≥50 years: recommendations of the Advisory Committee on Immunization Practices—United States, 2024. MMWR Morb Mortal Wkly Rep. 2025;74:1–8. https://doi.org/10.15585/mmwr.mm7401a1
7. Beall B, Walker H, Tran T, Li Z, Varghese J, McGee L, et al. Upsurge of conjugate vaccine serotype 4 invasive pneumococcal disease clusters among adults experiencing homelessness in California, Colorado, and New Mexico. J Infect Dis. 2021;223:1241–9. https://doi.org/10.1093/infdis/jiaa501
8. Centers for Disease Control and Prevention. Active Bacterial Core surveillance (ABCs): surveillance reports. 2024 [cited 2025 May 1]. https://www.cdc.gov/abcs/reports/index.html
9. Metcalf BJ, Chochua S, Gertz RE Jr, Li Z, Walker H, Tran T, et al.; Active Bacterial Core Surveillance Team. Using whole genome sequencing to identify resistance determinants and predict antimicrobial resistance phenotypes for year 2015 invasive pneumococcal disease isolates recovered in the United States. Clin Microbiol Infect. 2016;22:1002.e1–8. https://doi.org/10.1016/j.cmi.2016.08.001
10. Pilishvili T, Lexau C, Farley MM, Hadler J, Harrison LH, Bennett NM, et al.; Active Bacterial Core Surveillance/Emerging Infections Program Network. Sustained reductions in invasive pneumococcal disease in the era of conjugate vaccine. J Infect Dis. 2010;201:32–41. https://doi.org/10.1086/648593
11. Trotter RT II, Lininger MR, Camplain R, Fofanov VY, Camplain C, Baldwin JA. A survey of health disparities, social determinants of health, and converging morbidities in a county jail: a cultural-ecological assessment of health conditions in jail populations. Int J Environ Res Public Health. 2018;15:2500. https://doi.org/10.3390/ijerph15112500
12. Kinner SA, Young JT. Understanding and improving the health of people who experience incarceration: an overview and synthesis. Epidemiol Rev. 2018;40:4–11. https://doi.org/10.1093/epirev/mxx018
13. Yahiaoui RY, den Heijer CD, van Bijnen EM, Paget WJ, Pringle M, Goossens H, et al.; APRES Study Team. Prevalence and antibiotic resistance of commensal *Streptococcus pneumoniae* in nine European countries. Future Microbiol. 2016;11:737–44. https://doi.org/10.2217/fmb-2015-0011
14. Centers for Disease Control and Prevention. Summary of risk-based pneumococcal vaccination recommendations. 2025 [cited 2025 May 1]. https://www.cdc.gov/pneumococcal/hcp/vaccine-recommendations/risk-indications.html

Address for correspondence: Camden D. Gowler, North Carolina Department of Health and Human Services, 225 N McDowell St, Raleigh, NC 27603, USA; email: camden.gowler@dhhs.nc.gov

Extraintestinal *Entamoeba moshkovskii* Infection, Eastern India

Sanjib Kumar Sardar, Ajanta Ghosal,[1] Tapas Haldar,[1] Basudev Ganguly, Koushik Das, Sandipan Ganguly

Entamoeba moshkovskii is historically considered nonpathogenic. We report a case of severe extraintestinal infection in a patient from eastern India who had abdominal pain, fever, weight loss, anemia, and a splenic abscess. Molecular analysis confirmed *E. moshkovskii* as the causative agent. This case highlights this parasite's potential to cause severe illness.

For more than a century, the *Entamoeba histolytica* protozoan was considered the sole pathogenic amoeba to cause diarrhea, dysentery, and liver abscess. Microscopy was once the diagnostic standard, but because of the morphologic similarity among *Entamoeba* species, PCR is now recommended (*1*,*2*). Major morphologically identical species indistinguishable from *E. histolytica* include *E. dispar*, *E. moshkovskii*, and *E. bangladeshi* (*3*,*4*). This group of organisms (with *E. nuttalli*) is called the *E. histolytica* complex. Within this group, *E. moshkovskii* was historically regarded as nonpathogenic; however, emerging evidence suggests potential pathogenicity (*5*–*9*). Reported prevalence of *E. moshkovskii* varies widely (≈1%–25%) across epidemiologic settings (*5*–*10*).

In Bangladesh, one study reported a 21.1% infection rate in children, whereas another reported a 2.95% prevalence with an association to diarrhea in infants (*8*,*11*). Similarly, a 3-year surveillance study in eastern India identified a 3.12% prevalence among diarrheal patients, supporting its classification as an emerging pathogen rather than a nonpathogenic species (*5*,*6*). In a murine model of intestinal amebiasis, *E. moshkovskii* was also found to cause diarrhea, weight loss, and colitis (*8*).

Author affiliations: The University of Tokyo, Bunkyo, Japan (S.K. Sardar); ICMR–National Institute for Research in Bacterial Infections, Kolkata, India (S.K. Sardar, A. Ghosal, T. Haldar, B. Ganguly, S. Ganguly); Assam Downtown University, Guwahati, India (K. Das).

DOI: https://doi.org/10.3201/eid3203.251065

Emerging epidemiologic evidence suggests *E. moshkovskii* is a potential enteropathogen. We present a clinically documented case of an extraintestinal infection caused by *E. moshkovskii* that resulted in severe health complications in a patient from eastern India.

The Study

A 36-year-old man from Kolkata, in West Bengal, India, sought care in July 2024 for a 6-day history of intermittent fever, characterized by 1–2 spikes per day and a recorded high temperature of 102°F. The patient reported fever with malaise but no chills or rigors, along with a 5-day history of dull, continuous left upper quadrant abdominal pain that worsened with deep inspiration, sneezing, or when lying in the left lateral decubitus position. A slow-developing heavy feeling in the left upper abdomen, along with nausea, a bad taste in the mouth, and 1 episode of nonbilious vomiting, also occurred. The patient reported weight loss from 53 kg to 47 kg over 4 weeks, despite preserved appetite. In addition, he had a history of occasional nonproductive cough without wheezing, hemoptysis, or shortness of breath. The patient had a left-lobe hepatic abscess diagnosed in March 2023 in Kolkata and was treated empirically with intravenous injection and oral metronidazole. The causative agent was not identified. The bad taste in the patient's mouth was likely not related to the previous metronidazole treatment, because he had not been on the medication in the previous 3 weeks.

The patient was a cigarette smoker but had abstained from alcohol for 4 years. On examination, his heart rate was 104 beats/min and blood pressure 146/74 mmHg; oxygen saturation (98% room air) and respiratory rate (16 breaths/min) were unremarkable. Physical examination revealed pallor,

[1]These authors contributed equally to this article.

hepatomegaly (2 cm below right costal margin), splenomegaly (6 cm below left costal margin), and left upper quadrant tenderness. The patient had absent breath sounds over the left intercostal and subaxillary areas but showed no signs of cyanosis, clubbing, or lymphadenopathy. Neurologic examination results were unremarkable. Iron deficiency anemia was noted. Serologic testing revealed negative results for HIV, hepatitis B surface antigen, hepatitis C virus antibody, malarial parasite detection antigen, and *Brucella* IgM and IgG. The patient also had a nonreactive Rose Bengal plate test and standard tube agglutination test for *Brucella*. A chest radiograph revealed an elevated left hemidiaphragm and left pleural effusion. An abdominal ultrasound revealed hepatomegaly and a large splenic abscess (18 cm x 14 cm × 17 cm, 2000 mL) with mild subdiaphragmatic fluid. Contrast-enhanced computed tomography of the chest and abdomen confirmed a collapsed left lower lobe and a splenic abscess. The patient was managed with drainage and supportive care.

Pleural fluid analysis with Gram and Ziehl-Neelsen stains showed no microorganisms, and *Mycobacterium tuberculosis* was not detected. The wet mount showed predominantly macrophages, erythrocytes, epithelial cells, and many protozoal structures resembling *E. histolytica* with erythrophagia (Figure 1). However, splenic abscess aspirate did not reveal amoebae or amoeba-like structures. The direct smear revealed degenerated blood elements and necrosis, with no granuloma or malignant cells. We conducted additional characterization of the *E. histolytica*–like organism by using molecular methods.

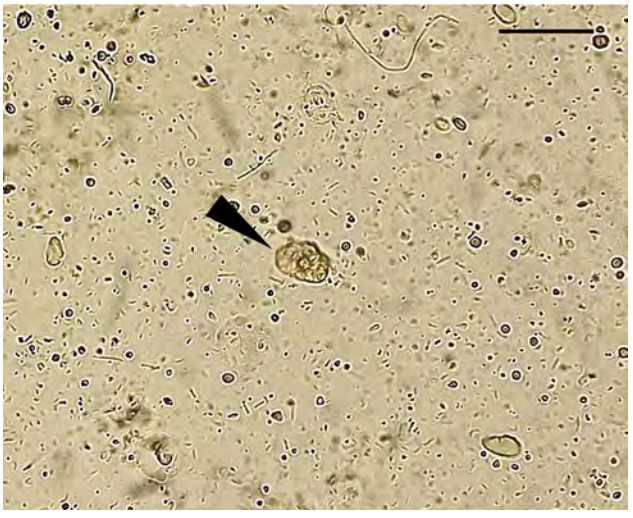

Figure 1. Microscopic view of *Entamoeba moshkovskii* trophozoites (arrowhead) observed in a pleural fluid sample recovered from a patient with an extraintestinal infection, eastern India. Slide used a wet-mount preparation. Scale bar indicates 30 μm.

We extracted DNA by using the QIAamp DNA Mini Kit (QIAGEN, https://www.qiagen.com). We

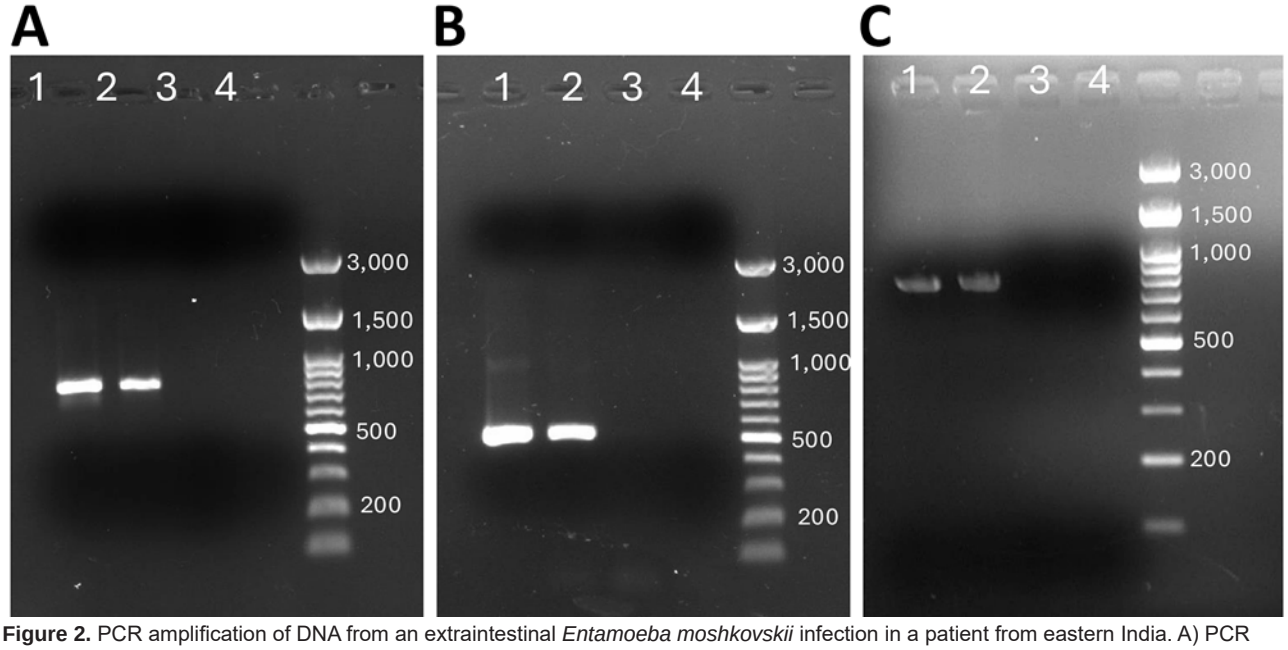

Figure 2. PCR amplification of DNA from an extraintestinal *Entamoeba moshkovskii* infection in a patient from eastern India. A) PCR amplification of the 18S rRNA locus of *E. moshkovskii* using DNA extracted from a splenic aspirate. The expected product size is 779 bp. B) PCR amplification of the chitinase locus of *E. moshkovskii* using DNA extracted from spleen aspirate samples. The expected product size is 480 bp. C) Amplification of the 18S rRNA locus of *E. moshkovskii* by PCR using DNA extracted from a stool sample. The expected product size is 779 bp. Lane 1, PCR product from patient sample; lane 2, positive control (*E. moshkovskii* genomic DNA); lane 3, *E. histolytica* genomic DNA; lane 4, negative control.

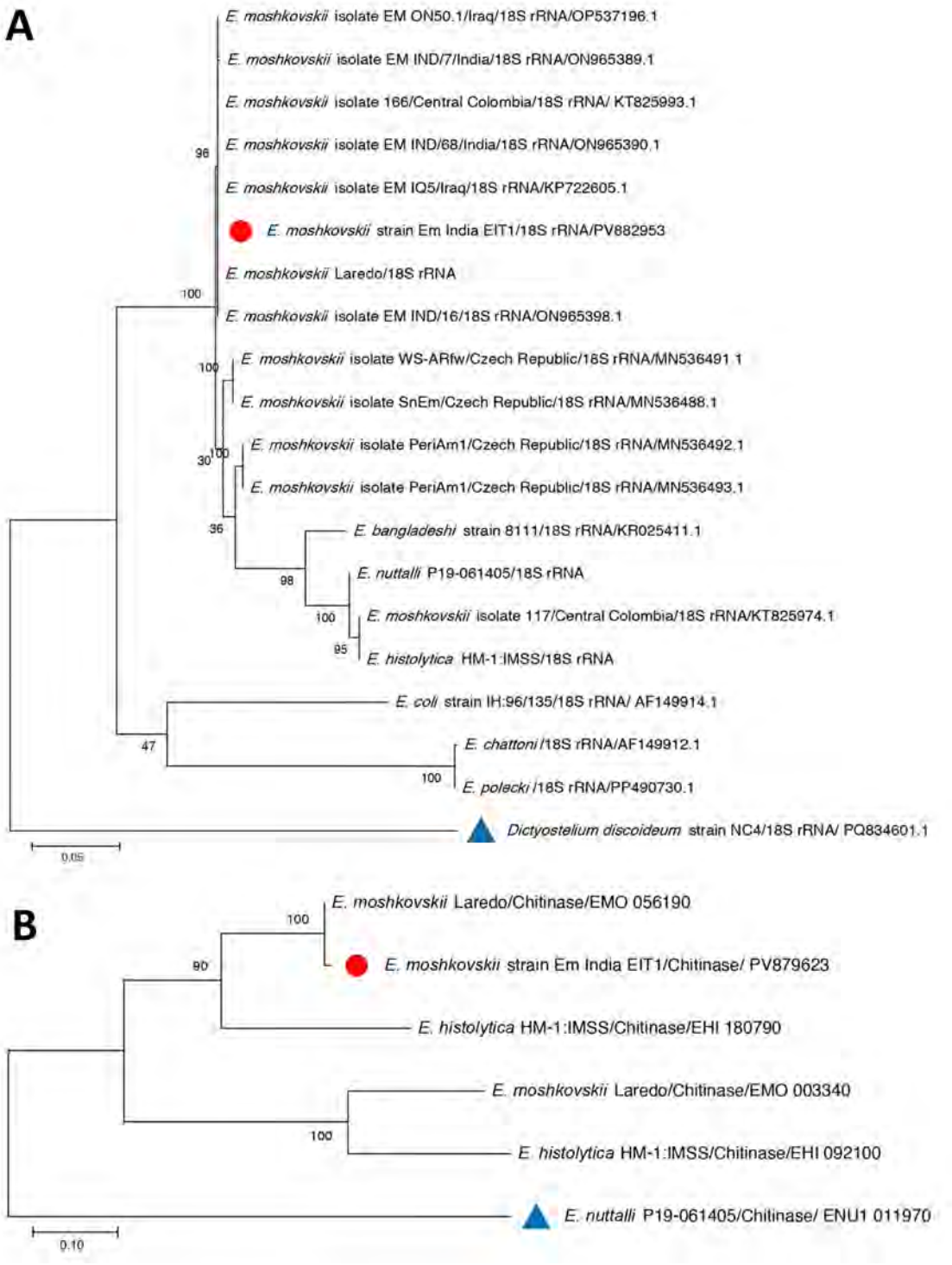

Figure 3. Phylogenetic trees constructed from the 18S rRNA and chitinase gene sequences obtained from *Entamoeba moshkovskii* isolates from a patient in eastern India (red circles) and reference sequences. A) Phylogenetic tree of 18S rRNA. The tree with the highest log-likelihood value (–2,562.32) is shown. Initial heuristic trees were generated automatically using the maximum parsimony approach. The model incorporated a proportion of invariant sites (45.63%). The analysis included 9 nucleotide sequences with 859 aligned positions in the final dataset. B) Phylogenetic tree of chitinase gene sequence. The tree with the highest log-likelihood value (−3,301.96) is presented. Initial heuristic searches were performed automatically using the maximum parsimony method. The final analysis included 20 nucleotide sequences, with a total of 939 positions in the final dataset. GenBank accession numbers are provided. Outgroup taxa are indicated with blue triangles. The phylogeny was inferred using the maximum likelihood method. Scale bars indicate substitutions per site.

performed conventional PCR targeting the 18S rRNA gene on splenic aspirate and pleural fluid by using previously published species-specific primers for *E. histolytica* and *E. moshkovskii* (*5*,*12*). Both the splenic abscess aspirate and pleural fluid DNA tested negative for *E. histolytica* but positive for *E. moshkovskii* (Figure 2, panel A). To confirm the presence of *E. moshkovskii*, we targeted the chitinase gene for testing. We designed primer sequences to amplify the upstream and downstream regions of the chitinase open reading frame (Appendix Table, http://wwwnc.cdc.gov/EID/article/32/3/25-1065-App1.pdf). Both splenic abscess aspirate and pleural fluid samples again tested positive for *E. moshkovskii* when targeting the chitinase locus (Figure 2 panel B). We then purified the PCR products by using the Roche PCR Gel Extraction kit (Roche, https://www.roche.com) and sequenced bidirectionally with the BigDye Terminator v3.1 kit (Thermo Fisher Scientific, https://www.thermofisher.com).

BLAST analysis (https://blast.ncbi.nlm.nih.gov) confirmed the organism as *E. moshkovskii*, showing 100% identity to the reference Laredo strain (18S rRNA; GenBank accession no. AF149906.1). However, the chitinase gene corresponding to AmoebaDB (https://amoebadb.org/amoeba/app) entry EMO_056190 exhibited 3 mutations at positions 36 T/C, 127 G/A, and *2 T/G. The mutation at position 36 was synonymous, whereas the substitution at position 127 resulted in a nonsynonymous change, replacing glutamic acid with lysine. We constructed phylogenetic trees generated from the obtained 18S rRNA and chitinase gene sequences to confirm species identity and evaluate evolutionary relationships (Figure 3, panels A, B).

Of note, PCR analysis of DNA isolated from the patient's stool samples by using the 18S rRNA targeted assay detected the presence of *E. moshkovskii* and not *E. histolytica* (Figure 2, panel C). In addition, results of ELISA testing for *E. histolytica*–specific IgG in serum were negative. Taken together, those findings indicate that neither the hepatic abscess nor the splenic abscess was associated with *E. histolytica* infection.

The patient was initially started on intravenous (IV) meropenem empirically. However, after confirmation of *E. moshkovskii* infection, we changed the treatment to IV metronidazole (750 mg IV/8 h for 1 d), followed by oral metronidazole (400 mg 3×/d after food for 7 d). The patient was also prescribed ferrous sulfate 200 mg (1 dose by mouth), B-complex tablets, and other medications as needed. Pigtail drainage continued for the first week. The patient recovered after 3 weeks.

Conclusions

E. moshkovskii DNA alongside *E. histolytica* in 5 of 115 liver abscess cases was previously reported; however, extraintestinal *E. moshkovskii* infection, particularly in pleural fluid, is extremely rare (*13*). In the case we report, *E. moshkovskii* might have reached the pleural cavity through direct extension or rupture of a splenic abscess.

Metronidazole is the primary drug for treating amoebiasis and was effective in this patient, showing empirical activity against *E. moshkovskii* (*14*). However, the optimal dosage for this species remains undefined. Drug sensitivity differs among *Entamoeba* spp.; for instance, *E. moshkovskii* is resistant to emetine, which is effective against *E. histolytica* (*15*). Diagnosis is also challenging. Molecular tests often target only *E. histolytica*, leaving *E. moshkovskii* infections unrecognized. In addition, *E. moshkovskii* produces fewer cysts than *E. histolytica*, reducing the reliability of microscopic detection and increasing the risk for false negatives (*5*).

Because of the high regional prevalence of *E. moshkovskii*, extraintestinal infections caused by this species need attention. Our case underscores the need to better understand transmission and to develop improved diagnostic methods to ensure effective management and prevent drug resistance in *E. moshkovskii*.

Acknowledgements

We thank the hospital staff for their support in sample collection and obtaining the patient's history.

This study was reviewed and approved by the Institutional Human Ethics Committee of the Indian Council of Medical Research—National Institute for Research in Bacterial Infections. Informed consent was obtained from the participant.

Representative sequences obtained in this study were deposited in GenBank under the accession numbers PV882953 for the 18S rRNA and PV879623 for the chitinase locus.

This study was funded by the Indian Council of Medical Research.

Author contributions: study conceptualization, S.K.S. and S.G.; study methodology, S.K.S, A.G., T.H., and B.G.; data curation, S.K.S., A.G., and T.H.; study validation, K.D. and S.G.; writing original draft, S.K.S.; formal statistical analysis, S.K.S.; visualization, S.G.; investigation, S.G.; funding acquisition, S.G.; manuscript review and editing, S.G.; study supervision, S.G.

About the Author

Dr. Sardar conducted his doctoral research at the Indian Council of Medical Research—National Institute for Research in Bacterial Infections and is currently a postdoctoral fellow at The University of Tokyo. His research focuses on the biology and pathogenicity of *Entamoeba* species.

References

1. Tanyuksel M, Petri WA Jr. Laboratory diagnosis of amebiasis. Clin Microbiol Rev. 2003;16:713–29. https://doi.org/10.1128/CMR.16.4.713-729.2003
2. Centers for Disease Control and Prevention. Post-travel diarrhea. In: CDC yellow book: health information for international travel. 2026 [cited 2026 Feb 28]. https://www.cdc.gov/yellow-book/hcp/post-travel-evaluation/post-travel-diarrhea.html
3. Ngui R, Angal L, Fakhrurrazi SA, Lian YL, Ling LY, Ibrahim J, et al. Differentiating *Entamoeba histolytica*, *Entamoeba dispar* and *Entamoeba moshkovskii* using nested polymerase chain reaction (PCR) in rural communities in Malaysia. Parasit Vectors. 2012;5:187. https://doi.org/10.1186/1756-3305-5-187
4. Royer TL, Gilchrist C, Kabir M, Arju T, Ralston KS, Haque R, et al. *Entamoeba bangladeshi* nov. sp., Bangladesh. Emerg Infect Dis. 2012;18:1543–5. https://doi.org/10.3201/eid1809.120122
5. Sardar SK, Ghosal A, Haldar T, Maruf M, Das K, Saito-Nakano Y, et al. Prevalence and molecular characterization of *Entamoeba moshkovskii* in diarrheal patients from Eastern India. PLoS Negl Trop Dis. 2023;17:e0011287. https://doi.org/10.1371/journal.pntd.0011287
6. Sardar SK, Ghosal A, Haldar T, Prasad A, Mal S, Saito-Nakano Y, et al. Genetic characterization of the *Entamoeba moshkovskii* population based on different potential genetic markers. Parasitology. 2024;151:429–39. https://doi.org/10.1017/S003118202400026X
7. Sharma D, Rattan D, Kaur U, Dutta U, Sehgal R. First report on PCR-based detection of *Entamoeba moshkovskii* from a tertiary care center in north India. J Pure Appl Microbiol. 2025;19:100–5. https://doi.org/10.22207/JPAM.19.1.34
8. Shimokawa C, Kabir M, Taniuchi M, Mondal D, Kobayashi S, Ali IK, et al. *Entamoeba moshkovskii* is associated with diarrhea in infants and causes diarrhea and colitis in mice. J Infect Dis. 2012;206:744–51. https://doi.org/10.1093/infdis/jis414
9. Kyany'a C, Eyase F, Odundo E, Kipkirui E, Kipkemoi N, Kirera R, et al. First report of *Entamoeba moshkovskii* in human stool samples from symptomatic and asymptomatic participants in Kenya. Trop Dis Travel Med Vaccines. 2019;5:23. https://doi.org/10.1186/s40794-019-0098-4
10. López MC, León CM, Fonseca J, Reyes P, Moncada L, Olivera MJ, et al. Molecular epidemiology of *Entamoeba*: first description of *Entamoeba moshkovskii* in a rural area from central Colombia. PLoS One. 2015;10:e0140302. https://doi.org/10.1371/journal.pone.0140302
11. Ali IK, Hossain MB, Roy S, Ayeh-Kumi PF, Petri WA Jr, Haque R, et al. *Entamoeba moshkovskii* infections in children, Bangladesh. Emerg Infect Dis. 2003;9:580–4. https://doi.org/10.3201/eid0905.020548
12. Mukherjee AK, Chowdhury P, Bhattacharya MK, Ghosh M, Rajendran K, Ganguly S. Hospital-based surveillance of enteric parasites in Kolkata. BMC Res Notes. 2009;2:110. https://doi.org/10.1186/1756-0500-2-110
13. Kumar M, Nath G, Parija SC. Detection of *Entamoeba dispar* and *Entamoeba moshkovskii* DNA in liver abscess pus: newer perspectives to be considered in diagnosis of amoebiasis. Int J Infect Dis. 2016;45:1364. https://doi.org/10.1016/j.ijid.2016.02.784
14. Shrivastav MT, Malik Z, Somlata. Revisiting drug development against the neglected tropical disease, amebiasis. Front Cell Infect Microbiol. 2021;10:628257. https://doi.org/10.3389/fcimb.2020.628257
15. Dreyer DA. Growth of a strain of *Entamoeba histolytica* at room temperature. Tex Rep Biol Med. 1961;19:393–6.

Address for correspondence: Sandipan Ganguly, ICMR–National Institute for Research in Bacterial Infections, P-33, C.I.T. Road, Scheme-XM, Beliaghata, Kolkata 700010, India; email: sandipanganguly@hotmail.com

Natural Hendra Virus Infections in Captive Australian Black Flying Foxes, Queensland, Australia

Victoria Boyd, Anjana Karawita, Jianning Wang, Shawn Todd, Sarah Riddell, Rachel Layton, Grace Taylor, Michael L. Kelly, Teegan Allen, Sarah Caruso, Christopher C. Broder, Richard J. Ploeg, Gough G. Au, Gary Crameri, Anthony W. Purcell, Michelle L. Baker

We provide evidence for natural Hendra virus infections and associated serology in a cohort of Australian black flying foxes (*Pteropus alecto*) transferred from Queensland to the Australian Centre for Disease Preparedness in Victoria, Australia. This study supports the likelihood that flying foxes undergo cycles of infection and reinfection and possibly recrudescence.

Bats, including flying foxes, are natural reservoirs for a variety of viruses, many highly pathogenic in other species, including the henipaviruses Hendra virus (HeV) and Nipah virus (NiV). In Australia, HeV antibodies have been detected in all 4 species of Australian flying foxes; however, the Australian black flying fox (*Pteropus alecto*) is the primary reservoir for the original HeV genotype 1 variant (HeVg1) (*1*,*2*). Spillover events occurring annually from flying foxes into horses pose a potential risk for subsequent transmission to humans (*1*,*2*).

Government biosecurity authorities in Australia have recorded 90 outbreaks of HeV since 1994, when the virus was first identified, with HeV spillover events occurring predominantly during winter (June–August) (*2*). Research has also implicated nutrition and life history events, including the mating and birthing seasons, as imparting a higher risk of infection in Australian flying foxes (*3*). More recent findings have identified such environmental factors as habitat loss, droughts, and the scarcity of winter-flowering plants as implicit in driving bats to relocate to agricultural and urban areas. In those settings, bats feed on suboptimal foods that are often in close proximity to livestock, increasing the potential for spillover. In contrast, an abundance of winter flowers, which alleviate nutritional stress, appears to have a protective effect against HeV spillover (*4*).

We describe changes in HeV serology and infection status among a cohort of 20 *P. alecto* bats held in captivity in Queensland, Australia, and transported to The Australian Centre for Disease Preparedness (ACDP) in Victoria, Australia. This study was approved by the ACDP animal ethics committee (ACDP22004).

The Study

We included in this study flying foxes submitted to bat rehabilitators because of minor injuries that were otherwise healthy but nonreleasable. The cohort was selected from 39 bats housed in outdoor rehabilitation enclosures in Queensland, separate from other bats and screened by an in-house Luminex indirect antibody assay as described previously (*5*) (Appendix Table, https://wwwnc.cdc.gov/EID/article/32/3/25-1350-App1.pdf). We selected 20 bats with the lowest HeV serostatus and best overall condition for transport (12 seronegative, 8 low-positive). We charted the age and sex of the cohort (Table), which included 15 adults (6 female, 9 male), 4 subadults (2 female, 2 male), and 1 juvenile male bat. Tests revealed no viral RNA for known zoonotic viruses (HeVg1, HeV genotype 2 variant, Menangle virus, and Australian bat lyssavirus) in swab or urine specimens before transport, and HeV serostatus remained stable over 3 sampling events for up to 6 months in captivity in Queensland. Three weeks after the final Queensland

Author affiliations: Commonwealth Scientific and Industrial Research Organisation, Health and Biosecurity, Geelong, Victoria, Australia (V. Boyd, S. Todd, S. Caruso, M.L. Baker); Commonwealth Scientific and Industrial Research Organisation Australian Animal Health Laboratory, Geelong (A. Karawita, J. Wang, S. Riddell, R. Layton, G. Taylor, M.L. Kelly, T. Allen, R.J. Ploeg, G.G. Au); Uniformed Services University, Bethesda, Maryland, USA (C.C. Broder); Monash University, Clayton, Victoria, Australia (A.W. Purcell)

DOI: http://doi.org/10.3201/eid3203.251350

Table. Sex, age, and location of origin of 20 bats included in study examining Hendra virus infections in captive Australian black flying foxes, Queensland, Australia*

Flying fox ID	Sex	Age	Location of origin	Housing at ACDP
1	M	Adult	Beaudesert	BSL3Z
2	M	Subadult	Beaudesert	BSL3Z
3	F	Adult	Beaudesert	BSL4
4	M	Adult	Beaudesert	BSL4
5	M	Adult	Logan Reserve	BSL4
6	M	Adult	Beaudesert	BSL4
7	M	Adult	Beaudesert	BSL4
8	F	Subadult	Beaudesert	BSL4
9	F	Adult	Beaudesert	BSL3Z
10	M	Adult	Beaudesert	BSL3Z
11	F	Adult	Logan Reserve	BSL4
12	M	Subadult	Beaudesert	BSL4
13	F	Subadult	Beaudesert	BSL4
14	M	Adult	Beaudesert	BSL4
15	F	Adult	Logan Reserve	BSL4
16	M	Adult	Beaudesert	BSL4
R-1	M	Adult	Beaudesert	BSL3Z
R-2	M	Juvenile	Beaudesert	BSL3Z
R-3	F	Adult	Beaudesert	BSL3Z
R-4	F	Adult	Beaudesert	BSL3Z

*After arrival at ACDP, flying foxes were either housed in a group aviary at BSL3Z or in individual cages in a BSL4 room. ACDP, Australian Centre for Disease Preparedness; BSL, Biosafety Level; ID, identification.

testing (April 2023), we transported the animals to ACDP in Victoria (Figure 1).

Samples collected 1 day after arrival at ACDP revealed that 11 bats had seroconverted positive to HeV during the 3 weeks between testing in Queensland and transport, including 6 previously seronegative and 5 low-seropositive bats (Figure 2). Nine of the 11 bats that had seroconverted to HeV according to the in-house Luminex assay also had neutralizing antibodies to HeV, with virus neutralization test (VNT) titers ranging from 10 to 160 (Figure 2). Two bats tested PCR-positive for HeVg1 RNA: 1 (bat R1) on day 1

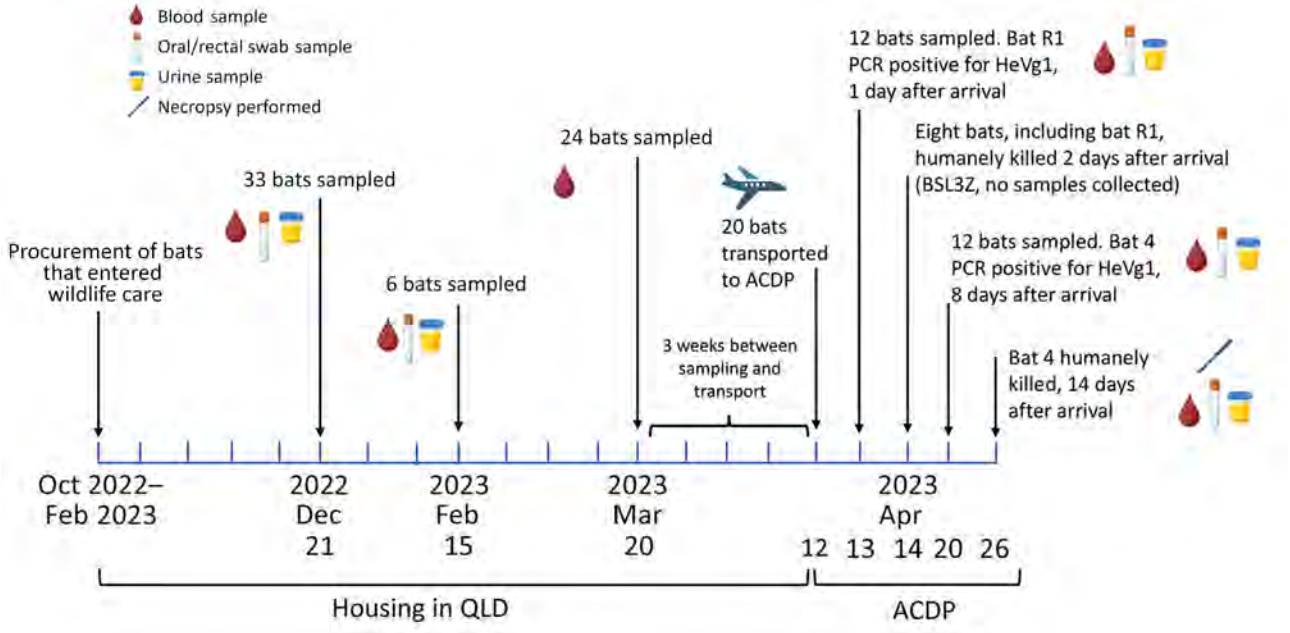

Figure 1. Timeline of events from inclusion of flying foxes in Queensland through to housing at ACDP from study of natural HeV infections in captive Australian black flying foxes, Queensland, Australia. Bats were added to the study as they became available December 2022–February 2023 after entering the care of bat rehabilitators in Queensland due to injuries. Samples collected from bat 4 at necropsy day 14 after arrival at ACDP included lung, liver, kidney, spleen, heart, ileum, large intestine, jejunum, salivary gland, retropharyngeal lymph node, submandibular lymph node, gonad, brain, cerebellum, urine, plasma, nasal wash, and oral and rectal swabs. Samples collected from individual bats are indicated on the timeline and included blood samples for serology and oral/rectal swab and urine samples for PCR. Urine was collected underneath individual cages for PCR testing on all days during the housing period at ACDP. ACDP, Australian Centre for Disease Preparedness; BSL, Biosafety Level; HeV, Hendra virus; HeVg1, HeV genotype 1 variant.

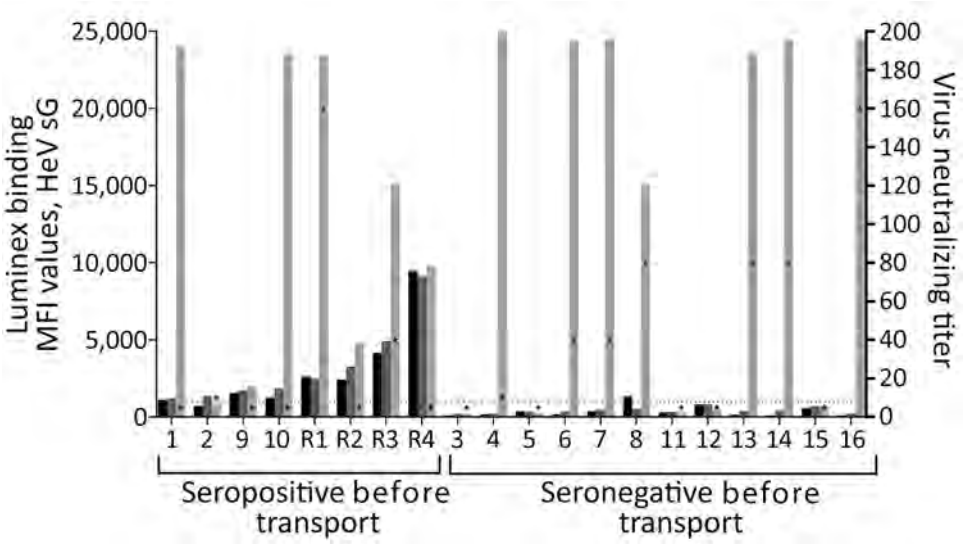

Figure 2. HeV serology of 20 flying foxes following arrival at Australian Centre for Disease Preparedness (ACDP) for a study of natural Hendra virus infections in captive Australian black flying foxes, Queensland, Australia. Detection of antibodies against HeV sG by an in-house Luminex indirect antibody binding serology assay in 20 flying foxes monitored in Queensland in December 2022 and February 2023 (black bars) and March 2023 (dark gray bars) before transport and 1 day after arrival at ACDP (light gray bars). Luminex data displayed as bars (left y-axis) representing MFI. Virus neutralization tests shown as star symbols (right y-axis). Samples with MFI >1000 (dotted line) considered positive. MFI values classified as high (>10,000), medium (4,000–10,000), low (1,000–4,000), and negative (<1,000). Virus neutralization test results were performed only on samples collected 1 day after arrival at ACDP. Bat identification numbers are indicated on the x-axis. All Luminex serologic testing on samples collected in Queensland and ACDP were performed at ACDP on a Bioplex 200 Array system integrated with Bio-Plex Manager Software 6.2 (Bio-Rad Laboratories, https://www.bio-rad.com). MFI, median fluorescence intensity.

postarrival in oral and rectal swab specimens (cycle threshold [Ct] = 33.9) and urine (Ct = 29) and 1 (bat 4) on day 8 in urine (Ct = 25). Both bats had already seroconverted in the 3 weeks between Queensland testing and arrival at ACDP, with bat R1 increasing from low Luminex seropositivity to a VNT titer of 160, and bat 4 from seronegative to VNT titer of 10 (Figure 2). Urine collected from underneath individual cages tested negative for known zoonotic viruses, except for those from bat 4, which were HeVg1 positive from days 9–14 at ACDP.

Because of biosafety constraints, we collected no tissues from bat R1, which was housed in a Biosafety Level (BSL) 3 facility (BSL3Z). Bat 4, housed in a BSL-4 facility (BSL4), had HeVg1 RNA detected at necropsy on day 14 in 2 of 14 tissues, the submandibular lymph node (Ct = 39.2) and spleen (Ct = 38.2), and in urine (Ct = 33). Virus isolation was unsuccessful from urine collected on arrival (bats R1 and 4) and from tissues collected from bat 4 at necropsy. Histopathologic analysis of tissues from bat 4 revealed apparent congestion of blood vessels throughout the lungs, as well as the expansion of perivascular tissues by edema. We also noted mild to moderate lymphoid follicular hyperplasia in bat 4, throughout lymphoid organs, but most pronounced in the spleen and mesenteric lymph nodes. No microscopic changes were evident in any other tissues. Viral antigen was only evident in isolated mononuclear cells scattered throughout the pulmonary interstitium (Figure 3).

Conclusions

This study provides evidence of natural HeV infections and seroconversion in a captive cohort of *P. alecto* bats, including detection of active HeV infections in apparently naive bats and in those with evidence of previous infections. Viral replication in seropositive animals implies that flying foxes undergo cycles of infection and reinfection, and it is thus unlikely that prior infection leads to lifelong immunity in *P. alecto* bats. This finding

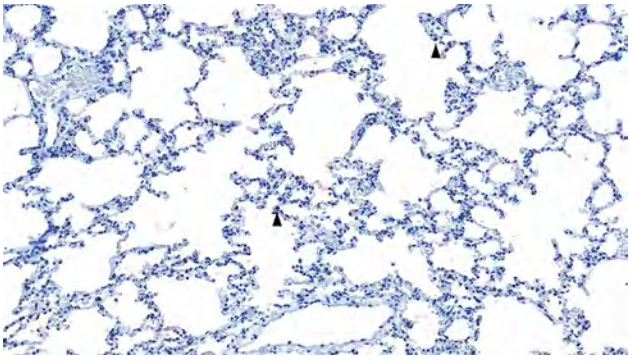

Figure 3. Histopathology of lung from a naturally infected flying fox from a study of natural Hendra virus infections in captive Australian black flying foxes, Queensland, Australia. Immunohistochemistry of bat 4, left caudal lung lobe for Hendra virus (nucleocapsid protein) using a cross-reactive Nipah virus nucleocapsid polyclonal antisera showing scattered interstitial mononuclear cells with finely granular cytoplasmic immunolabelling (arrowhead). Original magnification ×200.

contrasts nwith those for some other bat species, which appear to undergo higher rates of seroconversion with immunity to reinfection even after antibodies have waned (*6*,*7*).

The timing of infection—within 3 weeks before transport—is consistent with exposure having occurred in Queensland, either via exposure to HeV excretions from a wild bat outside the enclosure or because of recrudescence followed by horizontal transmission within the colony. Although evidence is insufficient to determine whether viral recrudescence occurred in the bats we studied, increasing evidence suggests that henipaviruses may establish latency and persist in humans and bats (*8*–*11*). Experimentally infected *P. alecto* bats typically begin shedding virus in throat and rectal swab specimens 2–7 days postinfection and in urine 7–19 days postinfection. Experimentally, development of HeV-neutralizing antibody has been inconsistent, but reports have noted low levels detected by 10 days postinfection (*12*–*14*). Thus, we speculate that the 2 flying foxes shedding HeV after arrival were likely infected with HeV ≥1 week before transport. Bat R1, which tested PCR-positive in both oral/rectal swab and urine specimen, likely experienced an active HeV infection within 10 days before transport to ACDP and continued shedding HeV upon arrival. In contrast, bat 4 may have undergone an active infection in Queensland that resolved before transport. Because those 2 bats were housed in separate rooms at ACDP, it is possible that bat 4 was reinfected immediately before transport or underwent viral recrudescence at ACDP.

We detected HeV neutralizing antibodies in 9 of the 11 seroconverted flying foxes upon arrival at ACDP; 3 had titers of 80 and 2 had titers of 160. Prior reports have revealed inconsistent antibody responses in flying foxes experimentally infected with HeV, with around 50% seroconverting with neutralizing titers of 10–80 by 10 days after oronasal inoculation (*14*,*15*). Given the unknown infection histories of bats in our study, higher titers may reflect anamnestic responses to HeV infection or could allude to differences between natural and experimental infections. Further studies will be required to determine the nature of antibody responses to infection and reinfections in flying foxes.

Our findings underscore the complexity of HeV maintenance in bat populations and highlight the need for further studies on immune dynamics, latency, and environmental drivers of recrudescence. Those insights are critical for understanding spillover risk and informing public health strategies.

Acknowledgments

The authors gratefully acknowledge bat carers from Wildlife Rescue Queensland and other bat carers from South-East Queensland, who are permitted under the Department of Environment and Heritage Protection. We gratefully acknowledge the teams at The Australian Centre for Disease Preparedness, including the Animal Studies Team for the care of flying foxes, the Biorisk Management Group for assistance with biosafety, and the Histology and Dangerous Pathogens Teams for assistance in sample processing. We also thank Som Walker, Donna Gillies, Honglei Chen, Ali Al-Saabary, Andre Attard, Nathan Fox, and the Australian Centre for Disease Preparedness Molecular Diagnostics Team for their assistance with molecular assays.

A.W.P. is supported by a National Health and Medical Research Council Investigator award (2016596). This study was supported by an award from the National Institutes of Health (R21AI169481) and a philanthropic bequest. The content is solely the responsibility of the authors and does not necessarily represent the official views of the National Institutes of Health.

About the Author

Ms. Boyd is a senior experimental scientist at the Commonwealth Scientific and Industrial Research Organisation's Australian Centre for Disease Preparedness in Geelong, Victoria, Australia. Her research interests include zoonotic batborne viruses, surveillance, and serological array assays.

References

1. Edson D, Peel AJ, Huth L, Mayer DG, Vidgen ME, McMichael L, et al. Time of year, age class and body condition predict Hendra virus infection in Australian black flying foxes (*Pteropus alecto*). Epidemiol Infect. 2019;147:e240. https://doi.org/10.1017/S0950268819001237
2. Business Queensland. Summary of Hendra virus incidents in horses. 2015 [cited 2025 Mar 4] https://www.business.qld.gov.au/industries/service-industries-professionals/service-industries/veterinary-surgeons/guidelines-hendra/incident-summary
3. Plowright RK, Field HE, Smith C, Divljan A, Palmer C, Tabor G, et al. Reproduction and nutritional stress are risk factors for Hendra virus infection in little red flying foxes (*Pteropus scapulatus*). Proc Biol Sci. 2008;275:861–9. https://doi.org/10.1098/rspb.2007.1260
4. Eby P, Peel AJ, Hoegh A, Madden W, Giles JR, Hudson PJ, et al. Pathogen spillover driven by rapid changes in bat ecology. Nature. 2023;613:340–4. https://doi.org/10.1038/s41586-022-05506-2
5. Bossart KN, McEachern JA, Hickey AC, Choudhry V, Dimitrov DS, Eaton BT, et al. Neutralization assays for differential henipavirus serology using Bio-Plex protein array systems. J Virol Methods. 2007;142:29–40. https://doi.org/10.1016/j.jviromet.2007.01.003

6. Schuh AJ, Amman BR, Sealy TK, Spengler JR, Nichol ST, Towner JS. Egyptian rousette bats maintain long-term protective immunity against Marburg virus infection despite diminished antibody levels. Sci Rep. 2017b;7:8763. https://doi.org/10.1038/s41598-017-07824-2
7. Kessler S, Stegen P, Zhan S, Schwemmle M, Reuther P, Schountz T, et al. Jamaican fruit bats mount a stable and highly neutralizing antibody response after bat influenza virus infection. Proc Natl Acad Sci U S A. 2024;121:e2413619121. https://doi.org/10.1073/pnas.2413619121
8. Playford EG, McCall B, Smith G, Slinko V, Allen G, Smith I, et al. Human Hendra virus encephalitis associated with equine outbreak, Australia, 2008. Emerg Infect Dis. 2010;16:219–23. https://doi.org/10.3201/eid1602.090552
9. Wong KT, Robertson T, Ong BB, Chong JW, Yaiw KC, Wang LF, et al. Human Hendra virus infection causes acute and relapsing encephalitis. Neuropathol Appl Neurobiol. 2009;35:296–305. https://doi.org/10.1111/j.1365-2990.2008.00991.x
10. Sohayati AR, Hassan L, Sharifah SH, Lazarus K, Zaini CM, Epstein JH, et al.; Henipavirus Ecology Research Group. Evidence for Nipah virus recrudescence and serological patterns of captive *Pteropus vampyrus*. Epidemiol Infect. 2011;139:1570–9. https://doi.org/10.1017/S0950268811000550
11. Epstein JH, Anthony SJ, Islam A, Kilpatrick AM, Ali Khan S, Balkey MD, et al. Nipah virus dynamics in bats and implications for spillover to humans. Proc Natl Acad Sci U S A. 2020;117:29190–201. https://doi.org/10.1073/pnas.2000429117
12. Middleton DJ, Morrissy CJ, van der Heide BM, Russell GM, Braun MA, Westbury HA, et al. Experimental Nipah virus infection in Pteropid bats (*Pteropus poliocephalus*). J Comp Pathol. 2007;136:266–72. https://doi.org/10.1016/j.jcpa.2007.03.002
13. Williamson MM, Hooper PT, Selleck PW, Westbury HA, Slocombe RF. Experimental Hendra virus infection in pregnant guinea-pigs and fruit bats (*Pteropus poliocephalus*). J Comp Pathol. 2000;122:201–7. https://doi.org/10.1053/jcpa.1999.0364
14. Halpin K, Hyatt AD, Fogarty R, Middleton D, Bingham J, Epstein JH, et al.; Henipavirus Ecology Research Group. Pteropid bats are confirmed as the reservoir hosts of henipaviruses: a comprehensive experimental study of virus transmission. Am J Trop Med Hyg. 2011;85:946–51. https://doi.org/10.4269/ajtmh.2011.10-0567
15. Williamson MM, Hooper PT, Selleck PW, Gleeson LJ, Daniels PW, Westbury HA, et al. Transmission studies of Hendra virus (equine morbillivirus) in fruit bats, horses and cats. Aust Vet J. 1998;76:813–8. https://doi.org/10.1111/j.1751-0813.1998.tb12335.x

Address for correspondence: Michelle Baker, Commonwealth Scientific and Industrial Research Organisation, Health and Biosecurity, Geelong, Victoria, Australia; email: michelle.baker@csiro.au

etymologia revisited

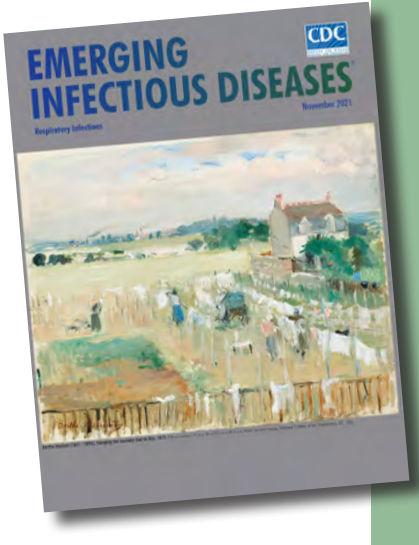

Originally published in November 2021

Prototheca

[pro”to-the’kə]

From the Greek *proto-* (first) + *thēkē* (sheath), *Prototheca* is a genus of variably shaped spherical cells of achloric algae in the family *Chlorellaceae*. Wilhelm Krüger, a German expert in plant physiology and sugar production, reported *Prototheca* microorganisms in 1894, shortly after spending 7 years in Java studying sugarcane. He isolated *Prototheca* species from the sap of 3 tree species. Krüger named these organisms as *P. moriformis* and *P. zopfii*, the second name as a tribute to Friedrich Wilhelm Zopf, a renowned botanist, mycologist, and lichenologist.

References

1. Davies RR, Spencer H, Wakelin PO. A case of human protothecosis. Trans R Soc Trop Med Hyg. 1964;58:448–51. https://doi.org/10.1016/0035-9203(64)90094-X
2. Dorland’s illustrated medical dictionary. 32nd ed. Philadelphia: Elsevier Saunders; 2012.
3. Kano R. Emergence of fungal-like organisms: Prototheca. Mycopathologia. 2020;185:747–54. https://doi.org/10.1007/s11046-019-00365-4
4. Krüger W. Brief characteristics of some lower organisms in the sap flow of deciduous trees [in German]. Hedwigia. 1894;33:241–66.
5. Todd JR, Matsumoto T, Ueno R, Murugaiyan J, Britten A, King JW, et al. Medical phycology 2017. Med Mycol. 2018;56(suppl 1):S188–204. https://doi.org/10.1093/mmy/myx162

https://wwwnc.cdc.gov/eid/article/27/11/21-1554_article

Everything is Tuberculosis: A Portrait of Connection

Nkuchia M. M'ikanatha

In 2019, author John Green visited Sierra Leone as a volunteer for Partners in Health, an international nonprofit organization, to learn about the maternal and neonatal healthcare system. While touring Lakka Government Hospital in Freetown, Sierra Leone, Green met Henry Reider, a 17-year-old tuberculosis (TB) patient. Green at first mistook him for a child—Henry's stature had been stunted by drug-resistant TB. Green writes:

> I figured Henry was someone's kid—a doctor, maybe, or a nurse, or one of the cooking or cleaning staff. Everyone seemed to know him, and everyone stopped their work to say hello and rub his head or squeeze his hand. I was immediately charmed by Henry—he had some of the mannerisms of my son, the same paradoxical mixture of shyness and enthusiastic desire for connection.

The two struck up an acquaintance, and the relationship opened up a world Green didn't know existed. *Everything is Tuberculosis*, the book that grew out of Green's experience with Henry, is part cultural history, part a meditation on friendship, and finally a call to action for effective and equally distributed treatment for this disease.

TB, Green writes, is one of the world's oldest diseases; signs of infection have been detected in human fossil remains. Before the modern era, many TB patients literally wasted away, just like Henry. Historically, shifting names for TB have reflected cultural attempts to characterize its devastating effects. The Chinese word was *huifu* (destroyed palace), in Hebrew the disease was described as *schachepheth* (wasting away), in Greek the name was *phthisis* (to decay), and in English "consumption" gained favor in the 1800s. Today, we take the name from the bacillus that causes the disease, *Mycobacterium tuberculosis*, identified and described by Robert Koch in 1882.

TB progression can seem random; a person may have an active case, then quiescence, and then relapse into another bout of active symptoms. Beyond the biological challenges, Green describes how cultural attitudes, deep-seated biases, and commercial incentives continue to complicate global treatment and prevention efforts.

After meeting Henry Reider and hearing his story, the author began to understand the enormity and complexity of TB and the factors that contribute to its persistence. He had thought of the disease, he writes, as "a disease of 19th century poets," but after becoming acquainted with Henry, Green began to see TB as "… both a form and expression of injustice."

Green notes that, in the 19th Century, the disease was strangely associated with fleeting youth and genius. Lord Byron famously remarked on his own pale appearance, wishing to die of consumption so women would find his "dying look" interesting. Poets like Keats called it a "delicious diligent disease," and even Henry Gilbert's 1842 medical treatise contained an ode to the "beauty of female consumptives," describing a "rosy tint" on the cheeks that was actually the fever of a dying patient:

> With step as noiseless as the summer air,
> Who comes in beautiful decay? Her eyes
> Dissolving with a feverish glow of light;
> ———————————and on
> Her cheek a rosy tint, as if the tip
> Of beauty's finger faintly press'd it there:
> Alas! Consumption is her name.

TB has been heavily stigmatized throughout history and continues to be so. Today, TB is often seen as a mark of disgrace because of its association with poverty, but it is also often associated with perceived choice and moral failures.

TB drugs are unavailable to many patients, especially in locations where healthcare is not as well supported, and the treatment requires long-term care involving many doses of antibiotics. In Sierra Leone, clinics are often some distance from towns and villages. The narratives notes, in places the drugs or the means to administer them are not there at all, and in dozens of countries, treatment either wasn't available or reached patients only sporadically. "It was as if the cure did not exist—because the cure is where the disease is not, and the disease is where the cure is not," Green writes.

After learning Henry Reider's story, Green returned to the United States, where he found he "could not shut up about tuberculosis." What he had

Author affiliations: Center for Clinical Epidemiology and Biostatistics, Perelman School of Medicine, University of Pennsylvania, Philadelphia, Pennsylvania, USA; The Pennsylvania State University, University Park, Pennsylvania, USA

DOI: https://doi.org/10.3201/eid3203.260264

seen and heard profoundly changed him. He found himself unable to grasp the enormous reach of tuberculosis and explained the struggle this way:

> The problem with statistics is that I cannot take in what it means to lose 1,250,000 people each year to a curable illness… That's more than a hundred thousand people a month. But how do I conceptualize such statistics? I've been in a stadium with a hundred thousand people, but I didn't know each of their families. I didn't know about the people they've loved, the heartbreaks they've endured, their constraints and encouragements, their frailty and resilience. I simply cannot fathom what 1,250,000 means.

The suffering that Henry Reider experienced—because of poverty, geography, and his misfortune of contracting this disease—led Green to consider not only the injustice of his situation but how it could be counteracted. His conclusion, in this highly personal account, is this:

> … when we know about suffering, when we are proximal to it, we are capable of extraordinary generosity. We can do and be so much for each other—but only when we see one another in our full humanity, not as statistics or problems, but as people who deserve to be alive in the world.

Everything is Tuberculosis is about friendship and how we can become changed—and charged—to pursue solutions to problems. The book is a portrait of connection, in both large and small ways. Green's portrait of Henry, and their developing closeness, drew him to the complex, colossal world of TB. He writes, "It's only because I met Henry Reider in 2019 that this book exists, and that I've found a hopefully good use for the curious megaphone I lucked into. TB has become the organizing principle of my professional life over the last 5 years."

The friendship Green forged with Henry serves as a model for how to move from statistics to action. Green argues that global health often fails because we view patients as data points, or part of a cost–benefit analysis, rather than as people. This text quietly straddles intimacy and action, appealing to researchers and the general audience alike. Its personal focus makes the content accessible in ways that raise awareness of TB—a treatable, preventable disease—and the systemic issues that keep it from being resolved. Green shows us we all have a stake in this collective effort.

By the final pages, Henry Rieder has become a close friend—"He and I talk all the time now"—leaving the reader to draw the connection that recognizing our shared humanity is what truly sustains progress in addressing the disease. Before closing the book, Green shows a picture of a beaming Reider in black and white. Reider is resting his elbow on a camera tripod and holds his head while looking at the reader. The men make videos, one in Sierra Leone and the other in the United States, their vision to overcome stigma created by geography and misunderstanding of the other, to ultimately address the pathogen that causes TB in the language microbes respect. As Green says,

> Imagining someone as more than human does as much the same work as imagining them as less than human. The ill are treated as fundamentally "other" because the social order is frightened by what their frailty reveals about everyone else's.

In addition to *M. tuberculosis*, this other, Green says, is what we need to overcome.

Acknowledgments

We thank Barbara and Paul Segal for their assistance in reviewing this manuscript.

About the Author

Dr. M'ikanatha is the lead epidemiologist for antimicrobial resistance response at the Pennsylvania Department of Health in Harrisburg, Pennsylvania, USA. He is an affiliate professor at Pennsylvania State University.

Bibliography

1. Green J. Everything is tuberculosis: the history and persistence of our deadliest infection. New York: Crash Course Books; 2025.

Address for correspondence: Nkuchia M. M'ikanatha, Pennsylvania Department of Health, 625 Forster St, Harrisburg, PA 17120, USA; email: nmikanatha@pa.gov

Detecting Influenza A(H5N1) Viruses through Severe Acute Respiratory Infection Surveillance, Cambodia

William W. Davis, Kathrine R. Tan, Borann Sar, Alyssa Finlay, Heng Seng, Vicheth Long, Savuth Chin, Darapheak Chau, Kim Sreng Leang, Mich Vann, Sovandara Lam, Dara Chan, Ly Vannara Tek, Sovann Ly, Timothy M. Uyeki

Author affiliations: US Centers for Disease Control and Prevention, Atlanta, Georgia, USA (W.W. Davis, K.R. Tan, B. Sar, A. Finlay, T.M. Uyeki); US Centers for Disease Control and Prevention, Phnom Penh, Cambodia (H. Seng, V. Long, S. Ly); Cambodia National Institute of Public Health, Phnom Penh (S. Chin, D. Chau); National Pediatric Hospital, Phnom Penh (K.S. Leang); Khmer Soviet Hospital, Phnom Penh (M. Vann); Kampot Provincial Hospital, Kampot, Cambodia (S. Lam); Svay Rieng Provincial Hospital, Svay Rieng, Cambodia (D. Chan); Kuntha Bopha Phnom Penh Hospital, Phnom Penh (L.V. Tek)

DOI: https://doi.org/10.3201/eid3203.250832

Of 19 human cases of avian influenza A(H5N1) virus infection detected during January 2023–March 2025 in Cambodia, 12 (63%) were detected directly by surveillance for severe acute respiratory infection (SARI) or indirectly by testing ill close contacts. SARI surveillance can supplement other surveillance sources for identifying H5N1 cases.

Novel influenza A viruses have pandemic potential, and early identification of infections in humans is crucial for rapid response and containment. Detection of human infection with a novel influenza A virus initiates response activities, including antiviral postexposure prophylaxis for close contacts, symptom monitoring, and implementation of interventions to reduce transmission risk. In addition, timely clinical suspicion and early diagnosis of novel influenza A virus infections in humans are critical for optimizing clinical management: the Centers for Disease Control and Prevention recommend persons with suspected novel influenza A virus infection be promptly isolated, tested for influenza A viruses, and started on empiric antiviral treatment without waiting for testing results (*1*).

The primary goal of sentinel surveillance for severe acute respiratory infection (SARI) (*2*) is to detect trends in severe seasonal influenza and other respiratory viruses (*3*). Typically, surveillance sites are referral hospitals where a subset of patients meeting the SARI case definition (acute respiratory illness causing temperature ≥38°C and cough that has onset within the previous 10 days and requires hospitalization) (*2*) have respiratory specimens collected and tested for seasonal and (if negative) novel influenza A viruses. A reliably functioning SARI surveillance system for seasonal influenza also provides an infrastructure for detecting novel influenza A virus infections, including rapid identification of severely ill patients, shipping and testing of specimens, and reporting chains for response.

During February 2023–March 2025, a total of 19 human cases of influenza A(H5N1) were identified in Cambodia. Nine (47%) of the 19 cases were detected by SARI surveillance; 3 (16%) additional cases that involved exposure to sick or dead poultry were identified by testing close contacts of those cases. Investigations concluded that findings were most consistent with poultry-to-human transmission, although in some cases human-to-human transmission could not be completely ruled out. Of the remaining 7 identified cases, 6 (26%) were suspected by clinicians on the basis of patients' history of exposure to sick or dead poultry, 1 (5%) was found through active case finding in response to one of those cases, and 1 (5%) was diagnosed by postmortem testing. Of the 19 H5N1 patients, 14 were <18 years of age; 7 pediatric cases were identified at SARI surveillance sites, and 3 of those 7 were detected at the National Pediatric Hospital in Phnom Penh. A highly pathogenic avian influenza A(H5N1) virus isolated from 1 patient was selected as an influenza A(H5) vaccine candidate (*4*).

Compared with the 5 cases diagnosed by clinicians, the 9 cases detected by SARI surveillance were diagnosed earlier (time from symptom onset

Table. SARI cases and influenza A and influenza A(H5N1) virus detections in humans, by surveillance site, Cambodia, January 2023–March 2025*

Detections	Surveillance site									Total
	AHC	CCH	KCH	KPH	KSH	KVH	NPH	PKH	SVH	
SARI cases	1,078	547	888	521	1,168	779	2,403	1,635	1,346	10,365
Influenza A virus detections	62	87	67	49	141	103	201	119	94	923
H5N1 virus detections	0	0	0	1	3	1	3	0	1	9

*All patients with SARI were tested for influenza. AHC, Angkor Hospital for Children, Siem Reap, Cambodia; CCH, Chey Chum Nas Hospital, Ta Khmau, Cambodia; KCH, Kampong Cham Hospital, Kampong Cham, Cambodia; KPH, Kampot Hospital, Kampot, Cambodia; KSH, Khmer Soviet Hospital, Phnom Penh, Cambodia; KVH, Kirivong Hospital, Takeo Province; NPH, National Pediatric Hospital, Phnom Penh; PKH, Preah Kosomak Hospital, Phnom Penh; SARI, severe acute respiratory infection; SVH, Svay Rieng Hospital, Svay Rieng, Cambodia.

to diagnosis: median 6 [range 3–9] days vs. median 8 [range 4–12] days) and treated with oseltamivir earlier (time from symptom onset to initiation of treatment: median 5 [range 2–7] days vs. median 7 [range 4–12] days). Oseltamivir treatment of H5N1 patients is associated with survival when initiated within 2 days of illness onset (*5*); however, most cases identified by SARI surveillance were identified much later. All but 1 of the 14 case-patients sought care at other healthcare facilities before seeking care at the hospital where they were diagnosed with influenza A(H5N1), highlighting an urgent need for clinician education to identify cases and start oseltamivir treatment as soon as possible.

SARI surveillance has limitations in detecting novel influenza A virus infections. Some novel influenza A case-patients might not develop SARI, and others with SARI might seek care at a private clinic that may not have influenza testing. Because SARI surveillance tests a subset of eligible SARI patients and does not usually have national coverage, H5N1 virus infections will be missed (*6*,*7*). SARI surveillance systems are costly, detections of novel influenza A viruses are rare (*8*)—in Cambodia, roughly 1 H5N1 virus was detected per 1,100 SARI cases (Table)—and other forms of surveillance are effective for detecting novel influenza A infections. For example, clinician suspicion led to diagnosis of 5 (25%) of 19 H5N1 cases in Cambodia during the study period. Thus, a combination of sentinel and event-based surveillance systems ideally should be used to detect novel influenza A viruses (*9*). Training clinicians at private clinics, outpatient settings, and nonsentinel site hospitals on the manifestations, diagnosis, and reporting of novel influenza A virus infections and expanding access to influenza testing, including for influenza A(H5) viruses, especially in areas with novel influenza A viruses circulating among poultry and other animals, is essential to improving detection of human cases.

In conclusion, during February 2023–March 2025, sentinel SARI surveillance in Cambodia directly or indirectly detected 63% (12/19) of human cases of influenza A(H5N1). To improve surveillance coverage and decrease times from symptom onset to detection, countries should consider multilayered surveillance systems, including event-based surveillance and educating clinicians on diagnosis of novel influenza A, especially in areas with high zoonotic transmission risk (*10*).

About the Author

Dr. Davis is an epidemiologist working as program director for the Influenza Division, National Center for Immunization and Respiratory Diseases, US Centers for Disease Control and Prevention, in Nonthaburi, Thailand. His primary research interest is influenza, particularly H5N1 outbreak response.

References

1. Centers for Disease Control and Prevention. Interim guidance on specimen collection and testing for patients with suspected infection with novel influenza A viruses associated with severe disease or with the potential to cause severe disease in humans. Atlanta: The Centers; 2024.
2. World Health Organization. Implementing the integrated sentinel surveillance of influenza and other respiratory viruses of epidemic and pandemic potential by the Global Influenza Surveillance and Response System: standards and operational guidance. Geneva: The Organization; 2024.
3. Alroy KA, Do TT, Tran PD, Dang TQ, Vu LN, Le NTH, et al. Expanding severe acute respiratory infection (SARI) surveillance beyond influenza: the process and data from 1 year of implementation in Vietnam. Influenza Other Respir Viruses. 2018;12:632–42. https://doi.org/10.1111/irv.12571
4. World Health Organization. Summary of status of development and availability of A(H5N1) candidate vaccine viruses and potency testing reagents. Geneva: The Organization; 2025.
5. Uyeki TM, Belser JA. Antivirals for novel influenza A virus infections. J Infect Dis. 2025;232(Supplement_3):S191–209. https://doi.org/10.1093/infdis/jiaf296
6. Brammer L, Blanton L, Epperson S, Mustaquim D, Bishop A, Kniss K, et al. Surveillance for influenza during the 2009 influenza A (H1N1) pandemic—United States, April 2009–March 2010. Clin Infect Dis. 2011;52(Suppl 1):S27–35. https://doi.org/10.1093/cid/ciq009
7. Biggerstaff M, Reed C, Epperson S, Jhung MA, Gambhir M, Bresee JS, et al. Estimates of the number of human infections with influenza A(H3N2) variant virus, United States, August 2011–April 2012. Clin Infect Dis. 2013;57(Suppl 1):S12–5. https://doi.org/10.1093/cid/cit273
8. Chen X, Wang W, Wang Y, Lai S, Yang J, Cowling BJ, et al. Serological evidence of human infections with highly pathogenic avian influenza A(H5N1) virus: a systematic review and meta-analysis. BMC Med. 2020;18:377. https://doi.org/10.1186/s12916-020-01836-y
9. World Health Organization. Crafting the mosaic: a framework for resilient surveillance for respiratory viruses of epidemic and pandemic potential. Geneva: The Organization; 2023.
10. Worsley-Tonks KEL, Bender JB, Deem SL, Ferguson AW, Fèvre EM, Martins DJ, et al. Strengthening global health security by improving disease surveillance in remote rural areas of low-income and middle-income countries. Lancet Glob Health. 2022;10:e579–84. https://doi.org/10.1016/S2214-109X(22)00031-6

Address for correspondence: William W. Davis, Centers for Disease Control and Prevention, 1600 Clifton Rd NE, Mailstop H24-7, Atlanta, GA 30329-4018, USA; email: lyo0@cdc.gov

Costs of Extrapulmonary Nontuberculous Mycobacteria Disease, Denmark, 2005–2017

Victor Naestholt Dahl, Andreas Arnholdt Pedersen, Michael Høffding Ibsen, Ole Hilberg, Anders Løkke, Andreas Fløe

Author affiliations: Aarhus University Hospital, Aarhus, Denmark (V.N. Dahl, A. Fløe); Odense University Hospital, Odense, Denmark (A.A. Pedersen); University of Southern Denmark, Odense (A.A. Pedersen, O. Hilberg, A. Løkke); i2minds, Aarhus (M.H. Ibsen); Lillebaelt Hospital, Vejle, Denmark (M.H. Ibsen, O. Hilberg, A. Løkke)

DOI: https://doi.org/10.3201/eid3203.251548

We estimated the direct and indirect costs associated with extrapulmonary nontuberculous mycobacteria (ENTM) disease in Denmark during 2005–2017. ENTM disease was associated with substantially higher healthcare costs, lower employment income, and increased public benefits before, around, and after diagnosis. Our findings highlight the substantial socioeconomic burden associated with ENTM disease.

Extrapulmonary nontuberculous mycobacteria (ENTM) disease comprises a heterogeneous group of clinical manifestations, from benign cervical lymphadenitis in children to severe skin and soft tissue infections complicated by osteomyelitis (*1*–*3*). Many ENTM cases occur from nosocomial infections and in persons without predisposing conditions (*4*,*5*). Healthcare costs associated with pulmonary nontuberculous mycobacteria are well-described (*6*,*7*), but ENTM-associated costs remain unexplored. We estimated direct and indirect costs associated with ENTM disease in Denmark.

This nationwide study included all patients ≥18 years of age with ENTM diagnosed during 2005–2017. We identified cases through the first occurrence of a nontuberculous mycobacteria diagnosis code (A31.1, A31.8, or A31.9) using the International Classification of Diseases, 10th Revision (ICD-10). We defined cases by using a previously described approach (*4*) (Appendix Table 1, https://wwwnc.cdc.gov/EID/article/32/3/25-1548-App1.pdf) and matched each case to 4 randomly selected comparators of the same age, sex, marital/cohabitation status, and municipality of residence in the diagnosis year.

We considered direct healthcare costs as expenses from primary care, prescription medications, and inpatient and outpatient secondary care. We estimated indirect costs by comparing employment income between case-patients and comparators, along with public benefits (unemployment benefits, social security, sick pay, disability pensions, early retirement pensions, and age pensions) for persons 18–64 years of age. We obtained 2002–2020 patient and cost data from national health and income registries in Denmark (*8*). We applied a 2-step generalized linear model with a gamma distribution and log link to estimate annual costs for cases and comparators over the 3 years before and after ENMT diagnosis. We incorporated mortality-adjusted weights to account for differential survival. Adjusted analyses included Charlson comorbidity index (CCI) on the basis of inpatient and outpatient ICD-10 diagnosis codes, and education level (*9*). We calculated costs in 2020 euros (€). We conducted analyses using Stata 16.1 (StataCorp LLC, https://www.stata.com) and SAS 9.4 (SAS Institute, Inc., https://www.sas.com) and generated visualizations in R version 4.2.3 (The R Project for Statistical Computing, https://www.r-project.org).

We included 406 cases and 1,580 matched comparators with a median age of 57 (IQR 30) years; of cases, 60.1% (n = 244) were among men and 39.9% (n = 162) among women (Appendix Table 2). Case-patients had lower education levels than comparators (31.3% vs. 28.6% with primary education only) and were less often employed (37.7% vs. 47.8%) (both p<0.001). Although underlying conditions were more prevalent among case-patients, most had none recorded (Appendix Table 3).

Analyses showed total direct healthcare costs for cases increased sharply around the time of diagnosis (year 0), peaking at diagnosis and remaining higher than for comparators throughout follow-up (Figure 1). Employment income was consistently lower for case-patients and declined in the 2 years preceding diagnosis. Public benefits increased substantially among case-patients, peaking around the time of diagnosis. Net costs (i.e., sum of direct costs and foregone earnings) peaked in the year before diagnosis (€21,924; 95% CI €21,017–€22,861) and at diagnosis (€20,747; 95% CI €19,960–€21,550). After adjusting for CCI and education level, direct healthcare costs were 4.3 (95% CI 3.8–4.8) times higher in cases than in comparators in the diagnosis year (Figure 2). Outpatient costs were elevated the year before diagnosis (cost ratio 4.0 [95% CI 3.6–4.5]), whereas inpatient costs peaked at diagnosis (cost ratio 6.9 [95% CI 6.2–7.7]) (Appendix Figure 1). Public benefits, specifically sick pay, disability, and early retirement pensions, rose substantially at diagnosis, and total public benefits were 1.4 (95% CI 1.2–1.6) times higher

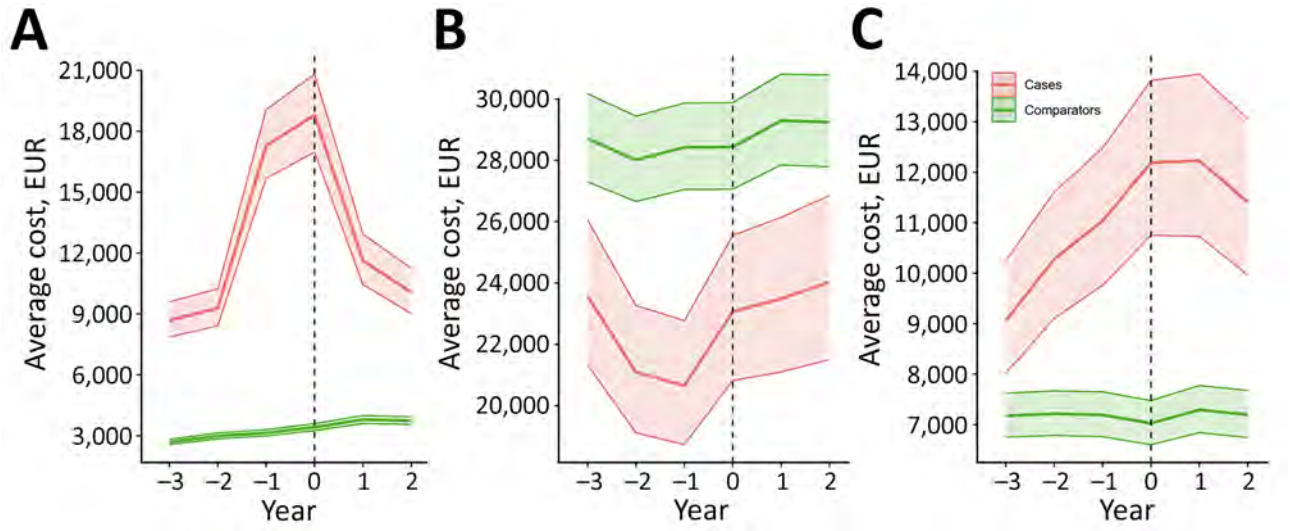

Figure 1. Annual average costs before and after extrapulmonary nontuberculous mycobacterial disease diagnosis, Denmark, 2005–2017. A) Total direct healthcare costs; B) employment income; C) total public benefits. Dotted vertical lines indicate year of diagnosis; solid center lines indicate average cost; shaded areas with borders indicate 95% CIs.

for case-patients than comparators in the diagnosis year (Appendix Figures 1, 2). Overall, ENTM cases incurred substantially higher direct and indirect costs than comparators, particularly in the peridiagnostic period.

ENTM disease is clinically heterogeneous and often requires prolonged diagnostic workup and multidisciplinary care. Rising primary care and outpatient costs before diagnosis likely reflect diagnostic delays and repeated healthcare contacts, whereas inpatient and prescription drug costs around the time of diagnosis more plausibly reflect treatment-related care. The decline in employment income and rise in public benefits before and around the time of diagnosis suggest substantial functional impairment. ENTM can occur as a device- or procedure-related infection, underscoring the need for procedural safety and infection prevention (*5*). Those infections, together with the observed cost patterns, point to opportunities for cost reduction through earlier recognition.

Although baseline socioeconomic differences might contribute to the observed cost differences, matching on key demographic variables and adjusting for education level and CCI partially addressed that concern, but we cannot exclude residual confounding. The nationwide design and registry data support the generalizability of findings to comparable

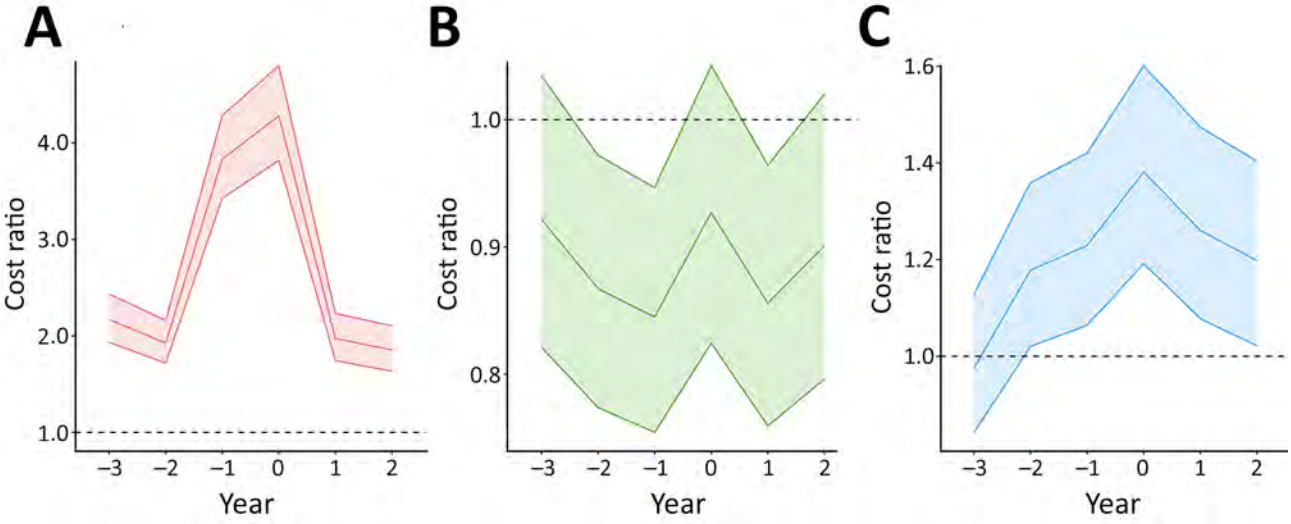

Figure 2. Cost ratios before and after extrapulmonary nontuberculous mycobacterial disease diagnosis, Denmark, 2005–2017. A) Total direct healthcare costs; B) employment income; C) total public benefits. Ratios adjusted for Charlson comorbidity index and educational level; values above 1 (dotted horizontal line) indicate higher costs for cases than comparators. Solid center lines indicate average cost; shaded areas with borders indicate 95% CIs.

tax-funded healthcare systems. However, the study was limited by a lack of species-level microbiological data and by an inability to separately quantify costs attributable to diagnostic workup, antimicrobial treatment, and surgical procedures.

In conclusion, ENTM was associated with substantial healthcare costs, reduced employment income, and increased reliance on public support in Denmark. Those findings highlight the broader socioeconomic impacts associated with ENTM before and after diagnosis. Although ENTM disease is rare (*2*,*3*), the associated costs highlight the need for early diagnosis and effective management to reduce healthcare utilization and productivity losses.

NordicInfu Care Denmark (https://www.infucare.com) funded the study. The funders of the study had no role in study design, data collection, data analysis, data interpretation, or writing of the report.

V.N.D., A.A.P., O.H., and A.F. are on an advisory board for NordicInfu Care Denmark, which distributes ARIKAYCE (amikacin liposome inhalation suspension) for Insmed (https://insmed.com); the other authors declare no competing interests.

About the Author

Dr. Dahl is a clinician-researcher at the Department of Infectious Diseases, Aarhus University Hospital, Aarhus, Denmark. His interests include complicated respiratory infections, such as tuberculosis and nontuberculous mycobacteria.

References

1. Malhotra AM, Arias M, Backx M, Gadsby J, Goodman A, Gourlay Y, et al. Extrapulmonary nontuberculous mycobacterial infections: a guide for the general physician. Clin Med (Lond). 2024;24:100016. https://doi.org/10.1016/j.clinme.2024.100016
2. Ricotta EE, Adjemian J, Blakney RA, Lai YL, Kadri SS, Prevots DR. Extrapulmonary nontuberculous mycobacteria infections in hospitalized patients, United States, 2009–2014. Emerg Infect Dis. 2021;27:845–52. https://doi.org/10.3201/eid2703.201087
3. Henkle E, Hedberg K, Schafer SD, Winthrop KL. Surveillance of extrapulmonary nontuberculous mycobacteria infections, Oregon, USA, 2007–2012. Emerg Infect Dis. 2017;23:1627–30. https://doi.org/10.3201/eid2310.170845
4. Pedersen AA, Dahl VN, Løkke A, Holden IK, Fløe A, Ibsen R, et al. Mortality rate and cause of death in adults with extrapulmonary nontuberculous mycobacteria infection, Denmark. Emerg Infect Dis. 2024;30:1790–8. https://doi.org/10.3201/eid3009.240475
5. Grigg C, Jackson KA, Barter D, Czaja CA, Johnston H, Lynfield R, et al. Epidemiology of pulmonary and extrapulmonary nontuberculous mycobacteria infections at 4 US Emerging Infections Program sites: a 6-month pilot. Clin Infect Dis. 2023;77:629–37. https://doi.org/10.1093/cid/ciad214
6. Chang S, Kim S, Kang YA, Park MS, Sohn H, Park Y. Medical costs of nontuberculous mycobacterial pulmonary disease, South Korea, 2015–2019. Emerg Infect Dis. 2024;30:1841–9. https://doi.org/10.3201/eid3009.231448
7. Ramsay LC, Shing E, Wang J, Marras TK, Kwong JC, Brode SK, et al. Costs associated with nontuberculous mycobacteria infection, Ontario, Canada, 2001–2012. Emerg Infect Dis. 2020;26:2097–107. https://doi.org/10.3201/eid2609.190524
8. Dahl VN, Pedersen AA, Ibsen MH, Hilberg O, Løkke A, Fløe A. Nontuberculous mycobacterial pulmonary disease: a nationwide cost analysis of healthcare costs, foregone earnings, and public benefits in a universal health care setting. ERJ Open Res. 2025 Dec 11 [Epub ahead of print]. https://doi.org/10.1183/23120541.00870-2025
9. Quan H, Li B, Couris CM, Fushimi K, Graham P, Hider P, et al. Updating and validating the Charlson comorbidity index and score for risk adjustment in hospital discharge abstracts using data from 6 countries. Am J Epidemiol. 2011;173:676–82. https://doi.org/10.1093/aje/kwq433

Address for correspondence: Victor Næstholt Dahl, Department of Infectious Diseases, Aarhus University Hospital, Palle Juul-Jensens Blvd 99, Aarhus DK-8200, Denmark; email: victor.dahl@rm.dk

Oestrus ovis Nasal Myiasis with Pupation in Human Host, Greece, October 2025

Ilias P. Kioulos, Emmanouil Kokkas, Evangelia-Theophano Piperaki

Author affiliations: Agricultural University of Athens, Athens, Greece (I.P. Kioulos); University of Crete, Heraklion, Greece (E. Kokkas); Foundation for Research and Technology Hellas, Institute of Molecular Biology and Biotechnology, Heraklion (E. Kokkas); National and Kapodistrian University of Athens Medical School, Athens (E.T. Piperaki)

DOI: https://doi.org/10.3201/eid3203.251077

We report a case of human *Oestrus ovis* nasal myiasis in Greece, in which pupation occurred within the human host. Ten larvae in various stages of development and 1 puparium were expelled or extracted from the patient's maxillary sinus. Diagnosis was confirmed through morphologic identification and by PCR, followed by DNA sequencing.

Oestrus ovis (Diptera: Oestridae), the sheep bot fly, is a cosmopolitan parasite of small ruminants, widespread in hot and dry regions, including countries bordering the Mediterranean Sea. Accidental human infestations by *O. ovis* flies have been reported from around the world (*1*,*2*). We report a case of human *O. ovis* nasal myiasis in which pupation occurred within the human host. The diagnosis was confirmed by molecular identification of the parasite using PCR followed by DNA sequencing.

The patient was a 58-year-old woman in Greece who worked outdoors on a Greek island, adjacent to a field with grazing sheep. It was September, during hot and dry weather, and she noticed numerous flies swarming around her face. Approximately 1 week later, she had onset of progressive maxillary pain, followed over the next 2–3 weeks by severe coughing. She reported no other symptoms. On October 15, she sought medical attention after she sneezed and "worms" started coming out of her nose. An otolaryngologist surgically removed 10 larvae of various stages and 1 pupa from her maxillary sinus. She was treated with nasal decongestants and made a complete recovery. None of her co-workers reported similar symptoms.

We examined 2 of the larvae and part of a puparium (Figure). The puparium fragment was ≈10 mm long, black, and wrinkled and contained remnants of the pupa. One larva was yellowish, measured ≈15 mm, and exhibited rows of spines ventrally, with a bare preanal bulge; its posterior peritremes were circular with a central button and no distinct suture. The second larva measured ≈20 mm, was light brown, and displayed broad transverse blackish bands dorsally. On the basis of size and morphology, we identified both larvae as third instar (L3) *O. ovis* bot fly.

We extracted genomic DNA from the pupal casing by using DNAzol (Molecular Research Center, https://www.mrcgene.com) according to the manufacturer's instructions. We amplified a 392-bp fragment of the mitochondrial cytochrome c oxidase I gene and a 190-bp fragment of the ribosomal DNA 28S gene, as previously described (*3*). Both PCR reactions produced specific bands at the expected sizes. We purified the products by using the GeneJet PCR Purification Kit (Thermo Fisher Scientific, https://www.thermofisher.com)

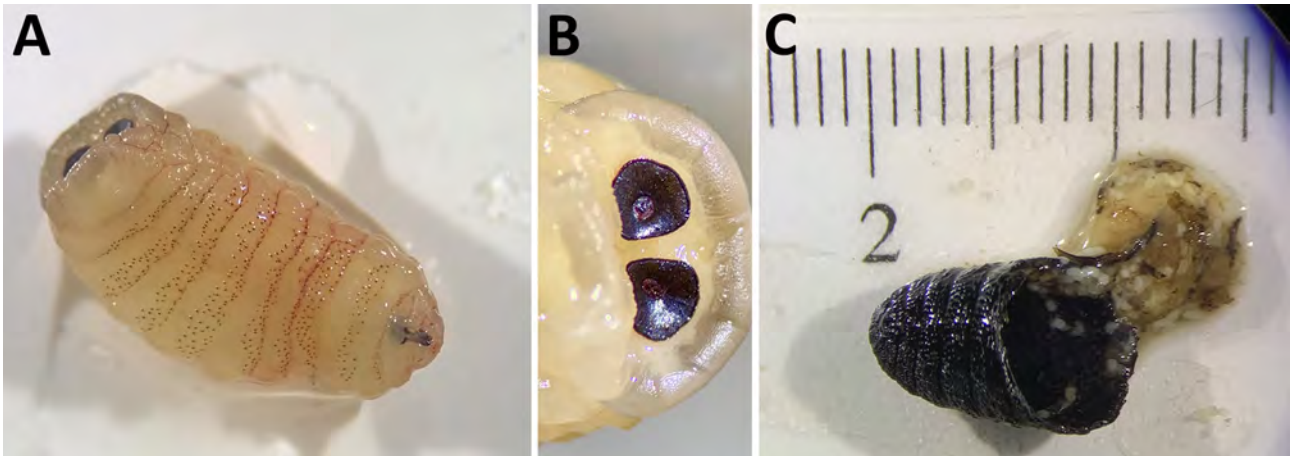

Figure. Third instar *Oestrus ovis* larva and puparium retrieved from nasal sinuses of a 58-year-old female patient, Greece. A) The third instar was yellowish, with rows of spines on the ventral surface. B) The posterior peritremes were circular with a central button. C) The broken puparium was black and wrinkled and contained remnants of the pupa.

and sequenced them (GENEWIZ, https://www.genewiz.com). Sequencing results demonstrated 100% identity of the amplified fragments with their corresponding GenBank sequences (accession no. KX268655.1 for *cox1* and KP974974.1 for 28S rDNA). We performed alignments by using the ClustaW function in BioEdit version 7.2.5 (https://thalljiscience.github.io).

Myiasis can be classified ecologically as obligatory (caused by larvae that require a living vertebrate host), facultative (caused by free-living larvae that may opportunistically develop in hosts), and accidental (caused by free-living larvae, unable to complete their life cycle in a host). Anatomically, myiasis is categorized by affected site as sanguinivorous, cutaneous (furuncular or migratory), wound, or cavitary (e.g., cerebral, aural, nasal, or ophthalmomyiasis) (*1*).

The *O. ovis* life cycle within its natural hosts, sheep and goats, is well-documented. The female deposits first instar (L1) larvae into the animal's nostrils, which migrate upward into the nasal passages and paranasal sinuses, where they feed, grow, and molt. They are expelled as third instar (L3) larvae, burrow into the soil, and pupate. *O. ovis* bot flies infrequently affect humans, most often depositing larvae in the conjunctival sac and rarely into the nostrils, mouth, or external auditory meatus. The most common clinical manifestation is acute catarrhal conjunctivitis, typically preceded by the sudden sensation of a foreign body (*1*). Until recently, it was believed that *O. ovis* larvae could not develop beyond the L1 stage in humans. In recent years, however, L2 (*4*) and L3 (*5*,*6*) larvae have been recovered from human case-patients, typically in the setting of immunosuppression or in patients with traumatic or anatomic abnormalities of the nasal passages. Of the 5 reported cases of *O. ovis* myiasis in travelers returning from Greece, 4 involved L1 (*7*–*10*) and 1 involved L2 larvae (*4*).

The patient we report had a severely deviated nasal septum and appears to have been inoculated with a large larval burden. From a purely anatomic perspective, we hypothesize that the combination of high larval numbers and septum deviation impeded normal egress from the nasal passages, permitting progression to the L3 stage and, in 1 instance, pupation. Of note, L3 larvae that become trapped within the sinuses of animals are not known to pupate; instead, they desiccate, liquefy, or calcify, with occasional bacterial superinfection. Pupation of *O. ovis* larvae within any mammalian host is considered biologically implausible. The paranasal sinus environment does not meet temperature and humidity requirements for pupation, and host secretions, immune responses, and resident microbiota create a hostile milieu for pupal development. In our patient, unidentified anatomic or physiologic factors within the paranasal sinuses, probably including her severe septum deviation, apparently permitted pupation. Alternatively, this case may represent an early indication of evolutionary adaptation, enabling *O. ovis* parasites to complete their life cycle in humans. In either scenario, additional cases and data are needed to understand this phenomenon, but clinicians should be aware of the potential for human bot fly infections in endemic areas.

About the Author

Dr. Kioulos is a medical entomologist at the Laboratory of Pesticide Science, Agricultural University of Athens, specializing in the control and insecticide resistance of mosquitoes and other important medical and veterinary arthropods. His research focuses on integrated vector management, resistance mechanisms, and the development of effective control strategies for disease vectors.

References

1. Francesconi F, Lupi O. Myiasis. Clin Microbiol Rev. 2012;25:79–105. https://doi.org/10.1128/CMR.00010-11
2. Pupić-Bakrač A, Pupić-Bakrač J, Škara Kolega M, Beck R. Human ophthalmomyiasis caused by *Oestrus ovis*—first report from Croatia and review on cases from Mediterranean countries. Parasitol Res. 2020;119:783–93. https://doi.org/10.1007/s00436-019-06599-x
3. Hu L, Zhao Y, Zhang W, Guan C, Zhang Y, Mi K. Morphological and molecular identification of *Oestrus ovis* (Diptera: Oestridae) larvae collected from a Chinese patient with conjunctival myiasis. Acta Parasitol. 2022;67:1273–81. https://doi.org/10.1007/s11686-022-00573-x
4. Einer H, Ellegård E. Nasal myiasis by *Oestrus ovis* second stage larva in an immunocompetent man: case report and literature review. J Laryngol Rhinol Otol. 2011;125:745–6. https://doi.org/10.1017/S002221511100096X
5. Lucientes J, Clavel A, Ferrer-Dufol M, Valles H, Peribanez MA, Gracia-Salinas MJ, et al. Short report: one case of nasal human myiasis caused by third stage instar larvae of *Oestrus ovis*. Am J Trop Med Hyg. 1997;56:608–9. https://doi.org/10.4269/ajtmh.1997.56.608
6. Hoyer P, Williams RR, Lopez M, Cabada MM. Human nasal myiasis caused by *Oestrus ovis* in the highlands of Cusco, Peru: report of a case and review of the literature. Case Rep Infect Dis. 2016;2016:2456735. https://doi.org/10.1155/2016/2456735
7. Wölfelschneider P, Wiedemann P. External ophthalmic myiasis cause by Oestrus ovis (sheep and goat botfly) [in German]. Klin Monbl Augenheilkd. 1996;209:256–8. https://doi.org/10.1055/s-2008-1035314
8. Fries FN, Pattmöller M, Seitz B, Berger F, Kampen H, Szentmáry N, et al. Ophthalmomyiasis externa due to

Oestrus ovis in a traveller returning from Greece. Travel Med Infect Dis. 2018;23:101–2. https://doi.org/10.1016/j.tmaid.2018.05.007
9. Hartmannová L, Mach R, Záruba R, Pavlovský M. External ophthalmomyiasis caused by *Oestrus ovis* (a case report). Ces Slov Oftalmol. 2020;76:130–4. https://doi.org/10.31348/2020/22
10. Griffin B, Hawrami A, Stephenson J, Narang A. Ophthalmomyiasis externa caused by *Oestrus ovis*. BMJ Case Rep. 2022;15:e249796. https://doi.org/10.1136/bcr-2022-249796

Address for correspondence: Evangelia-Theophano Piperaki, National and Kapodistrian University of Athens, Medical School, Mikras Asias 75, 11527 Athens, Greece; email: epiper@med.uoa.gr

CCHFV Seroprevalence among Hunter-Gatherers, Northeastern Democratic Republic of the Congo

Dacquin M. Kasumba, Samuel M. Shamamba, Ange Y. Mubiala, Bobo N. Bazola, Amanda C. Horton, Charles Ndawula, Jean-Jacques Muyembe-Tamfum, Jean-Christophe Sabue Mulangu

Author affiliations: Institut National de Recherche Biomédicale, Kinshasa, Democratic Republic of the Congo (D.M. Kasumba, S.M. Shamamba, A.Y. Mubiala, B.N. Bazola, J.-J. Muyembe-Tamfum, J.-C.S. Mulangu); Université de Kinshasa Faculty of Medicine, Kinshasa (D.M. Kasumba, J.-C.S. Mulangu); United Kingdom Health Security Agency, Porton Down, UK (A.C. Horton); National Livestock Resources Research Institute, Entebbe, Uganda (C. Ndawula); Global Medical Affairs, Ridgeback Biotherapeutics, Miami, Florida, USA (J.-C.S. Mulangu)

DOI: https://doi.org/10.3201/eid3203.251171

We evaluated human Crimean-Congo hemorrhagic fever virus (CCHFV) seroprevalence in hunter-gatherer populations of northeastern Democratic Republic of the Congo. We tested blood from 300 participants for CCHFV antibodies; 4% were CCHFV-positive. CCHFV likely has been circulating undetected in the country, indicating the need for a more robust surveillance system.

Crimean-Congo hemorrhagic fever (CCHF) is a tickborne viral disease that is endemic to sub-Saharan Africa and has a widespread global distribution (*1*). CCHF virus (CCHFV) belongs to the *Orthonairovirus* genus, in the Nairoviridae family of the Bunyaviridae order (*2*). *Hyalomma* spp. ticks transmit CCHFV through bites, but the virus also can be transmitted to humans via contact with infected blood (*1*). During outbreaks, case-fatality rates can be as high as 60%, and the incubation period is ≈1–6 days, depending on the transmission route. Infections are characterized by a wide range of symptoms, including but not limited to nonspecific fever, myalgia, headache, diarrhea, nausea, and vomiting (*3*).

In the Democratic Republic of the Congo (DRC), reported cases have been limited to 2 zoonotic transmissions since 1956 (*4*,*5*). Even so, CCHF cases are likely undetected because of limited surveillance in the country. Furthermore, no serologic evaluation in humans has been reported from DRC. To shed light on CCHFV prevalence in the country, we examined blood samples taken from a pygmy hunter-gatherer population in Watsa, in northeastern DRC, a population that has frequent contact with wildlife (*6*). We recruited 300 participants from 39 different settlements, 150 men and 150 women, whose mean age was 32.2 (SD ±14.6) years. Study participants were invited to the study site, where they received informed consent before we administered a questionnaire and collected blood samples. We used a database previously generated as part of a Marburg hemorrhagic fever virus seroprevalence investigation (*7*) (Appendix, https://wwwnc.cdc.gov/EID/article/32/3/25-1171-App1.pdf) to record interview responses and find evidence of CCHFV circulating within the region.

Using an ELISA assay, we observed a 4% (n = 12) IgG seroprevalence. Most (83.3%, n = 10) of those positive were female; only 2 men were seropositive (odds ratio [OR] = 5.286; p = 0.035). We noted no significant difference in age between the seropositive and seronegative population, and the mean age of seropositive participants did not deviate from mean age of the study population (Table).

Our investigation questionnaire did not ask whether volunteers were involved in farming. Because pygmies' subsistence activities do not include farming (*6*), seropositive donors more likely encountered viral vectors in the forest during traditional hunter-gatherer activities. Sociologically, male members of the community are predominantly expected to hunt, bringing home carcasses to be butchered by female members. Among participants, 60% stated they practiced hunting as their primary means of subsistence; the other

Table. Characteristics of subjects in a study of CCHFV seroprevalence among hunter-gatherers, northeastern Democratic Republic of the Congo *

Characteristics	CCHFV serology, no. (%)			p value	OR (95% CI)
	Total, n = 300	Negative, n = 288	Positive, n = 12		
Sex					
M	150 (50)	148 (51.4)	2 (16.7)		
F	150 (50)	140 (48.6)	10 (83.3)	0.035	5.286 (1.138–24.549)
Mean age, y ±SD	32.2 ±14.6	32.3 ±14.5	29.9 ±17.5	0.649†	0.988 (0.948–1.031)
Professional activity					
Hunting	180 (60)	178 (61.8)	2 (16.7)	0.004	8.091 (1.740–37.616)
Other/not described	120 (40)	110 (38.2)	10 (83.3)		
Animal contact‡					
Rat	216 (72.0)	209 (72.6)	7 (58.3)	0.282	1.890 (0.583–6.128)
Bat	224 (74.7)	215 (74.7)	9 (75)	0.978	0.982 (0.259–3.724)
Monkey	273 (91.0)	261 (90.6)	12 (100)	0.610	0 (0–0.018)

*p value calculated by Fisher exact test, except as indicated. CCHFV, Crimean-Congo hemorrhagic fever virus; OR, odds ratio.
†p value calculated by Student *t*-test.
‡>1 animal exposure type possible.

40% performed other, unspecified, activities. In contrast to our expectations, nonhunting participants had a higher probability for seropositivity than hunting participants (Table; Appendix Table 1).

Because most seropositive participants were women who did not routinely hunt, and considering the lifestyle of pygmy populations, we speculate that gathering food or butchering carcasses constituted greater CCHFV risk factors (*1*). However, we cannot exclude the possibility that the nonhunting seropositive female members also undertook farming activities for additional subsistence. Nevertheless, data suggest the possibility that nonfarming activities in the forest could expose humans to CCHFV tick vectors, either through direct interaction in the bushes or via wild animals harboring ticks (*8*–*10*).

To help clarify the risk mediated by exposure via wild animals, we asked participants about animal contacts. Rats, bats, monkeys, and other animals in the area are known to carry ticks responsible for CCHFV transmission (*8*–*10*). We asked participants whether they touched, ate, or had been bitten by animals; 72% reported encountering rodents (particularly rats), 74.7% encountered bats, and 91% encountered monkeys. Although all 12 seropositive participants confirmed previous contact with monkeys, we did not have sufficient elements to statistically confirm that association (OR = 0; p = 0.610) (Table).

Of the 12 seropositive participants, 6 (50%) reported previously having hemorrhagic fever (HF) symptoms; however, we found no significant correlation between seropositivity and HF symptoms (OR = 0.834; p = 0.776). In addition, we found no correlation between seropositivity and direct or indirect contact with another HF patient or a dead body (Appendix Table 2). That finding supports the possibility that CCHFV seroprevalence and transmission was not through direct or indirect human contact within this community, but rather through zoonotic transmission, further supported by the established correlation between reported subsistence activities and seropositivity (Table).

In conclusion, we documented serologic evidence of CCHF in DRC hunter-gatherer populations, indicating that the disease has been circulating undetected in the country. The lack of previously reported cases is probably the consequence of a nonexistent surveillance system. In addition, the lack of specific diagnostic tools in DRC is a challenge to understanding the epidemiology of the disease. Our findings highlight the need for greater scrutiny into risk factors of CCHFV exposure, particularly among populations exposed to wildlife as part of their lifestyles and in regions with diverse human population groups and cultures.

Acknowledgments

We thank members of the Watsa Rural Health Zone Central Office and the interviewers who made this investigation possible despite the difficult working conditions characterized by security issues. We also thank Antoine Tshomba for facilitating the administrative procedures with local authorities and Janusz Paweska and his team for their crucial and fruitful discussions and support in this analysis.

D.M.K. is supported by the European Union (grant no. DCI-PANAF/2020/420-028) through the African Research Initiative for Scientific Excellence pilot program. ARISE is implemented by the African Academy of Sciences with support from the European Commission and the African Union Commission. D.M.K. also receives additional support from the National Institutes of Health Fogarty Program Global Infectious Diseases through the

Emerging and Re-Emerging Pathogens Research Training Program in DRC (EREP-RTP-DRC). The contents of this document are the sole responsibility of the authors and can under no circumstances be regarded as reflecting the position of the European Union, the African Academy of Sciences, the African Union Commission, the National Institutes of Health, the UK Health Security Agency, or the British government.

About the Author

Dr. Kasumba is an associate professor at the University of Kinshasa and a scientist at the National Institute for Biomedical Research, Kinshasa, DRC. His research interests focus on host-microbe interactions to improve and develop mitigation approaches against infectious diseases.

References

1. Temur AI, Kuhn JH, Pecor DB, Apanaskevich DA, Keshtkar-Jahromi M. Epidemiology of Crimean-Congo hemorrhagic fever (CCHF) in Africa—underestimated for decades. Am J Trop Med Hyg. 2021;104:1978–90. https://doi.org/10.4269/ajtmh.20-1413
2. Kuhn JH, Alkhovsky SV, Avšič-Županc T, Bergeron É, Burt F, Ergünay K, et al. ICTV virus taxonomy profile: *Nairoviridae* 2024. J Gen Virol. 2024;105:4.
3. Frank MG, Weaver G, Raabe V; State of the Clinical Science Working Group of the National Emerging Pathogens Training; Education Center's Special Pathogens Research Network2; State of the Clinical Science Working Group of the National Emerging Pathogens Training Education Center's Special Pathogens Research Network. Crimean-Congo hemorrhagic fever virus for clinicians—epidemiology, clinical manifestations, and prevention. Emerg Infect Dis. 2024;30:854–63. https://doi.org/10.3201/eid3005.231647
4. Simpson DI, Knight EM, Courtois G, Williams MC, Weinbren MP, Kibukamusoke JW. Congo virus: a hitherto undescribed virus occurring in Africa. I. Human isolations—clinical notes. East Afr Med J. 1967;44:86–92.
5. Woodall JP, Williams MC, Simpson DI. Congo virus: a hitherto undescribed virus occurring in Africa. II. Identification studies. East Afr Med J. 1967;44:93–8.
6. Fa JE, Olivero J, Farfán MA, Lewis J, Yasuoka H, Noss A, et al. Differences between Pygmy and non-Pygmy hunting in Congo Basin forests. PLoS One. 2016;11:e0161703. https://doi.org/10.1371/journal.pone.0161703
7. Borchert M, Mulangu S, Swanepoel R, Tshomba A, Afounde A, Kulidri A, et al. Pygmy populations seronegative for Marburg virus. Emerg Infect Dis. 2005;11:174–7. https://doi.org/10.3201/eid1101.040377
8. Müller MA, Devignot S, Lattwein E, Corman VM, Maganga GD, Gloza-Rausch F, et al. Evidence for widespread infection of African bats with Crimean-Congo hemorrhagic fever-like viruses. Sci Rep. 2016;6:26637. https://doi.org/10.1038/srep26637
9. Lacroux C, Bonnet S, Pouydebat E, Buysse M, Rahola N, Rakotobe S, et al. Survey of ticks and tick-borne pathogens in wild chimpanzee habitat in Western Uganda. Parasit Vectors. 2023;16:22. https://doi.org/10.1186/s13071-022-05632-w
10. Omoga DCA, Tchouassi DP, Venter M, Ogola EO, Osalla J, Kopp A, et al. Transmission dynamics of Crimean-Congo haemorrhagic fever virus (CCHFV): evidence of circulation in humans, livestock, and rodents in diverse ecologies in Kenya. Viruses. 2023;15:1891. https://doi.org/10.3390/v15091891

Address for correspondence: Dacquin Muhandwa Kasumba, Institut National de Recherche Biomédicale, 5345 Ave de la Démocratie, Kinshasa-Gombe BP1197, Democratic Republic of the Congo; email: dacquin.kasumba@unikin.ac.cd

Occupational Transmission of Extensively Drug-Resistant Tuberculosis, France

Corentin Poignon, Frédéric Vandenbos, Karine Risso, Delphine Viard, Esther Gydé, Alice Gaudart, David Chirio, Nicolas Veziris, Michel Carles

Author affiliations: Centre d'Immunologie et des Maladies Infectieuses, Sorbonne Université, CNR Mycobactéries, APHP, Paris, France (C. Poignon, E. Gydé, N. Veziris); Hôpital Pasteur Centre de Lutte Antituberculeuse de Nice, Nice, France (F. Vandenbos, K. Risso); Hôpital Archet, Nice (K. Risso, A. Gaudart, D. Chirio, M. Carles); Centre Hospitalie r Universitaire de Nice, Nice (D. Viard).

DOI: https://doi.org/10.3201/eid3203.251099

We report occupational transmission of extensively drug-resistant tuberculosis (TB) to a healthcare worker in France receiving tumor necrosis factor α inhibitor therapy. Despite airborne precautions, the healthcare worker contracted TB working in a high-risk unit. This case underscores that immunocompromised healthcare workers should not be assigned to frontline TB care in high-risk settings.

In France, multidrug-resistant tuberculosis (TB) represents <3% of all notified TB cases annually; variable case counts ranged from 44 cases in 2021 to 110 in 2014. The World Health Organization defines extensively drug-resistant TB (XDR TB) by resistance to rifampin, isoniazid, and fluoroquinolones in addition to bedaquiline or linezolid, representing the most difficult-to-treat forms of the disease. Tumor necrosis

factor α (TNF-α) inhibitors (e.g., infliximab, adalimumab) disrupt granuloma integrity and increase the risk for latent TB reactivation or new infection by up to 25-fold (*1*). We report a case of occupational transmission of XDR TB to a healthcare worker in France receiving TNF-α inhibitor therapy, despite airborne precautions.

In December 2023, a 57-year-old woman sought care after experiencing several weeks of fatigue. Her medical history included ankylosing spondylitis treated by the TNF-α inhibitor adalimumab since 2017. Pretherapeutic QuantiFERON (QIAGEN, https://www.qiagen.com) testing was negative, and she had no personal history of TB or prior exposure. Since 2020, she had worked as a nursing assistant in an infectious diseases department.

Computed tomography revealed hypermetabolism of right upper lobe alveolar consolidation (Figure 1). Because of the absence of sputum production, bronchoscopy with culture was performed. An acid-fast bacilli smear result was negative, but Xpert MTB/RIF Ultra (Cepheid, https://www.cepheid.com) testing detected rifampin-resistant *M. tuberculosis*. Occupational TB transmission was assumed.

The bronchoscopy culture was positive and sent to the French National Reference Center for Mycobacteria (Nice, France), where we conducted targeted next-generation sequencing by using Deeplex Myc-TB (Illumina, https://www.illumina.com), whole-genome sequencing analysis (Illumina), and phenotypic drug susceptibility testing. Genotypic analysis revealed resistance to 7 drugs, including rifampin, isoniazid, fluoroquinolones, and an insertion in the *rv0678* gene resulting in a frameshift associated with bedaquiline and clofazimine resistance. Phenotypic susceptibility testing confirmed genotypic resistance to bedaquiline and clofazimine (MICs >2 mg/L) but susceptibility to aminoglycosides, delamanid, linezolid, and cycloserine, confirming XDR TB.

Before susceptibility test results were available, we started the patient on bedaquiline (400 mg 1×/d for 2 weeks, followed by 200 mg 3×/wk), linezolid (600 mg/d), delamanid (100 mg 2×/d), cycloserine (500 mg/d), and amikacin (10 mg/kg/d) for the first 3 months. Bedaquiline was maintained in the treatment protocol because *rv0678* mutations usually confer low-level MIC increases, and a negative effect on treatment outcome is unconfirmed (*2*). Cultures were identified within 1 month. The patient completed 13 months of treatment (1 year after identification) and remained clinically well with stable imaging at 6 months posttreatment. After a multidisciplinary provider discussion to balance rheumatologic needs and infectious disease risk, TNF-α inhibitor therapy was resumed after 3 months of treatment, clinical improvement, and documented culture identification.

A review of department cases discovered a smear-positive cavitary XDR TB patient hospitalized 3 months earlier. Whole-genome comparison confirmed both isolates were identical (0 single-nucleotide polymorphism difference). The index patient was isolated with airborne precautions, including filtering face piece class 2 mask use by all staff, but he was autonomous, and mask compliance outside direct care activities could not be ensured. He stayed 10 days before he was transferred to another hospital without treatment. During that period, the patient we describe provided routine close-contact care, during which exposure might have occurred.

TNF-α inhibitors have greatly improved outcomes in chronic inflammatory diseases (*1*,*3*). Pretreatment screening for active TB or latent TB is standard practice (*4*,*5*), but infection can still occur after treatment initiation (*4*).

In France, nosocomial TB transmission among healthcare workers has decreased because of declining TB incidence and stringent airborne precautions (*5*). Nevertheless, departments regularly managing TB patients remain high-risk areas (*6*). Among patients receiving TNF-α inhibitors for irritable bowel disease, 44 TB cases were reported, including 6 (14%) in healthcare workers (*7*). Another publication determined that healthcare workers receiving TNF-α inhibitors for irritable bowel disease do not have increased risk for infections except for TB (*8*). Our case

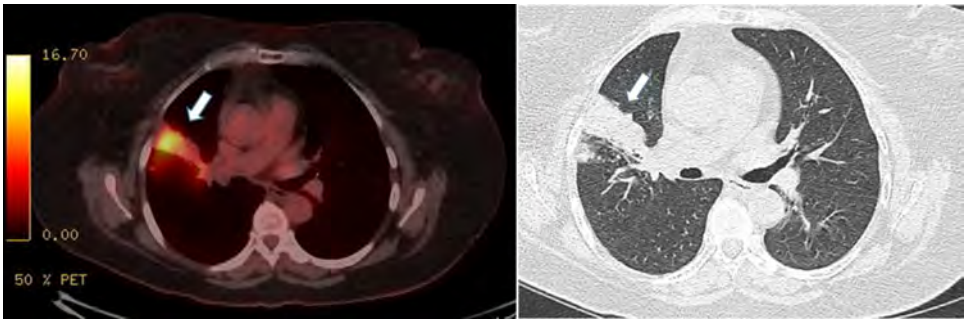

Figure. Computed tomography scans of a healthcare workers with occupationally transmitted extensively drug-resistant tuberculosis, France. Scan revealed hypermetabolism (standardized update value 9.1) of the right upper lobe alveolar consolidation, indicated by white arrows.

confirms this occupational susceptibility in high-exposure environments.

A healthcare worker receiving TNF-α inhibitors who contracted TB despite minimal contact was previously reported (*9*). Genotyping confirmed transmission from a TB patient, suggesting that even brief or indirect exposure might be sufficient for infection under immunosuppressive conditions (*9*). Similar to our case, despite routine infection control measures, exposure to a cavitary XDR TB patient led to transmission. Infection prevention protocols in France are extensive but might not be sufficient for immunosuppressed staff in a TB high-risk unit, especially before efficient treatment is initiated when drug-resistant TB is involved (*10*).

After this event, hospital policy was revised. Newly hired staff already receiving TNF-α therapy will no longer be assigned to pulmonology, infectious diseases, or emergency departments. Current staff in those departments that are beginning TNF-α inhibitors will be offered reassignment. The occupational health revisions reflect a local institutional policy change; further studies will be needed before national or international recommendations can be proposed.

Our case demonstrates confirmed occupational transmission of XDR TB to an immunocompromised healthcare worker despite airborne precautions. Our findings underscore the vulnerability of immunosuppressed healthcare workers and support the need to reconsider their assignment to frontline TB care in high-risk departments.

The patient gave her written informed consent to the publication of case details.

Whole-genome data are available in the National Center for Biotechnology Information Sequence Read Archive (https://www.ncbi.nlm.nih.gov/sra; BioProject no. PRJNA1345252, accession nos. SRR35790521 and SRR35790522).

About the Author

Dr. Poignon is a clinical microbiologist specialized in mycobacteriology and currently works at the Department of Bacteriology at Pitié-Salpêtrière Hospital and at the French National Reference Center for Mycobacteria. His research focuses on development of omics for identification and drug resistance study in tuberculous and nontuberculous mycobacteria.

References

1. Keane J, Gershon S, Wise RP, Mirabile-Levens E, Kasznica J, Schwieterman WD, et al. Tuberculosis associated with infliximab, a tumor necrosis factor α–neutralizing agent. N Engl J Med. 2001;345:1098–104. https://doi.org/10.1056/NEJMoa011110
2. Kaniga K, Lounis N, Zhuo S, Bakare N, Andries K. Impact of *Rv0678* mutations on patients with drug-resistant TB treated with bedaquiline. Int J Tuberc Lung Dis. 2022;26:571–3. https://doi.org/10.5588/ijtld.21.0670
3. Fragoulis GE, Nikiphorou E, Dey M, Zhao SS, Courvoisier DS, Arnaud L, et al. 2022 EULAR recommendations for screening and prophylaxis of chronic and opportunistic infections in adults with autoimmune inflammatory rheumatic diseases. Ann Rheum Dis. 2023;82:742–53. https://doi.org/10.1136/ard-2022-223335
4. Kucharzik T, Ellul P, Greuter T, Rahier JF, Verstockt B, Abreu C, et al. ECCO guidelines on the prevention, diagnosis, and management of infections in inflammatory bowel disease. J Crohns Colitis. 2021;15:879–913. https://doi.org/10.1093/ecco-jcc/jjab052
5. Gehanno JF, Abiteboul D, Rollin L. Incidence of tuberculosis among nurses and healthcare assistants in France. Occup Med (Lond). 2017;67:58–60. https://doi.org/10.1093/occmed/kqw138
6. Baussano I, Nunn P, Williams B, Pivetta E, Bugiani M, Scano F. Tuberculosis among health care workers. Emerg Infect Dis. 2011;17:488–94. https://doi.org/10.3201/eid1703.100947
7. Abitbol Y, Laharie D, Cosnes J, Allez M, Nancey S, Amiot A, et al.; GETAID. Negative screening does not rule out the risk of tuberculosis in patients with inflammatory bowel disease undergoing anti-TNF treatment: a descriptive study on the GETAID cohort. J Crohns Colitis. 2016;10:1179–85. https://doi.org/10.1093/ecco-jcc/jjw129
8. Gagnière C, Bourrier A, Seksik P, Gornet JM, DeWit O, Nancey S, et al.; GETAID INFOPRO study group. Risk of serious infection in healthcare workers with inflammatory bowel disease: a case-control study of the Groupe d'Etude Thérapeutique des Affections Inflammatoires du tube Digestif (GETAID). Aliment Pharmacol Ther. 2018;48:713–22. https://doi.org/10.1111/apt.14926
9. Murphy ME, Wilmore S, Satta G, Witney A, Atzeni A, Sturgeon K, et al. Occupational tuberculosis despite minimal nosocomial contact in a health care worker undergoing treatment with a tumor necrosis factor inhibitor. Ann Am Thorac Soc. 2016;13:2275–7. https://doi.org/10.1513/AnnalsATS.201608-582LE
10. Stoltz A, Nathavitharana RR, de Kock E, Ueckermann V, Jensen P, Mendel CM, et al. Estimating the early transmission inhibition of new treatment regimens for drug-resistant tuberculosis. J Infect Dis. 2025;232:143–51. https://doi.org/10.1093/infdis/jiaf005

Address for correspondence: Nicolas Veziris, Assistance Publique Hôpitaux de Paris, Hôpital Saint-Antoine, 184 rue du Faubourg Saint-Antoine, 75012 Paris, France; email: nicolas.veziris@aphp.fr

Mycobacterium nanjing sp. nov. Isolated from Cutaneous Infection, China

Yidie Zou,[1] Youming Mei,[1] Wenyue Zhang, Ying Shi, Haiqin Jiang, Yukun Huang, Hongsheng Wang

Authors affiliation: Chinese Academy of Medical Sciences and Peking Union Medical College, Nanjing, China

DOI: https://doi.org/10.3201/eid3203.252001

We report a case of a cutaneous infection in an immunocompetent person in China caused by an uncharacterized *Mycobacterium* strain. The patient isolate was identified as a novel species by whole-genome sequencing. We propose *Mycobacterium nanjing* sp. nov. as the name for this new species.

Mycobacterial infections are a major public health concern and pose a continued threat to human health. The incidence and prevalence of nontuberculosis mycobacteria (NTM) infections are on the rise in certain regions and might surpass the rates of tuberculosis (*1*). In southeastern coastal China, the *Mycobacterium avium* complex, particularly *M. intracellulare*, predominates, followed by rapidly growing mycobacteria such as the *M. abscessus* complex. *M. kansasii* has been reported in some coastal cities (*2*). The relatively high NTM case count might be associated with warm climates, urban water systems, and improved laboratory detection (*3*–*5*). We report a case of cutaneous infection in Jiangsu Province, China, caused by an uncharacterized *Mycobacterium* strain, for which we propose the name *Mycobacterium nanjing* sp. nov.

In 2025, an 86-year-old man was admitted to the outpatient department with a subcutaneous nodule on his left palm. The patient reported the nodule appeared 1 month earlier after a minor penetrating trauma to the left palm caused by a wooden splinter during carpentry work. Physical examination revealed 2 red subcutaneous nodules on the left hand, 1 in the palm and 1 on the back of the hand, each measuring 0.5 cm (Figure). Laboratory tests revealed a reduced erythrocyte count of 3.82×10^9 cells/L (reference range $4.3–5.8 \times 10^{12}$ cells/L) and hemoglobin of 117 g/L (reference range 130–175 g/L). Serologic tests for syphilis, HIV, hepatitis B and C viruses, and tuberculosis were all negative.

Color doppler ultrasound revealed 3 hypoechoic masses in the dermis and subcutaneous fat layer of the left palm and back of hand lesions. The larger mass was in the palm, with uneven echo in the inner part, irregular shape, approximately 2.25 × 1.17 cm in size, approximately 0.93 cm in thickness, unclear boundary, no capsule, and enhanced echo in the surrounding soft tissue. Abundant blood flow was seen in and around the masses.

Histopathologic examination revealed hyperplasia of the epidermis and lymphocyte-dominated inflammatory cell infiltration in the superficial dermis. We conducted PCR testing on skin specimens by using common mycobacterial primers and cultured the samples on Löwenstein–Jensen slants. All PCRs included a no-template negative control that remained amplification-free. Direct PCR results were inconclusive. After 15 days of incubation at 37°C, we observed light yellow colonies on modified Löwenstein–Jensen medium slants (Figure). The organism was photochromogenic with a smooth appearance and slow growth rate.

We extracted DNA from the colonies for PCR analysis and aligned the sequences by using BLAST (https://blast.ncbi.nlm.nih.gov/Blast.cgi) for species identification. The partial sequence of the *hsp65* gene (736-bp) shared greatest similarity with *Mycolicibacterium gilvum* Spyr1 (95.18%), and the *rpoB* gene (435-bp) shared greatest similarity with *Mycolicibacterium vanbaalenii* strain L1I3 (97.30%). On the basis of those results, we propose this strain might be a new member of the *Mycobacterium* genus.

For precise pathogen species identification, we subjected the patient isolate, ZZG, to whole-genome sequencing on the DNBSEQ platform (MGI, https://mgi-tech.eu) at the Beijing Genomics Institute (Shenzhen, China), yielding 1,177 Mb of data at 195× depth. Whole-genome sequencing yielded a genome assembly of 5.75 Mb (6,029,915 bp) for isolate ZZG, with an overall GC content of 67.87%. We submitted the whole genome to the type strain genome server (https://tygs.dsmz.de) to evaluate digital DNA-DNA hybridization with all available mycobacterial genomes (Table). The result suggests this strain is closest to *M. vaccae* (ATCC no. 15483). The digital DNA-DNA hybridization value is 28.9% and was calculated by using the genome-to-genome distance calculator formula, which is far from the threshold value for species delineation (70%). For phylogenetic analysis, the 5 species most closely related to isolate ZZG identified by the Type Strain Genome Server were involved; *M. marinum* (ATCC no. 927) was the outgroup. We constructed a phylogenetic tree from core genes by using RAxML (https://github.com/amkozlov/raxml-ng) under

[1]These first authors contributed equally to this article.

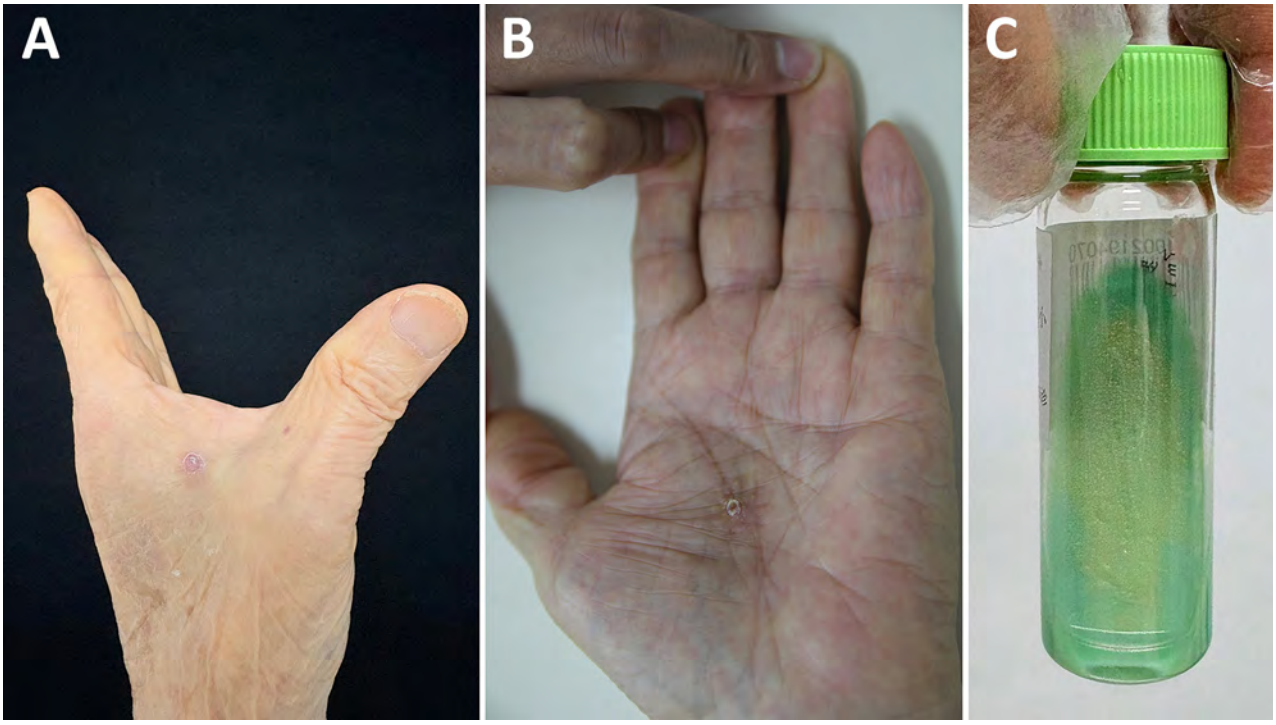

Figure. Novel cutaneous *Mycobacterium* infection in an 86-year-old man in China. A, B) Subcutaneous nodules on the left hand of the patient. C) *Mycobacterium* colonies grown on modified Löwenstein–Jensen medium slants.

the general time-reversible plus invariable site plus discrete Gamma model with 1,000 bootstrap replicates, which demonstrated that strain ZZG was a distinct monophyletic clade, independent of its closest relatives (Appendix Figure, http://wwwnc.cdc.gov/EID/article/32/3/25-2001-App1.pdf). We propose *Mycobacterium nanjing* sp. nov. as the name for this potential new species.

We initially treated the patient with moxifloxacin (400 mg 1×/d), and clarithromycin (250 mg 2×/d) for 14 days. Antimicrobial drug susceptibility testing then revealed susceptibility to meropenem, linezolid, ciprofloxacin, moxifloxacin, tobramycin, minocycline, trimethoprim/sulfamethoxazole, doxycycline, amikacin, and rifabutin but resistance to rifampin and amoxicillin. We prescribed a roxithromycin regimen (150 mg 2×/d) for the patient on the basis of those results.

In summary, we isolated a distinct *Mycobacterium* species from a patient with a cutaneous infection. We propose the name *Mycobacterium nanjing* sp. nov. for this species. *M. nanjing* can cause disease in immunocompetent patients and shows susceptibility to multiple antimicrobial drugs. Despite the advantages of direct molecular detection in sensitivity and convenience, culture remains the standard and an indispensable component of a complementary diagnostic strategy, particularly for emerging mycobacterial species. The combination of surgical resolutions with antimicrobial therapy could be a good option for patients with *Mycobacterium*–caused cutaneous infections.

This whole-genome project has been deposited at the DNA Data Bank of Japan, the European Nucleotide Archive, and GenBank (accession nos. JBTBFV000000000 and JBTBFV010000000).

Table. Genomic relatedness of novel strain ZZG recovered from patient with cutaneous *Mycobacterium* infection to closely related *Mycobacterium* species, China*

Subject strain	dDDH (95% CI), %†	G+C content difference
M. vaccae ATCC 15483	28.9 (26.5–31.4)	0.71
M. vanbaalenii PYR-1	28.4 (26.1–30.9)	0.08
M. austroafricanum DSM 44191	28.2 (25.9–30.7)	0.19
M. parafortuitum CCUG 20999	24.8 (22.5–27.3)	0.66
M. gilvum NCTC 10742	24.4 (22.1–26.9)	0.23
M. rufum DSM 45406	23.7 (21.4–26.1)	1.37

*dDDH, digital DNA-DNA hybridization.
†Calculated using the genome-to-genome distance calculation formula.

This study was supported by the Jiangsu Provincial Medical Key Laboratory, Jiangsu Province Capability Improvement Project through Science, Technology and Education (grant no. ZDXYS202204), National Natural Science Foundation of China (grant nos. 81972950, 82173431, 82103748), the Nanjing Incubation Program for National Clinical Research Center (grant no. 2019060001), and the Chinese Academy of Medical Sciences Innovation Fund for Medical Science (grant no. 2022-I2M-C&T-B-094).

About the Author

Ms. Zou is a medical student at the Institute of Dermatology, Chinese Academy of Medical Sciences and Peking Union Medical College in Nanjing, China. Her primary research interest is mycobacterial infectious diseases.

References

1. Shenjie T, Liang L, Xiaofeng Y, Meiying W. Guidelines for the diagnosis and treatment of nontuberculous mycobacteriosis (2020 edition). Chinese Journal of Tuberculosis and Respiratory. 2020;43:918–46. https://doi.org/10.3760/cma.j.cn112147-20200508-00570
2. Xu X, Lei Y, Zheng L. Non-tuberculous mycobacterial infections in mainland China and Taiwan: a systematic review and meta-analysis of epidemiology, species distribution, and drug resistance (2013–2024). Front Public Health. 2025;13:1676715. https://doi.org/10.3389/fpubh.2025.1676715
3. Faverio P, Del Castello L, Spotti M, Rebora P, Maggioni EC, Salerno R, et al.; METEO-NTM study group. How do climate conditions and urbanisation impact nontuberculous mycobacterial infections? An Italian nationwide case-control study. ERJ Open Res. 2025;11:00044–02025. https://doi.org/10.1183/23120541.00044-2025
4. Dowdell KS, Potgieter SC, Olsen K, Lee S, Vedrin M, Caverly LJ, et al. Source-to-tap investigation of the occurrence of nontuberculous mycobacteria in a full-scale chloraminated drinking water system. Appl Environ Microbiol. 2024;90:e0060924. https://doi.org/10.1128/aem.00609-24
5. Wang L, Chen Y, Wang Q, Pan J, Bao R, Jin W, et al. Comparison of molecular testing methods for diagnosing non-tuberculous mycobacterial infections. Eur J Clin Microbiol Infect Dis. 2025;44:109–16. https://doi.org/10.1007/s10096-024-04981-x

Address for correspondence: Hongsheng Wang, Chinese Academy of Medical Sciences and Peking Union Medical College, St. 12 Jiangwangmiao, Nanjing, Jiangsu, China; email: whs33@vip.sina.com

Cutaneous *Paraconiothyrium cyclothyrioides* Infection in Lung Transplant Recipient, Georgia, USA

Carolyn Mackey, Stephanie Thomas, Lucy S. Witt, Elizabeth Sajewski, Shawn R. Lockhart, Stephanie M. Pouch, Justin Cheeley, Jamie B. MacKelfresh, Jeremy A.W. Gold

Author affiliations: Georgia Emerging Infections Program, Atlanta, Georgia, USA (C. Mackey, S. Thomas, L.S. Witt, S.M. Pouch); Atlanta Veterans Affairs Health System, Decatur, Georgia, USA (C. Mackey, S. Thomas, L.S. Witt, S.M. Pouch); Emory University School of Medicine, Atlanta (C. Mackey, S. Thomas, L.S. Witt, S.M. Pouch, J. Cheeley, J.B. MacKelfresh); Centers for Diseases Control and Prevention, Atlanta (E. Sajewski, S.R. Lockhart, J.A.W. Gold)

DOI: http://doi.org/10.3201/eid3203.251042

We report a cutaneous infection caused by *Paraconiothyrium cyclothyrioides*, a rare environmental mold, in a lung transplant recipient in Georgia, USA. The infection resolved with posaconazole after substantial diagnostic delays and related side effects. This case underscores the need for improved clinical awareness, diagnostic testing, treatments, and surveillance for such infections.

Environmentally acquired infections caused by rare molds are a growing public health concern because of potential disease severity, rising numbers of susceptible immunocompromised persons, and changes to the natural environment that are shifting fungal disease epidemiology (*1*,*2*). *Paraconiothyrium cyclothyrioides*, a Coelomycete, is an environmental mold found on plants and in soil (*3*). Seven cases of human *P. cyclothyrioides* infection have been reported, most cutaneous (*3*–*9*). The incidence of *P. cyclothyrioides* and other rare mold infections might be underestimated, however, because routine laboratory methods often cannot identify them or classify them as contaminants. Reliable identification usually requires molecular diagnostics that are not commonly performed. Thus, data to inform clinical recognition, treatment, and future surveillance efforts are sparse. We present a case of cutaneous *P. cyclothyrioides* infection in a lung transplant recipient in Georgia, USA, identified through Centers for Disease Control and Prevention's Emerging Infections Program (EIP) invasive mold diseases surveillance system.

The EIP is a collaborative effort among public health agencies, healthcare providers, and academic

institutions aimed at enhancing public health capacity to address emerging infectious threats (https://www.cdc.gov/emerging-infections-program/php/about/index.html). The EIP invasive mold diseases team in Georgia conducts active, sentinel, laboratory-based surveillance at Atlanta-area healthcare facilities using a standardized case report form to collect patients' data from electronic medical records. Georgia EIP surveillance activities were approved by the Institutional Review Board, granting a consent and HIPAA waiver.

A 67-year-old man underwent unilateral lung transplantation for idiopathic pulmonary fibrosis. He received basiliximab for induction immunosuppression and a regimen of mycophenolate mofetil, tacrolimus, and prednisone for maintenance immunosuppression. At time of transplantation, after isolation of *Aspergillus niger* from the donor airway, physicians treated the patient with inhaled amphotericin B and oral posaconazole. The patient experienced acute cellular rejection ≈9 months posttransplantation, which physicians treated with thymoglobulin. Thereafter, the patient completed a 16-month course of posaconazole, ending treatment because of fatigue. Physicians identified environmental molds *Penicillium* and *Fonsecaea* species in separate bronchoalveolar lavage cultures shortly after the patient completed posaconazole treatment but did not administer treatment, considering both to be contaminants.

Twenty-eight months after the transplant (1 year after completing posaconazole), the patient noticed a nodule on his shin. He visited a dermatology clinic 4 months later for 2 verrucous pink nodules on his right shin. Skin biopsies done for histopathology and culture showed polymorphic dematiaceous hyphal elements not further speciated, and clinicians initiated no treatment at that first visit. The patient gained referral to an academic dermatology clinic and sought treatment there 3 months later. His lesions had not substantially spread or evolved (Figure 1). Clinicians submitted another tissue biopsy for culture and histopathology. Histopathologic examination revealed numerous polymorphic forms within the superficial dermis, with overlying epidermal pseudoepitheliomatous hyperplasia (Figure 2).

Pending species identification, and under the supervision of an infectious diseases physician, the patient began oral posaconazole treatment. Treating physicians initially prescribed isavuconazole, but the treatment was cost prohibitive. The patient achieved therapeutic posaconazole levels (trough 1.8 μg/mL) and, after 6 weeks of treatment, the skin lesions healed, leaving 2 residual scars. His treatment course was complicated by tremor and insomnia related to drug-drug interactions between posaconazole and tacrolimus, despite appropriate tacrolimus dose reduction. Posaconazole was discontinued after 6 weeks, with clinical resolution.

Technicians ultimately identified dematiaceous mold from the patient's culture, initially speciated by a reference laboratory as *Phanerochaete* species. Two months after the specimen was collected (8 months after the lesions first appeared and after treatment completion), DNA sequencing analysis revealed the mold to be *P. cyclothyrioides*. The isolate was unavailable for antifungal drug susceptibility testing.

This case of cutaneous *P. cyclothyrioides* in a lung transplant recipient highlights the pathogen as a potential cause of chronic, indolent skin infections in immunocompromised persons. Biopsy and culture

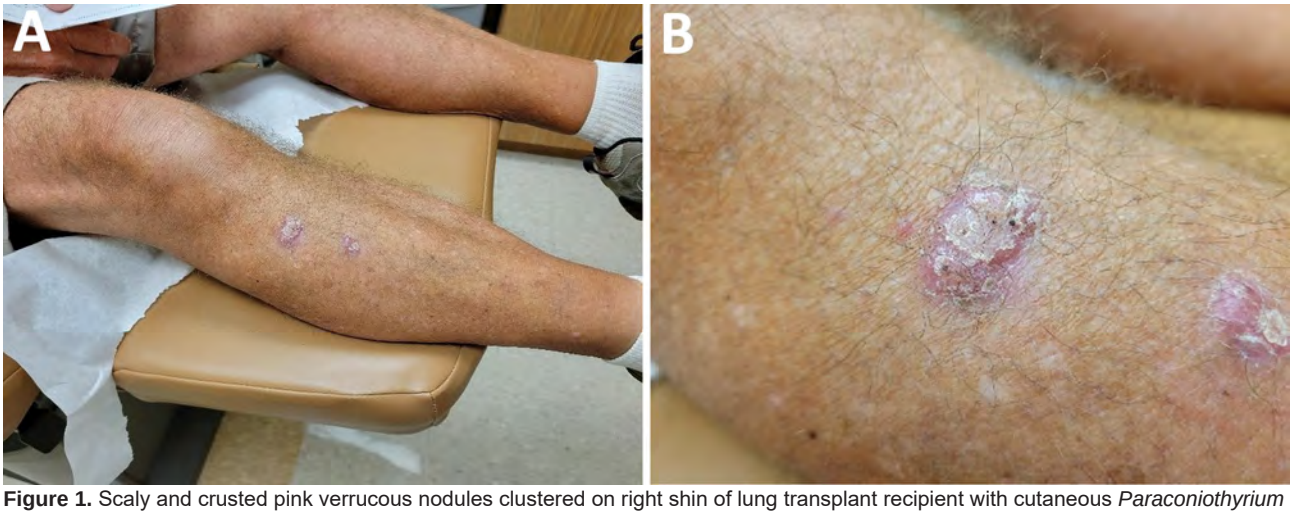

Figure 1. Scaly and crusted pink verrucous nodules clustered on right shin of lung transplant recipient with cutaneous *Paraconiothyrium cyclothyrioides* infection, Georgia, USA.

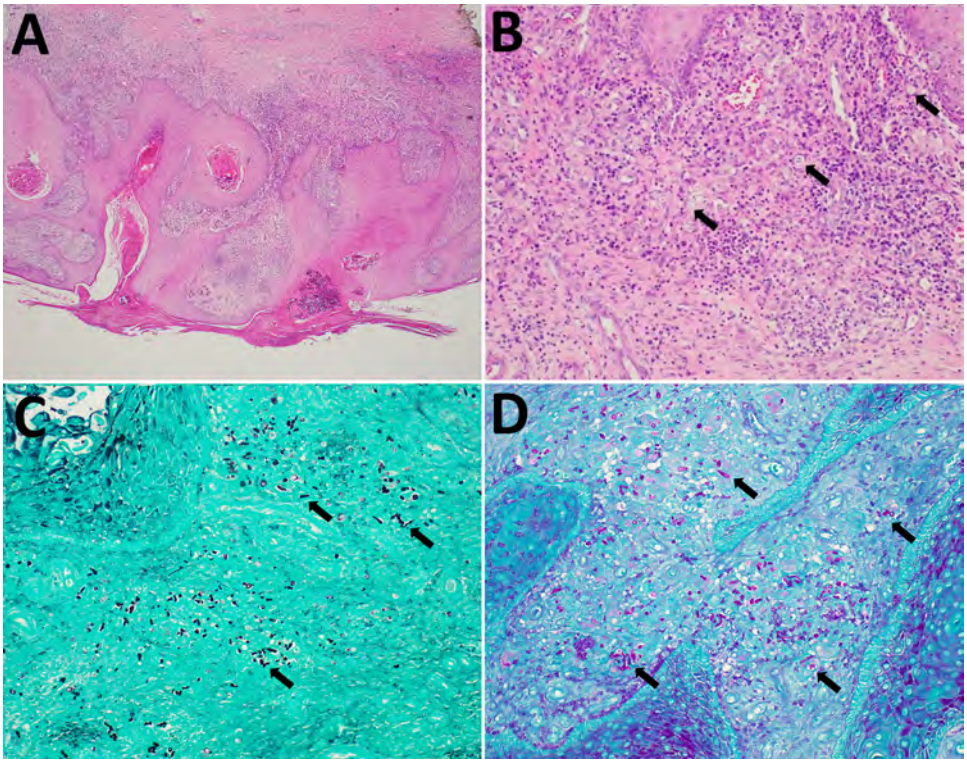

Figure 2. Histologic (A, B) and histochemical (C, D) findings from case of cutaneous *Paraconiothyrium cyclothyrioides* in lung transplant recipient, Georgia, USA. A) Skin biopsy from right shin revealed psuedoepitheliomatous hyperplasia of the epidermis overlying a mixed dermal inflammatory infiltrate. Hematoxylin and eosin stain; original magnification ×40. B) Polymorphic fungal elements (arrows) seen within the superficial dermis. Hematoxylin and eosin stain; original magnification ×200. C) Numerous fungal hyphal elements and yeast-like forms (arrows) highlighted within the dermis. Grocott methenamine silver stain; original magnification ×200. D) Fungal hyphal elements and yeast-like forms (arrows) noted by Periodic acid–Schiff stain; original magnification ×200.

are essential for diagnosing cutaneous infections in immunocompromised patients, and DNA sequencing is required to identify *P. cyclothyrioides*. Prompt referral to an infectious diseases specialist or a larger medical center with experience in transplantation can help promote accurate diagnosis and treatment while final speciation results are pending. If the biopsy or culture reveals fungus and species identification is delayed or not possible, healthcare providers should consider broad-spectrum antifungal therapies. The prolonged time needed for diagnosis, therapy initiation, and causative species identification in this case report aligns with previous reports (*3*–*8*), emphasizing the importance of heightened clinical suspicion. Further, the timeline of this case reinforces the need to develop rapid diagnostic tests to identify rare molds and distinguish between infection, colonization, and contamination (*1*,*2*).

In summary, our report underscores the need for heightened clinical awareness, improved diagnostics, and better antifungal options for rare mold infections such as *P. cyclothyrioides* and emphasizes the importance of ongoing surveillance. Treatment challenges associated with rare mold infections are common, as illustrated in this case, because appropriate antifungal drugs can be expensive, cause marked side effects, and interact with other drugs, including immunosuppressants frequently used by at-risk patients (*1*,*2*). In this instance, the patient's infection resolved successfully with posaconazole. Prior *P. cyclothyrioides* case reports involved successful infection resolution following treatment with posaconazole, itraconazole, isavuconazole, or voriconazole (*3*,*5*–*9*).

Acknowledgments

We acknowledge the work that Ana Mesa Restrepo contributed in reviewing the medical record for this patient, and we thank the rest of the Georgia Emerging Infections Program and staff who collected and maintained this data or the specimens.

This activity was reviewed by CDC, deemed not research, and was conducted consistent with applicable federal law and CDC policy (see e.g., 45 C.F.R. part 46.102(l)(2), 21 C.F.R. part 56; 42 U.S.C. §241(d); 5 U.S.C. §552a; 44 U.S.C. §3501 et seq.)

ChatGPT (OpenAI) was used for assistance with language editing of this manuscript; all intellectual content is the sole responsibility of the authors.

About the Author

C. Mackey is project coordinator for the Invasive Mold Disease Surveillance Team within the Georgia Emerging Infections Program, Atlanta, Georgia. Her research interests include the epidemiology of fungal and bacterial infections.

References

1. van Rhijn N, Bromley M. The consequences of our changing environment on life threatening and debilitating fungal diseases in humans. J Fungi (Basel). 2021;7:367. https://doi.org/10.3390/jof7050367
2. World Health Organization. WHO fungal priority pathogens list to guide research, development and public health action. Geneva: World Health Organization. 2022 [cited 2025 Jul 10]. https://www.who.int/publications/i/item/9789240060241.
3. Gordon RA, Sutton DA, Thompson EH, Shrikanth V, Verkley GJ, Stielow JB, et al. Cutaneous phaeohyphomycosis caused by *Paraconiothyrium cyclothyrioides*. J Clin Microbiol. 2012;50:3795–8. https://doi.org/10.1128/JCM.01943-12
4. Colombier MA, Alanio A, Denis B, Melica G, Garcia-Hermoso D, Levy B, et al. Dual invasive infection with *Phaeoacremonium parasiticum* and *Paraconiothyrium cyclothyrioides* in a renal transplant recipient: case report and comprehensive review of the literature of Phaeoacremonium phaeohyphomycosis. J Clin Microbiol. 2015;53:2084–94. https://doi.org/10.1128/JCM.00295-15
5. Hamed A, Bosshardt Hughes O, Palavecino EL, Jakharia N. Cutaneous infection caused by *paraconiothyrium cyclothyrioides* in a renal transplant recipient. Transpl Infect Dis. 2021;23:e13624. https://doi.org/10.1111/tid.13624
6. Malaure C, Hoang S, Bagny K, Tauziède-Espariat A, Garcia-Hermoso D, Kamus L, et al. Multifocal cutaneous phaeohyphomycosis caused by *Paraconiothyrium cyclothyrioides* in an immunocompromised patient: a case report. J Dermatol. 2023;50:e179–80. https://doi.org/10.1111/1346-8138.16706
7. Li J, Yaqoob MD, Liu K, Sun H, Qiu Q, Ke X, et al. A cutaneous phaeohyphomycosis case caused by *Paraconiothyrium cyclothyrioides* in southern China. Infect Drug Resist. 2024;17:2401–4. https://doi.org/10.2147/IDR.S470026
8. Mori H, Hayashi S, Okamoto M, Nagaoka S, Suzuki T, Igawa K. *Paraconiothyrium cyclothyrioides* infected on the sole of a healthy person: a case report. J Dermatol. 2022;49:e278–9. https://doi.org/10.1111/1346-8138.16403
9. Aulakh P, Leon J, Gonzales Zamora JA. *Paraconiothyrium cyclothyroides* pneumonia: report of a unique case. D48 Lung infection case reports I: fungal infections. Am J Respir Crit Care Med. 2016;193:A7147.

Address for correspondence: Carolyn Mackey, Emory University, 1462 Clifton Rd NE, 5th Fl, Mail Code 1370-005-1AA, Atlanta, GA 30322, USA; email: cmacke6@emory.edu

Indeterminant Interferon-γ Release Assays in Refugee Children with Splenomegaly, Uganda, 2020–2023

Christina R. Phares, Moses Mwesigwa, Sean R. Toney

Author affiliations: Centers for Disease Control and Prevention, Atlanta, Georgia, USA (C.R. Phares, S.R. Toney); Migration Health Division, International Organization for Migration, Geneva, Switzerland (M. Mwesigwa)

DOI: http://doi.org/10.3201/eid3203.251200

We observed a novel association between splenomegaly and indeterminate interferon-γ release assays in refugee children 5–14 years of age in Uganda. Those demonstrating splenomegaly were 4 times more likely to have indeterminate results. Among refugee children 2–4 years of age, >10% had indeterminate results even without splenomegaly.

Refugees bound for the United States must undergo a health assessment before US entry; results are recorded in the Centers for Disease Control and Prevention (CDC) Electronic Disease Notification (EDN) system. In East Africa and other areas with a high burden of tuberculosis (TB), the assessment includes an interferon-γ release assay (IGRA) to detect infection (*1*). Before October 2024, the IGRA requirement applied to applicants 2–14 years of age living in countries with a World Health Organization (WHO)–estimated TB incidence rate ≥20 cases/100,000 population. This requirement has since been expanded to applicants ≥2 years of age. A 2023 CDC review of EDN data for refugees 2–14 years of age noted the proportion of indeterminate IGRA results in Uganda exceeded the expected frequency of ≤2.5% for the QuantiFERON-TB Gold Plus (QIAGEN, https://www.qiagen.com) package insert.

Splenomegaly is a clinical concern among refugees in Uganda. In a 2015 investigation of 987 US-bound Congolese refugees examined in Uganda, nearly 15% had splenomegaly (*2*). Although the investigation did not establish a definitive etiology, hyperreactive malarial splenomegaly syndrome is a leading cause of massive splenomegaly in malaria-endemic countries (*3*). Prompted by those findings, panel physicians added an enhanced abdominal examination to predeparture health assessments in Uganda that included physical examination and, for

palpable spleens, an ultrasound. The abdominal examination occurs before presumptive treatments for malaria and intestinal parasites, which are routinely provided to refugees in Uganda (*4*). Splenomegaly is defined as spleen size by ultrasound >2 SD above the height-adjusted mean. Factors affecting the immune system have been linked to indeterminate IGRA results (*5*,*6*), and splenomegaly can be linked to immune dysregulation. Therefore, we analyzed health assessment data to determine whether splenomegaly was associated with indeterminate IGRA results among refugee children in Uganda.

Overall, 11,721 refugees 2–14 years of age who were examined in East Africa arrived in the United States during fiscal years 2020–2023 (October 2019–September 2023). Among 1,863 mostly Congolese (86.8%) children examined in Uganda, 87.5% of IGRA test results were negative, 5.7% were positive, and 6.8% were indeterminate. In comparison, among 9,858 mostly Congolese (93.0%) children examined elsewhere in East Africa, 2.9% had an indeterminate IGRA.

In Uganda, the proportion of indeterminate results among older children (5–14 years) was 17.0% for those with splenomegaly and 4.2% for those without splenomegaly; among younger children (2–4 years), proportions were 16.7% and 10.6% (Table). We also modeled the relative prevalence of indeterminate IGRA results by splenomegaly status (Appendix, https://wwwnc.cdc.gov/EID/article/32/3/25-1200-App1.pdf) and found splenomegaly was associated with a significantly increased prevalence of indeterminate results for older children but not younger children (Table).

Results for repeated IGRAs performed in the United States, typically within 3 months of arrival, were available in EDN for 60 children. Four (7.4%) of 54 older children and 0 of 6 younger children had an indeterminate or borderline result in the United States. US data are limited because results from domestic examination are only captured by EDN for refugees assigned an overseas TB classification. Among the 1,863 refugee children examined in Uganda during the period we studied, 1,754 lacked such a classification, including all 126 children with an indeterminate IGRA result overseas. In addition, a repeat domestic IGRA test is not recommended for those with a positive prior IGRA or with a recent (<6 months) negative IGRA and no TB signs or symptoms (*7*). However, retesting still occurs in practice, as in the case of the 60 children retested in the context of this study.

Our findings suggest a previously unrecognized correlation between splenomegaly and indeterminate IGRA results for refugee children 5–14 years of age in Uganda. Interpreting this correlation is complicated because research has also linked conditions associated with splenomegaly, including malaria, helminthiases, anemia, and HIV infection (*8*), with indeterminate IGRA results (*5*,*6*). Thus, it is unclear whether the observed association is mediated by the pathology causing splenomegaly, impaired splenic function, or other factors. We also noted a high proportion of indeterminate IGRA results for younger children, as others have found (*5*,*6*), even among those without splenomegaly.

The first limitation of this retrospective and programmatic analysis is that the underlying cause of splenomegaly among refugees in Uganda remains uncertain. We lacked systematic data on infections and other clinical factors, limiting inference. IGRA results were qualitative only, preventing assessment of whether indeterminate results related to mitogen control failures or elevated responses in the negative control.

Our observations should be interpreted as hypothesis-generating. Additional investigation is needed to identify the causes of splenomegaly and determine whether the association with increased QFT-Plus indeterminate results reflects splenomegaly itself, its etiologies, comorbidities, or a combination. Further work is also needed to determine whether a link exists for other IGRA tests, other age groups, or other populations with splenomegaly. When a high

Table. Interferon-γ release assay result by splenomegaly status and age group among US-bound refugee children examined in Uganda, 2020–2023*

Age group and splenomegaly status	Assay result, no. (%)		Prevalence ratio (95% CI)
	Indeterminate, n = 126	Not indeterminate, n = 1,737	
Age 2–14 y, N = 1,863			
Splenomegaly, n = 177	30 (16.9)	147 (83.1)	3.0 (2.0–4.1)
No splenomegaly, n = 1,686	96 (5.7)	1,590 (94.3)	NA
Age 2–4 y, n = 419			
Splenomegaly, n = 24	4 (16.7)	20 (83.3)	1.6 (0.6–4.0)
No splenomegaly, n = 395	42 (10.6)	353 (89.4)	NA
Age 5–14 y, n = 1,444			
Splenomegaly, n = 153	26 (17.0)	127 (83.0)	4.1 (2.6–6.3)
No splenomegaly, n = 1,291	54 (4.2)	1,237 (95.8)	NA

*NA, not applicable.

number of indeterminate IGRA results coincide with prevalent splenomegaly, we advise caution in attributing such results solely to splenomegaly without investigating other potential causes, such as mishandling specimens or errors in processing. This study underscores the prudence of a repeat IGRA after arrival in the United States for any refugee with an indeterminate or borderline IGRA result (*1*).

Acknowledgments

We thank Alison Zabron (International Organization for Migration, Tanzania), Alex Klosovsky (International Organization for Migration, Geneva, Switzerland), Abena Asante (International Organization for Migration, Washington, DC), and Elizabeth Soda and Kimberly Skrobarcek (Division of Global Migration Health, National Center for Emerging and Zoonotic Infectious Diseases, Centers for Disease Control and Prevention) for their valuable contributions to this work.

We conducted this activity consistent with applicable federal law and CDC policy. The CDC reviewed the activity prior to its undertaking, deeming it not research. The findings and conclusions of this report are those of the authors and do not represent the official position of the Centers for Disease Control and Prevention or the institutions with which the authors are affiliated.

About the Author

Dr. Phares is a senior scientist with the CDC National Center for Emerging and Zoonotic Infectious Diseases, Division of Global Migration Health, Immigrant and Refugee Health Branch, Atlanta. Her areas of interest include migration health and tuberculosis.

References

1. Centers for Disease Control and Prevention. Tuberculosis technical instructions for panel physicians; 2024 May 15 [cited 2025 Aug 6]. https://www.cdc.gov/immigrant-refugee-health/hcp/panel-physicians/tuberculosis.html
2. Goers M, Ope MO, Samuels A, Gitu N, Akandwanaho S, Nabwami G, et al. Notes from the field: splenomegaly of unknown etiology in Congolese refugees applying for resettlement to the United States—Uganda, 2015. MMWR Morb Mortal Wkly Rep. 2016;65:943–4. https://doi.org/10.15585/mmwr.mm6535a5
3. Leoni S, Buonfrate D, Angheben A, Gobbi F, Bisoffi Z. The hyper-reactive malarial splenomegaly: a systematic review of the literature. Malar J. 2015;14:185. https://doi.org/10.1186/s12936-015-0694-3
4. Centers for Disease Control and Prevention. Refugee health overseas guidance; 2024 May 15 [cited 2025 Aug 6]. https://www.cdc.gov/immigrant-refugee-health/hcp/overseas-guidance/index.html
5. Banfield S, Pascoe E, Thambiran A, Siafarikas A, Burgner D. Factors associated with the performance of a blood-based interferon-γ release assay in diagnosing tuberculosis. PLoS One. 2012;7:e38556. https://doi.org/10.1371/journal.pone.0038556
6. Zhou G, Luo Q, Luo S, Chen H, Cai S, Guo X, et al. Indeterminate results of interferon gamma release assays in the screening of latent tuberculosis infection: a systematic review and meta-analysis. Front Immunol. 2023;14:1170579. https://doi.org/10.3389/fimmu.2023.1170579
7. Centers for Disease Control and Prevention. Refugee health domestic guidance; 2024 July 25 [cited 2025 Nov 20]. https://www.cdc.gov/immigrant-refugee-health/hcp/domestic-guidance/tuberculosis.html
8. Suttorp M, Classen CF. Splenomegaly in children and adolescents. Front Pediatr. 2021;9:704635. https://doi.org/10.3389/fped.2021.704635

Address for correspondence: Christina Phares, Centers for Disease Control and Prevention, 1600 Clifton Rd NE, Mailstop H16-4, Atlanta, GA 30329-4018, USA; email: cphares@cdc.gov

Two Cases of Posttraumatic *Kosakonia* Infection, Argentina, 2023

Claudia Barberis, Maria Sol Haim, Paula Zomero, Germán Traglia, Alejandro Ellis, Roxana Cittadini, Tomás Poklépovich, Marisa Almuzara, Carlos Vay

Author affiliations: University of Buenos Aires, Faculty of Pharmacy and Biochemistry, "Hospital de Clínicas José de San Martín", Buenos Aires, Argentina (C. Barberis, P. Zomero, M. Almuzara, C. Vay); National Center for Genomics and Bioinformatics Unit, ANLIS "Dr. Carlos G. Malbrán", Buenos Aires (M.S. Haim, T. Poklépovich); CENUR Litoral Norte Genomics and Bioinformatics Unit, University of the Republic, Salto, Uruguay (G. Traglia); Sanatorio Mater Dei, Buenos Aires (A. Ellis, R. Cittadini, C. Vay)

DOI: http://doi.org/10.3201/eid3203.251714

We describe 2 plant-associated posttraumatic *Kosakonia* infections in Argentina. Facing biochemical and matrix-assisted laser desorption/ionization time-of-flight mass spectrometry limitations, we used whole-genome sequencing to successfully identify *K. cowanii* and *K. oryzae* as the causative agents. Our data highlight the crucial role of genomics in correctly identifying these underestimated emerging pathogens.

Medical literature recognized the genus *Kosakonia* in 2013, after the systematic reorganization of *Enterobacter* genus (*1*). Largely known as plant growth–promoting bacteria, or phytopathogens (*2*), the species included in this genus are rapidly gaining relevance as opportunistic human pathogens. However, because of the bacteria's phenotypic similarities with *Enterobacter* and *Pantoea*, clinicians frequently misidentify *Kosakonia* infections, leading to an underestimation of their true clinical incidence (*3*–*5*). We describe 2 cases of osteomyelitis in Argentina caused by *Kosakonia* species associated with environmental trauma.

Case 1 involved a 12-year-old girl with an open supracondylar elbow fracture sustained falling from a horse and involving soil contamination. Despite surgical fixation and cephalosporin prophylaxis, she sought treatment 10 days later for purulent discharge. Cultures yielded a gram-negative rod (isolate CMVA41). We treated the suspected osteomyelitis with intravenous piperacillin/tazobactam and clindamycin, followed by oral ciprofloxacin and clindamycin for 6 weeks, resulting in complete resolution.

Case 2 involved a 20-year-old man with chronic posttraumatic knee osteomyelitis following a puncture with a tree thorn. We cultured a gram-negative rod (isolate CMVA47) from surgical samples. We administered vancomycin and piperacillin/tazobactam, followed by a course of oral amoxicillin and ciprofloxacin for 6 weeks, achieving clinical cure.

We performed a polyphasic identification approach for both cases. Colonies were yellow and lactose-fermenting on eosin methylene blue (Levine) agar. Initial phenotypic identification using conventional biochemical tests failed to provide reliable genus-level identification (Appendix Table, https://wwwnc.cdc.gov/EID/article/32/3/25-1714-App1.pdf). We subsequently performed matrix-assisted laser desorption/ionization time-of-flight (MALDI-TOF) mass spectrometry (Bruker Biotyper, library v13.0; https://www.bruker.com). We identified isolate CMVA47 as *Kosakonia cowanii* with a secure species-level score (2.052). In contrast, we initially misidentified isolate CMVA41 as *K. radicincitans* with a low confidence score (1.717), indicating probable genus-level identification but species uncertainty. This result highlighted a limitation: the spectral library lacked a reference profile for *K. oryzae*, leading to potential misclassification (*6*).

To resolve those uncertainties, we performed whole-genome sequencing (WGS) using the Illumina NovaSeq6000 platform (https://www.illumina.com). For strain CMVA41, the 16S rRNA gene sequence showed 100% identity with the reference

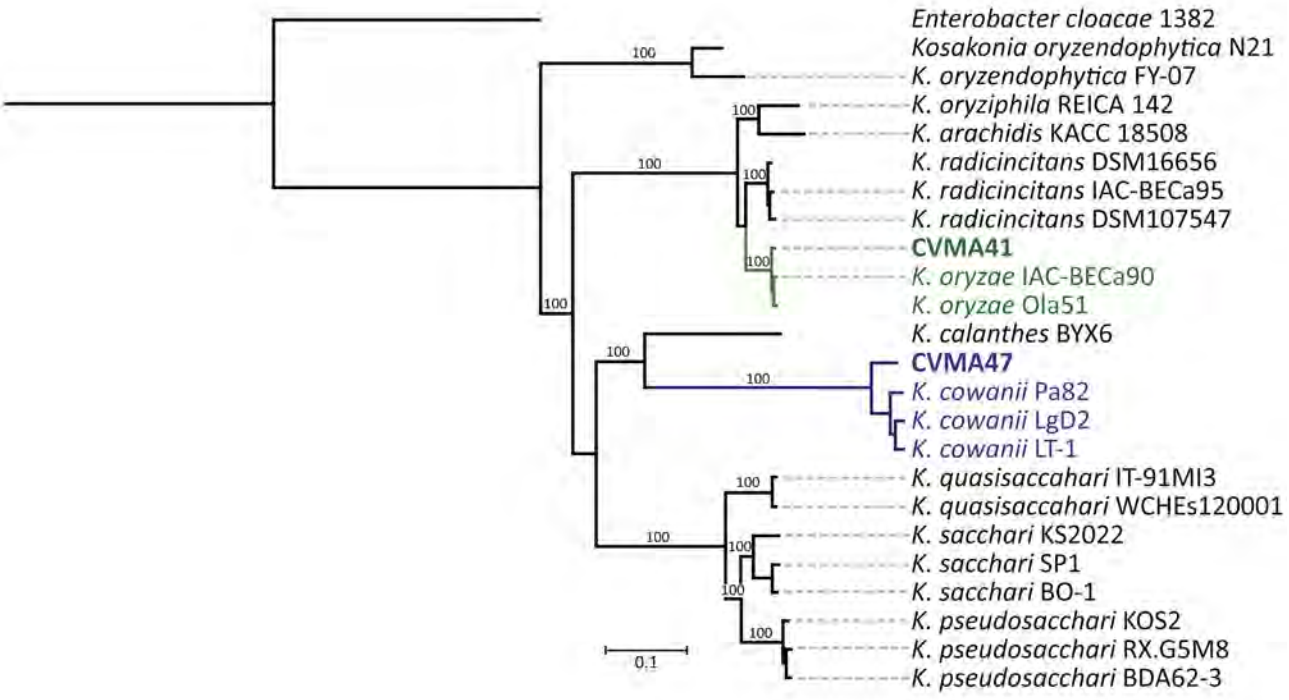

Figure. Data from a study of 2 cases of posttraumatic *Kosakonia* infection, Argentina, 2023. Maximum-likelihood phylogeny calculated using 1,214,977 single-nucleotide variants from a core-gene alignment of 3,232 genes from genomes of *Kosakonia*-described species with 1,000 bootstraps. Green indicates CVMA41 clusters, violet indicates CVMA47 clusters. Tree rooted in an *Enterobacter cloacae* genome included as an outgroup. Scale bar indicates substitutions per site.

K. oryzae sequence Ola 51. Relative to the same reference, we noted an average nucleotide identity value of 98.83% and a digital DNA-DNA hybridization value of 91.6%, with ribosomal multilocus sequence typing identifying the strain as the same species with 94% support. Those results differed from MALDI-TOF mass spectrometry identification and indicated *K. oryzae* as a clinically relevant human pathogen. For strain CMVA47, although the 16S rRNA gene (99.77% identity) and average nucleotide identity (95.94%) supported identification as *K. cowanii*, the digital DNA-DNA hybridization value (65.1%) fell below the 70% threshold typically used for species delineation.

We produced a core genome phylogeny analysis based on concatenated sequences of 3,232 core genes that shared ≥50% sequence identity and were present in ≥80% of the included genomes (1 reference genome of each *Kosakonia* species, if present, downloaded from the National Center for Biotechnology Information RefSeq database [https://www.ncbi.nlm.nih.gov/refseq]). CVMA41 clustered with *K. oryzae* and CVMA47 clustered with *K. cowanii*, with 100% bootstrap support (Figure). The genomic divergence observed in CMVA47 suggested that revisiting genomic thresholds within the *Kosakonia* genus might be necessary, as seen in other genera (*7*).

Antimicrobial susceptibility testing revealed that both isolates were susceptible to aminoglycosides, fluoroquinolones, trimethoprim/sulfamethoxazole, extended-spectrum cephalosporins, and carbapenems. Of note, although CMVA41 was susceptible to all tested agents, CVMA47 exhibited resistance to ampicillin and intermediate susceptibility to cefazolin. This phenotypic profile serves as a marker distinguishing *Kosakonia* spp. from *Enterobacter cloacae* complex. *Enterobacter cloacae* complex typically exhibits intrinsic resistance to ampicillin/sulbactam and carries an inducible chromosomal *ampC* β-lactamase that can lead to third-generation cephalosporin resistance upon derepression, but both *Kosakonia* isolates remained susceptible to these agents. Genomic analysis confirmed the absence of *ampC* and its regulator *ampR* in both strains. This distinction is clinically relevant, supporting the use of ampicillin/sulbactam or cephalosporins as therapeutic options, sparing carbapenems. Consequently, we theorized that the ampicillin resistance in CVMA47 was likely attributable to the putative chromosomic β-lactamase KSA-1, which was identified in *Kosakonia sacchari*, showing 78.6% similarity to this class A extended-spectrum β-lactamase, rather than an AmpC-type enzyme (*8*). Our results further support that genomic divergence in CVMA47 is biologically meaningful. Researchers noted similar findings regarding *Kluyvera* spp., where the presence of intrinsic β-lactamases were linked to species differentiation and the proposal of refined taxonomic thresholds (*9*).

Identifying *Kosakonia* isolates in this study illustrates the challenges that clinical laboratories face with emerging pathogens. The cases we describe contribute to the growing evidence that *Kosakonia* infections are strongly associated with traumatic inoculation of plant material, although reports have described endogenous infections (*3*,*10*). The identification of *K. oryzae* as a human pathogen expands the spectrum of *Kosakonia* species with clinical relevance. MALDI-TOF mass spectrometry represents a considerable improvement over biochemical tests, but the reliability of such analysis is contingent on updated databases (*6*). WGS thus stands as the standard for accurate identification of such environmental pathogens, essential for defining their epidemiology and guiding antimicrobial stewardship.

Short reads for both sequenced isolates have been submitted to the National Center for Biotechnology Information Short Read Archive (accession no. PRJNA1389793).

This study was conducted in accordance with the Ethics Committee of Hospital de Clínicas José de San Martín, Buenos Aires, Argentina, and the Declaration of Helsinki (2024 version), the National Ministry of Health Resolution 1480/11, and the National Law on Personal Data Protection No. 25.326

About the Author

Dr. Barberis is an adjunct professor at the University of Buenos Aires and serves at the "Hospital de Clínicas José de San Martín", Buenos Aires, Argentina, as a biochemist and bacteriologist. Her areas of clinical interest include microbiology teaching, identification and taxonomy of emerging pathogens, and the challenges in clinical diagnostics, including proteomics and antimicrobial resistance.

References

1. Brady C, Cleenwerck I, Venter S, Coutinho T, De Vos P. Taxonomic evaluation of the genus *Enterobacter* based on multilocus sequence analysis (MLSA): proposal to reclassify *E. nimipressuralis* and *E. amnigenus* into *Lelliottia* gen. nov. as *Lelliottia nimipressuralis* comb. nov. and *Lelliottia amnigena* comb. nov., respectively, *E. gergoviae* and *E. pyrinus* into *Pluralibacter* gen. nov. as *Pluralibacter gergoviae* comb. nov. and *Pluralibacter pyrinus* comb. nov., respectively, *E. cowanii*, *E. radicincitans*, *E. oryzae* and *E. arachidis* into *Kosakonia* gen.

nov. as *Kosakonia cowanii* comb. nov., *Kosakonia radicincitans* comb. nov., *Kosakonia oryzae* comb. nov. and *Kosakonia arachidis* comb. nov., respectively, and *E. turicensis*, *E. helveticus* and *E. pulveris* into *Cronobacter* as *Cronobacter zurichensis* nom. nov., *Cronobacter helveticus* comb. nov. and *Cronobacter pulveris* comb. nov., respectively, and emended description of the genera *Enterobacter* and *Cronobacter*. Syst Appl Microbiol. 2013;36:309–19. https://doi.org/10.1016/j.syapm.2013.03.005

2. Peng G, Zhang W, Luo H, Xie H, Lai W, Tan Z. *Enterobacter oryzae* sp. nov., a nitrogen-fixing bacterium isolated from the wild rice species *Oryza latifolia*. Int J Syst Evol Microbiol. 2009;59:1650–5. https://doi.org/10.1099/ijs.0.005967-0
3. Berinson B, Bellon E, Christner M, Both A, Aepfelbacher M, Rohde H. Identification of *Kosakonia cowanii* as a rare cause of acute cholecystitis: case report and review of the literature. BMC Infect Dis. 2020;20:366. https://doi.org/10.1186/s12879-020-05084-6
4. Merlino J, Pillay K, Rizzo S, Baskar SR, Seed D, Siarakas S, et al. Bacterial skin infection caused by a plant pathogen *Kosakonia cowanii*: identification with the MALDI Biotyper sirius one and susceptibility testing. Access Microbiol. 2025;28;7:000923.v3.
5. Washio M, Sonobe K, Teshima T. Rhabdomyolysis due to bacteremia from *Enterobacter cowanii* caused by a rose thorn prick. J Dermatol. 2018;45(11):e313–4. https://doi.org/10.1111/1346-8138.14341
6. Singhal N, Kumar M, Kanaujia PK, Virdi JS. MALDI-TOF mass spectrometry: an emerging technology for microbial identification and diagnosis. Front Microbiol. 2015;6:791. https://doi.org/10.3389/fmicb.2015.00791
7. Elbir H. Updating the relationship between the threshold value of average nucleotide identity and digital DNA-DNA hybridization for reliable taxonomy of *Corynebacterium*. Vet Sci. 2024;11:661. https://doi.org/10.3390/vetsci11120661
8. Fournier C, Nordmann P, de la Rosa JO, Kusaksizoglu A, Poirel L. KSA-1, a naturally occurring Ambler class A extended spectrum β-lactamase from the enterobacterial species *Kosakonia sacchari*. J Glob Antimicrob Resist. 2024;39:6–11. https://doi.org/10.1016/j.jgar.2024.07.008
9. Rodriguez MM, Gutkind G. Re-updating the taxonomy of *Kluyvera* genus for a better understanding of CTX-M β-lactamase origin. Microbiol Spectr. 2024;12:e0405423. https://doi.org/10.1128/spectrum.04054-23
10. Duployez C, Edun-Renard ME, Kipnis E, Dessein R, Le Guern R. Bacteremia due to *Kosakonia cowanii* in a preterm neonate. J Pediatr Infect Dis. 2021;16(4):183-186. doi: 10.1055/s-0040-1721448

Address for correspondence: Claudia Barberis, Hospital de Clíncas. Facultad de Farmacia y Bioquimica–Bioquímica Clínica, Av. Córdoba 2351 Capital Federal, Buenos Aires 1120, Argentina; email: claudiabar07@gmail.com

Mycobacterium riyadhense Pulmonary Disease after Relocation from Saudi Arabia, Japan

Takuya Ozawa, Takeshi Komine, Sohei Nakayama, Yusuke Suzuki, Naoki Hasegawa, Koichi Fukunaga, Ho Namkoong, Hanako Fukano, Takanori Asakura

Author affiliations: Keio University School of Medicine, Tokyo, Japan (T. Ozawa, N. Hasegawa, K. Fukunaga, H. Namkoong, T. Asakura); Japan Institute for Health Security, Tokyo (T. Komine, H. Fukano); Kitasato University Kitasato Institute Hospital, Tokyo (S. Nakayama, Y. Suzuki, T. Asakura); Kitasato University School of Pharmacy, Tokyo (Y. Suzuki, T. Asakura)

DOI: https://doi.org/10.3201/eid3203.251418

We report a case of *Mycobacterium riyadhense* pulmonary disease in a patient who relocated from Saudi Arabia to Japan. Epidemiologic data and whole-genome analyses of the isolated strains suggested that the infection might have been acquired in Saudi Arabia and persisted, rather than a recent local acquisition in Japan.

Mycobacterium riyadhense, first isolated in Saudi Arabia, has been reported mainly in the Middle East (*1*) and sporadically elsewhere (*2*,*3*). We describe a patient who experienced slowly progressive pulmonary deterioration caused by *M. riyadhense* infection after she relocated from Saudi Arabia to Japan. Because *M. riyadhense* has not been reported in Japan, genomic analysis of the patient's isolates was more consistent with within-host persistence of a preexisting infection than recent local acquisition from environmental exposure in Japan.

A 47-year-old woman was referred to Kitasato University Kitasato Institute Hospital (Tokyo, Japan) after granular opacities were detected in the right lung on screening. She had lived in Saudi Arabia for 2 years, where she had chronic exposure to sand and dust. A visibly contaminated, uncleaned air-conditioning unit at her home housed a bird's nest for 7 months and remained in use. She took only showers and rarely cleaned the shower room. She also gardened regularly. Shortly before her initial visit for care, she returned to Japan, bringing back only clothing and no other household belongings. She resumed tub bathing; the showerhead was replaced 4 years after her return, while her illness was being monitored.

Computed tomography (CT) revealed multiple small nodular opacities in the right upper and middle

lobes and the lingular segment, along with bronchial wall thickening; those findings suggested the nodular bronchiectatic form of nontuberculous mycobacterial pulmonary disease (Figure 1, panel A, B). Bronchial wash from the right upper lobe was negative for acid-fast bacilli (AFB) by smear and culture. Because she was asymptomatic, we monitored her for 2 years. CT imaging showed progressive worsening (Figure 1, panel C, D). A repeat bronchial wash from the same site in the right upper lobe was negative by AFB smear; culture yielded *M. riyadhense*, identified by matrix-assisted laser desorption/ionization time-of-flight (MALDI-TOF) mass spectrometry using the MALDI Biotyper system with the Mycobacteria Library version 6.0 (Bruker, https://www.bruker.com) (4). Because she was asymptomatic without lung cavities, we deferred treatment.

Five years after her initial visit, radiology-detected progression prompted a third bronchoscopy. Bronchial washes from 2 sites yielded *M. riyadhense* (strains 484719 and 537489), which we confirmed by MALDI-TOF mass spectrometry. We assembled draft genomes of the 2 strains from Illumina MiniSeq short-read sequencing data (https://www.illumina.com) using SPAdes version 3.15.5 (https://github.com/ablab/spades) (Appendix 1, https://wwwnc.cdc.gov/EID/article/32/3/25-1418-App1.pdf). Average nucleotide identity heatmap analysis using PyANI version 0.2.12 (https://github.com/widdowquinn/pyani) demonstrated that the isolates clustered with *M. riyadhense*, with ≥99.08% identity (Appendix 1 Figure 1; Appendix 2 Table 1, https://wwwnc.cdc.gov/EID/article/32/3/25-1418-App2.xlsx). Phylogenetic analysis based on 4,753 core genes from 12

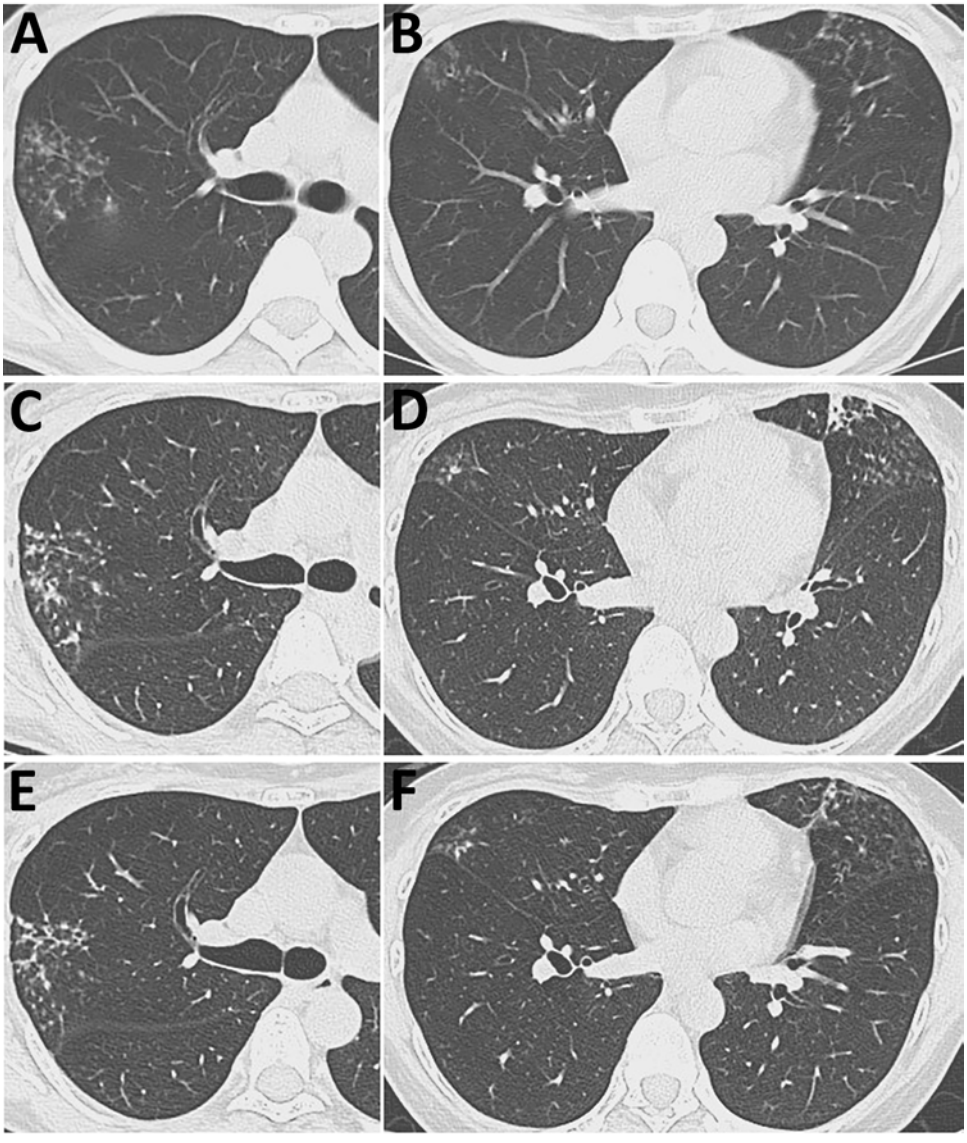

Figure 1. Serial axial chest computed tomography images over time from patient with *Mycobacterium riyadhense* pulmonary disease after relocation from Saudi Arabia, Japan. A, B) Images taken at initial hospital visit, demonstrating multiple scattered small nodular opacities in the right upper and middle lobes (A) and the lingular segment (B), accompanied by bronchial wall thickening. C, D) Images taken 2 years later, showing progression of the lesions in the right upper/middle lobes (C) and lingular segment (D). E, F) Images taken after treatment showing improvement of the lesions in the right upper/middle lobes (E) and lingular segment (F).

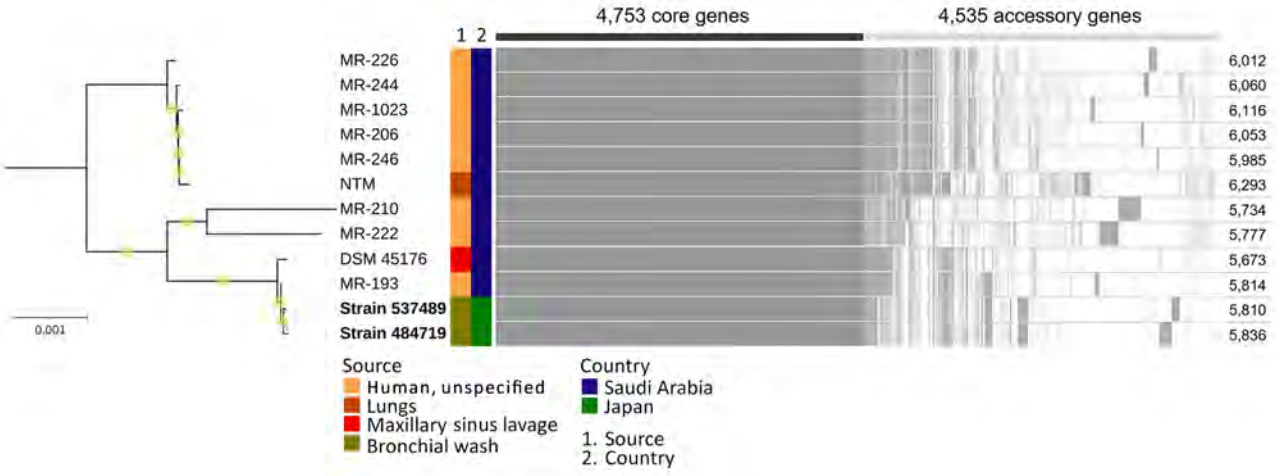

Figure 2. Midpoint-rooted maximum-likelihood tree based on 4,753 core genes of *Mycobacterium riyadhense* isolates from study of *Mycobacterium riyadhense* pulmonary disease after relocation from Saudi Arabia to Japan. Strains 484719 and 537489 (bold), obtained from clinical specimens in this study, were more closely related to strains MR-193 and DSM 45176 from Saudi Arabia. Yellow circles indicate ultrafast bootstrap values of 100%. Numbers at right indicate the number of coding sequences detected. Scale bar represents 0.001 substitutions per site.

M. riyadhense genomes, including publicly available genomes from the National Center for Biotechnology Information database (Appendix), further showed that isolates from both specimens were closely related to strains reported from Saudi Arabia (Figure 2). We called 7 single-nucleotide polymorphisms (SNPs) using Snippy version 4.6.0 (https://github.com/tseemann/snippy) and Gubbins version 3.4 (https://github.com/nickjcroucher/gubbins) within the 2 isolated strains (Appendix 1 Figures 2, 3). Fourteen-day broth microdilution susceptibility testing showed favorable results (Appendix 2 Table 2). Four months later, sputum culture also yielded *M. riyadhense*. Azithromycin (250 mg/d) plus ethambutol (500 mg/d) achieved sputum culture conversion and radiologic improvement (Figure 1, panel E, F). Sputum cultures have remained negative on repeated follow-up.

We did not identify published case reports of *M. riyadhense* in Japan (Appendix). Recent studies showed that shower aerosols and certain soil types are common sources of NTM exposure (*5*,*6*). The patient had prolonged exposure to such environmental conditions while living in Saudi Arabia. Although the environmental reservoir of *M. riyadhense* is not completely defined, culture-independent surveys have detected *M. riyadhense*–consistent signatures in freshwater and soil samples, which suggests those habitats could represent potential sources of exposure (*7*,*8*). Our isolates differed from MR-193 by 11–12 SNPs, whereas they were substantially more distant from other publicly available genomes. However, neither a molecular clock nor SNP threshold for *M. riyadhense* has been established, so interpretation is limited; more genomes from the same cluster are needed to infer transmission. Nevertheless, considering the patient's exposure history, clinical course, and the absence of previous detection reports of *M. riyadhense* in Japan, we considered within-host persistence of a preexisting infection to be a plausible explanation in this case.

No standard regimen for *M. riyadhense* infection has been established. Therapeutic approaches in previous cases have varied (*1*). A study summarizing previous cases of *M. riyadhense* (*9*) demonstrated efficacy of macrolide-based regimens combined with rifampin or fluoroquinolone, reporting a cure or improvement rate of 87.5%. In the case we describe, the isolate was susceptible to macrolides and other major drugs; therefore, we selected combination therapy with azithromycin and ethambutol. After initiating therapy, sputum cultures converted to negative within 2 months, with no evidence of recurrence. Subsequent imaging confirmed improvement in the lungs, providing further support for the efficacy of macrolide-based therapy against *M. riyadhense*.

Our findings contribute to understanding of the epidemiology and clinical course of *M. riyadhense* pulmonary disease. Given our whole-genome sequencing results and the absence of previous reports in Japan, this case might represent within-host persistence of a preexisting infection, distinct from recent local acquisition from environmental sources.

Acknowledgments

We thank Osamu Takeuchi and Masaharu Taga for their assistance with the transportation of mycobacteria.

This study was supported by a grant-in-aid for scientific research, Japan Society for the Promotion of Science (grant nos. JP25K02695 to T.A., JP22K16382 to H.F., JP24K19189 to T.K.).

Author contributions: T.O. and T.A. prepared the initial draft of the manuscript. S.N., Y.S., N.H., K.F., H.N., and H.F. revised subsequent versions. T.A. was responsible for the clinical management of the patient. T.K. and H.F. contributed to the bacteriologic diagnosis. All authors contributed to and approved the final manuscript.

About the Author

Dr. Ozawa is a physician specializing in respiratory medicine at the Division of Respiratory Medicine, Department of Internal Medicine, Keio University School of Medicine. He is pursuing a PhD, focusing on bronchiectasis and respiratory infectious diseases, particularly chronic infections such as nontuberculous mycobacterial pulmonary disease.

References

1. Varghese B, Enani MA, Althawadi S, Johani S, Fernandez GM, Al-Ghafli H, et al. *Mycobacterium riyadhense* in Saudi Arabia. Emerg Infect Dis. 2017;23:1732–4. https://doi.org/10.3201/eid2310.161430
2. Godreuil S, Marchandin H, Michon AL, Ponsada M, Chyderiotis G, Brisou P, et al. *Mycobacterium riyadhense* pulmonary infection, France and Bahrain. Emerg Infect Dis. 2012;18:176–8. PubMed https://doi.org/10.3201/eid1801.110751
3. Choi JI, Lim JH, Kim SR, Lee SH, Park JS, Seo KW, et al. Lung infection caused by *Mycobacterium riyadhense* confused with *Mycobacterium tuberculosis*: the first case in Korea. Ann Lab Med. 2012;32:298–303. https://doi.org/10.3343/alm.2012.32.4.298
4. Markanović M, Makek MJ, Glodić G, Kuliš T, Mareković I. Evaluation and clinical impact of MALDI Biotyper Mycobacteria Library v6.0 for identification of nontuberculous mycobacteria by MALDI-TOF mass spectrometry. J Mass Spectrom. 2023;58:e4915. https://doi.org/10.1002/jms.4915
5. DeFlorio-Barker S, Egorov A, Smith GS, Murphy MS, Stout JE, Ghio AJ, et al. Environmental risk factors associated with pulmonary isolation of nontuberculous mycobacteria, a population-based study in the southeastern United States. Sci Total Environ. 2021;763:144552. https://doi.org/10.1016/j.scitotenv.2020.144552
6. Tzou CL, Dirac MA, Becker AL, Beck NK, Weigel KM, Meschke JS, et al. Association between *Mycobacterium avium* complex pulmonary disease and mycobacteria in home water and soil. Ann Am Thorac Soc. 2020;17:57–62. https://doi.org/10.1513/AnnalsATS.201812-915OC
7. King HC, Khera-Butler T, James P, Oakley BB, Erenso G, Aseffa A, et al. Environmental reservoirs of pathogenic mycobacteria across the Ethiopian biogeographical landscape. PLoS One. 2017;12:e0173811. https://doi.org/10.1371/journal.pone.0173811
8. Pontiroli A, Khera TT, Oakley BB, Mason S, Dowd SE, Travis ER, et al. Prospecting environmental mycobacteria: combined molecular approaches reveal unprecedented diversity. PLoS One. 2013;8:e68648. https://doi.org/10.1371/journal.pone.0068648
9. Alsaeed M, Alanazi K, Alhamdan A, Faqihi M, Alibrahim A, Alshehri S, et al. Exploring *Mycobacterium riyadhense*: epidemiology, clinical presentation, and treatment outcome. Open Forum Infect Dis. 2025;12:ofaf461. https://doi.org/10.1093/ofid/ofaf461

Address for correspondence: Takanori Asakura, Division of Pulmonary Medicine, Department of Medicine, Keio University School of Medicine, 35 Shinanomachi, Shinjuku-ku, Tokyo 160-8582, Japan; email: takanori.asakura@keio.jp

lsaC and Tandem *lsaE-lnuB* Resistance Genes in Invasive Group A *Streptococcus*

Bernard Beall, Saundra Mathis, Zhongya Li, Joy Rivers, Anne-Kathryn Venero, Benjamin J. Metcalf, Lesley McGee, Sopio Chochua

Author affiliations: Applied Science, Research & Technology, Inc., Atlanta, Georgia, USA (B. Beall, S. Mathis, Z. Li, A.-K. Venero); Centers for Disease Control and Prevention, Atlanta (J. Rivers, B.J. Metcalf, L. McGee, S. Chochua)

DOI: https://doi.org/10.3201/eid3203.251776

Among >16,500 recently recovered invasive *Streptococcus pyogenes* isolates, we detected 9 independent acquisitions of *lsaC* or tandem *lsaE-lnuB* genes, which are known to confer resistance to pleuromutilins and clindamycin. Continued awareness of the evolving *S. pyogenes* antimicrobial resistosome is important for future infection treatment considerations.

Group A *Streptococcus* (GAS) commonly causes noninvasive infections affecting the skin and throat and invasive infections that can involve any tissue of the human body. Treatment of GAS infections is primarily with β-lactam antimicrobial drugs; macrolides and clindamycin are alternatives for patients allergic to β-lactam antimicrobial drugs (*1*). GAS co-resistance to macrolides and clindamycin has increased (*2*), which compromises macrolide usage

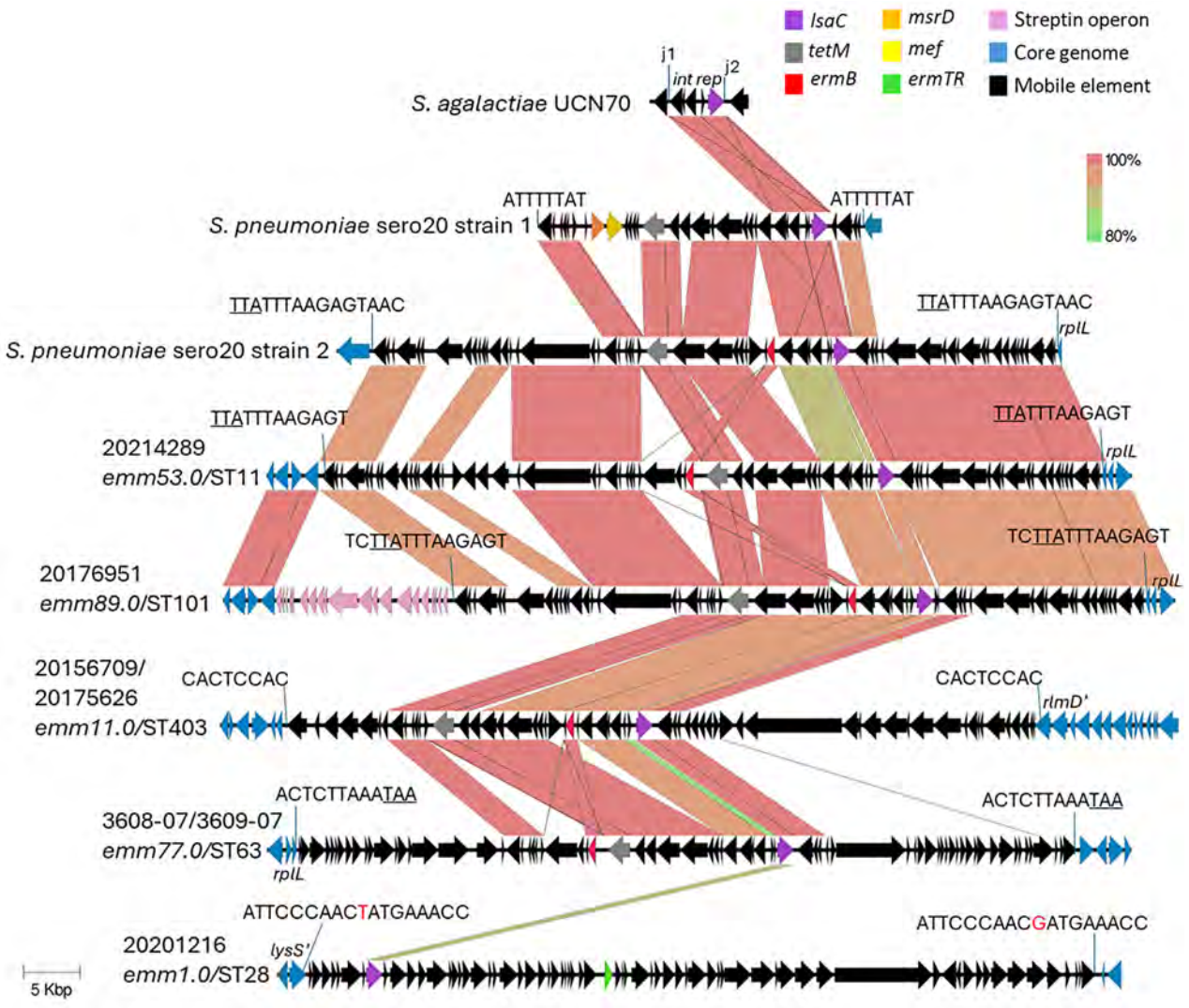

Figure 1. Alignments of 5 different group A Streptococcus *lsaC*-carrying accessory elements from study of repeated acquisitions of *lsaC* and tandem *lsaE-lnuB* resistance genes. Alignments include a partial element from *S. agalactiae* strain UCN70 (6) and 2 complete elements recently described in pneumococci (9). The j1 and j2 (junctions 1 and 2) sequences depict 24–25 bp sequences that demarcate a 5,258–5,816 bp mobilizable *lsaC*-carrying cassette that is highly conserved between all of the strains shown except for iGAS strain 20201216 (Appendix Figure 1, panel B, https://wwwnc.cdc.gov/EID/article/32/3/25-1776-App1.pdf). The 8–18 bp target sequence repeat flanking each complete element shown is perfect except in strain 20201216 (nonconserved base in red font). Underlined text indicates the stop codon of the *rplL* gene in 4 strains (including *S. pneumoniae* strain 2). The insertion within strain 20156709/20175626 targeted an 8-bp internal sequences within the *rlmD* gene, resulting in a truncated allele, *rmlD*'; the insertion within strain 20201216 targeted an 18-bp internal sequence within the *lysS* gene, resulting another truncated allele, *lysS'*. Scale bar indicates 5,000 base pairs. ST, sequence type.

for noninvasive infections and combined clindamycin with penicillin for severe disease (*1*). The 2 main streptococcal macrolide resistance mechanisms are 23S rRNA methylation by *erm* gene–encoded methylases, which confers resistance to macrolides, lincosamides (including clindamycin), and streptogramin B antimicrobials, and macrolide efflux by *mef*-encoded and *msrD*-encoded proteins (*3*). The *lnu* genes confer lincosamide resistance, whereas *lsa* genes confer resistance to lincosamides, streptogramin A drugs, and pleuromutilins. The pleuromutilin lefamulin is approved in the United States for systemic treatment of community-acquired bacterial pneumonia in adults (*4*) and has potent antibacterial activity against β-hemolytic streptococci (*5*). Although *lsa* and *lnu* genes are documented in group B *Streptococcus* (*6*,*7*) only 1 GAS isolate carrying tandem *lsaE-lnuB* determinants has been reported (*8*).

We identified 11 invasive GAS (iGAS) blood isolates positive for *lsa* or *lnu* genes, 7 *lsaC* and 4 *lsaE/lnuB*, from >16,500 iGAS isolates recovered during 2015–2023 and 335 isolates screened before 2015

through Active Bacterial Core surveillance (ABCs). We detected the positive isolates on 1 of 9 distinct mobile elements (Figures 1, 2; Appendix Table, Figures 1–9, https://wwwnc.cdc.gov/EID/article/32/3/25-1776-App1.pdf). Each element was found within 1 of 7 different iGAS strains (7 *emm* type/sequence type [ST] combinations; for example, *emm89.0*/ST101). Two strains were represented by indistinguishable (360807 and 360907) or nearly identical (20156709 and 20175626) isolate genome sequences available under BioProject PRJNA395240 (Appendix Table).

We found 5 large (61,501–78,917 bp) accessory elements carrying *lsaC* in combination with *ermB* and *tetM* in 6 isolates from 5 strains and with *ermTR* in isolate 20201216 (Figure 1). All 6 elements were flanked by short genomic target repeats, indicative of genomic insertion through precisely targeted transposition (*7*). Three of the 5 elements were inserted at the *rplL* 3′ end, 1 within the *rlmD* gene, and 1 within the *lysS* gene.

Four iGAS strains, including 1 *S. equisimilis* isolate (*10*), carried an identical *lnuB* allele and conserved *lsaE* alleles sharing 98%–100% sequence identity on 4 distinct accessory elements (Appendix Figure 2, panel B). As with 3 *lsaC*-carrying elements (Figure 1), 2 of the 4 elements carrying *lsaE-lnuB* mapped at the *rplL* 3′ end and were also apparently inserted through precise transposition events. For 2 strains, we were unable to map element genomic insertion sites because of incomplete assembly.

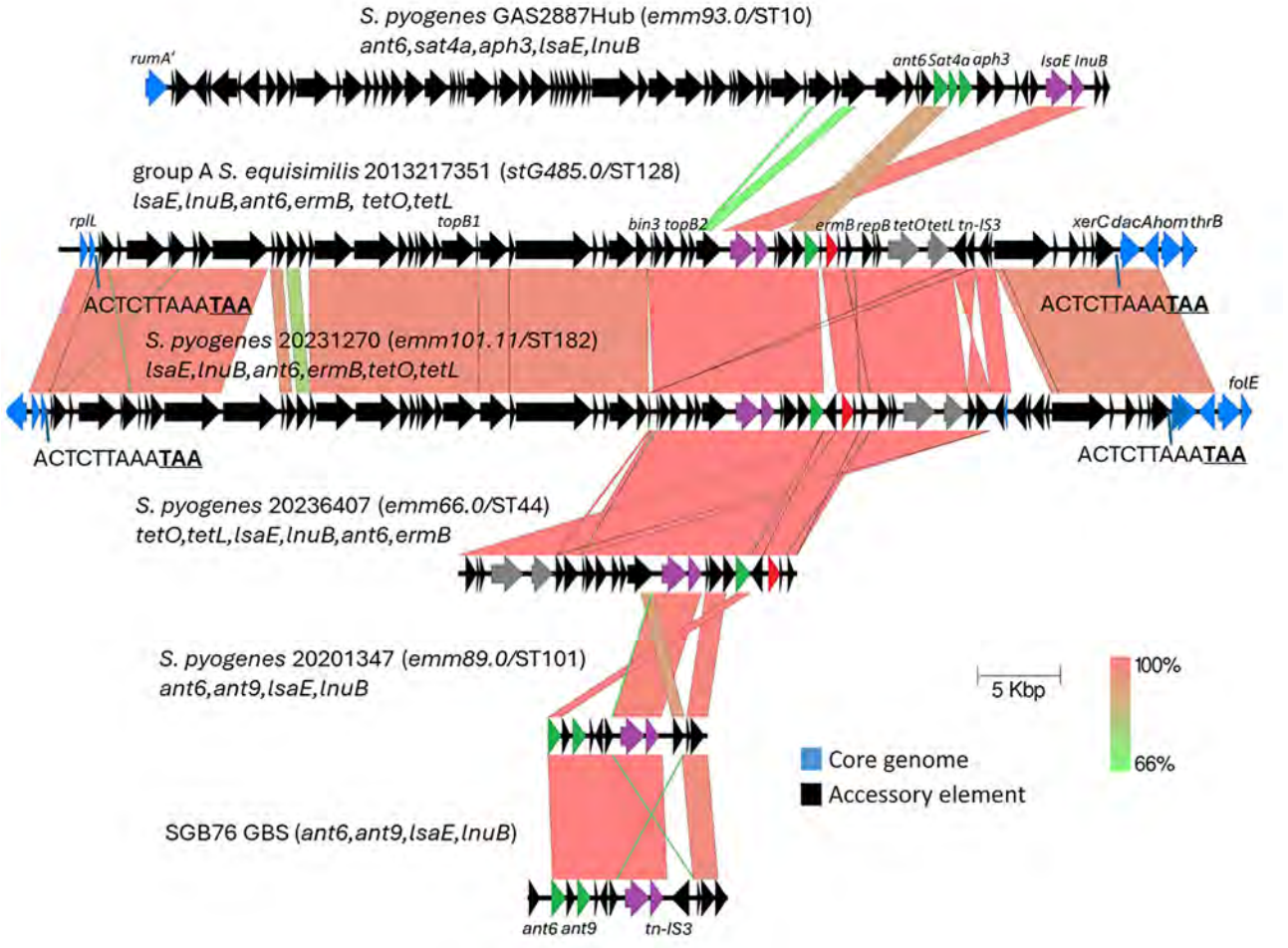

Figure 2. Alignment of complete and partial *lsaE*-carrying elements from study of repeated acquisitions of *lsaC* and tandem *lsaE-lnuB* resistance genes by group A *Streptococcus.* Alignments shown are from group A ABCs strains 2013217351 and 20231270 with partial elements from strains 20236407 and 20201347. Also included are complete elements from GAS2887Hub (*8*) and GBS strain SGB76 (GenBank accession no. KF772204). Antimicrobial resistance genes include 3 aminoglycoside 6-adenyltransferase genes (*ant6, aph3,* and *ant9*), and the streptothricin acetyltransferase gene *aph3.* Prokka annotations include *topB* (DNA topoisomerase genes), *bin3* (DNA invertase gene), *repB* (DNA replication gene), *tn-IS3* (IS3 family transposase gene), and *xerC* (tyrosine recombinase gene). Underlined bold text indicates the stop codon of the *rplL* gene in 2 strains. Scale bar indicates 5,000 base pairs. ABCs, Active Bacterial Core surveillance; sero, serotype; ST, sequence type.

The 4 deduced 492 residue LsaE proteins shared 52.2%–53.7% sequence identity with the 5 deduced 494 residue LsaC protein sequences. Other than resistance determinants, few genes were conserved between the 4 mobile elements carrying *lsaE-lnuB* from this study with the prophage described from *S. pyogenes* strain Gas2887Hub (*8*) also carrying those genes (Figure 2). The iGAS *S. equisimilis* strain 2013217351 and *S. pyogenes* 20231270 carried closely related transposons, each inserted at the 12-mer *rplL* 3′ terminus conserved between the 2 species.

The 5 *lsaC*-carrying elements represented 4 phylogenetically distinct *lsaC* alleles (Appendix Figure 1) with 90.4%–99.8% sequence identity to the *S. agalactiae* UCN70 *lsaC* allele (*6*). The 4 elements carrying *lsaC*, *ermB*, and *tetM* each contained a small (5,258–5,816 bp) conserved *lsaC* self-mobilizing element inserted within a consensus Tn916 *ori*T site sequence (Appendix Figure 1, panel B) described in *S. agalactiae* (*7*) and recently described in 2 distinct pneumococcal elements (*9*). There was wide sequence divergence between the 4 small *ori*T-targeting iGAS *lsaC* mobile elements, despite identical 24–25 bp sequences flanking their insertion sites. For the *lsaC*-containing element in strain 20156709/20175626, genomic insertion and phylogenetic data were consistent with the sequential genomic insertion of a Tn916 family element before a more recent second precise insertion of the 5546 bp *lsaC*–carrying element into its *ori*T site (Appendix Figure 2, panels A, B). For 2 other *lsaC*-carrying elements, phylogenetic data suggested recent introduction of the complete composite element, consisting of a Tn916-related element carrying an integrated small *lsaC* element (Appendix Figures 3–4).

Ten of the 11 study isolates were resistant to both erythromycin and clindamycin (Appendix Table); that resistance is associated with the presence of *ermB* and *lsaC* (6 isolates), *ermTR* and *lsaC* (1 isolate), or *ermB*, *lsaE*, and *lnuB* (3 isolates). One strain, 20201347 (*lsaE*+, *lnuB*+), was erythromycin susceptible but clindamycin-resistant, indicating *lsaE*- and *lnuB*-conferred clindamycin resistance. That finding in strain 20201347 was consistent with masking of *lsaE*- and *lnuB*-conferred clindamycin resistance in the other 10 isolates because of *erm* gene–encoded methylase activity. The 4 isolates carrying *lsaE-lnuB* had high MICs for the pleuromutilin lefamulin (MIC >2 μg/mL), whereas the 7 *lsaC*-positive isolates had low MICs for lefamulin (MICs ≤0.25 μg/mL) (Appendix Table). We conclude that expansion of *lsaE*-positive iGAS lineages could compromise future potential use of lefamulin, and *lsaC*- or *lsaE-lnuB*–positive strains could further undermine the use of clindamycin for treating β-hemolytic streptococcal infections.

Acknowledgments

We thank everyone involved in ABCs and are gratified to be involved ourselves.

ABCs is a collaboration between the Centers for Disease Control and Prevention, state health departments, and universities that has been ongoing since 1995 (https://www.cdc.gov/abcs/index.html).

About the Author

Dr. Beall has been conducting streptococcal strain surveillance and ABCs-related streptococcal research since 1994. After retiring in 2021 from the National Center for Immunization and Respiratory Diseases, Centers for Disease Control and Prevention, in 2021, he continues to work on ABCs-related streptococcal surveillance projects.

References

1. Khan ZZ. Group A streptococcal (GAS) infections treatment & management, 2024 [cited 2026 Feb 1]. https://emedicine.medscape.com/article/228936-treatment
2. Li Y, Rivers J, Mathis S, Li Z, McGee L, Chochua S, et al. Continued increase of erythromycin nonsusceptibility and clindamycin nonsusceptibility among invasive group A streptococci driven by genomic clusters, United States, 2018–2019. Clin Infect Dis. 2023;76:e1266–9. https://doi.org/10.1093/cid/ciac468
3. Schwarz S, Shen J, Kadlec K, Wang Y, Brenner Michael G, Feßler AT, et al. Lincosamides, streptogramins, phenicols, and pleuromutilins: mode of action and mechanisms of resistance. Cold Spring Harb Perspect Med. 2016;6:a027037. https://doi.org/10.1101/cshperspect.a027037
4. File TM Jr, Goldberg L, Das A, Sweeney C, Saviski J, Gelone SP, et al. Efficacy and safety of intravenous-to-oral lefamulin, a pleuromutilin antibiotic, for the treatment of community-acquired bacterial pneumonia: the phase III Lefamulin Evaluation Against Pneumonia (LEAP 1) trial. Clin Infect Dis. 2019;69:1856–67. https://doi.org/10.1093/cid/ciz090
5. Paukner S, Sader HS, Ivezic-Schoenfeld Z, Jones RN. Antimicrobial activity of the pleuromutilin antibiotic BC-3781 against bacterial pathogens isolated in the SENTRY antimicrobial surveillance program in 2010. Antimicrob Agents Chemother. 2013;57:4489–95. https://doi.org/10.1128/AAC.00358-13
6. Malbruny B, Werno AM, Murdoch DR, Leclercq R, Cattoir V. Cross-resistance to lincosamides, streptogramins A, and pleuromutilins due to the *lsa*(C) gene in *Streptococcus agalactiae* UCN70. Antimicrob Agents Chemother. 2011;55:1470–4. https://doi.org/10.1128/AAC.01068-10
7. Douarre PE, Sauvage E, Poyart C, Glaser P. Host specificity in the diversity and transfer of *lsa* resistance genes in group B *Streptococcus*. J Antimicrob Chemother. 2015;70:3205–13.
8. Berbel D, Càmara J, García E, Tubau F, Guérin F, Giard JC, et al. A novel genomic island harbouring *lsa*(E) and *lnu*(B) genes and a defective prophage in a *Streptococcus pyogenes* isolate resistant to lincosamide, streptogramin A and pleuromutilin antibiotics. Int J Antimicrob Agents. 2019;54:647–51. https://doi.org/10.1016/j.ijantimicag.2019.08.019

9. Beall B, Lin W, Li Z, Tran T, Metcalf BJ, Anderson BJ, et al. Two independent acquisitions of multidrug resistance gene *lsaC* in *Streptococcus pneumoniae* serotype 20 multilocus sequence type 1257. Emerg Infect Dis. 2025;31:2098–108. https://doi.org/10.3201/eid3111.251101
10. Chochua S, Rivers J, Mathis S, Li Z, Velusamy S, McGee L, et al. Emergent invasive group A *Streptococcus dysgalactiae* subsp. *equisimilis*, United States, 2015–2018. Emerg Infect Dis. 2019;25:1543–7. https://doi.org/10.3201/eid2508.181758

Address for correspondence: Bernard Beall, Centers for Disease Control and Prevention, 1600 Clifton Rd NE, Mailstop C02, Atlanta, GA 30329-4018, USA; email: beb0@cdc.gov

EMERGING INFECTION NETWORKS LETTERS

Query into Tuberculosis Infection Screening and Management among Pregnant Migrants, Europe

Filippo Cioli Puviani,[1] Amina Zaffagnini,[1] Cristina Mazzi, Daniela Maria Cirillo, Francesco Di Gennaro, Ferenc Balázs Farkas, Lorenzo Guglielmetti, Yousra Kherabi, Heinke Kunst, Chiara Sepulcri, Christian Wejse, Laura Todaro, Tamara Ursini

Author affiliations: University of Verona, Verona, Italy (F. Cioli Puviani); IRCCS Sacro Cuore Don Calabria Hospital, Negrar di Valpolicella, Italy (A. Zaffagnini, C. Mazzi, L. Guglielmetti, T. Ursini); Emerging Bacterial Pathogens Unit, IRCCS San Raffaele Scientific Institute, Milan, Italy (D.M. Cirillo, C. Sepulcri); University of Bari, Bari, Italy (F. Di Gennaro); Institute of Medical Microbiology, Faculty of Medicine, Semmelweis University, Budapest, Hungary (F.B. Farkas); Pediatric Center, Semmelweis University, Budapest (F.B. Farkas); Bichat-Claude Bernard Hospital, Assistance Publique-Hôpitaux de Paris, Université Paris Cité, Paris, France (Y. Kherabi); Université Paris Cité, Inserm, Paris (Y. Kherabi); Queen Mary & Barts Health Tuberculosis Centre, Blizard Institute, Faculty of Medicine & Dentistry, London, UK (H. Kunst); University of Genoa, Genoa, Italy (C. Sepulcri); Aarhus University Hospital, Aarhus, Denmark (C. Wejse); Center for Global Health, Aarhus University, Aarhus (C. Wejse); Provincial Hospital of Bolzano, Bolzano-Bozen, Italy (L. Todaro)

DOI: https://doi.org/10.3201/eid3203.251775

Pregnant migrant women face increased tuberculosis vulnerability. We queried clinicians in Europe on *Mycobacterium tuberculosis* infection screening and management among pregnant migrants. Fewer than half reported routinely performing screening, and diagnostic and preventive practices varied widely. Those responses highlight substantial heterogeneity and uncertainty in current *M. tuberculosis* infection screening practices.

[1]These first authors contributed equally to this article.

Tuberculosis (TB), caused by *Mycobacterium tuberculosis*, remains a major global health threat. The World Health Organization (WHO) European Region reported 172,300 TB cases and 22,500 deaths in 2023 (*1*,*2*). Migrants from high-incidence countries are disproportionately affected by TB (*3*). Pregnancy further increases vulnerability because of immunologic changes and healthcare barriers (*4*). Early identification of *M. tuberculosis* infection during pregnancy could represent an opportunity for prevention; however, evidence on the balance between potential benefits and risks remains limited (*5*). Current WHO recommendations restrict TB preventive treatment (TPT) during pregnancy to persons living with HIV and are largely derived from high-burden settings, which have limited applicability to migrant populations in Europe (*6*). Although drugs included in TPT regimens are used for treating TB during pregnancy, safety data remain limited (*6*). Given those gaps, we queried clinicians in Europe on *M. tuberculosis* infection screening and preventive practices for pregnant migrant women.

We disseminated an online query during March 4–May 31, 2025 (Appendix 1, https://wwwnc.cdc.gov/EID/article/32/3/25-1775-App1.pdf; Appendix 2, https://wwwnc.cdc.gov/EID/article/32/3/25-1775-App2.pdf), to gather information on *M. tuberculosis* infection screening and management practices for pregnant migrants in Europe. The query was endorsed by the European Society of Clinical Microbiology and Infectious Diseases Study Group for Infections in Travelers and Migrants and Study Group for Mycobacterial Infections. We descriptively summarized responses.

A total of 101 professionals responded, 74.3% (75/101) of whom were infectious diseases specialists, and most worked in hospitals. Participants represented 20 different countries, most within the WHO European Region (Appendix 1 Table). Only 27.7% (28/101) reported routinely offering *M. tuberculosis* infection screening to pregnant migrants, but 36.6%

(37/101) reported screening migrants who had specific risk factors, such as HIV infection, recent (<5 years) arrival from high-incidence countries, immunosuppression, or close contact with a TB case (Table).

Among screening tools, of participants who reported screening pregnant migrants for *M. tuberculosis* infection, 82.6% (57/69) reported using interferon-γ release assays (IGRAs), and 27.5% (19/69) used chest radiographs. Tuberculin skin testing was less commonly adopted, serving as the main diagnostic tool for only 24.6% (17/69). To diagnose *M. tuberculosis* infection, 60.9% (42/69) of respondents reported using a sequential diagnostic approach in which positive tuberculin skin test or IGRA result was followed by chest radiograph to rule out TB disease among IGRA-positive women. An additional 37.7% (26/69) used a similar approach but relied on clinical assessment instead of imaging to exclude TB disease.

Approaches to TPT during pregnancy varied widely among respondents; 30.4% (21/69) reported routinely offering TPT to all pregnant migrants with diagnosed *M. tuberculosis* infection, 40.6% (28/69) did so only under specific conditions, and 23.2% (16/69) postponed treatment until after delivery. When TPT was initiated during pregnancy, most respondents started therapy as soon as *M. tuberculosis* infection diagnosis was made, regardless of fetal gestational age. The most common regimens were isoniazid plus rifampin or isoniazid monotherapy.

Participants reported barriers to *M. tuberculosis* infection screening and treatment in pregnant migrants; 53.6% (37/69) identified challenges in performing screening and 62.7% (42/67) reported difficulties in prescribing or ensuring adherence to TPT (Table). The most common reported barriers to screening included concerns about radiation exposure from chest radiographs, unclear protocols, and uncertainty about timing for safely administering chest radiographs during pregnancy. Additional issues for both screening and treatment included patient adherence, limited resources, and lack of clear guidelines (Table).

Regarding TPT, respondents reported the main difficulties were patient-related, such as language and cultural barriers and fears about gestational risks and side effects. Among healthcare provider–related concerns, reported difficulties included uncertainty about which stage of pregnancy is considered safe for starting TPT and lack of training. Participants also noted healthcare system challenges, such as fragmented follow-up pathways and limited availability of dedicated services. Estimated TPT adherence rates varied, and only one third of respondents estimated high (>80%) adherence.

Table. Risk factors and barriers reported by respondents to a network query into TB screening and management among pregnant migrants, Europe, 2025*

Risk factor or barrier	No. (%) respondents
Risk factors considered when screening offered during pregnancy, n = 37†	
Recent TB contact	34 (91.9)
HIV infection	34 (91.9)
Immunosuppression	31 (83.8)
Recent migration, <5 y	22 (59.4)
Homelessness	12 (32.4)
Diabetes	7 (18.9)
Malnutrition	6 (16.2)
Risk factors considered when TB preventive treatment offered during pregnancy, n = 31†	
HIV infection	30 (96.8)
Recent TB contact	27 (87.1)
Immunosuppression	22 (71)
Recent migration, <5 y	11 (35.5)
Diabetes	7 (22.6)
Malnutrition	7 (22.6)
Homelessness	5 (16.1)
Perceived barriers to TB infection screening, n = 37†	
Chest radiograph issues‡	28 (75.7)
Patient adherence	11 (29.7)
Financial or healthcare system barriers	10 (27)
Guideline gaps	8 (21.6)
Perceived barriers to TB preventive treatment, n = 42†	
Patient-related factors	33 (78.6)
Healthcare provider–related factors	20 (47.6)
Guideline or policy gaps	16 (38.1)
Healthcare system barriers	12 (28.6)

*TB, tuberculosis.
†Multiple responses were permitted.
‡Includes concerns regarding radiation exposure, which trimester radiographs can safely be administered, and patient acceptance of chest radiography during pregnancy.

Slightly more than one third (35.7%, 35/98) of respondents reported following specific guidelines for *M. tuberculosis* infection screening in pregnant women, predominantly international guidelines (*6*–*8*) and, to a lesser extent, national guidelines (*9*,*10*). However, only 23.2% (23/99) considered the available guidelines adequate. Guideline limitations included a lack of evidence specific to pregnancy, insufficient guidance on when and how to screen and treat pregnant women, and inconsistent national recommendations. Respondents noted training gaps, and one third of participants had received no specific training on *M. tuberculosis* infection screening and treatment. Respondents emphasized the need for additional resources, particularly standardized protocols, training, better access to guidelines, and the involvement of cultural mediators.

In this query among clinicians in Europe, respondents reported substantial heterogeneity in *M. tuberculosis* infection screening and TPT practices for pregnant migrants. Screening was most often restricted to women with specific risk factors, and diagnostic and preventive approaches varied widely across settings. Given the convenience sampling approach and the open-link dissemination strategy (response rates not assessable), the patterns described here should not be interpreted as representative of all settings in Europe. However, the responses to our query underscore areas of clinician uncertainty regarding *M. tuberculosis* infection screening and treatment in pregnant women that warrant further investigation, training, and guidelines.

Acknowledgments

We thank all members of the ESCMID Study Group for Infections in Travelers and Migrants (ESGITM) and the Study Group for Mycobacterial Infections (ESGMYC), as well as other professionals who contributed to this work. We are also grateful to our colleagues at the Department of Infectious–Tropical Diseases and Microbiology, IRCCS Sacro Cuore Don Calabria Hospital, for their valuable review and input during the development phase.

This work was partly funded by the Italian Ministry of Health (current search line no. L3P5) with funds to IRCCS Sacro Cuore Don Calabria Hospital. The funding source had no role in study design, writing, and submission.

About the Author

Dr. Tamara Ursini is an infectious diseases specialist at the Department of Infectious–Tropical Diseases and Microbiology, IRCCS Sacro Cuore Don Calabria Hospital, Negrar di Valpolicella, Verona, Italy. Her main research interests include migrant and refugee health, tuberculosis, and neglected tropical diseases.

References

1. World Health Organization. Tuberculosis global report 2024. Geneva: The Organization; 2024.
2. World Health Organization, Regional Office for Europe. Tuberculosis—fact sheet. Copenhagen: The Organization; 2025.
3. Kunst H, Lange B, Hovardovska O, Bockey A, Zenner D, Andersen AB, et al.; TBnet. Tuberculosis in adult migrants in Europe: a TBnet consensus statement. Eur Respir J. 2025;65:2401612. https://doi.org/10.1183/13993003.01612-2024
4. Zenner D, Kruijshaar ME, Andrews N, Abubakar I. Risk of tuberculosis in pregnancy: a national, primary care-based cohort and self-controlled case series study. Am J Respir Crit Care Med. 2012;185:779–84. https://doi.org/10.1164/rccm.201106-1083OC
5. Mathad JS, Gupta A. Tuberculosis in pregnant and postpartum women: epidemiology, management, and research gaps. Clin Infect Dis. 2012;55:1532–49. https://doi.org/10.1093/cid/cis732
6. World Health Organization. WHO consolidated guidelines on tuberculosis. Module 1: prevention—tuberculosis preventive treatment, second edition. Geneva: The Organization; 2024.
7. Migliori GB, Sotgiu G, Rosales-Klintz S, Centis R, D'Ambrosio L, Abubakar I, et al. ERS/ECDC Statement: European Union standards for tuberculosis care, 2017 update. Eur Respir J. 2018;51:1702678. https://doi.org/10.1183/13993003.02678-2017
8. European Centre for Disease Prevention and Control. Programmatic management of latent tuberculosis infection in the European Union. Stockholm: The Centre; 2018.
9. Istituto Superiore di Sanità. Physiological pregnancy [in Italian]. Rome: The Institute; 2023.
10. Schaberg T, Brinkmann F, Feiterna-Sperling C, Geerdes-Fenge H, Hartmann P, Häcker B, et al. Tuberculosis in adulthood—the Sk2-Guideline of the German Central Committee against Tuberculosis (DZK) and the German Respiratory Society (DGP) for the diagnosis and treatment of adult tuberculosis patients [in German]. Pneumologie. 2022;76:727–819. https://doi.org/10.1055/a-1934-8303

Address for correspondence: Tamara Ursini, Department of Infectious, Tropical Diseases and Microbiology, IRCCS Sacro Cuore Don Calabria Hospital, Viale Luigi Rizzardi 4, Negrar di Valpolicella 37024, Italy; email: tamara.ursini@sacrocuore.it

Correction: Vol. 32, No. 1

Funding information was missing for Detection of Avian Influenza H5–Specific Antibodies by Chemiluminescent Assays (A.C. Márquez et al.). The article has been corrected online (https://wwwnc.cdc.gov/eid/article/32/1/25-1117_article).

Joseph Severn, *Portrait of Keats, listening to a nightingale on Hampstead Heath*, 1845 (detail). Oil on canvas. 114 cm × 97 cm (45 in × 38 in). Guildhall Art Gallery, London, UK. On display at Keats House, Hampstead, UK.

Romanticism at the Edge of Death

Terence Chorba

Fade softly from my eyes, and be once more
In masque-like figures on the dreary urn;
Farewell! I yet have visions for the night,
And for the day faint visions there is store;
Vanish, ye Phantoms! from my idle spright,
Into the clouds, and never more return!

—John Keats, *Ode on Indolence*, lines 55–60 (*1*)

Author affiliation: Centers for Disease Control and Prevention, Atlanta, Georgia, USA

DOI: https://doi.org/10.3201/eid3203.AC3203

John Keats (1795–1821), a renowned poet of the English Romantic movement, died at just 25 years of age, a victim of what was then called consumption; in 1829, Johann Schonlein, a German physician, renamed the disease tuberculosis (*2*). As a young man, Keats was apprenticed to an apothecary and trained to be a physician at Guy's Hospital in London, obtaining the Licentiate of the Society of Apothecaries in 1816, which made him eligible to practice both pharmacy and medicine (*3*). Although he achieved the rank of assistant surgeon at age 20, Keats was enamored of the beauty of poetry and truncated his medical practice.

The severity of Keats' illness was presaged by the deaths from tuberculosis of his mother when he was 14 (*4*) and of a younger brother, Thomas (1799–1818), 3 years before his own death (*5*). His illness deeply shaped his creative output and posthumous legacy. Students of English poetry are awed when they learn how, in a single year, 1819, Keats composed 6 elaborately structured odes (*Ode on a Grecian Urn*, *Ode on Indolence*, *Ode on Melancholy*, *Ode to a Nightingale*, *Ode to Psyche*, and *To Autumn*) that rank among his best known poems, together with numerous sonnets and other works. Although not widely known in his brief lifetime but well launched toward literary immortality, Keats had to confront the reality of his own impending death from tuberculosis when, in February 1820, he coughed up blood and noted (as a physician) that it "was arterial"—"my death warrant" (*6*).

In early 19th Century Europe, Keats' disease would have been interpreted through a dominant framework of heredity, because the disease was so often observed in the context of families who had shared airspace (*7*). In 1865, by demonstrating that inoculation with tuberculin material from human lymph nodes would result in the development of tubercular lesions in rabbits, Jean-Antoine Villemin provided evidence to the scientific community that tuberculosis was infectious, a position that largely went ignored (*8*). At the time, in the absence of common knowledge of a communicable etiology and of a known cure, a common prescription for consumption was a change of climate. That was before the definitive breakthrough revelation by Robert Koch on March 24, 1882, that the etiology of this disease was infection with a *Mycobacterium* (*9*); the date has been designated as World TB Day by the World Health Organization and is why March issues of *Emerging Infectious Diseases* always have tuberculosis as their central and cover themes.

For Keats, a change of climate meant setting sail for Italy in September 1820, accompanied by his friend Joseph Severn (1793–1879), in the hopes that the mild Mediterranean air would ease his suffering. Severn was an English portrait painter who had developed a reputation as a good miniaturist, and for his artwork, he won a medal and 3-year traveling fellowship from the Royal Academy. It is thought that Severn had first met Keats in 1816, and in London's Royal Academy Exhibition of 1819, Severn exhibited a portrait miniature, *J. Keats, Esq.* (Figure). Although Severn had an exceedingly successful artistic career as a realist and genre painter after Keats' death, helped establish the British Academy of Arts in Rome, and later served as British consul (1861–1872) in Rome at the time of Italian unification under Giuseppi Garibaldi, he is best known for his role in nursing Keats through his final days and for the several artistic depictions that he made of the poet. On this issue's cover is a depiction of the poet painted by Severn in 1845, *Keats Listening to a Nightingale on Hampstead Heath.* In this posthumous portrait, Severn pictures a distracted Keats seated in an environment that is at once day and night, two scenes in one, with his book set aside, the poet gazing toward a small bird silhouetted against a full moon.

Figure. Joseph Severn, *John Keats, Esq.*, 1819. Oil on ivory miniature. 105 × 79 mm. National Portrait Gallery, London, UK. https://www.npg.org.uk/collections/search/portrait/mw03554/John-Keats

After arriving in Rome in November 1820 enduring rapid disease progression, and after numerous contemporary medical interventions including starvation and bloodletting, Keats died in Rome in February 1821 (*10*). Soon thereafter, his room and its contents were burned, the walls scraped, and the apartment cleansed, all consistent with the then-still-unproven theory that consumption might be infectious in origin (*11*).

Because tuberculosis was so widespread in 19th Century Europe populations, accounting for estimates of 1 in 4 deaths at the time (*12*), the presence of many young, talented artists and poets among its victims resulted in the disease being romanticized by some as ennobling. With no effective treatment available, it was a slow and painful disease, characterized by coughing, fever, night sweats, weight loss, and wasting. Contemporary with Keats, a host of other English literary giants believed to have had tuberculosis include Percy Bysshe Shelley, Elizabeth Barrett Browning, and the famed Brontë siblings, Emily, Anne, and Charlotte.

The poignancy of Keats' rapid decline, his artistic drive and boundless productivity, his extreme physical suffering and lack of effective therapy, and his own awareness of his impending demise are all parts of a tragic tale of 19th Century genius cut short by infectious disease that in the modern era is preventable and treatable. Still, from his suffering and endurance came some of the most luminous poetry in the English language—poems of yearning, mortality, and an intense experience of fleeting beauty.

The author acknowledges using AI tools for locating references in writing this essay.

References

1. Keats J. The poems of John Keats. de Sélincourt E, editor. New York: Dodd, Mead & Company; 1905. p. 249–50 [cited 2026 Feb 25]. https://archive.org/details/poemsofjohnkeats00keat/page/n9/mode/2up
2. Jay SJ, Kırbıyık U, Woods JR, Steele GA, Hoyt GR, Schwengber RB, et al. Modern theory of tuberculosis: culturomic analysis of its historical origin in Europe and North America. Int J Tuberc Lung Dis. 2018;22:1249–57. https://doi.org/10.5588/ijtld.18.0239
3. Smith H. John Keats: poet, patient, physician. Rev Infect Dis. 1984;6:390–404. https://doi.org/10.1093/clinids/6.3.390
4. Cantwell JD. On John Keats and Blue Zones. Proc Bayl Univ Med Cent. 2016;29:220–3 https://doi.org/10.1080/08998280.2016.11929425
5. The Morgan Library & Museum. Here lies One Whose Name was writ in Water [cited 2026 Feb 25]. https://www.themorgan.org/exhibitions/online/keats/here-lies-one-whose-name-was-writ-water
6. Kim Blank G. Mapping Keats' progress: a critical chronology. 2018 [cited 2026 Feb 25]. https://johnkeats.uvic.ca/1820-02.html
7. Lauer S. The social impact of the misconceptions surrounding tuberculosis. The Iowa Historical Review. 2017:55–78 [cited 2026 Feb 25]. https://pubs.lib.uiowa.edu/iowa-historical-review/article/1618/galley/110615/view
8. Daniel TM. The history of tuberculosis. Respir Med. 2006;100:1862–70. https://doi.org/10.1016/j.rmed.2006.08.006
9. Cambau E, Drancourt M. Steps towards the discovery of *Mycobacterium tuberculosis* by Robert Koch, 1882. Clin Microbiol Infect. 2014;20:196–201. https://doi.org/10.1111/1469-0691.12555
10. Hughes SP, Snell N. Is the criticism of John Keats's doctors justified? A bicentenary re-appraisal. The Keats-Shelley Review. 2021;35:41–55. https://doi.org/10.1080/09524142.2021.1911181
11. Birkenhead S. Against oblivion: the life of Joseph Severn. London: The MacMillan Company; 1944.
12. Barberis I, Bragazzi NL, Galluzzo L, Martini M. The history of tuberculosis: from the first historical records to the isolation of Koch's bacillus. J Prev Med Hyg. 2017;58:E9–12.

Address for correspondence: Terence Chorba, Centers for Disease Control and Prevention, 1600 Clifton Rd NE, Mailstop H24-4, Atlanta, GA 30329-4018, USA; email: tlc2@cdc.gov

EMERGING INFECTIOUS DISEASES®

Upcoming Issue

- Pediatric Meningoencephalitis Cluster Caused by Snowshoe Hare Virus, Whistler, British Columbia, Canada, 2024
- Frequency of Use and Yield of Epidemiologic and Ecological Investigative Strategies to Determine Human Plague Exposure Sites, United States, 1991–2018
- Enterovirus D68 Circulation in Europe from 2014 to 2024—Circulation Patterns, Genetic Diversity, and Public Health Implications
- Enhanced Detection of *Coccidioides* spp. Fungi from Environmental Samples Using Digital Droplet PCR
- Dengue Incidence, Seroprevalence, and Expansion Factors from Active Surveillance in Brazil, 2016–2021
- Emergence of a LEE-Negative Shiga Toxin–Producing *Escherichia coli* Strain Causing an Outbreak of Severe Hemolytic Uremic Syndrome in Adults, France, 2025
- Evaluation of Respirable Aerosols Produced during Processing of Chickens in Bangladesh
- Retrospective Genomic Surveillance of St. Louis Encephalitis Virus in Texas, 2009–2024
- Confirming ERVEBO Vaccination via Vector Immunity Detection to Support Ebola Virus Surveillance in Endemic Countries
- Seroprevalence of Crimean-Congo Hemorrhagic Fever Virus Infection in Humans and Domestic Ruminants in the Democratic Republic of the Congo
- Chronic Wasting Disease in Farmed Cervids, South Korea, 2001–2024
- Outbreak of Dengue Virus Serotype 3, Republic of the Marshall Islands, 2019–2021
- Treatment of Severe Ocular Mpox with Cidofovir and Tecovirimat
- Use of Nitroxoline for Disseminated Acanthamoeba Infection Presenting as Necrotic Skin Lesions and Granulomatous Vasculitis in Elderly Man on Dupilumab
- Recombinant Mosaic Coxsackievirus A9 Strain Associated with Severe Inflammatory Cardiomyopathy in Previously Healthy Child, Northeastern France, 2024
- Whole-Genome Analysis of *Treponema pallidum* subsp. *endemicum* Among Men Who Have Sex with Men in Japan, 2020–2023
- Community Outbreak with Panton-Valentine Leukocidin-Encoding CC398 Methicillin-Resistant *Staphylococcus aureus* (MRSA) in the Netherlands, November 2023–June 2024
- Guillain-Barré Syndrome and Visual Impairment Associated with an Emerging Oropouche Virus Lineage, Brazil, 2024
- Rapid Spread of Recombinant African Swine Fever Virus Genotypes I and II in Vietnam during 2023–2024
- The Weight of Waiting
- Acute Febrile Illness Surveillance Provides Population Immunity Estimates Comparable to a Household Serosurvey
- Seroepidemiologic Study of Oropouche Virus in Amazonas State, Brazil, 2015–2016
- *Rickettsia lanei* Rickettsiosis, Oregon, USA, 2025

Complete list of articles in the April issue at https://wwwnc.cdc.gov/eid/#issue-330

Earning CME Credit

To obtain credit, you should first read the journal article. After reading the article, you should be able to answer the following, related, multiple-choice questions. To complete the questions (with a minimum 75% passing score) and earn continuing medical education (CME) credit, please go to http://www.medscape.org/journal/eid. Credit cannot be obtained for tests completed on paper, although you may use the worksheet below to keep a record of your answers.

You must be a registered user on http://www.medscape.org. If you are not registered on http://www.medscape.org, please click on the "Register" link on the right hand side of the website.

Only one answer is correct for each question. Once you successfully answer all post-test questions, you will be able to view and/or print your certificate. For questions regarding this activity, contact the accredited provider, CME@medscape.net. For technical assistance, contact CME@medscape.net. American Medical Association's Physician's Recognition Award (AMA PRA) credits are accepted in the US as evidence of participation in CME activities. For further information on this award, please go to https://www.ama-assn.org. The AMA has determined that physicians not licensed in the US who participate in this CME activity are eligible for *AMA PRA Category 1 Credits*™. Through agreements that the AMA has made with agencies in some countries, AMA PRA credit may be acceptable as evidence of participation in CME activities. If you are not licensed in the US, please complete the questions online, print the AMA PRA CME credit certificate, and present it to your national medical association for review.

Article Title

Blastomyces Urine Antigen Testing for Active Case Identification During Blastomycosis Outbreaks

CME Questions

1. Which of the following statements regarding infection with blastomycosis is most accurate?

A. The most common symptoms are cough, chest pain, and fever
B. Over 80% of infections are symptomatic
C. The incubation period before infection is 1 to 2 weeks
D. Reactivation of latent infection with blastomycosis has not been documented

2. Which of the following statements regarding testing for blastomycosis is most accurate?

A. Skin testing remains a standard for diagnosing blastomycosis
B. New blood enzyme immunoassay (EIA) testing has not improved on test sensitivity
C. Urine antigen testing has low sensitivity
D. Urine antigen testing is limited by specificity between different fungal pathogens

3. Which of the following statements regarding urine antigen testing results in the current study cohort is most accurate?

A. Urine testing was positive in approximately half of all patients
B. Most individuals with a positive urine test were asymptomatic
C. Treatment for blastomycosis was associated with a higher rate of negative urine samples
D. Time from study initiation to urine testing did not affect the rate of positive urine samples

4. Which of the following variables was most associated with a positive urine antigen test for blastomycosis in the current study?

A. Being a man
B. The presence of symptoms
C. Older age
D. A history of immunocompromise